

INFN-LNL-269/2022

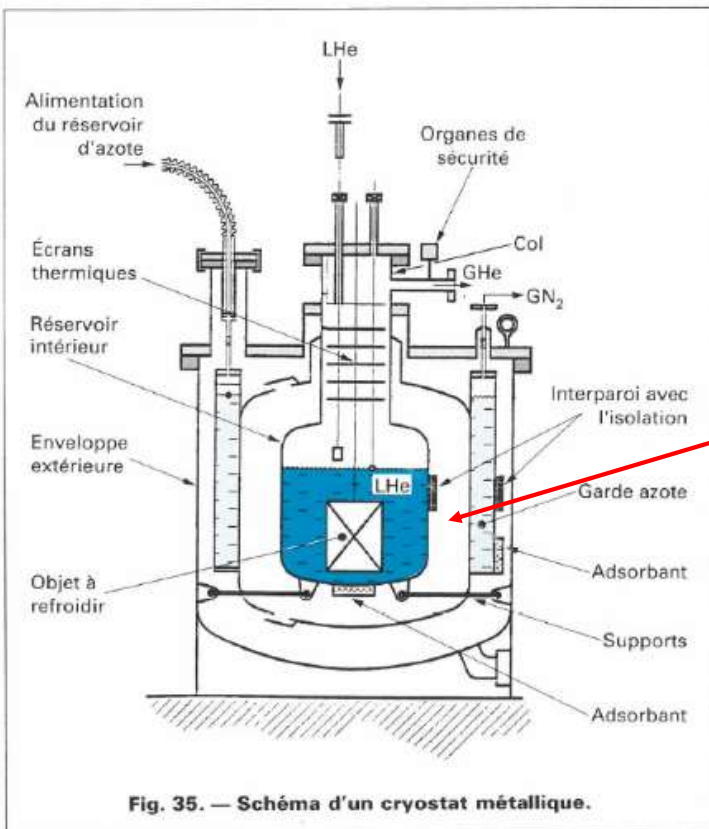
CORSO INFN DI CRIOGENIA

RUGGERO PENGO

INFN-LNL

Programma del corso		slides
Cryostat design	Introduzione	2-13
	Definizioni utili	14-19
Refrigerazione	Throtteling, sistemi adiabatici aperti	20-25
	Temperatura d'inversion, Joule-Thomson effect, cooling by external work, refrigerator vs liquefier	26-41
Altri cicli termici di refrigerazione	Stirling, Gifford-Mc Mahon, Pulse tube, TS diagram for He, H, N, O	42-58
Proprieta' dei materiali	Temperatura di Debye, Calcolo dell'Entalpia, caratteristiche dei materiali, Thermal expansion	59-86
Trasmissione del calore	Conduzione nei solidi, conduzione nel gas residuo, interfaccia solido/liquido, natural convection, irraggiamento, cryopumping, current leads, altri tipi d'isolamento	87-140
Linee di trasferimento	Caduta di pressione, termosifone, convezione forzata (pompe), calcolo di Kv di una valvola, guarnizioni a freddo, dimensionamento di una valvola di sicurezza	141-174
Cenni di criogenia a T< 4 K	Cenni di superfluidita', resistenza di Kapitza, refrigerazione He-3 He-4, superconduttività per magneti e cavità RF, giunzioni Josephson	175-205

Cryostat design



3.1 Enceintes.

Les cryostats réalisés actuellement sont en général métalliques (acier inoxydable le plus souvent). Dans quelques cas particuliers, on utilise toujours des cryostats en verre : ce matériau fragile est poreux à l'hélium au-dessus de 77 K. Un cryostat comporte toujours une **enceinte à paroi double**; entre ces parois, on réalise un vide d'isolement thermique poussé ($\leq 10^{-4}$ Pa).

Outlook on different cryogenic fluids:

Table 1
Characteristic temperatures of cryogenic fluids [K]

Cryogen	Triple point	Normal boiling point	Critical point
Methane	90.7	111.6	190.5
Oxygen	54.4	90.2	154.6
Argon	83.8	87.3	150.9
Nitrogen	63.1	77.3	126.2
Neon	24.6	27.1	44.4
Hydrogen	13.8	20.4	33.2
Helium	2.2*	4.2	5.2

* λ point

1. PROPRIÉTÉS DES FLUIDES

Tableau A. – Propriétés physiques usuelles des fluides cryogéniques (1).

Fluide	^3He	^4He	H_2	D_2	Ne	N_2	O_2	Ar	CH_4
Température d'ébullition à p normale (K)	3,2	4,2	20,4	23,6	27,1	77,3	90,2	87,3	111,7
Point triple	néant	néant	13,95	18,7	24,5	83,14	54,40	84,0	90,7
Pression (10 ² Pa)	néant	néant	72	170	424	125	1,5	670	116
Point critique	Température (K)	3,33	5,20	33,2	38,3	44,4	126,1	154,4	160,8
Pression (10 ² Pa)	1,16	2,23	12,8	16,5	26,6	33,1	49,5	47,7	45,8
Volume de gaz provenant de 1 L de liquide	à T d'ébullition et p normale (L)	2,5	7,3	54,6	70	127	180	260	250
	à T et p normales (L)	455	700	780	900	1355	648	798	784
Enthalpie de formation à la température d'ébullition sous p normale (kJ/kg)	8,2	21	452	305	86	199	213	167	510
Enthalpie sensible entre T_{de} et 300 K (kJ/kg)	2080	1550	3800	2048	280	233	193	112	402
Rapport enthalpie sensible enthalpie de formation	255	74	8,4	6,7	3,25	1,17	0,90	0,71	0,8
Taux d'évaporation (Wh/L)	0,14	0,7	9	13,6	29	45	68	61	60
Conductivité thermique du gaz à T_{de} et p normale (mW/(m.K))	*	10	15	< 40	8	7,6	9	8	8,7
Conductivité thermique du gaz à 300 K et p normale (mW/(m.K))	*	152	181	137	50	26	27	18	31
Masse volumique du liquide couplant à p normale (kg/m ³)	59	125	71	161	1210	810	1140	1400	425
Masse volumique de la vapeur saturante à p normale (kg/m ³)	24	17	1,3	2,3	9,5	4,5	4,4	5,8	1,7
Masse volumique du gaz à p et T normales (kg/m ³)	0,13	0,18	0,09	0,18	0,90	1,25	1,43	1,80	0,55
Viscosité du liquide à T_{de} ($\mu\text{Pa.s}$)	2	3,6	13	16,2	125	160	190	260	120
Viscosité du gaz à T_{de} ($\mu\text{Pa.s}$)	1,2	1,0	1,0	1,5	4,5	5,0	7,0	8	4,4
Viscosité du gaz à température ambiante ($\mu\text{Pa.s}$)	*	20	9	13	30	17	20	22	11
Permittivité du liquide	*	1,05	1,23	1,27	1,19	1,44	1,48	1,54	1,68

(1) p normale = $p_{\text{atm}} = 1,013 \times 10^5$ Pa.

* non transcrit dans la littérature.

How can we cool a superconducting material

Superconductor properties

Superconductor	Crystal structure*	Lattice constants [\AA] [†]			T_c [K]	$\mu_0 H_{c2}(0 \text{ K})$ [T]	$\lambda_{\text{GL}}(0 \text{ K})^{\ddagger}$ [nm]	$\xi_{\text{GL}}(0 \text{ K})^{\ddagger}$ [nm]
		a	b	c				
<i>Low T_c</i>								
Nb–Ti ^e	A2				9.3 ^j	13	300	4
V ₃ Ga ^e	A15	4.816 ⁿ	—	—	15	23	90	2–3
V ₃ Si ^e	A15	4.722 ⁿ	—	—	16	20	60	3
Nb ₃ Sn ^e	A15	5.289 ⁿ	—	—	18	23	65	3
Nb ₃ Al ^e	A15	5.187 ⁿ	—	—	18.9	32		
Nb ₃ Ga ^e	A15	5.171 ⁿ	—	—	20.3	34		
Nb ₃ (Al ₇₅ Ge ₂₅) ^b	A15				20.5	41		
Nb ₃ Ge ^e	A15	5.166 ⁿ	—	—	23	38	90	3
NbN ^e	B1				16	15	200	5
V ₂ (Hf,Zr) ^o	C15				10.1	24 ^k		
PbMo ₆ S ₈ ^e	Chevrel				15	60	200	2
MgB ₂	hexagonal	3.086 ^m	—	3.521 ⁿ	39	~16 (a, b) ^l	140 ^k	5.2 ^k
<i>High T_c</i>								
La _{1-x} Sr _x CuO _{4-t} ^e	I4/mmm	3.779	3.779	1.323	40	50	80 (a, b) 400 (c)	~4 (a, b) 0.7 (c)
YBa ₂ Cu ₃ O _{7-δ} ^d (YBCO)	Pmmm	3.818	3.884	11.683	90	670 (a, b) 120 (c)	150 (a, b) 900 (c)	~2 (a, b) 0.4 (c)
Bi ₂ Sr ₂ CaCu ₃ O _{7-δ} ^d (Bi-22212)	A2aa	5.410	5.420	30.930	90	280 (a, b) 32 (c)	300 (a, b)	~3 (a, b) 0.4 (c)
(Bi,Pb) ₂ Sr ₂ Ca ₂ Cu ₃ O _{7+δ} ^e (Bi-2223)	Perovskite (orthorhombic)	5.39	5.40	37	110			
Tl ₂ Ba ₂ CaCu ₃ O _{8-δ} ^{d,p} (Tl-2212)	I4/mmm	3.856	3.856	29.260	110		215 (a, b)	2.2 (a, b) 0.5 (c)
Tl ₂ Ba ₂ Ca ₂ Cu ₃ O _{10-δ} ^{d,p} (Tl-2223)	I4/mmm	3.850	3.850	35.88	125	120	205 (a, b) 480 (c)	1.3 (a, b)
HgBa ₂ Ca ₂ Cu ₃ O _{8+δ} ^e	Pmmm	3.85	—	15.85	133	160 ⁱ		1.42 (a, b) ^q

Notation:

* Crystal structures for the low- T_c superconductors are listed here mostly by the Strukturbericht designation, whereas for the high- T_c materials they are mostly listed by the Space group designation. Tables of cross lists to different nomenclatures are given in the appendixes to the ASM Handbook (1992), Vol. 3, *Alloy Phase Diagrams*, ASM International, Materials Park, OH.

^a (a, b) refers to magnetic field, penetration depth, or coherence length being coplanar with the a, b crystallographic direction or Cu–O planes (usually parallel to the flat faces of practical conductors); (c) refers to an orientation along the c-axis; that is, perpendicular to the Cu–O planes (usually perpendicular to the flat faces of most practical conductors).

^b The penetration depth $\lambda_{\text{GL}}(0 \text{ K})$ is the constant prefactor in the Ginzburg–Landau expression $\xi_{\text{GL}}(T) = \xi_{\text{GL}}(0 \text{ K}) (1 - T/T_c)^{-0.5}$.

^c The coherence length $\xi_{\text{GL}}(0 \text{ K})$ is the constant prefactor in the Ginzburg–Landau expression $\xi_{\text{GL}}(T) = \xi_{\text{GL}}(0 \text{ K}) (1 - T/T_c)^{-0.5}$.
(References continued)

Superconductor properties

Superconductor	Crystal structure*	Lattice constants [\AA] [†]			T_c [K]	$\mu_0 H_{c2}(0 \text{ K})$ [T]	$\lambda_{\text{GL}}(0 \text{ K})^{\ddagger}$ [nm]	$\xi_{\text{GL}}(0 \text{ K})^{\ddagger}$ [nm]
		a	b	c				
<i>Low T_c</i>								
Nb–Ti ^e	A2				9.3 ^j	13	300	4
V ₃ Ga ^e	A15	4.816 ⁿ	—	—	15	23	90	2–3
V ₃ Si ^e	A15	4.722 ⁿ	—	—	16	20	60	3
Nb ₃ Sn ^e	A15	5.289 ⁿ	—	—	18	23	65	3
Nb ₃ Al ^e	A15	5.187 ⁿ	—	—	18.9	32		
Nb ₃ Ga ^e	A15	5.171 ⁿ	—	—	20.3	34		
Nb ₃ (Al ₇₅ Ge ₂₅) ^b	A15				20.5	41		
Nb ₃ Ge ^e	A15	5.166 ⁿ	—	—	23	38	90	3
NbN ^e	B1				16	15	200	5
V ₂ (Hf,Zr) ^o	C15				10.1	24		
PbMo ₆ S ₈ ^e	Chevrel				15	60	200	2
MgB ₂	hexagonal	3.086 ^m	—	3.521 ⁿ	39	~16 (a, b) ^l	140 ^k	5.2 ^k
<i>High T_c</i>								
La _{1-x} Sr _x CuO _{4-t} ^e	I4/mmm	3.779	3.779	1.323	40	50	80 (a, b) 400 (c)	~4 (a, b) 0.7 (c)
YBa ₂ Cu ₃ O _{7-δ} ^d (YBCO)	Pmmm	3.818	3.884	11.683	90	670 (a, b) 120 (c)	150 (a, b) 900 (c)	~2 (a, b) 0.4 (c)
Bi ₂ Sr ₂ CaCu ₃ O _{7-δ} ^d (Bi-22212)	A2aa	5.410	5.420	30.930	90	280 (a, b) 32 (c)	300 (a, b)	~3 (a, b) 0.4 (c)
(Bi,Pb) ₂ Sr ₂ Ca ₂ Cu ₃ O _{7+δ} ^e (Bi-2223)	Perovskite (orthorhombic)	5.39	5.40	37	110			
Tl ₂ Ba ₂ CaCu ₃ O _{8-δ} ^{d,p} (Tl-2212)	I4/mmm	3.856	3.856	29.260	110		215 (a, b)	2.2 (a, b) 0.5 (c)
Tl ₂ Ba ₂ Ca ₂ Cu ₃ O _{10-δ} ^{d,p} (Tl-2223)	I4/mmm	3.850	3.850	35.88	125	120	205 (a, b) 480 (c)	1.3 (a, b)
HgBa ₂ Ca ₂ Cu ₃ O _{8+δ} ^e	Pmmm	3.85	—	15.85	133	160 ⁱ		1.42 (a, b) ^q

Table 1
Characteristic temperatures of cryogenic fluids [K]

Cryogen	Triple point	Normal boiling point	Critical point
Methane	90.7	111.6	190.5
Oxygen	54.4	90.2	154.6
Argon	83.8	87.3	150.9
Nitrogen	63.1	77.3	126.2
Neon	24.6	27.1	44.4
Hydrogen	13.8	20.4	33.2
Helium	2.2*	4.2	5.2

* λ point

A1.5 PROPERTIES OF COMMON CRYOGENIC FLUIDS (SEC. 1.2)

Additional data on the vapor-pressure vs. temperature dependence of these cryogenic fluids are given in Appendix A5.1.

Fluid: property	³ He	⁴ He	H ₂ ^a (Para)	H ₂ ^a (Normal)	Ne	N ₂	Ar	O ₂	CH ₄ (Methane)
Molecular weight	3.0160	4.0026	2.0159	2.0159	20.179	28.013	39.948	31.999	16.043
Critical temp. [K]	3.324	5.195	32.93	33.18	44.49	126.2	150.7	154.6	190.6
Critical pressure [atm]	1.145	2.245	12.67	12.98	26.44	33.51	47.99	49.27	45.39
Boiling point [K]	3.191	4.230	20.27	20.27	27.10	77.35	87.30	90.20	111.7
Melting point [K]	—	4.2 (at 140 atm)	13.80	13.95	24.56	63.15	83.81	54.36	90.72
Liquid density at B.P. [g/mL]	0.05722	0.1247	0.07080	0.07080	1.207	0.8061	1.395	1.141	0.4224
Gas density at 0°C and 1 atm [g/L]	0.1345	0.1785	0.08988	0.08988	0.8998	1.250	1.784	1.429	0.7175
Vapor density at B.P. [g/L]	24.51	16.76	1.339	1.339	9.577	4.612	5.774	4.467	1.816
Liquid thermal conductivity at B.P. [mW/(m·K)]	—	18.66	103.4	103.4	155.0	145.8	125.6	151.6	183.9
Liquid isobaric specific heat at B.P. [J/(g K)]	24.80	5.299	9.659	9.667	1.862	2.041	1.117	1.699	3.481
Latent heat of vaporization at B.P.	7.976 J/g (0.4564 J/mL)	20.75 (2.589)	445.4 (31.54)	445.4 (31.54)	85.75 (103.5)	199.2 (160.6)	161.1 (224.9)	213.1 (243.1)	510.8 (215.8)
Latent heat of fusion at M.P. [J/g]	—	30.5	—	58.2	16.6	25.5	27.8	13.8	58.7
Vapour pressure of solid at M.P. [kPa]	—	—	7.04	7.20	43.46	12.52	68.89	0.146	11.5

A1.5 PROPERTIES OF COMMON CRYOGENIC FLUIDS (SEC. 1.2)

Additional data on the vapor-pressure vs. temperature dependence of these cryogenic fluids are given in Appendix A5.1.

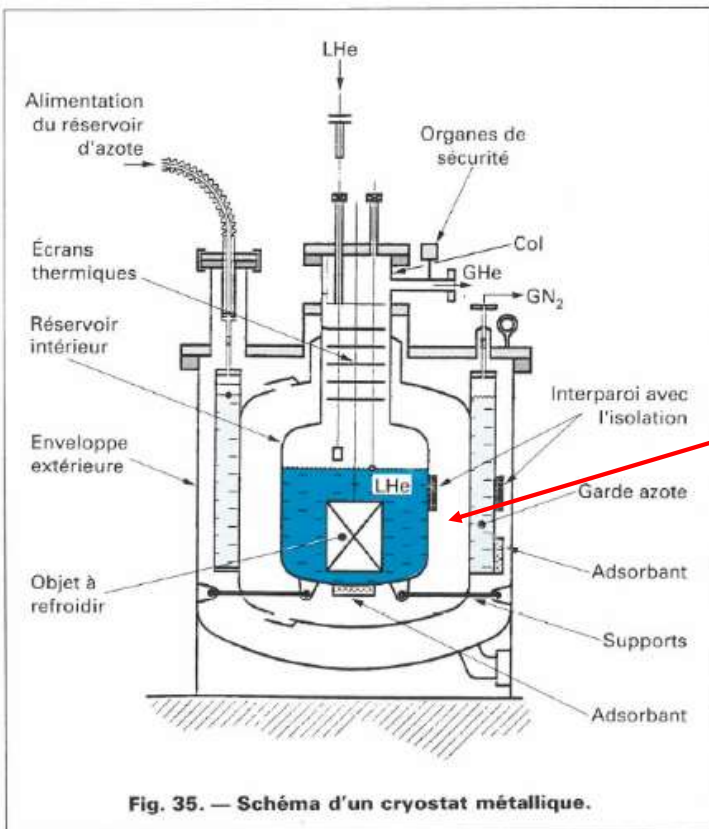
Fluid: property	³ He	⁴ He	H ₂ ^a (Para)	H ₂ ^a (Normal)	Ne	N ₂	Ar	O ₂	CH ₄ (Methane)
Molecular weight	3.0160	4.0026	2.0159	2.0159	20.179	28.013	39.948	31.999	16.043
Critical temp. [K]	3.324	5.195	32.93	33.18	44.49	126.2	150.7	154.6	190.6
Critical pressure [atm]	1.145	2.245	12.67	12.98	26.44	33.51	47.99	49.77	45.39
Boiling point [K]	3.191	4.230	20.27	20.27	27.10	77.35	87.30	90.20	111.7
Melting point [K]	—	4.2 (at 140 atm)	13.80	13.95	24.56	63.15	83.81	54.36	90.72
Liquid density at B.P. [g/mL]	0.05722	0.1247	0.07080	0.07080	1.207	0.8061	1.395	1.141	0.4224
Gas density at 0°C and 1 atm [g/L]	0.1345	0.1785	0.08988	0.08988	0.8998	1.250	1.784	1.429	0.7175
Vapor density at B.P. [g/L]	24.51	16.76	1.339	1.339	9.577	4.612	5.774	4.467	1.816
Liquid thermal conductivity at B.P. [mW/(m·K)]	—	18.66	103.4	103.4	155.0	145.8	125.6	151.6	183.9
Liquid isobaric specific heat at B.P. [J/(g K)]	24.80	5.299	9.659	9.667	1.862	2.041	1.117	1.699	3.481

Latent heat of vaporization at B. P.	7.976 J/g (0.4564 J/mL)	20.75 (2.589)	445.4 (31.54)	445.4 (31.54)	85.75 (103.5)	199.2 (160.6)	161.1 (224.9)	213.1 (243.1)	510.8 (215.8)
Latent heat of fusion at M.P. [J/g]	—	30.5	—	58.2	16.6	25.5	27.8	13.8	58.7
Vapour pressure of solid at M.P. [kPa]	—	—	7.04	7.20	43.46	12.52	68.89	0.146	11.5

To cool a material the latent heat $c_\lambda = H_{\text{vap}} - H_{\text{liq}}$ is used, with or without the gas enthalpy. H_{vap} and H_{liq} are computed at the boiling point temperature.

Note: Latent Heat of water is ca. 2200 J/g

Cryostat design

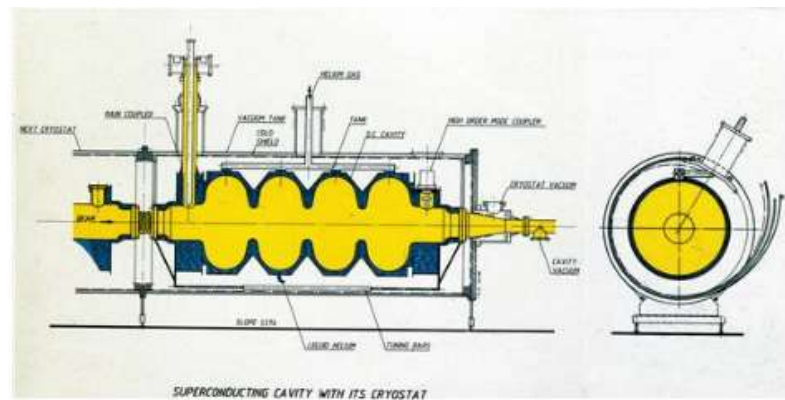
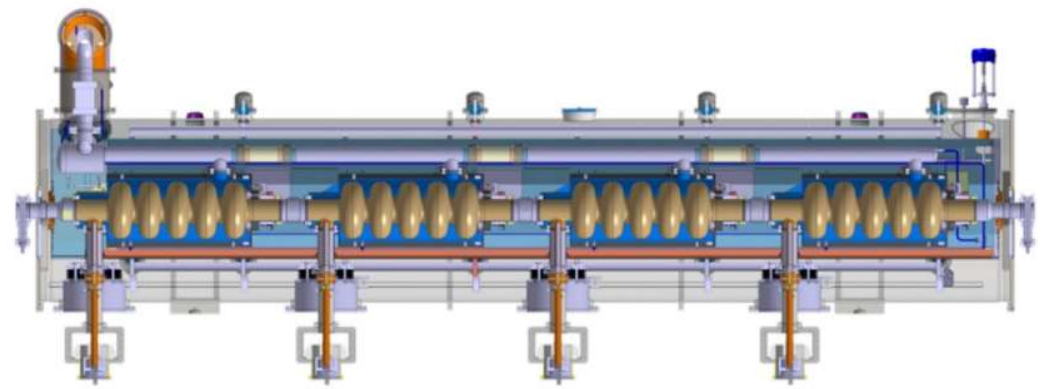


3.1 Enceintes.

Les cryostats réalisés actuellement sont en général métalliques (acier inoxydable le plus souvent). Dans quelques cas particuliers, on utilise toujours des cryostats en verre : ce matériau fragile est poreux à l'hélium au-dessus de 77 K. Un cryostat comporte toujours une **enceinte à paroi double**; entre ces parois, on réalise un vide d'isolement thermique poussé ($\leq 10^{-4}$ Pa).



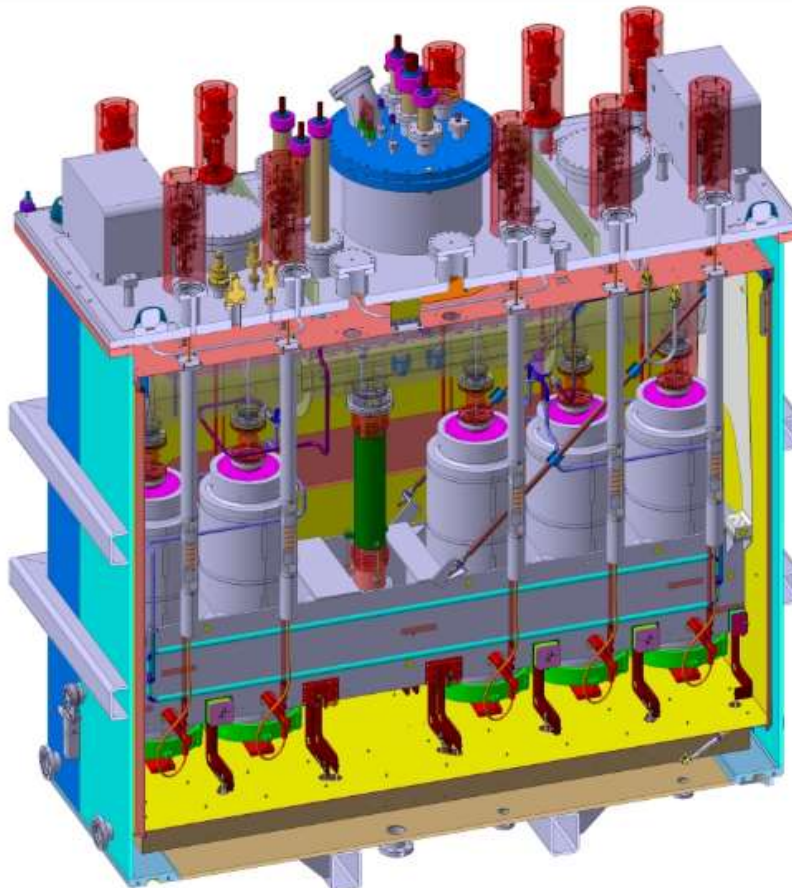
Cryostat design



Cryostat design



Cryostat design



Eur. Phys. J. A (2016) 52: 334



Fig. 7. The picture, taken in April 2015, shows the complete assembly of the first cryomodule. One can see the 5 cavities, the helium vessel on the top and the support frame hiding the solenoid placed between the third and fourth cavity.

The HIE-ISOLDE project [1] [2] looks at the overall upgrade of the ISOLDE facility, i.e. an increase of the final energy of the radioactive ion beam, an improvement of the beam quality and flexibility and an increase of the beam intensity. The linac upgrade will consist of a superconducting machine [3] [4] providing 39.6 MV of

Bologna ottobre 2019

11

Cryostat design

Magnetic Birefringence of Vacuum: the PVLAS Experiment

6 Cryostat with lambda plate for superfluid helium (He II)

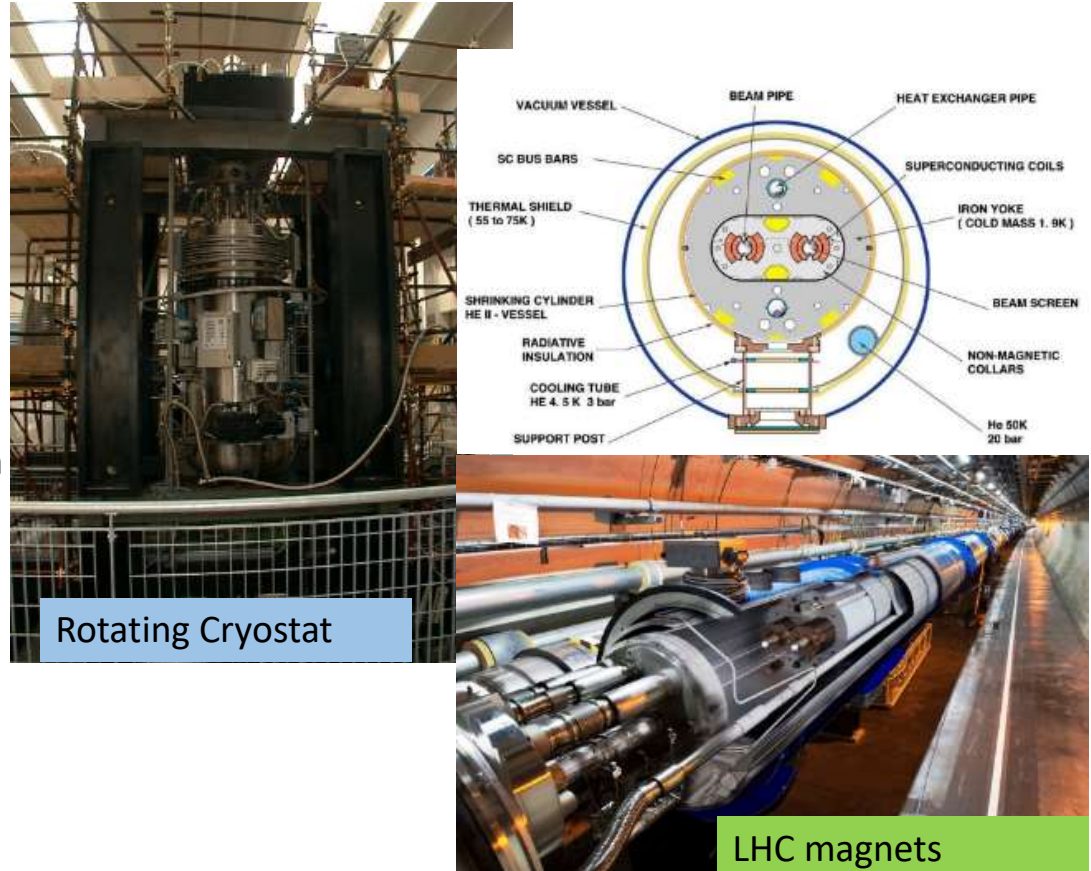
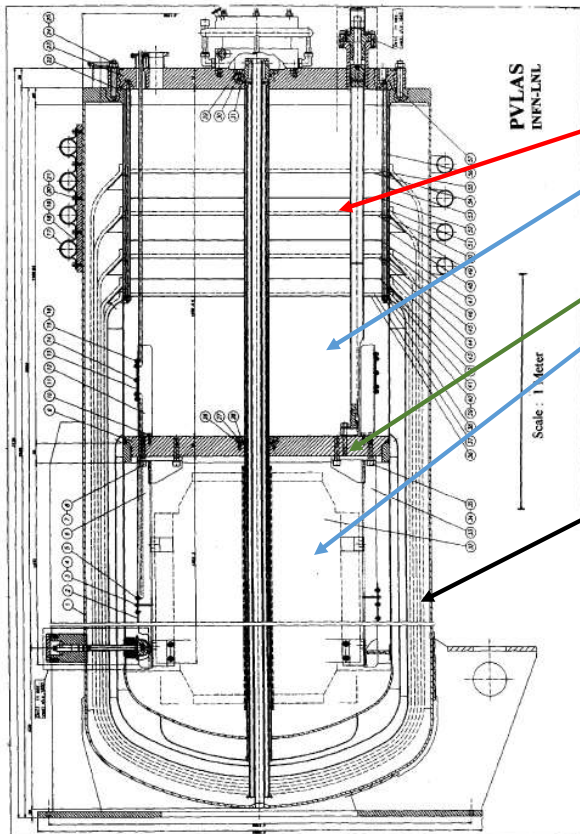


Figure 5. Mechanical drawing of the cryostat.

Cryostat design

To house and thermally insulate a superconducting device (e.g. s/c RF cavities, s/c magnets,...) or a cryogenic fluid (e.g. Liquid Argon) in which detectors are immersed.

The following disciplines are necessary/involved:

- Low temperature mechanical engineering (e.g. to chose the proper material)
- Heat transfer (e.g. to properly insulate the devices and so to reduce the consumption of the cryogenic fluid used)
- (low) temperature fluid mechanics for the fluid transfer and control
- Instrumentation such as measurements of flow, temperature, level, pressure at low temperature
- Safety measures to be adopted both for the personnel and the apparatus protection (e.g. use of the proper material, pressure relief valves PRV,...)
- Vacuum is an important part (not treated in these lectures).

Temperature scales



ENTALPIA

$$H = U + PV \quad \text{funzione di stato}$$

$$dH = dU + P dV + V dP$$

importante per sistemi semplicemente comprimibili:

- trasf. isobare $\Delta H = \Delta Q$
- caso di sistemi aperti con flusso di materia: estensione del 1° principio $\rightarrow H$ è la proprietà che conta per la materia entra/esce (es. scambiatore di calore)
- espansione strozzata: refrigerazione Joule-Thomson

CAPACITÀ TERMICA e CALORE SPECIFICO

$$C = \frac{dQ}{dT} \quad [\text{J/K}] \quad C = \frac{1}{m} \frac{dQ}{dT} \quad [\text{J/kg K}] \text{ or } [\text{J/mol K}]$$

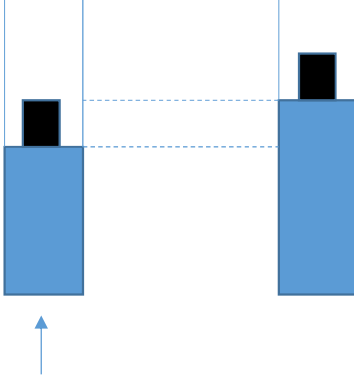
come dQ , anche C dipende dalla trasformazione

SISTEMA SEMPLICEMENTE COMPRIMIBILE:

- isocora: $C_V = \left(\frac{dQ}{dT} \right)_V = \left(\frac{dU}{dT} \right)_V$ tutto Q va in U
- isobara: $C_P = \left(\frac{dQ}{dT} \right)_P = \left(\frac{dH}{dT} \right)_P > C_V$ parte di Q va in L
- $C_P \approx C_V$ per solidi e liquidi

Tabella 11.1 Confronto fra U e H

Energia interna U	Entalpia H
In generale $dU = dQ - PdV$ $\left(\frac{\partial U}{\partial T} \right)_V = C_V$	In generale $dH = dQ + VdP$ $\left(\frac{\partial H}{\partial T} \right)_P = C_P$
Trasformazioni isocore $U_f - U_i = Q$ $U_f - U_i = \int_i^f C_V dT$	Trasformazioni isobare $H_f - H_i = Q$ $H_f - H_i = \int_i^f C_P dT$
Trasformazioni adiabatiche $U_f - U_i = - \int_i^f P dV$	Trasformazioni adiabatiche $H_f - H_i = \int_i^f V dP$
Espansione libera $U_f = U_i$	Espansione strozzata $H_i = H_f$
Per un gas ideale $U = \int C_V dT + \text{cost.}$	Per un gas ideale $H = \int C_P dT + \text{cost.}$
Trasformazioni reversibili $dU = TdS - PdV$ $T = \left(\frac{\partial U}{\partial S} \right)_V$ $P = \left(\frac{\partial U}{\partial V} \right)_S$	Trasformazioni reversibili $dH = TdS + VdP$ $T = \left(\frac{\partial H}{\partial S} \right)_P$ $V = \left(\frac{\partial H}{\partial P} \right)_S$



Heat Q at
constant
pressure

Difference between Internal Energy and Enthalpy

Process at constant pressure $P = 12 \text{ bar}$

The heat added $Q = 125 \text{ kJ}$

Volume increase $\Delta V = 12.4 \text{ liter}$

Calculate the change of internal Energy ΔE and the change of Enthalpy ΔH

$$\Delta E = Q + \text{Work} = Q - P \Delta V$$

$$\text{Work} = 12 \text{ bar} \cdot 12.4 \text{ liter}$$

$$= 12 \cdot 10^5 \text{ Pa} \cdot 12.4 \cdot 10^{-3} \text{ m}^3 \\ = 14.9 \cdot 10^3 \text{ J} = 14.9 \text{ kJ}$$

$$\Delta E = 125 \text{ kJ} - 14.9 \text{ kJ} = \mathbf{110.1 \text{ kJ}}$$

$$\Delta H = \Delta E + \Delta(PV) = \Delta E + P \Delta V + V \Delta P = \Delta E + P \Delta V$$

$$\Delta H = (Q + \text{Work}) + P \Delta V$$

$$= Q - P \Delta V + P \Delta V = Q$$

$$\Delta H = \mathbf{125 \text{ kJ}}$$

Definizioni utili

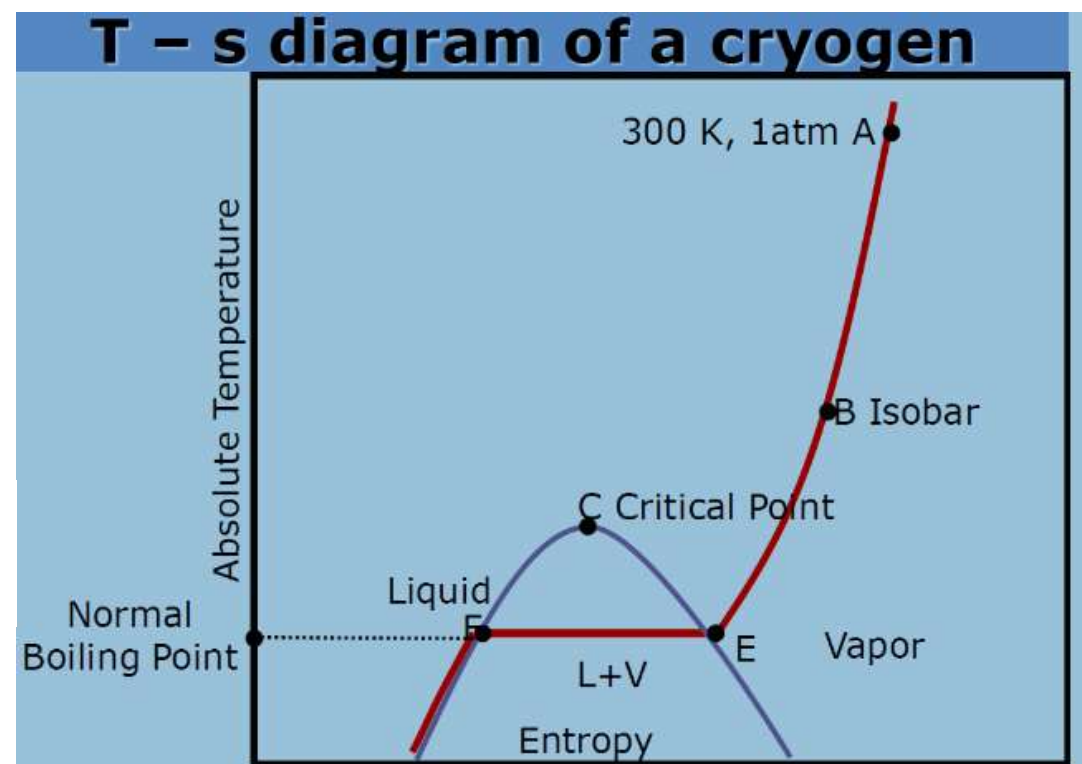
- Temperatura (K)
- Entalpia $H(J) = U + PV$ o più usata «specific enthalpy» $H/m = h = u + p/\rho$ (J/kg) or (J/g) or (J/mol)
- Entropia (J/K) o più usata «specific entropy» (J/kg-K) or (J/g-K) or (J/mol-K)

The Helmholtz energy for the ideal gas is given by

$$A^0 = U^0 - TS^0 = H^0 - RT - TS^0$$

$$A^0 = H_0^0 + \int_{T_0}^T C_p^0 dT - RT - T \left[S_0^0 + \int_{T_0}^T \frac{C_p^0}{T} dT - R \ln \left(\frac{\rho T}{\rho_0 T_0} \right) \right]$$

Richard T. Jacobsen, Thermodynamic Properties of Cryogenic Fluids (International Cryogenics Monograph Series), 1997



Useful definitions

- Temperatura (K)
- Entalpia $H(J) = U + PV$ o più usata «specific enthalpy» $H/m = h = u + p/\rho$ (J/kg) or (J/g) or (J/mol)
- Entropia (J/K) o più usata «specific entropy» (J/kg-K) or (J/g-K) or (J/mol-K)

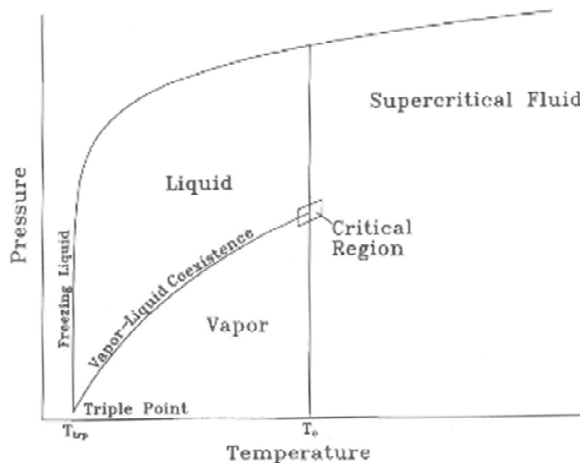
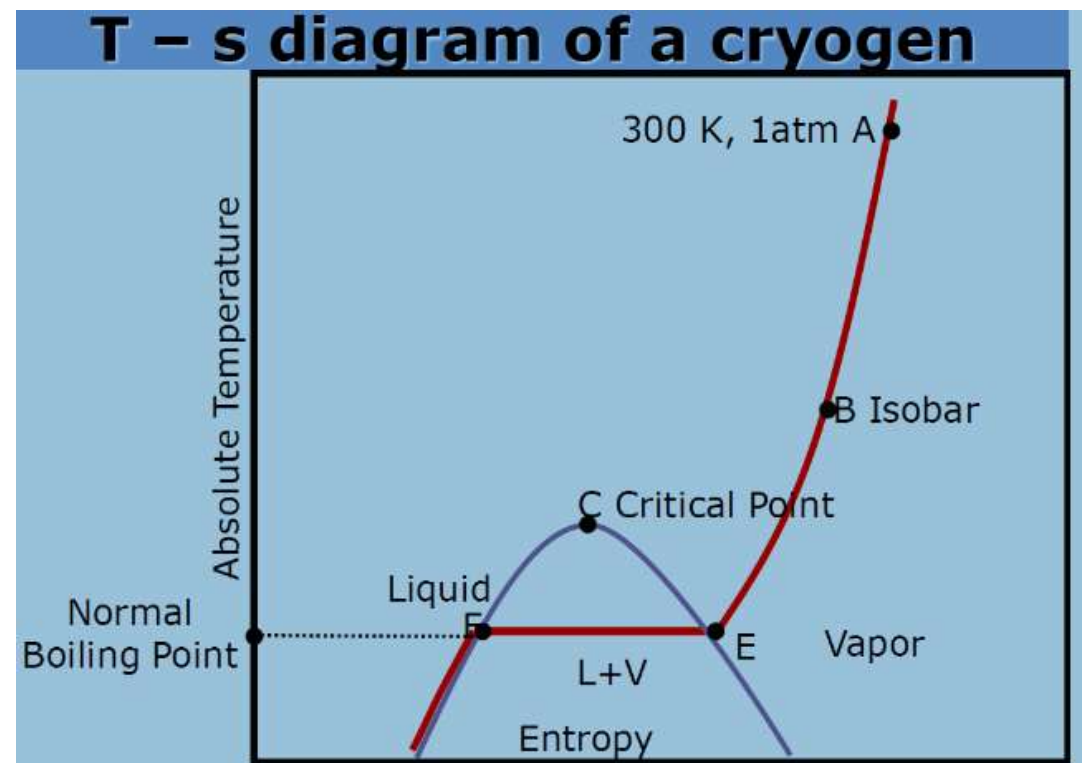


Fig. 1.1. Regions of the thermodynamic surface.



Per un sistema PVT l'Entalpia e' definita:

$$H = U \text{ (Energia interna in Joule)} + PV$$

$$\text{Da cui segue: } dH = dU + d(PV) = dU + dP \cdot V + P \cdot dV$$

Ovvero (1^ Princio della termodinamica):

$$\delta Q = dU - \delta W$$

$$dU = \delta Q + \delta W$$

$$dU = \delta Q - PdV ;$$

$$dH = \delta Q + \delta W + d(PV)$$

$$dH = \left(\frac{\partial H}{\partial T}\right)_V dT + \left(\frac{\partial H}{\partial V}\right)_T dV \quad f(T, V)$$

$$dH = \left(\frac{\partial H}{\partial P}\right)_T dP + \left(\frac{\partial H}{\partial T}\right)_P dT \quad f(P, T) \quad \left(\frac{\partial H}{\partial T}\right)_P dT \equiv C_p$$

$$dU = \left(\frac{\partial U}{\partial T}\right)_V dT + \left(\frac{\partial U}{\partial V}\right)_T dV \quad f(T, V) \quad \left(\frac{\partial U}{\partial T}\right)_V dT \equiv C_v$$

$$dH = \left(\frac{\partial U}{\partial P}\right)_T dP + \left(\frac{\partial U}{\partial T}\right)_P dT \quad f(P, T)$$

L'Energia interna U e l'Entalpia H svolgono ruoli analoghi nelle descrizioni di alcune trasformazioni a V costante e a P costante (Per sistemi PVT).

VOLUME COSTANTE (QUASI STATICÀ)

$$dU = \delta Q - PdV \rightarrow dU = \delta Q$$

$$\text{ovvero } U = \Delta U$$

Il calore trasmesso e' uguale alla variazione dell'energia interna!

PRESSIONE COSTANTE (QUASI STATICÀ)

$$dH = \delta Q + \delta W + d(PV)$$

$$= dH = \delta Q - PdV + d(PV) = \delta Q - PdV + PdV + V dP =$$

$$= \delta Q - V dP = \delta Q$$

$$\delta Q = dH \rightarrow Q = \Delta H$$

Il calore trasmesso e' uguale alla variazione di Entalpia

Molte trasformazioni in ingegneria criogenica sono a P costante!

SISTEMA A A CONTATTO TERMICO CON IL SISTEMA B

IL SISTEMA COMPLESSIVO (A+B) COMPIE UNA TRASFORMAZIONE ADIABATICA IN CUI A & B NON COMPIONO LAVORO

ES. IMMERGO UN PEZZO DI METALLO IN ACQUA E SUPPONGO (A RAGIONE δ) CHE IL SISTEMA ACQUA + METALLO NON SCAMBI CALORE CON L'ESTERNO

$$\begin{array}{ll} \text{SISTEMA } \underline{A} : & \Delta U_A = Q_A + W_A \\ \text{ " } \underline{B} : & \Delta U_B = Q_B + W_B \end{array}$$

$$\underline{\Delta U_A + \Delta U_B = (Q_A + Q_B) + (W_A + W_B)}$$

1° PRINCIPIO PER A
" PER B

$$\begin{array}{ll} \text{SISTEMA COMPLESSIVO} & \Delta U = Q + W \Rightarrow W = \Delta U \\ & \downarrow = 0 \text{ PERCHE' ADIABATICO} \end{array}$$

DAL CONFRONTO SI HA

$$\Delta U_A + \Delta U_B = \Delta U$$

$$W_A + W_B = W$$

$$Q_A + Q_B = Q = \phi \Rightarrow Q_A = -Q_B$$

CIOE' IL CALORE CEDUTO DA A E' UGUALE A QUELLO ASSORBITO DA B.

$$\text{SISTEMA } \underline{A} \quad 2 \text{ kg Fe @ } T = 75^\circ\text{C} ; c_p = 460 \frac{\text{J}}{\text{kg} \cdot \text{K}}$$

$$\underline{B} \quad 5 \text{ kg H}_2\text{O @ } T = 25^\circ\text{C} ; c_p = 1 \text{ cal/g} \cdot \text{K} \\ = 4180 \frac{\text{J}}{\text{kg} \cdot \text{K}}$$

$$c_p = \left(\frac{\delta Q}{dT} \right)_p \quad c = \lim_{T_2 \rightarrow T_1} \frac{Q}{T_2 - T_1} = \lim_{\Delta T \rightarrow 0} \frac{Q}{\Delta T}$$

$$\text{POICHÉ'} \quad Q_A = -Q_B \quad \text{cioè} \quad Q_A + Q_B = Q = \phi$$

$$\begin{aligned} \delta Q_A &= m_A c_{pA} dT_A & Q_A &= \int \delta Q_A = m_A c_{pA} \int_{T_A}^{T_f} dT_A \\ \delta Q_B &= m_B c_{pB} dT_B & Q_B &= \int \delta Q_B = m_B c_{pB} \int_{T_B}^{T_f} dT_B \end{aligned}$$

$$Q_A = m_A c_{pA} [T_f - T_A] \quad ; \quad Q_B = m_B c_{pB} [T_f - T_B]$$

T_f = TEMPERATURA FINALE DEL SISTEMA

$$[T_f - T_A] m_A c_{pA} + m_B c_{pB} [T_f - T_B] = \phi \quad \text{ADIABATICA}$$

$$m_A c_{pA} T_f + m_B c_{pB} T_f - [m_A c_{pA} T_A + m_B c_{pB} T_B] = 0$$

$$T_f = \frac{m_A c_{pA} T_A + m_B c_{pB} T_B}{m_A c_{pA} + m_B c_{pB}} =$$

$$T_f = \frac{m_A c_{pA} + T_A + m_B c_{pB} T_B}{m_A c_{pA} + m_B c_{pB}} =$$

$$T_f = \frac{2 \text{ kg} \cdot 460 \frac{\text{J}}{\text{kg K}} \cdot (75 + 273,15) \text{K} + 5 \text{ kg} \cdot 4180 \frac{\text{J}}{\text{kg K}} (25 + 273,15)}{2 \text{ kg} \cdot 460 \frac{\text{J}}{\text{kg K}} + 5 \text{ kg} \cdot 4180 \frac{\text{J}}{\text{kg K}}}$$

$$T_f = 300,3 \text{ K} \quad t_f = 27,1 \text{ }^{\circ}\text{C}$$

THROTTLING O FENOMENO DI STROZZAMENTO (IMPORTANZA DELL'ENTALPIA)

PISTONI SPOSTATI SIMULTANEAMENTE MANTENENDO A SINISTRA P_1 E A DESTRA P_2 [ES. UN REGOLATORE DI PRESSIONE A SX A P_1 E A DX P_2]

$$P_2 < P_1$$

$$\Delta H = Q + W + \Delta(PV);$$

$$H_2 - H_1 = Q + W + P_2 V_2 - P_1 V_1 \quad Q=0 \text{ (SISTEMA ISOLATO)}$$

$$W = - \int_{V_1}^0 P_1 dV - \int_0^{V_2} P_2 dV = - (-P_1 V_1) - P_2 V_2 = - (P_2 V_2 - P_1 V_1)$$

$$\Delta H = H_2 - H_1 = 0 - (P_2 V_2 - P_1 V_1) + (P_2 V_2 - P_1 V_1) = 0$$

$$H_2 = H_1$$

LA QUANTITA' DI GAS ALL'INIZIO E' UGUALE ALLA QUELLA FINALE

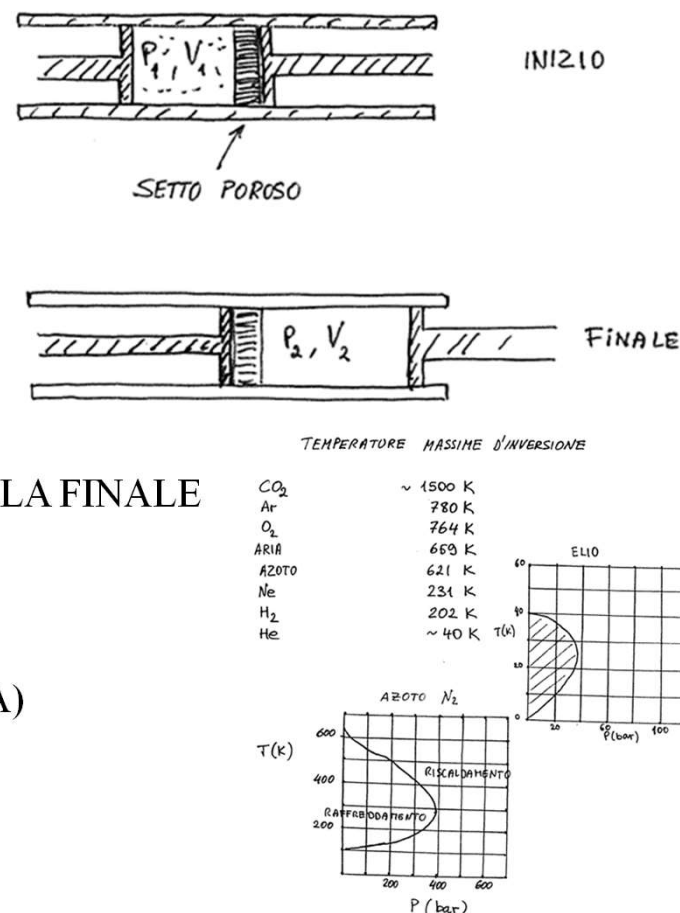
L'ENTALPIA INIZIALE E' UGUALE ALL'ENTALPIA FINALE:

TRASFORMAZIONE ISENTALPICA

ES: UNA VALVOLA PARZIALMENTE APERTA (O STROZZATA)

SI PUO' MANTENERE PER IL TEMPO VOLUTO,

AD ESEMPIO CON UNA POMPA AD ALTA PRESSIONE



SISTEMI APERTI ADIABATICI ($\Sigma Q=0$)

SI PUO' DIMOSTRARE CHE PER ESSI VALE:

$$\Delta H + \Delta u^2/g_c + \Delta z (g/g_c) = \Sigma Q + W_s$$

PER LA STESSA ALTEZZA z, $\Delta z (g/g_c)=0$

$$\Delta H + \Delta u^2/g_c = W_s$$

CASO a): UGELLO $W_s = 0$, $\rightarrow \Delta H = \Delta u^2/g_c$ (propulsione). Se la velocita' prodotta non e' usata per ricavare lavoro (oppure e' piccola), il processo e' isentalpico (throtteling).

CASO b): TURBINA $\Delta u^2/g_c = 0 \rightarrow \Delta H = W_s$ L'energia cinetica e' trascurabile, cosi' anche la sua differenza.

Se $\Delta Q = 0$ AND $\Delta S = 0 \rightarrow W_s = (\Delta H)_s$, e' il massimo shaft work (isentropic)

W_s (actual) = ΔH , l'efficienza e'
 $\eta = \Delta H / (\Delta H)_s$ expansion

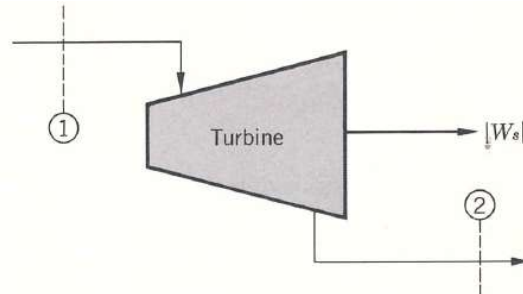


Fig. 10-11
Expansion in a turbine produces shaft work.

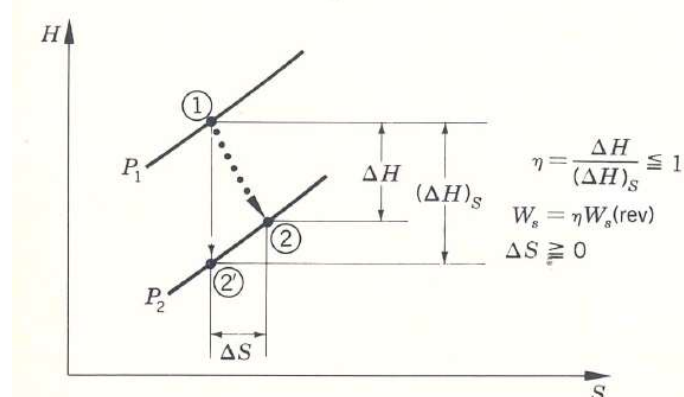


Fig. 10-12
Expansion processes.

SISTEMI APERTI ADIABATICI ($\Sigma Q=0$)

CASO c): COMPRESSORE $\Delta u^2/g_c = 0 \rightarrow \Delta H = W_s$

L'energia cinetica e' trascurabile, cosi' anche la sua differenza.

Se $\Delta Q = 0$ AND $\Delta S = 0 \rightarrow W_s = (\Delta H)_S$, e' il MINIMO shaft work (isentropic)

W_s (actual) = ΔH , l'efficienza e'

$$\eta = (\Delta H)_s / \Delta H$$

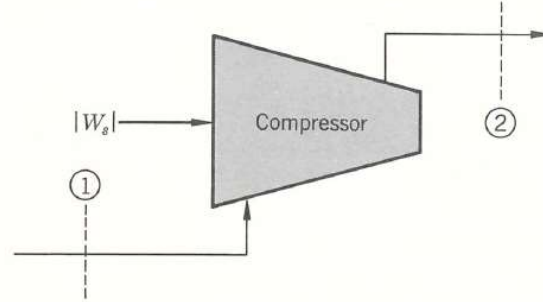


Fig. 10-13

Compression in a flow process as a result of shaft work.

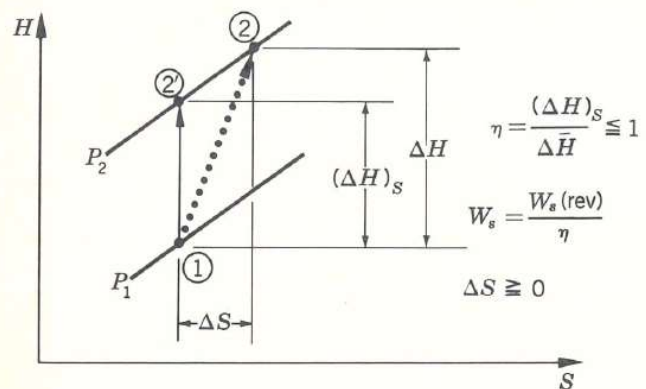


Fig. 10-14

Compression processes.

SISTEMI APERTI ADIABATICI

SI PUÒ DEMONSTRARE CHE PER ESSI VALE:

$$\Delta H + \frac{\Delta u^2}{2g_c} + \Delta z \left(\frac{g}{g_c} \right) = \sum Q + W_s$$

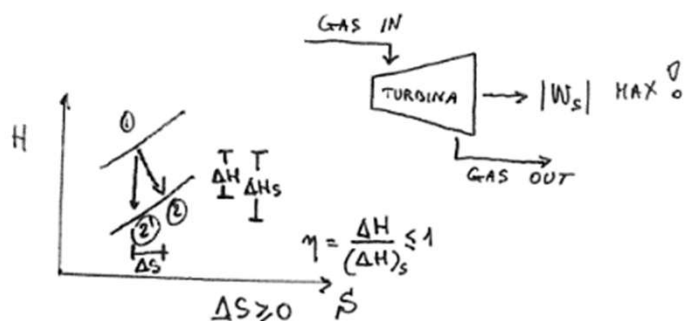
≈ 0 $\stackrel{<}{\approx} 0$

$$\Delta H + \frac{\Delta u^2}{2g_c} = W_s$$



a) UGELLO $W_s = 0 \Rightarrow \Delta H = \frac{\Delta u^2}{2g_c}$

b) TURBINA
(o COMPRESSORE) $\frac{\Delta u^2}{2g_c} = 0 \Rightarrow \Delta H = W_s$



A refrigerator ,must extract heat at low temperature and reject it at ambient temperature: this is achieved by doing work.

The most efficient refrigerator is the Carnot reversed cycle for which the work W done to the heat Q extracted at low temperature T_c for ambient temperature T₀ is

$W/Q = T_0/T_c - 1$, known as *figure of merit* always >1. (the inverse of *COP, coefficient of performance*)

Or $W = Q (T_0/T_c - 1)$.

For constant temperature is as follows:

Table 13.1
Ideal Refrigerator Performance at Some Common Cryogenic Temperatures (T_c) with an Ambient Temperature of 300 K

T_c (K)	120	77	20	4.2	1
W/Q	1.5	2.9	14	70	299

In reality if the gas is used as coolant the ideal work can be assumed as the sum of a series of Carnot refrigerators working between T_h and T_L. If $Q = C_p dT$ gives

$$W = \int_{T_L}^{T_H} C_p \left(\frac{T_0}{T} - 1 \right) dT$$

Liquefaction as the sum of the work to cool it from 300 K to boiling point plus the work to liquefy it. The last work to liquefy it is $W = Q (T_0 / T_c - 1) = W = \lambda (T_0 / T_c - 1)$, λ is the latent heat.

$$W_r = \int_{T_s}^{T_0} Cp \left(\frac{T_0}{T} - 1 \right) dT + \lambda \left(\frac{T_0}{T} - 1 \right) = T_0 \int_{T_s}^{T_0} Cp \frac{dT}{T} + T_0 \frac{\lambda}{T_s} - [\int_{T_s}^{T_0} Cp dT - \lambda] = \\ T_0 \left[\int_{T_s}^{T_0} \frac{CpdT}{T} + \frac{\lambda}{T_s} \right] - [\int_{T_s}^{T_0} Cp dT - \lambda] = T_0 [S_0 - S_L] - [h_0 - h_L];$$

$$\text{Exergy} = [h_0 - h_L] - T_0 [S_0 - S_L] = dh - T_0 ds, \text{ availability}$$

$$\text{For helium: } [h_0 - h_L] = 1.57 \cdot 10^6 - 9.59 \cdot 10^3 = \mathbf{1560 \text{ kJ/kg}} = \Delta h$$

$$T_0 [S_0 - S_L] = 300 [3.14 \cdot 10^4 - 8.6 \cdot 10^3] = \mathbf{6840 \text{ kJ/kg}} \text{ (cooling)}$$

$$W = Q [T_0/T_c - 1] = \lambda [T_0/T_c - 1] = 20.9 [300/4.2 - 1] = \mathbf{1472 \text{ kJ/kg}} \text{ (condensation)}$$

Table 13.2
Minimum Work of Liquefaction

Gas	Δh (kJ/kg)			Minimum work (kJ/kg)		
	Cooling	Condensation	Total	Cooling	Condensation	Total
Nitrogen	224	199	423	197	580	777
Hydrogen	3413	434	3847	6100	6090	12190
Helium	1509	21	1530	6900	1488	8389

6840 J/g+1472 J/g-1560 J/g=6752 J/g
i.e. for 1 g/s we need 6752 W

Inversion temperature

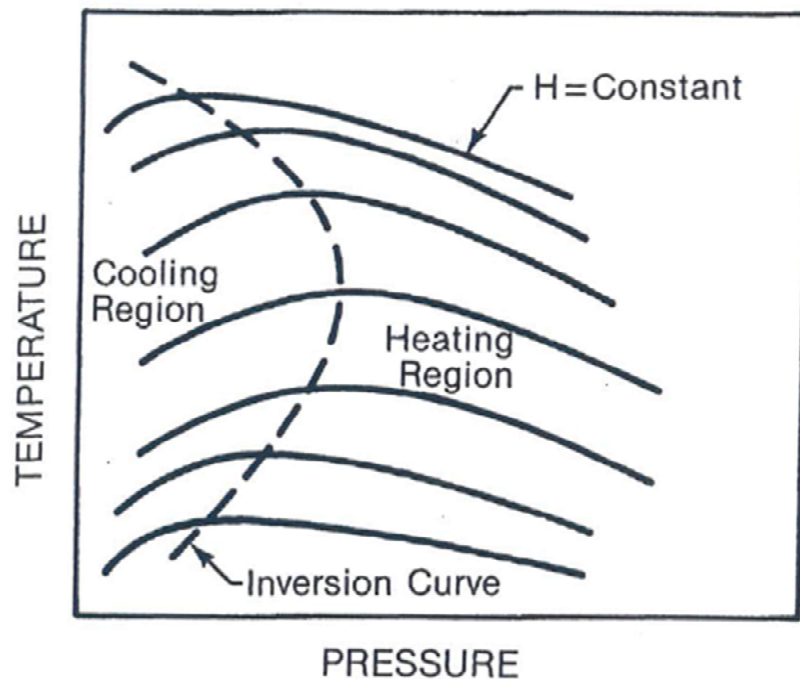


FIGURE 2.8 Joule–Thomson inversion curve.

$$\mu = \left(\frac{\partial T}{\partial P} \right)_H$$

TABLE 2.4 Maximum Inversion Temperature

Fluid	Maximum inversion temperature	
	K	°R
Oxygen	761	1370
Argon	722	1300
Nitrogen	622	1120
Air	603	1085
Neon	250	450
Hydrogen	202	364
Helium	40	72

1

Table 10
Maximum values of Joule-Thomson inversion temperature

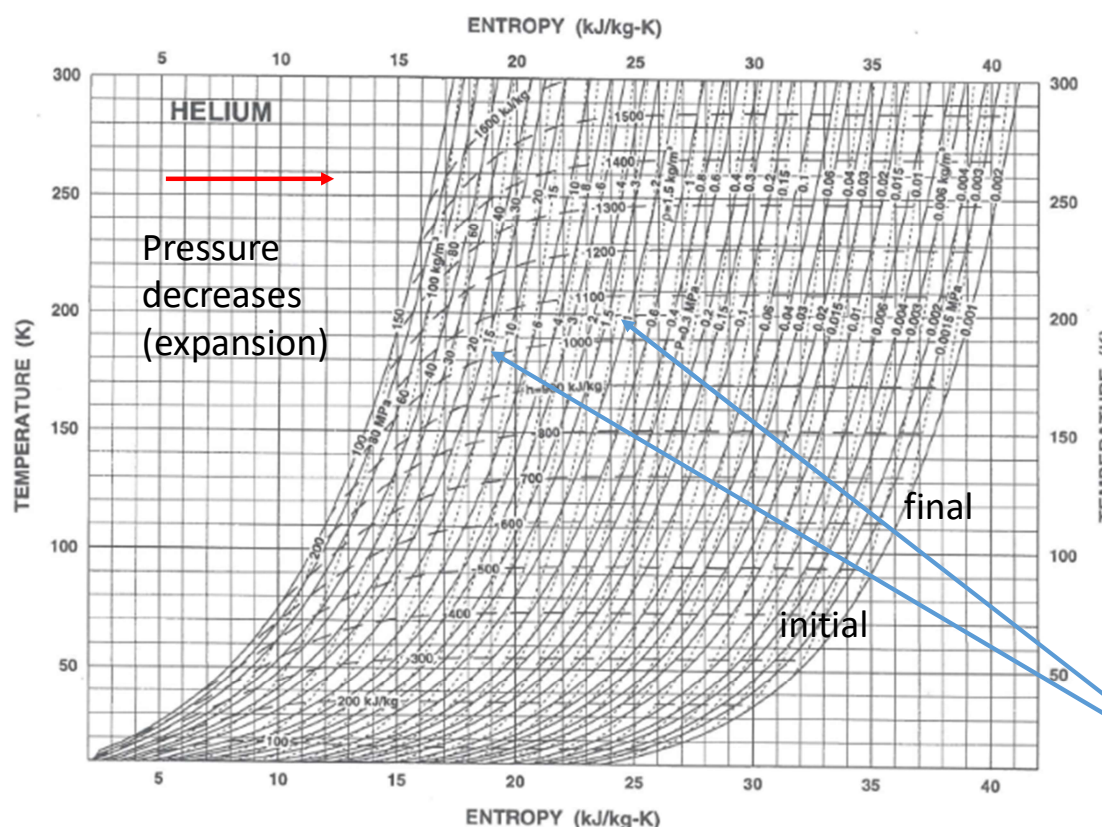
Cryogen	Maximum inversion temperature [K]
Helium	43
Hydrogen	202
Neon	260
Air	603
Nitrogen	623
Oxygen	761

The fluid used, gaseous at normal temperature, has to be liquefied. If the J-T method is used, it must be taken below its inversion temperature.

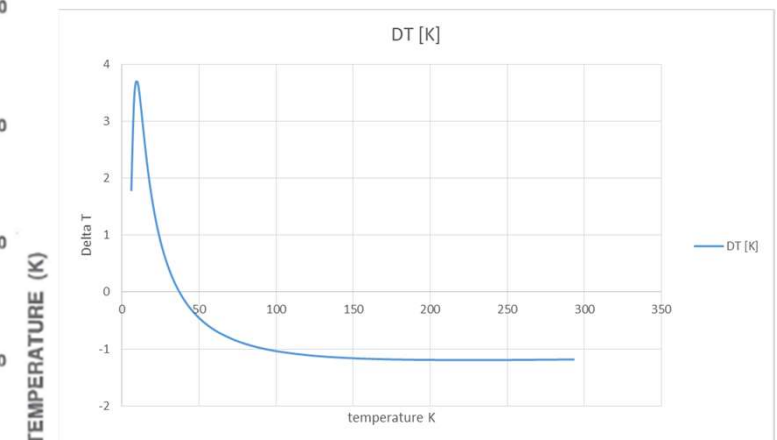
$$\mu = \left(\frac{\partial T}{\partial P} \right)_H$$

TABLE 2.4 Maximum Inversion Temperature

Fluid	Maximum inversion temperature	
	K	°R
Oxygen	761	1370
Argon	722	1300
Nitrogen	622	1120
Air	603	1085
Neon	250	450
Hydrogen	202	364
Helium	40	72

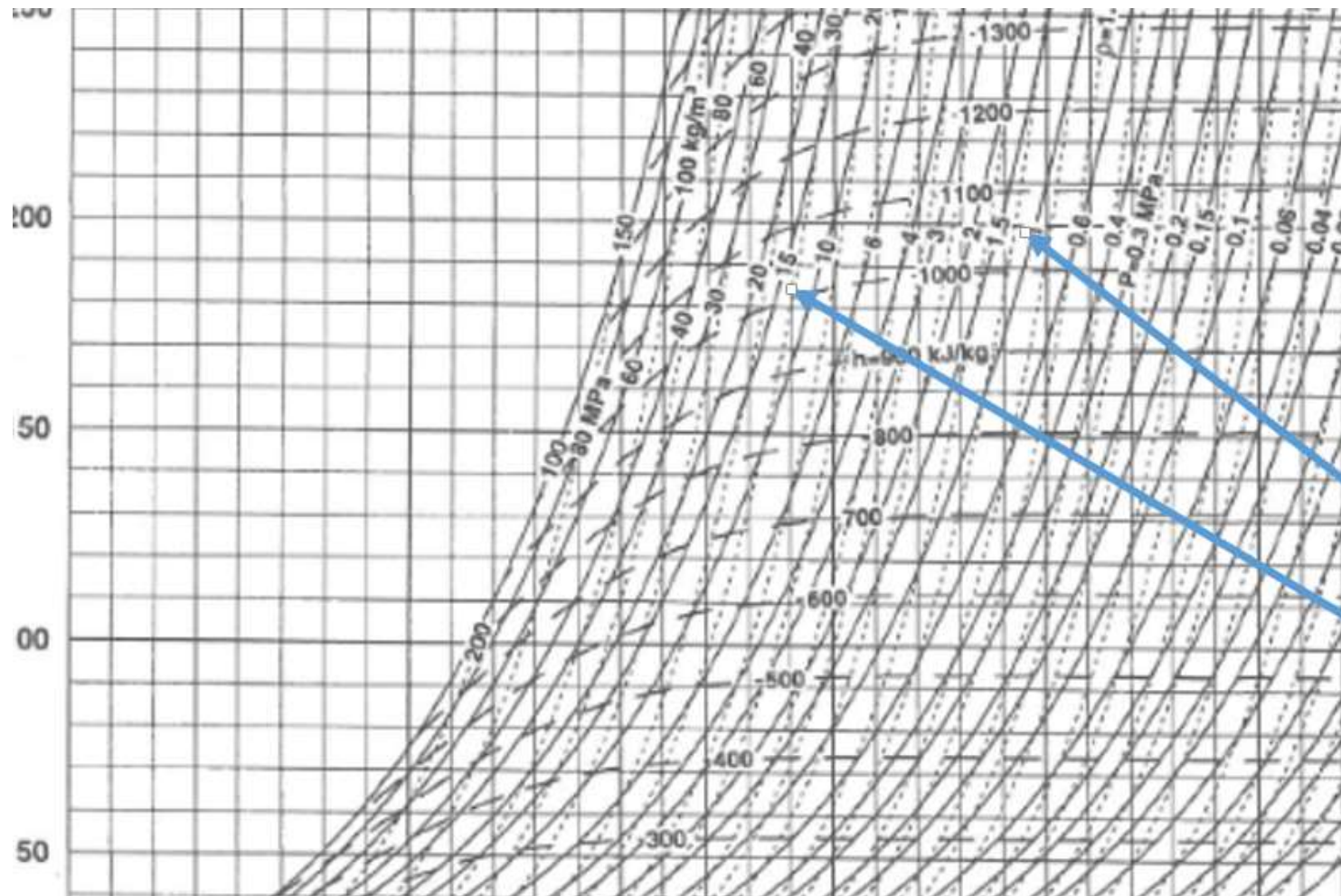


Inversion temperature



$\Delta T = T_i - T_f < 0$: The temperature increases for the same Enthalpy (isenthalpic transformation)

Inversion temperature



Inversion temperature

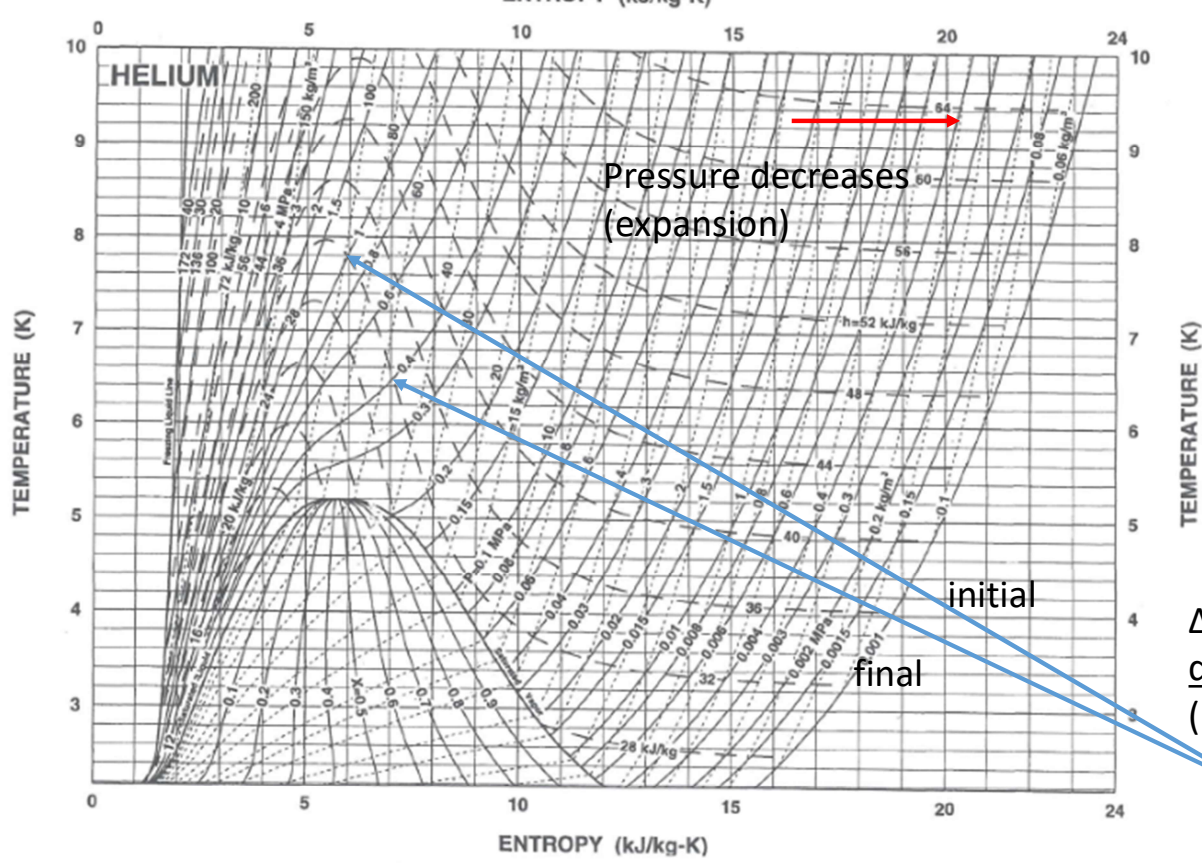
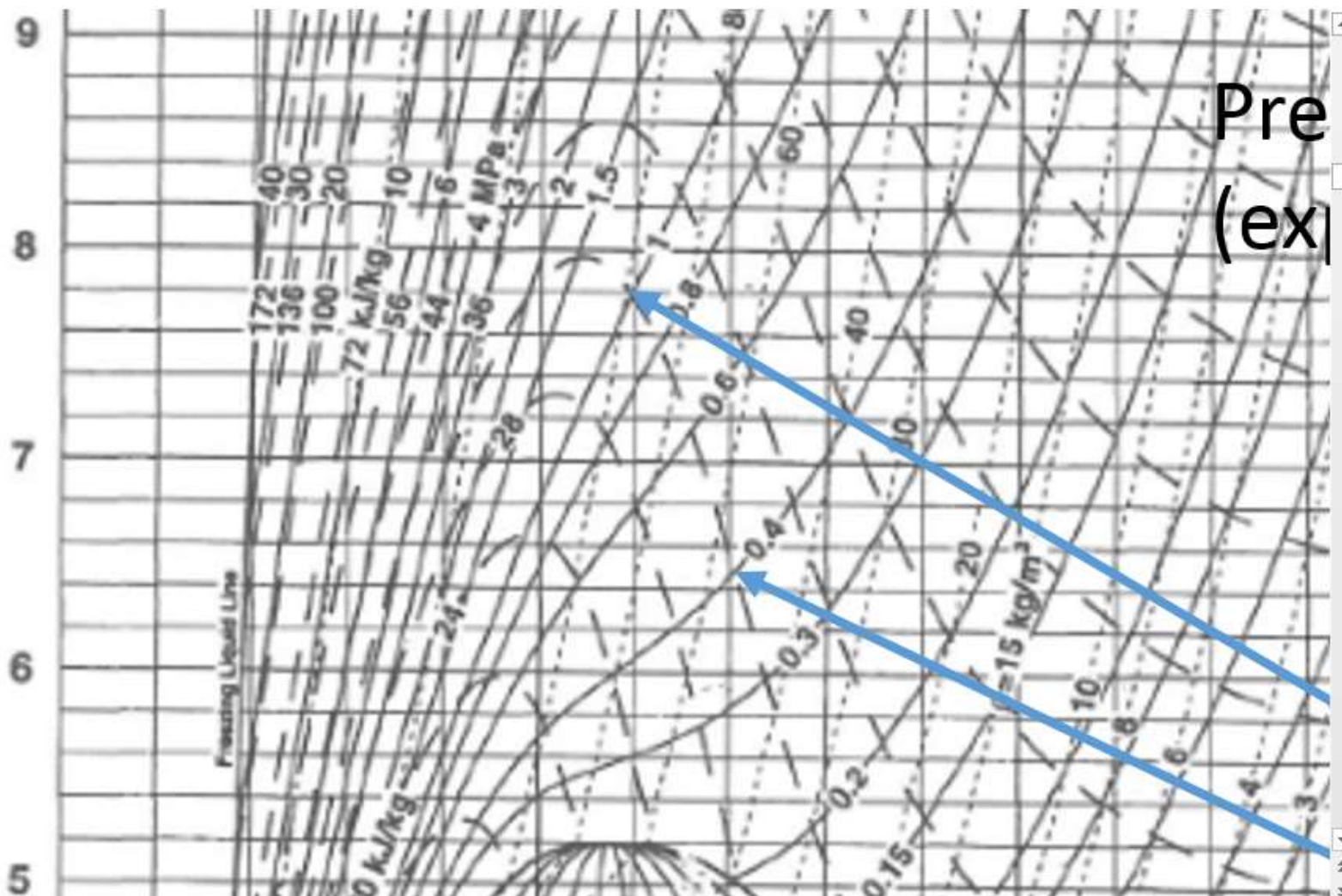


Fig. 5.15. $T-S$ diagram for helium ($T = 2-10$ K)

$\Delta T = T_i - T_f > 0$: The temperature decreases for the same Enthalpy (isenthalpic transformation)



Gas liquefaction by the Joule-Thomson Effect

The condensation (liquefaction) of a gas is due to the high intermolecular forces. At temperatures slightly above the condensation temperature the forces are so strong that the work against them during expansion causes significant cooling of the gas and the partially condenses: the process is Joule Thomson liquefaction.

In practice a real gas at high pressure is forced through a needle valve (or a nozzle) from where it exits at a lower pressure and a lower temperature. In the picture aside the work is given by P_2V_2 (recovered from the gas) – P_1V_1 (done on the gas) = $W=0$. The enthalpy is the same since $W=0$.

$H_1 = H_2$: isenthalpic expansion

Note: for an ideal gas $H = 5/2 \cdot N \cdot T$ then $T_1 = T_2$, there is no cooling!

In real gases a small temperature change occurs because the internal of work done by the molecules during expansion. The sign of the change in temperature depends on the initial temperature. All gases have an inversion temperature, below which the JT expansion cools.

Note: For a real gas the Enthalpy is:

$$H = 5/2 \cdot N \cdot T + (N^2/V) \cdot (bT - 2a) \text{ and } b > 0, a > 0$$

$$T_{inv} = 2a/b = 27/4 \cdot T_c$$

For Helium theoretically T_{inv} would be $27/4 \cdot 5.2 = 35.1 \text{ K}$

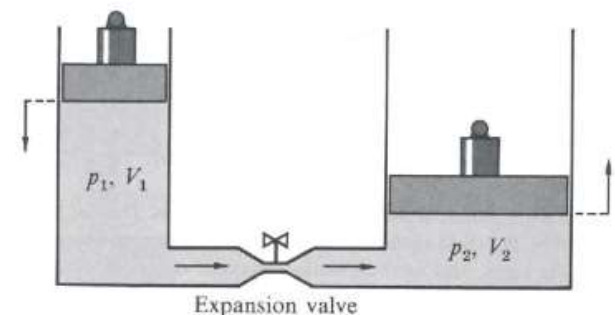


Figure 12.2 The Joule-Thomson effect. A gas is pushed through an expansion valve. If the gas is nonideal, there will be a temperature change during the expansion because of work done against the intermolecular forces. If the temperature is initially below a certain inversion temperature, τ_{inv} , the gas will cool on Joule-Thomson expansion.

Gas liquefaction by the Joule-Thomson Effect

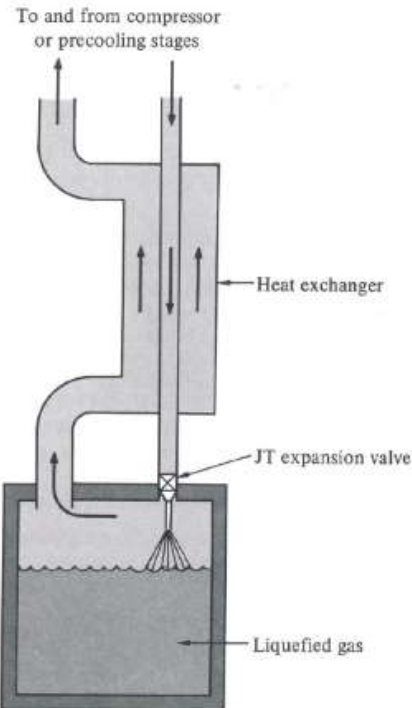


Figure 12.3 The Linde cycle. Gas is liquefied by combining Joule-Thomson expansion with a counterflow heat exchanger.

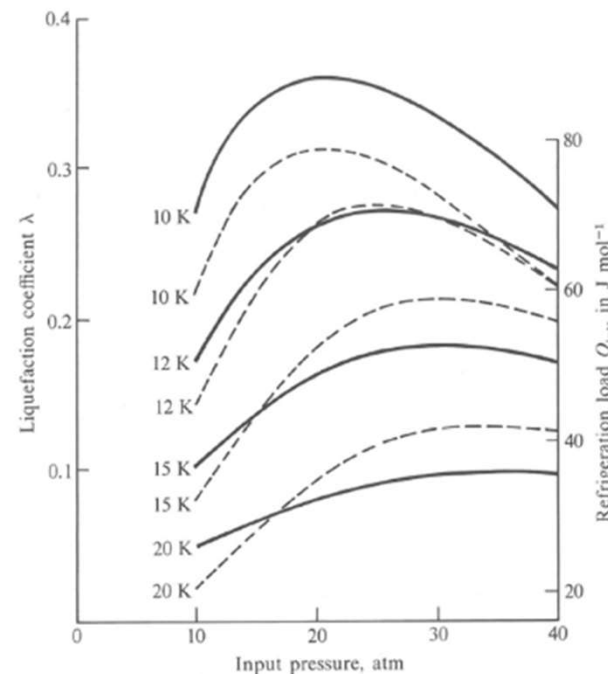


Figure 12.4 Performance of helium liquefiers operating by the Linde cycle, as a function of the input pressure, for an output pressure of 1 atm and for various values of the input temperature. The solid curves give the liquefaction coefficient. The broken curves give $Q_{int} = H_{out} - H_{in}$, the internal refrigeration load available at 4.2 K if the load is placed inside the liquefier and the still cold helium gas boiled off by the load is returned through the heat exchanger rather than boiled off into the atmosphere. See Problem 3. After A. J. Croft in *Advanced cryogenics* (C. A. Bailey, ed.), Plenum, 1971, p. 187.

Gas liquefaction by the Joule-Thomson Effect

The combination heat exchanger-expansion valve is a constant enthalpy arrangement. Let one mole of gas enter the combination; suppose that the fraction λ is liquefied. Constant enthalpy requires that

$$H_{in} = \lambda H_{liq} + (1 - \lambda)H_{out}. \quad (6)$$

Here $H_{in} = H(T_{in}, p_{in})$ and $H_{out} = H(T_{in}, p_{out})$ are the enthalpies per mole of gas at the input and output pressures, both at the common upper temperature of the heat exchanger. H_{liq} is the enthalpy per mole of liquid at its boiling temperature under the pressure p_{out} . From (6) we obtain the fraction

$$\lambda = \frac{H_{out} - H_{in}}{H_{out} - H_{liq}}, \quad (7)$$

called the liquefaction coefficient.

Liquefaction takes place when $H_{out} > H_{in}$; that is, when

$$H(T_{in}, p_{out}) > H(T_{in}, p_{in}). \quad (8)$$

Only the enthalpies at the input temperature of the heat exchanger matter. If the Joule-Thomson expansion at this temperature cools the gas, liquefaction will take place.

The three enthalpies in (7) are known experimentally. Figure 12.4 shows the liquefaction coefficient calculated from them for helium. The liquefaction coefficient drops rapidly with increasing T_{in} , because of the decrease of the numerator in (7) and the increase of the denominator. To obtain useful liquefaction, say $\lambda > 0.1$, input temperatures below one-third of the inversion temperature are usually required. For many gases this requires precooling of the gas by an expansion engine. The combination of an expansion engine and a Linde cycle is called a **Claude cycle**. The expansion engine is invariably preceded by another heat exchanger, as in Figure 12.1.

Ref.:C.Kittel, Thermal Physics, New York,
1980

Cooling by external work

Isentropic transformation: for a monoatomic gas $T_1^{3/2} \cdot V_1 = T_2^{3/2} \cdot V_2$ or since $PV=NT$ it results : $T_1^{5/2}/P_1 = T_2^{5/2}/P_2$ and $T_2 = T_1 \cdot (P_2/P_1)^{2/5}$.

Suppose $P_1=31$ bar, $P_2=1$ bar and $T_1=300$ K it follows that $T_2=75$ K. For Helium the above equation is a very good approximation if the cooling is reversible.

In practice, since in real processes friction is present (no perfect lubricants exist), all real transformations are irreversible and the expansion cooling instead follows the scheme shown aside.

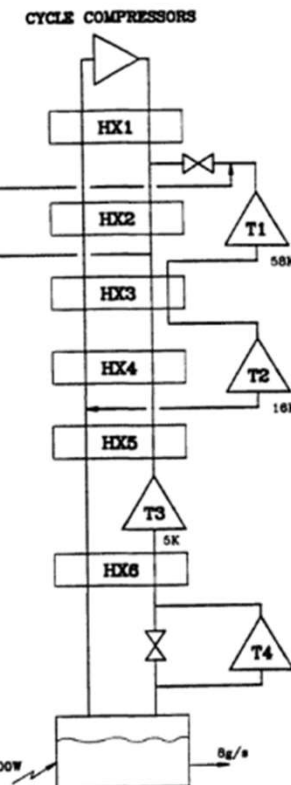
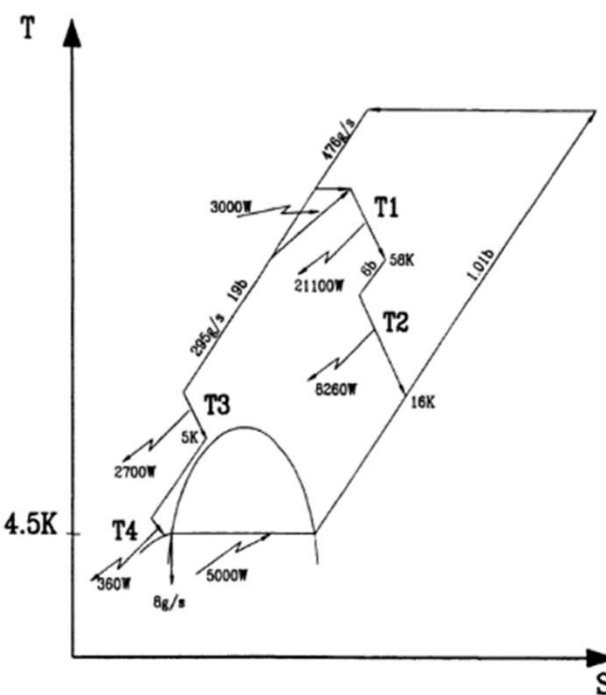


Figure 1. The 6 kW cycle.

Cooling by external work

- Gas is compressed at or above room temperature (ca. 80 C) and the heat is ejected in the atmosphere (air and/or water).
- The gas enters the expansion engine (gas bearing turbine) after a counterflow heat exchanger HX where it is cooled, i.e. It exits at a lower pressure and lower temperature. It enters the working volume (sample) which is cooled.
- Then it enters at low pressure the HX which further cools the gas that enters the expansion turbine. And so on.

The work extracted by the turbine is the enthalpy difference ΔH between the input and the output gas.

$$W = (U_1 + P_1 V_1) - (U_2 + P_2 V_2) = H_1 - H_2 = \Delta H$$

- The process described above continues to reach a temperature close to the liquefaction temperature. It is not possible to introduce a mixture of gas and liquid into the turbine (an exception is for the *wet reciprocating expander*, old fashion), which would produce instability/damage.
- The final stage of liquefaction is achieved by means of *Joule-Thomson effect*, or JT expansion valve.

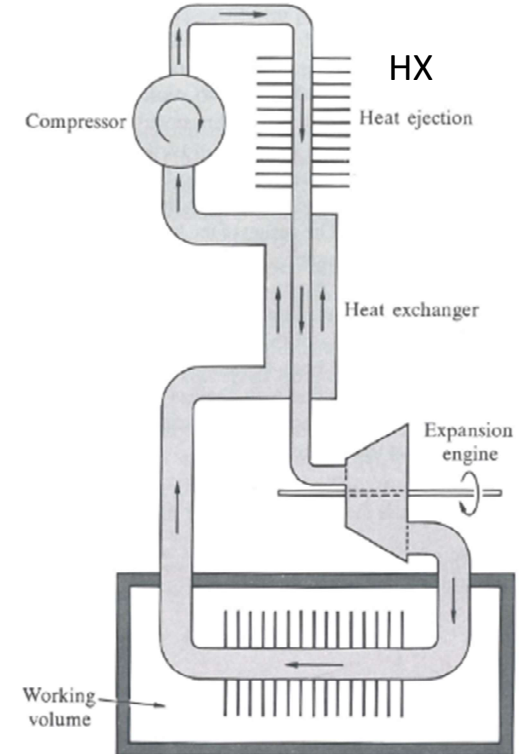
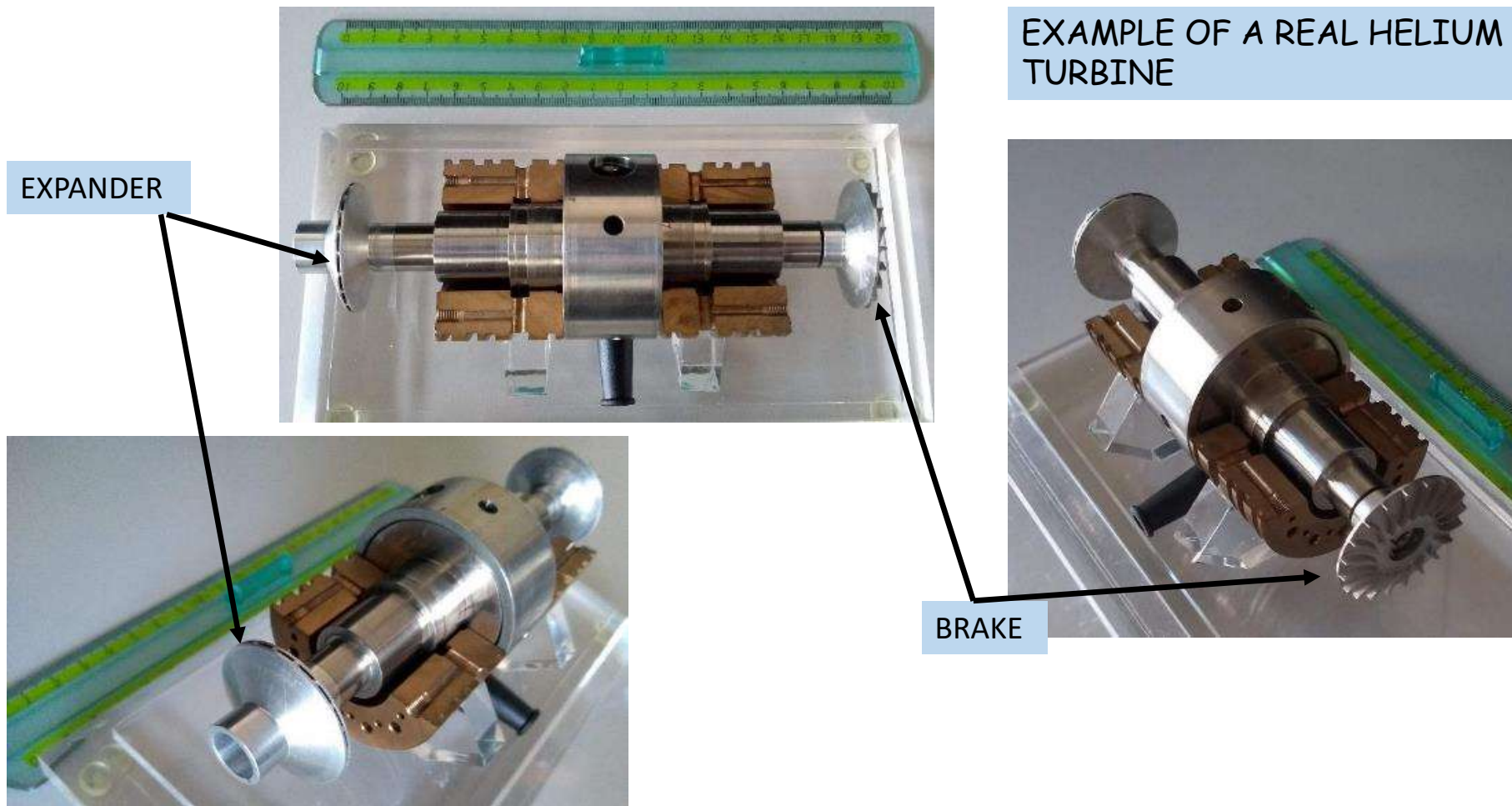


Figure 12.1 Simple expansion refrigerator. A working gas is compressed; the heat of compression is ejected into the environment. The compressed room temperature gas is precooled further in the counterflow heat exchanger. It then does work in an expansion engine, where it cools to a temperature below that of the working volume. After extracting heat from the working volume, the gas returns to the compressor via the heat exchanger.

Cooling by external work



Cooling by external work: The compressor

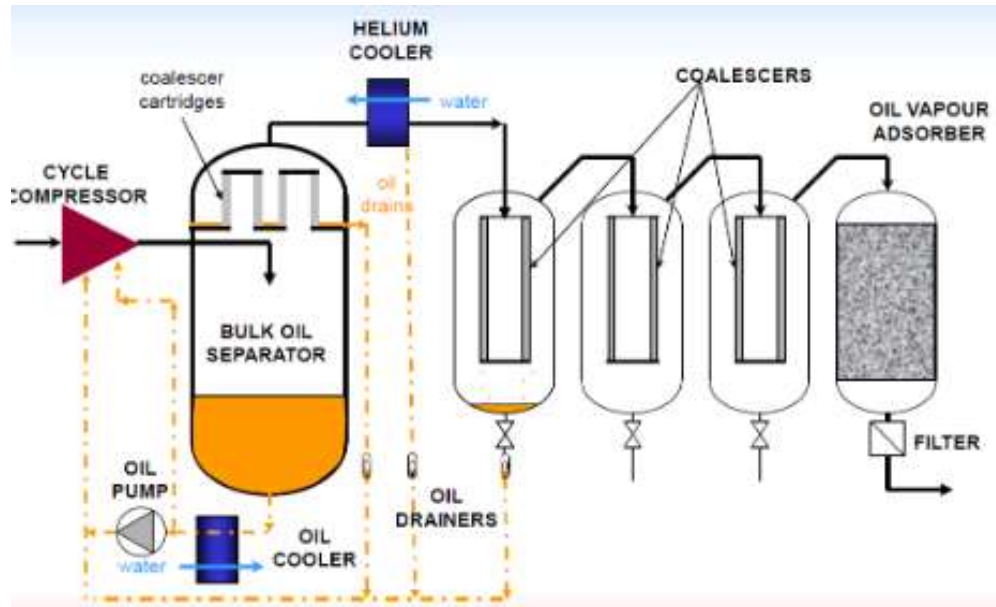
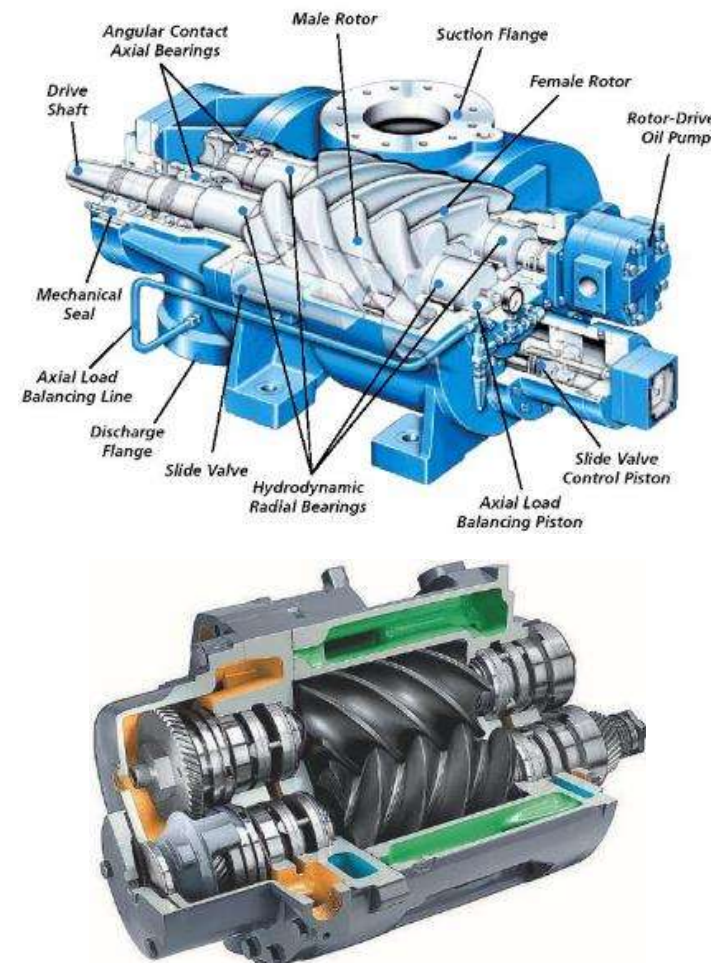
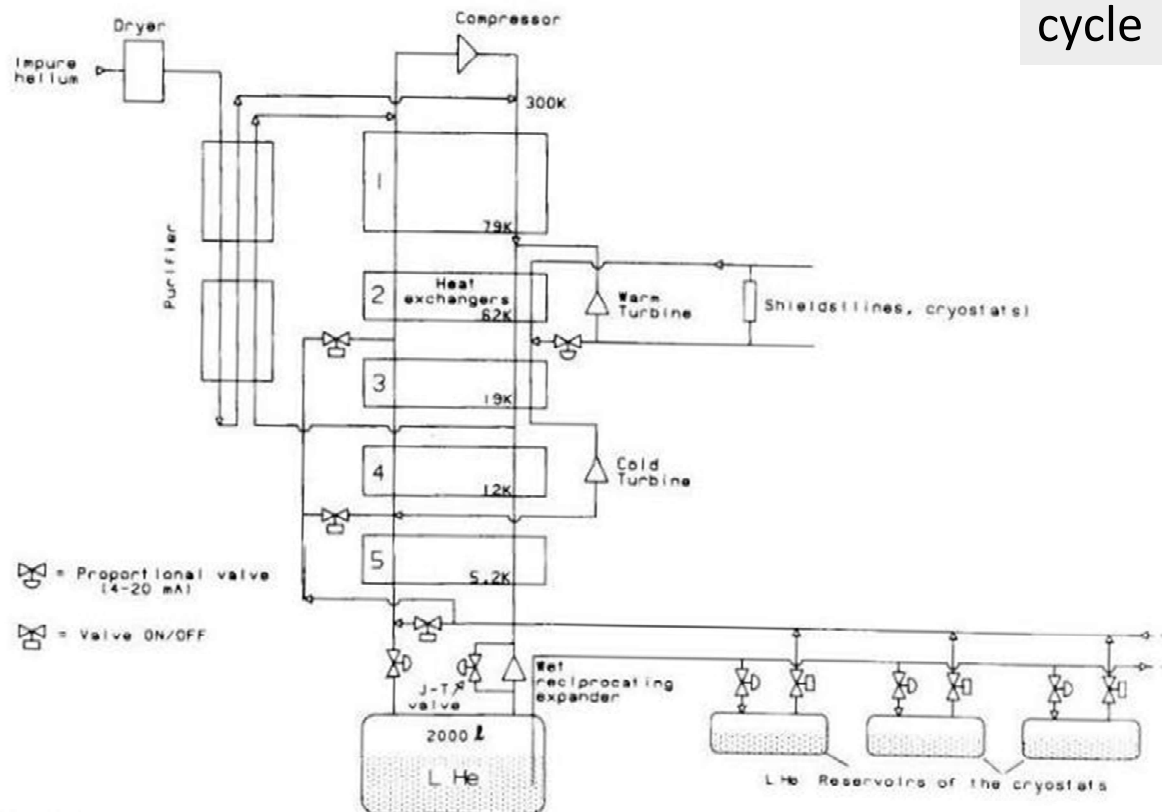


Figure 6: LHC Oil Removal System [2]

Gas liquefaction by the Joule-Thomson Effect plus preliminary work extraction: the Claude cycle

R. Pengo et al. / Cryogenics of the ALPI linac

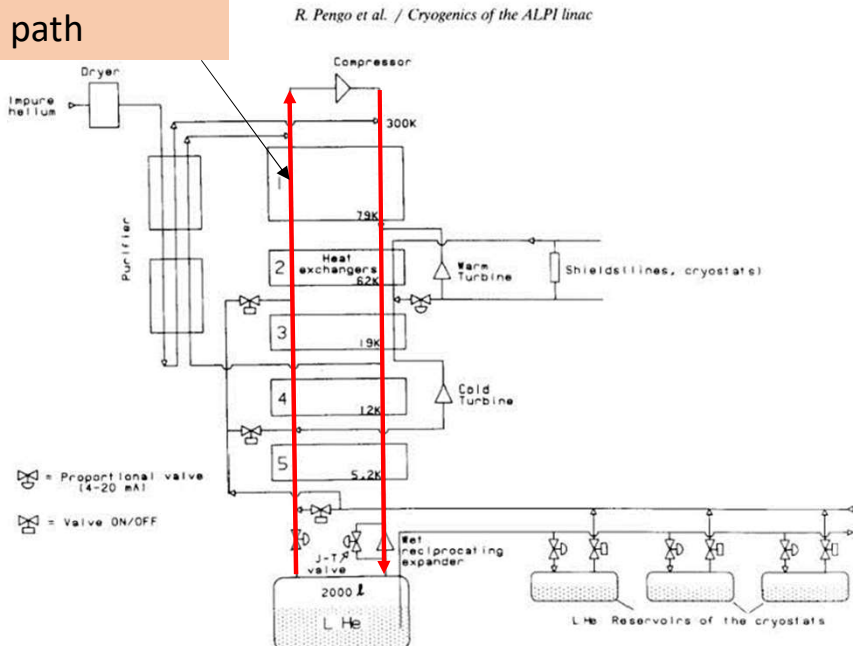


Claude cycle: ALPI superconducting Linac accelerator, INFN-LNL

Fig. 7. Schematic drawing (courtesy of L'Air Liquide) of the helium cycle. The gas compressed at 16 bar absolute is expanded in two turbines and passes through five heat exchangers. The liquefaction of helium is performed by means of a Joule-Thomson and/or a reciprocating wet expander. Gaseous helium at 7 bar absolute and 60 K can be used for the shields of the transfer lines and of the cryostats, where liquid nitrogen is not used.

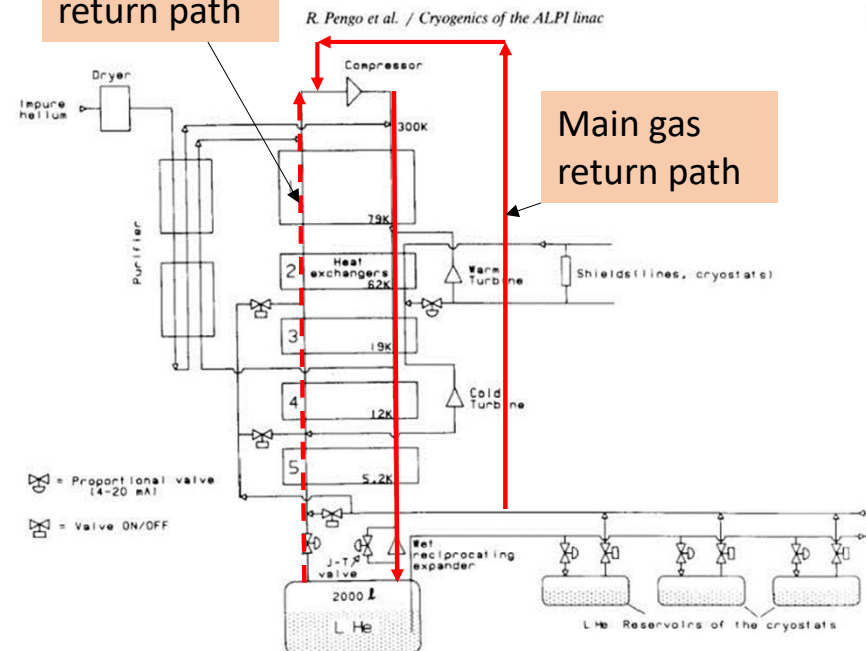
Refrigerator vs Liquefier

Total return path



Refrigerator

Minor gas return path



Liquefier

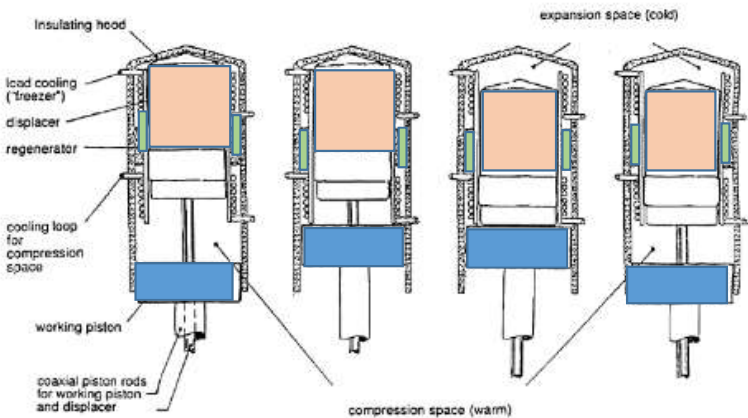
Refrigerator vs Liquefier

Question: what is the refrigeration power @ 4.3 K of 1 g/s helium liquefaction?

VERY HIGH VALUE!!

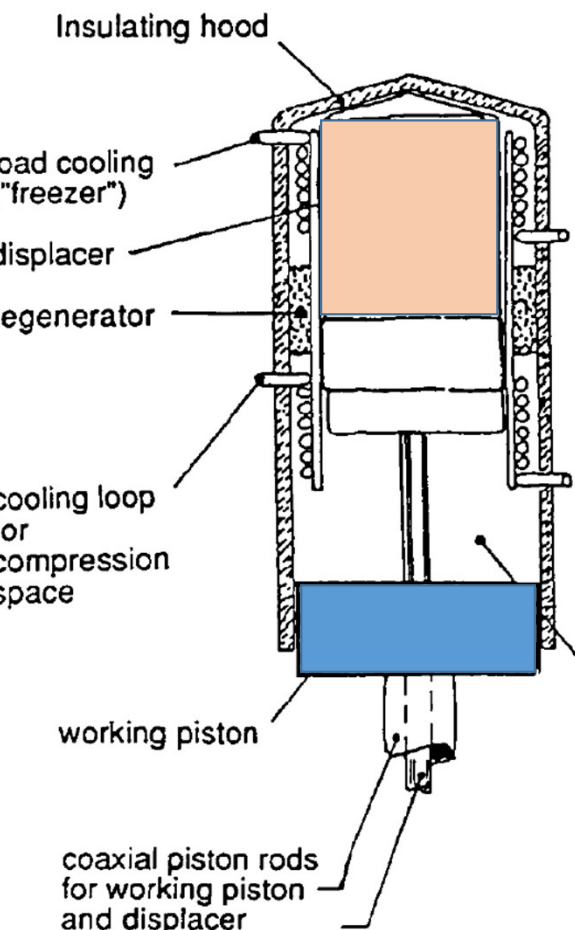
Other types of refrigerator: the Stirling cycle

Working principle of the Stirling engine ↓

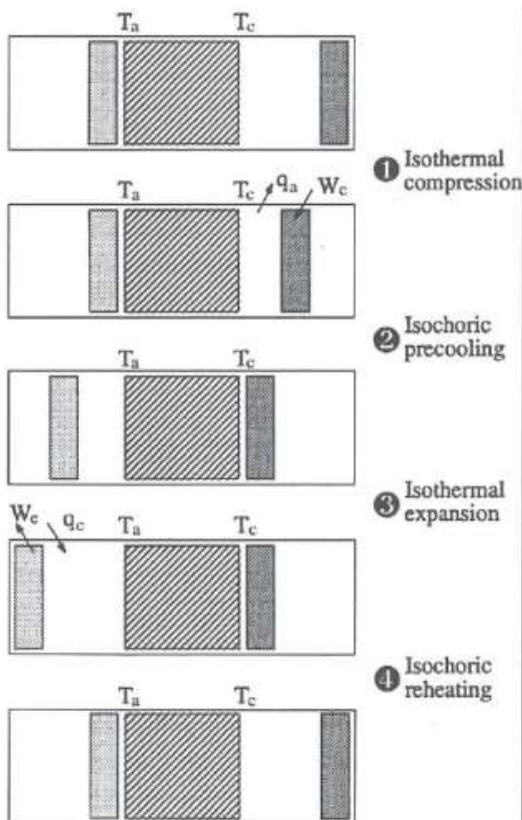


Operational phases of the Stirling cycle

Phase	Working piston position	Displacer position	Gas mainly located in
1	down	up	compression space
1→2			compression
2	up	up	compression space
2→3			gas displacement warm → cold
3	up	down	expansion space
2→4			expansion
4	down	down	expansion space
4→1			gas displacement cold → warm
1	down	up	compression space
...			...



Other types of refrigerator: the Stirling cycle



- Phase (1)—Isothermal Compression: The expansion piston is kept close to the regenerator. The compression piston is moved to compress the gas isothermally in the compression volume. The compression work w_c is transmitted to the gas, and heat q_a is rejected at ambient temperature.
- Phase (2)—Isochoric Precooling: Both pistons are now moved simultaneously to transfer the compressed gas at constant volume through the regenerator from the compression volume to the expansion volume. The gas is cooled from the ambient temperature to the cooling temperature, transferring heat to the regenerator matrix.
- Phase (3)—Isothermal Expansion: The compression piston is kept close to the regenerator. The expansion piston is moved to expand the gas in the expansion volume. The expansion work w_e is extracted from the gas. The cooling effect q_c theoretically assumed to occur at constant temperature can be used for refrigeration.
- Phase (4)—Isochoric Reheating: Both pistons are now moved simultaneously to transfer the expanded gas at constant volume through the regenerator from the expansion volume back to the compression volume. The gas is heated from the cooling temperature to the ambient temperature. The heat transferred from the regenerator matrix to the gas theoretically equals the heat previously transferred from the gas to the regenerator.

Figure 7-4 Schematic operation of a Stirling cooler.

Other types of refrigerator: the Stirling cycle

- Phase (1)—Isothermal Compression: The expansion piston is kept close to the regenerator. The compression piston is moved to compress the gas isothermally in the compression volume. The compression work w_c is transmitted to the gas, and heat q_a is rejected at ambient temperature.
- Phase (2)—Isochoric Precooling: Both pistons are now moved simultaneously to transfer the compressed gas at constant volume through the regenerator from the compression volume to the expansion volume. The gas is cooled from the ambient temperature to the cooling temperature, transferring heat to the regenerator matrix.
- Phase (3)—Isothermal Expansion: The compression piston is kept close to the regenerator. The expansion piston is moved to expand the gas in the expansion volume. The expansion work w_e is extracted from the gas. The cooling effect q_c theoretically assumed to occur at constant temperature can be used for refrigeration.
- Phase (4)—Isochoric Reheating: Both pistons are now moved simultaneously to transfer the expanded gas at constant volume through the regenerator from the expansion volume back to the compression volume. The gas is heated from the cooling temperature to the ambient temperature. The heat transferred from the regenerator matrix to the gas theoretically equals the heat previously transferred from the gas to the regenerator.

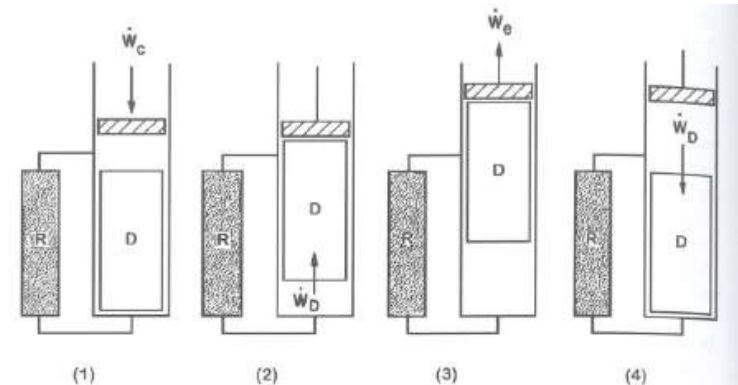


Fig. 8.21 Stirling cycle refrigerator

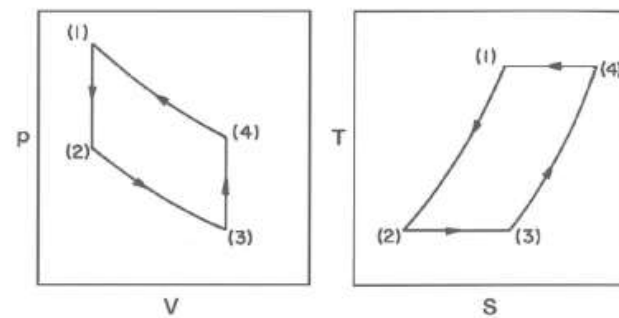


Fig. 8.22 p - V and T - S diagrams for Stirling cycle

Figure 7-4 Schematic operation of a Stirling cooler.

Other types of refrigerator: the Stirling cycle

Example 8.4

Calculate the performance of a Stirling cycle refrigerator is to operate between 100 and 300 K with an inlet pressure of 0.1 MPa and compressor output at 2 MPa. This can be compared to the Reverse Brayton cycle refrigerator discussed above.

Since these temperatures and pressures are far above the critical point for helium, it is fair to approximate the helium gas as an ideal gas for the present calculations. Since steps (1)–(2) and (3)–(4) are isochoric, we can use the ideal gas law to calculate p_2 and p_4 .

$$p_1 = 2 \text{ MPa}; p_2 = p_1(T_2/T_1) = 0.67 \text{ MPa}; p_3 = 0.1 \text{ MPa}; \\ p_4 = p_3(T_4/T_3) = 0.3 \text{ MPa}$$

Then the isothermal heat removal rate at low temperature is,

$$\frac{Q_c}{m} = \frac{R}{M} T_c \ln \frac{p_2}{p_3} = 2.08 \text{ kJ/kg K} \times 100 \text{ K} \times \ln(0.67/0.1) = 395 \text{ kJ/kg}$$

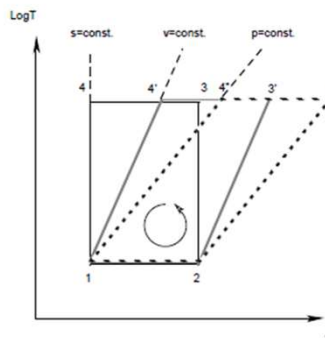


Fig. 5 Carnot cycle (1,2,3,4), Stirling cycle (1,2,3',4') and Ericsson cycle (1,2,3'',4'').

Example 8.4 (continued)

And the heat rejected into the high temperature reservoir is,

$$\frac{Q_h}{m} = \frac{R}{M} T_h \ln \frac{p_4}{p_1} = 2.08 \text{ kJ/kg K} \times 300 \text{ K} \times \ln(0.33/2) = -1184 \text{ kJ/kg}$$

Thus, the coefficient of performance for this cycle is,

$$COP = \frac{Q_c}{Q_h - Q_c} = \frac{395}{1184 - 395} = 0.5 = \frac{T_c}{T_h - T_c}$$

Note that this is the same *COP* as for a Carnot cycle. Although the Stirling cycle has theoretically the same *COP* as the Carnot cycle, there is an important difference. Since the Stirling cycle has two isochoric processes, heat is stored (or recovered) at constant volume during those stages of the cycle. Thus, the Stirling cycle moves more heat for the same cooling power, which can result in further inefficiencies in its practical application. On the other hand, as a Stirling cycle refrigerator does not require such high compression ratios as Carnot it provides a more practical approach for applications.

Other types of refrigerator: the Stirling cycle

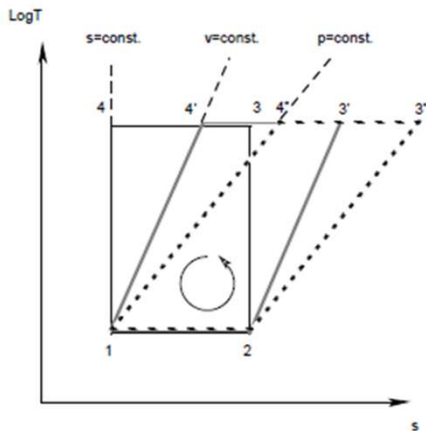


Fig. 5 Carnot cycle (1,2,3,4), Stirling cycle (1,2,3',4') and Ericsson cycle (1,2,3'',4'').

Example 8.4 (continued)

And the heat rejected into the high temperature reservoir is,

$$\frac{Q_h}{m} = \frac{R}{M} T_h \ln \frac{P_4}{P_1} = 2.08 \text{ kJ/kg K} \times 300 \text{ K} \times \ln(0.33/2) = -1184 \text{ kJ/kg}$$

Thus, the coefficient of performance for this cycle is,

$$COP = \frac{Q_c}{Q_h - Q_c} = \frac{395}{1184 - 395} = 0.5 = \frac{T_c}{T_h - T_c}$$

Note that this is the same *COP* as for a Carnot cycle. Although the Stirling cycle has theoretically the same *COP* as the Carnot cycle, there is an important difference. Since the Stirling cycle has two isochoric processes, heat is stored (or recovered) at constant volume during those stages of the cycle. Thus, the Stirling cycle moves more heat for the same cooling power, which can result in further inefficiencies in its practical application. On the other hand, as a Stirling cycle refrigerator does not require such high compression ratios as Carnot it provides a more practical approach for applications.

Other types of refrigerator: the Gifford-McMahon cycle

Fig. 8.23: Gifford-McMahon cycle

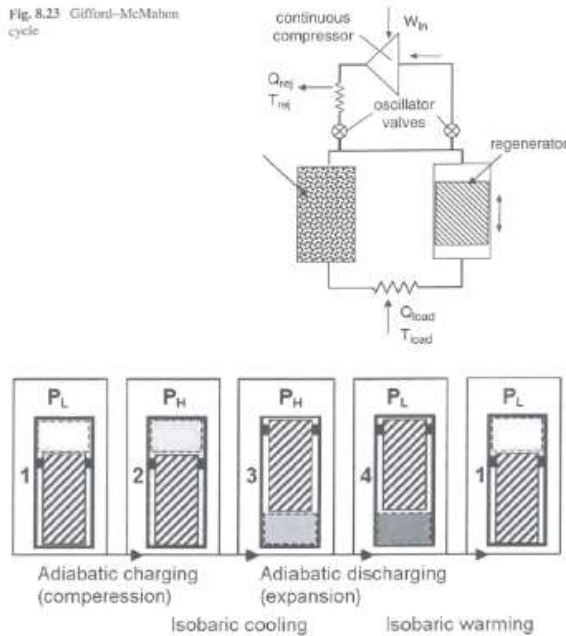


Fig. 8.24: Cycle description for the GM refrigerator

The Gifford–McMahon cycle was originally proposed in the early 1960s as a regenerative cycle that could potentially reach the helium temperature range [14, 15]. The GM cycle is similar to the Stirling cycle except that the oscillatory flow is achieved by cycling valves that select where the flow distributes in the cycle, see Fig. 8.23.

The GM cycle description is shown in Fig. 8.24. At the beginning of the first stage of the cycle, the displacer is at its lowest position with the outlet (return) valve closed. The inlet (high pressure) valve is opened to allow high pressure helium gas to fill the regenerator and space above the displacer at room temperature. Then, with the inlet valve still open, the displacer is moved to its upper position. The high pressure gas passes through the regenerator and is cooled isobarically by the matrix. Cold gas then fills the space below the displacer. Next, with the displacer at its

upper position, the inlet valve is closed and the outlet valve is opened. The gas in the regenerator and cold space below the displacer undergoes expansion, which produces the refrigeration. Finally, with the outlet valve still open, the displacer moves back to the lowest position. The low pressure cold gas is warmed isobarically by the matrix refilling the space above the displacer at room temperature completing the cycle.

Thermodynamically, the GM cycle is slightly more complex than the Stirling cycle. The cooling and warming processes are isobaric while the compression and expansion processes are isothermal. However, neither the compression nor expansion processes involve a constant mass since there is flow into and out of the system through the valves. The significant pressure drop occurring at the valves reduces the overall thermodynamic efficiency of the GM cycle compared with that of the Stirling cycle.

Such machines require about 7 kW of compressor power therefore operating at about 10% of Carnot efficiency.

Other types of refrigerator: the Gifford-McMahon cycle

Fig. 8.23 Gifford-McMahon cycle

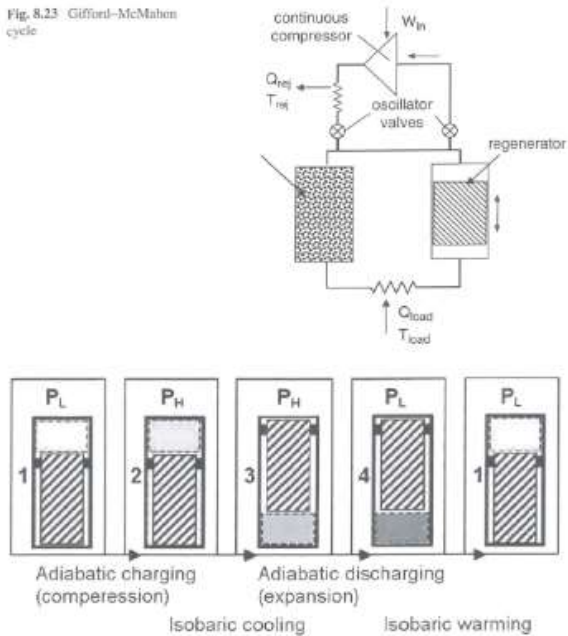


Fig. 8.24 Cycle description for the GM refrigerator

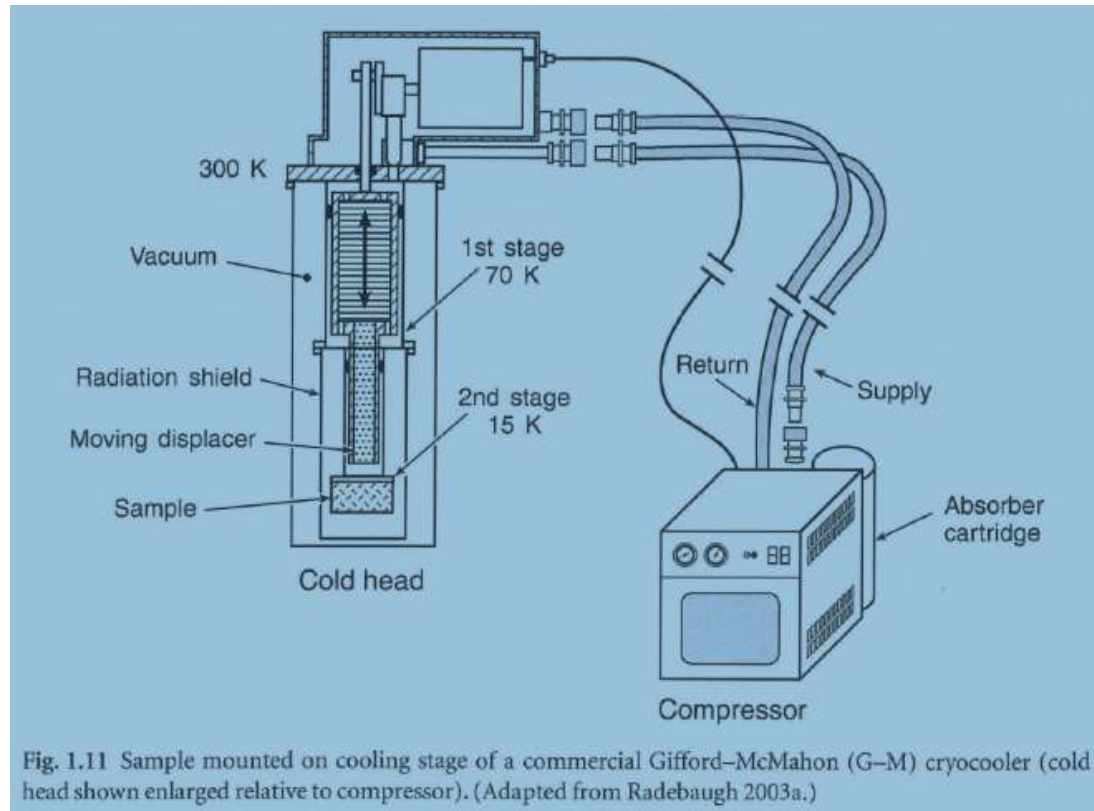


Fig. 1.11 Sample mounted on cooling stage of a commercial Gifford-McMahon (G-M) cryocooler (cold head shown enlarged relative to compressor). (Adapted from Radebaugh 2003a.)

Other types of refrigerator: Pulse Tube

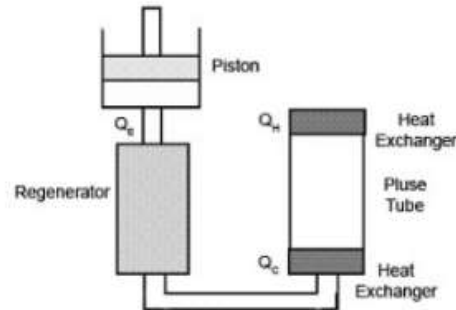


Fig. 1: Basic pulse tube refrigerator.

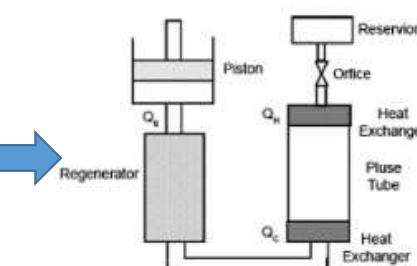


Fig. 3: Orifice pulse tube refrigerator.

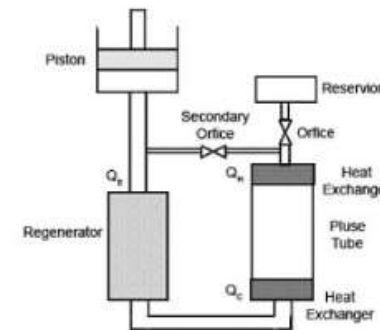


Fig. 5: Double inlet pulse tube refrigerator.
Gas flow through the regenerator into the pulse tube and through the secondary orifice directly to the warm end

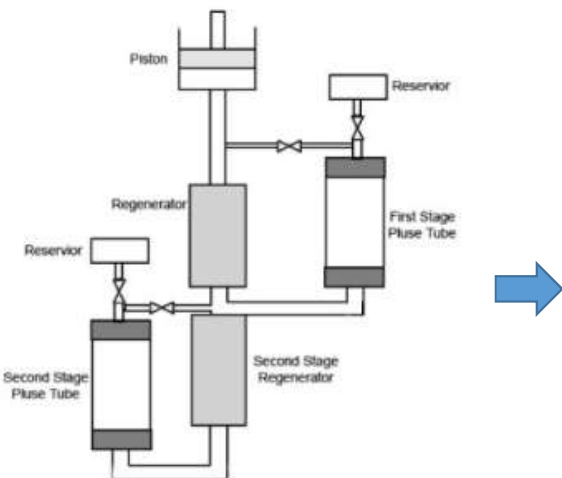


Fig. 6: Series arrangement of a multistage pulse tube.

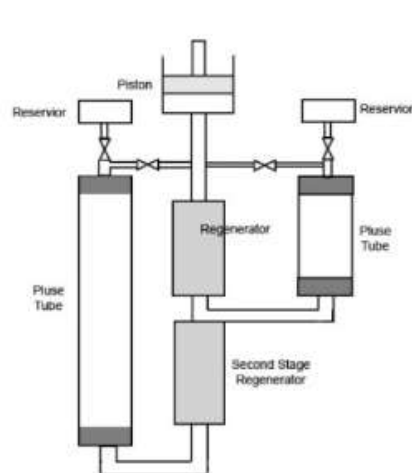


Fig. 7: Parallel arrangement of a multistage pulse tube.

J. Bert, Stanford University, 2007

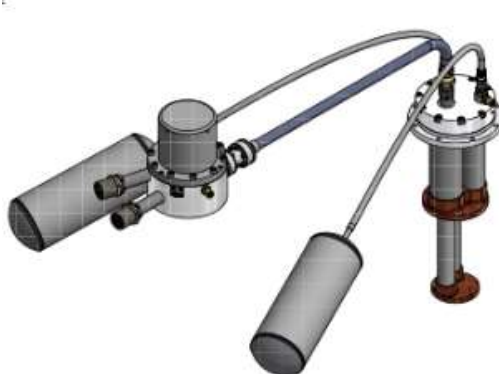
Other types of refrigerator: Pulse Tube



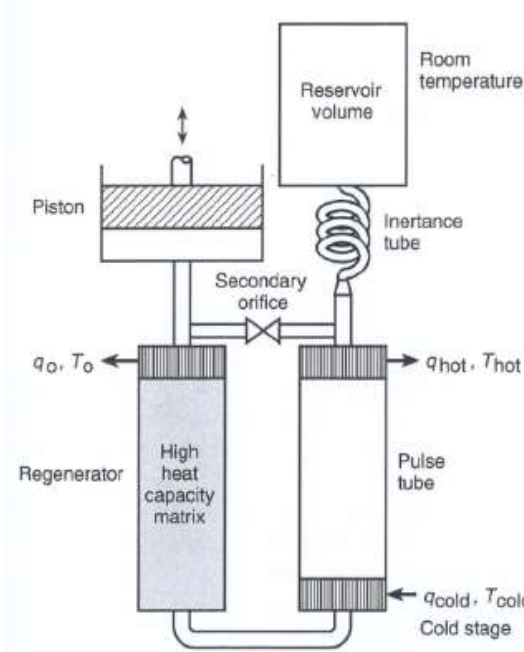
CRYOMECH



SHI 
Cryogenics Group



Other types of refrigerator: Pulse Tube



1. Compression of the gas by the piston
2. Temperature rises due to adiabatic compression
3. The gas passes the T_{cold} and goes into the tube
4. Then back to ambient temperature through T_{hot}
5. Then through an orifice to the reservoir
6. Pressure in the tube and reservoir is the same (no flow)
7. The piston goes upwards and expand adiabatically the gas in the tube
8. The gas is cooled
9. The gas flows back to the HX T_{cold}
10. Absorbs heat from the HX (cools the HX T_{cold})
11. The piston cycle starts again

Other types of refrigerator: Pulse Tube

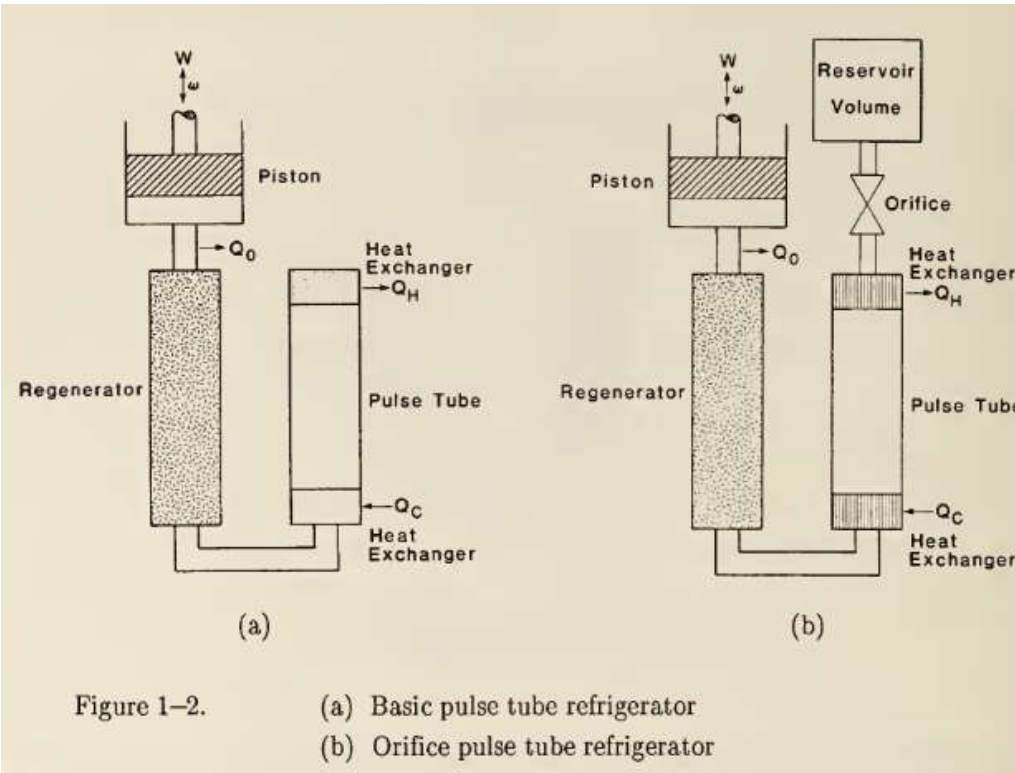
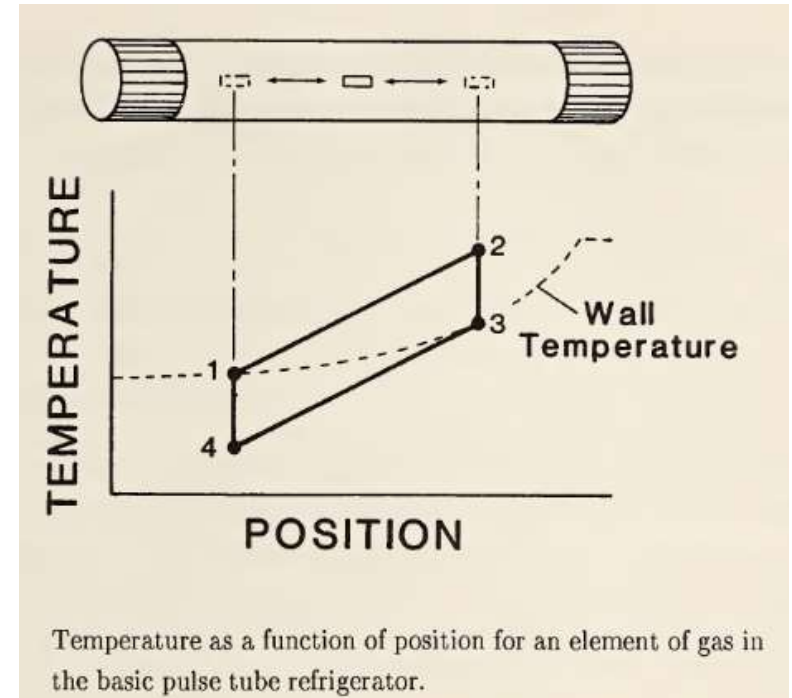


Figure 1–2.

- (a) Basic pulse tube refrigerator
- (b) Orifice pulse tube refrigerator



Temperature as a function of position for an element of gas in the basic pulse tube refrigerator.

Other types of refrigerator: Pulse Tube

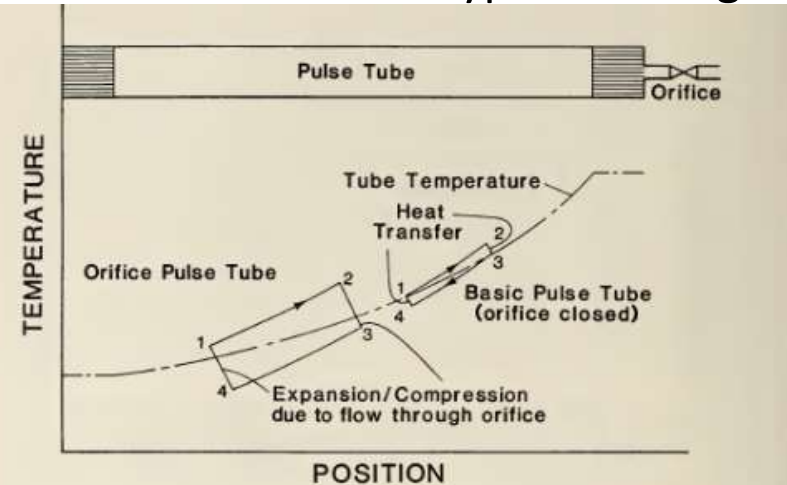


Figure 4-6. Temperature as a function of position for an element of gas in a pulse tube with the orifice open and with the orifice closed.

Another method of describing the refrigeration process in the orifice pulse tube involves a T-S diagram. It is impossible to represent pulse tube refrigeration on a T-S diagram in the traditional sense since each element of gas in the system follows a different path. For example, the buffer gas in the center of the tube traces out a simple vertical line on the T-S diagram since it experiences only the constant entropy processes of adiabatic compression and expansion. The gas which moves in and out of the ends of the pulse tube is more interesting. Figure 4-7 shows a T-S diagram for an element of gas which enters and leaves the cold end of the tube. Starting in the compressor at point 1 in the figure, the gas is cooled to the cold end temperature as it is moved by the piston through the regenerator and the cold end heat exchanger (1-2). The gas then experiences adiabatic compression in the tube and follows path (2-3). At this point, the gas in the OPTR follows path (3-4) and is cooled by adiabatic expansion due to flow of other gas elements

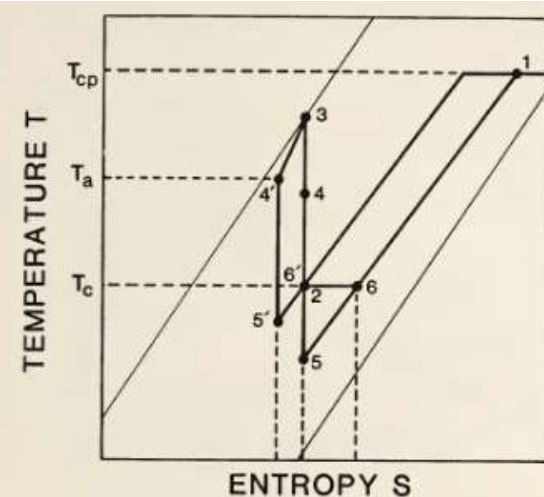
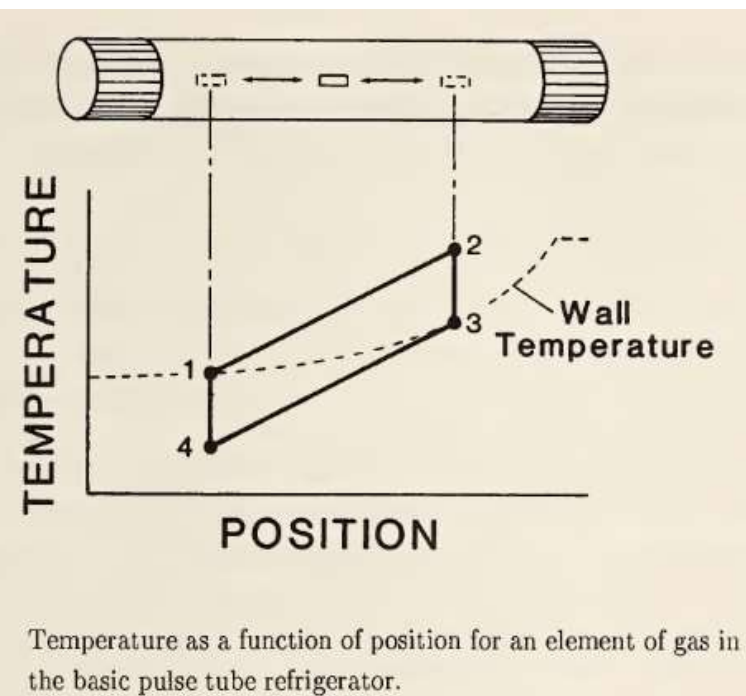


Figure 4-7. T-S diagram representing the thermodynamic cycle of an element of gas at the cold end of the tube.

out the orifice and into the reservoir. The path corresponds to path (2-3) on the T-x diagram in Figure 4-6 where gas moves toward the hot end as it cools below the average temperature. In the BPTR, however, cooling occurs at constant volume (3-4'), due to heat transfer with the tube wall and is limited to the wall temperature. The piston then moves gas back toward the cold end and the element of gas cools adiabatically from 4 to 5 in the OPTR and from 4' to 5' in the BPTR. The gas flows back through the cold-end heat exchanger and heat is absorbed at constant pressure along the paths (5-6) and (5'-6'). The gas completes the cycle back at point 1 in the compressor. The area under the curves (5-6) and (5'-6') represent the refrigeration power generated in the OPTR and BPTR, respectively. Just as shown in the T-x diagram in figure 4-6, the area is greater for the OPTR than for the BPTR.

Other types of refrigerator: Pulse Tube



1. Compression, the gas is cooled through the regenerator at T_{cold} end
2. The element of gas (1) is compressed adiabatically, is heated, and travels towards the closed end (1 -> 2)
3. During the relaxation period cooling occurs: heat is rejected at the hot end (to ambient)
4. The gas element is cooled transferring heat with the wall (2 -> 3)
5. The piston now goes back and the gas moves back towards the regenerator
6. The element of gas in the tube is expanded adiabatically and cools towards T_{cold} (3 -> 4)
7. During the relaxation time at constant volume heating occurs at low pressure (4 -> 1)
8. The gas at the cold end HX absorbs heat from the load while gas in the tube is heated by the wall

For the OPTR the relaxation time is given by the orifice, during this time the gas is cooled (expanded adiabatically) while the gas enters the reservoir. As gas flows back into the tube from the reservoir. Gas in the tube is adiabatically compressed and heats up.

Other types of refrigerator: Pulse Tube

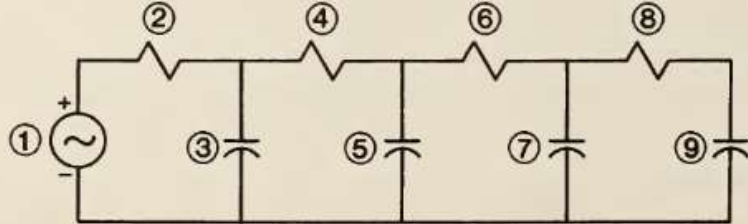


Figure 1–4. Analogous A C circuit for the orifice pulse tube refrigerator.

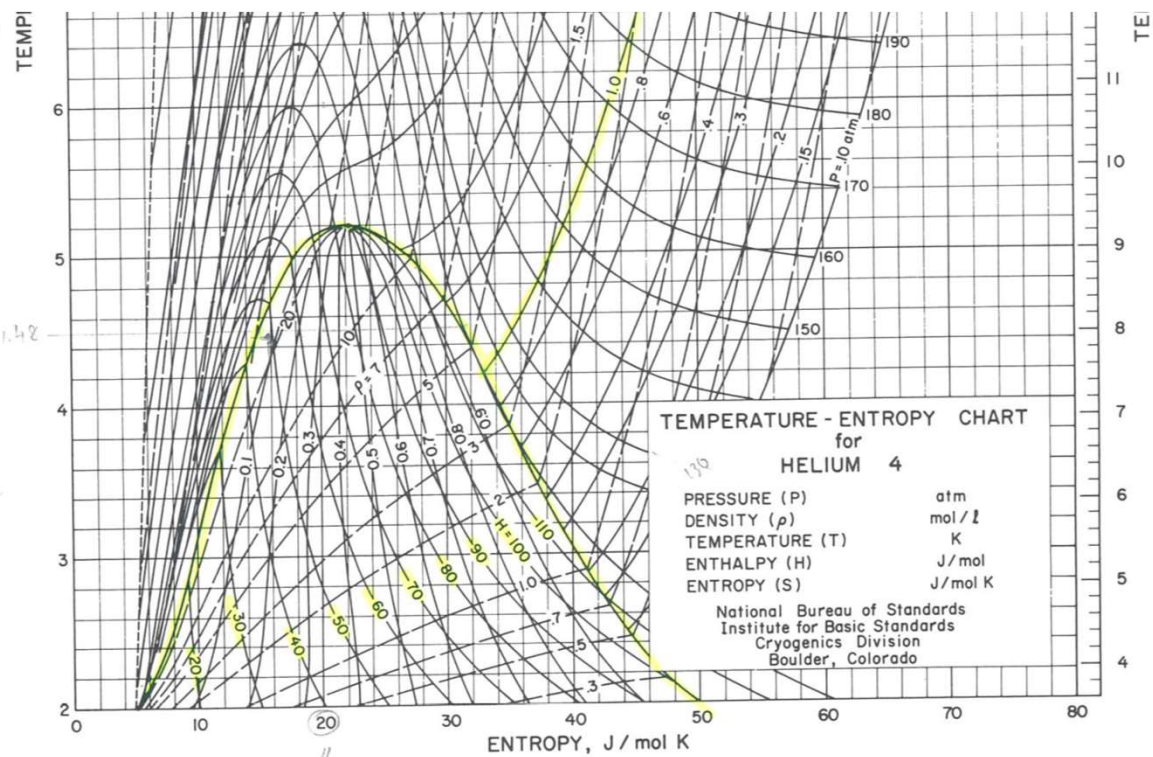
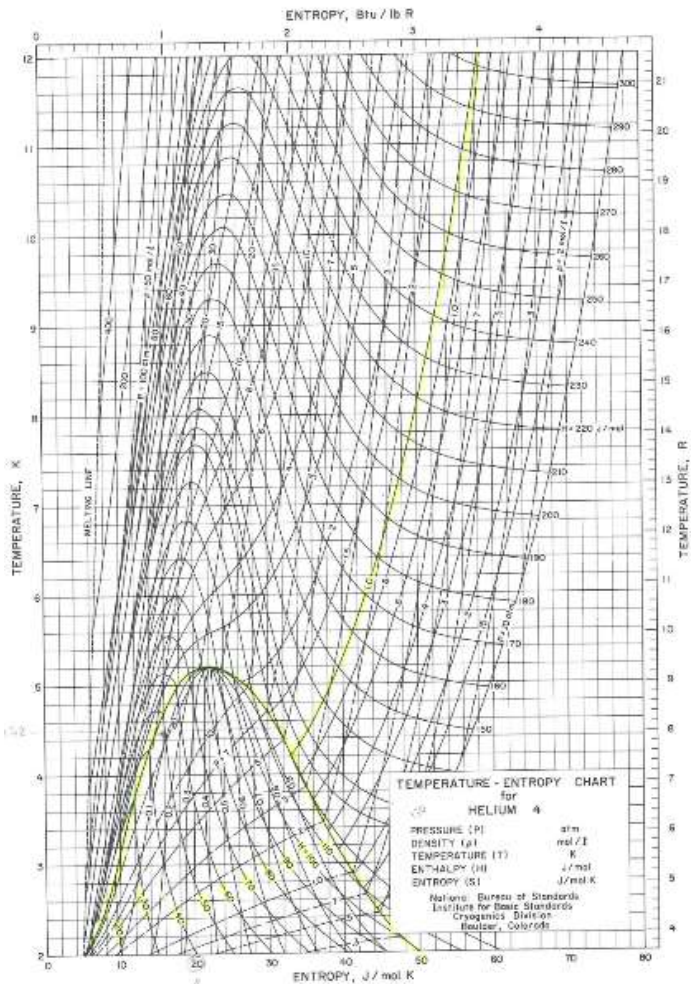
Analytical Model for the Refrigeration Power of the Orifice Pulse Tube Refrigerator

Peter J. Storch
Ray Radebaugh
James E. Zimmerman

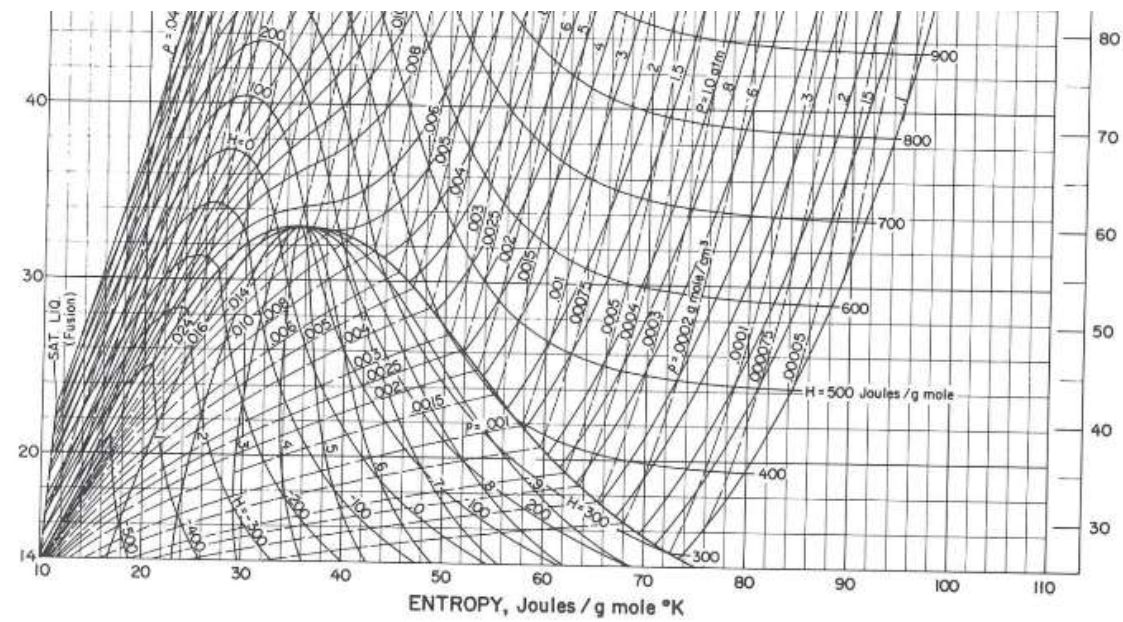
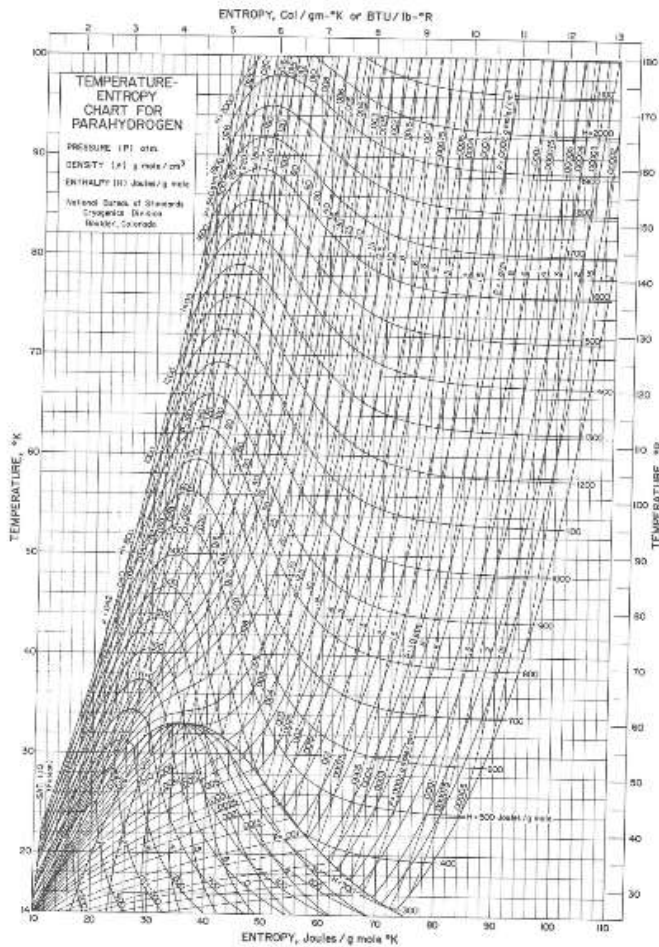
National Institute of Standards and Technology Technical Note 1343

The analogous circuit is shown in figure 1–4. The AC voltage source (element 1) produces a sinusoidal voltage and current in the electrical system in much the same way the compressor produces sinusoidal pressure and mass flow oscillations in the pulse tube. However, for large pressure oscillations, there is significant deviation from sinusoidal behavior and the compressor behaves more like a variable capacitor. Current from the voltage source flows through the first resistor (element 2), which represents the solid matrix in the regenerator, and a drop in voltage or pressure occurs. At this point, current is diverted in the circuit to charge a capacitor (element 3), just as part of the mass flow from the compressor is required to pressurize the regenerator void volume. The resulting current then encounters the next two resistor–capacitor sets (elements 4, 5 and elements 6, 7), which represent dead volume and pulse tube volume with similar effect. Each volume in the pulse tube can be associated with a resistance and a capacitance in the circuit. The last resistor in the circuit (element 8) models the flow impedance of the orifice at the hot end of the pulse tube. Again, a drop in voltage or pressure occurs here as charge or mass flows into the large capacitor (element 9) representing the reservoir volume.

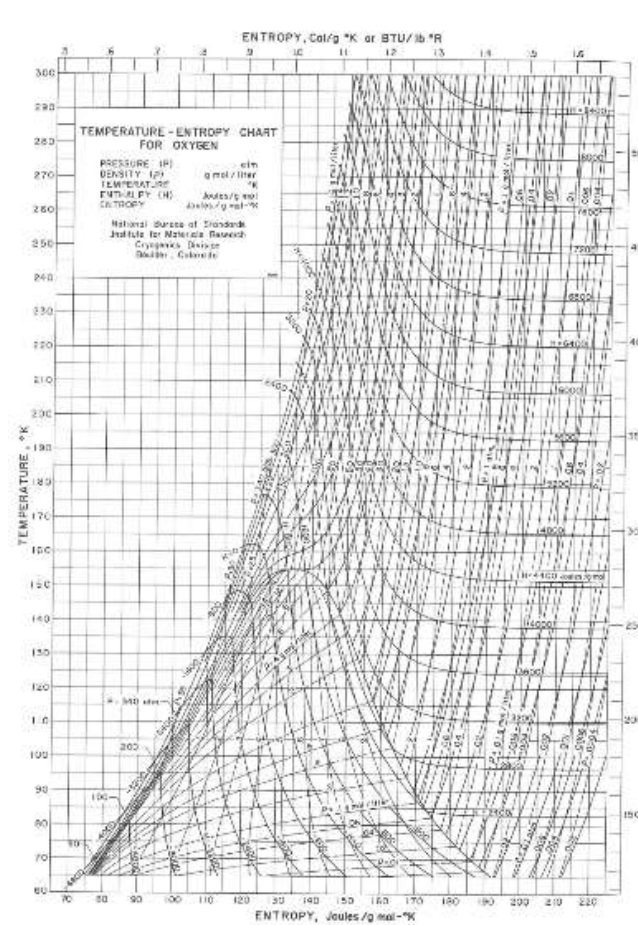
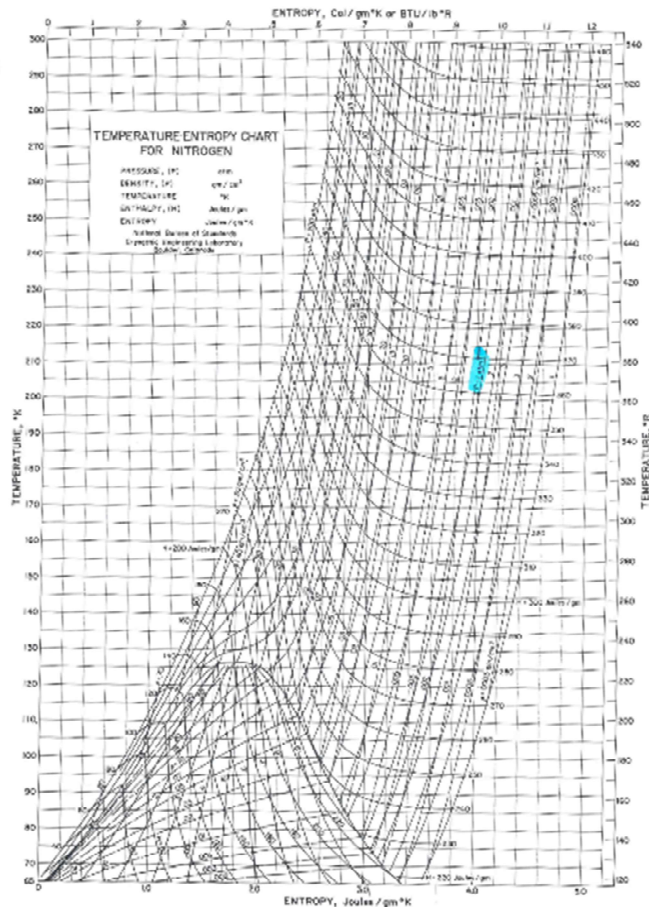
TS diagram for Helium



TS diagram for Para-Hydrogen ↑ ↓



TS diagram for Nitrogen & Oxygen



PROPRIETA' DEI MATERIALI:

- Entalpia (Temperatura di Debye)
- Scelta del materiale
- Contrazione termica
- Conducibilita' termica

TRASMISSIONE DEL CALORE

- Nei solidi
- Nei gas
- Irraggiamento
- Isolamento termico
- Cenni di crio-pompaggio
- Current Leads (discendenti di corrente)

LINEE DI TRASFERIMENTO

- Caduta di pressione
- Termosifone
- Pompe di circolazione
- Valvole criogeniche
- Giunzioni a bassa temperatura
- Dimensionamento di valvole di sicurezza

**Al fine di voler raffreddare un materiale e' necessario sapere:
Quanta energia e' contenuta in un materiale ad una determinata temperatura?**

Teoria di Debye: se si introduce la temperatura di Debye θ_D , caratteristica di un materiale, il «lattice specific heat» di un materiale e' dato dall'espressione (vedi grafico):

$$c_v = \frac{9RT^3}{\theta_D^3} \int_0^{\theta_D/T} \frac{x^4 e^x dx}{(e^x - 1)^2} = 3R \left(\frac{T}{\theta_D}\right)^3 D\left(\frac{T}{\theta_D}\right)$$

- θ_D e' detta Temperatura Caratteristica di Debye (vedi tabella)
- Per $T > \theta_D$ tende a $3R$ (Dulong Petit formula)
- Per $T < \theta_D/12$:
$$c_v = \frac{12\pi^4 RT^3}{5\theta_D^3} = \frac{233.78 RT^3}{\theta_D^3}$$
- Spesso e' piu' utile conoscere il C_p anziche' il C_v , ma la differenza $C_p - C_v$ e' generalmente cosi' piccola da poter essere trascurata se confrontata con l'incertezza della stima

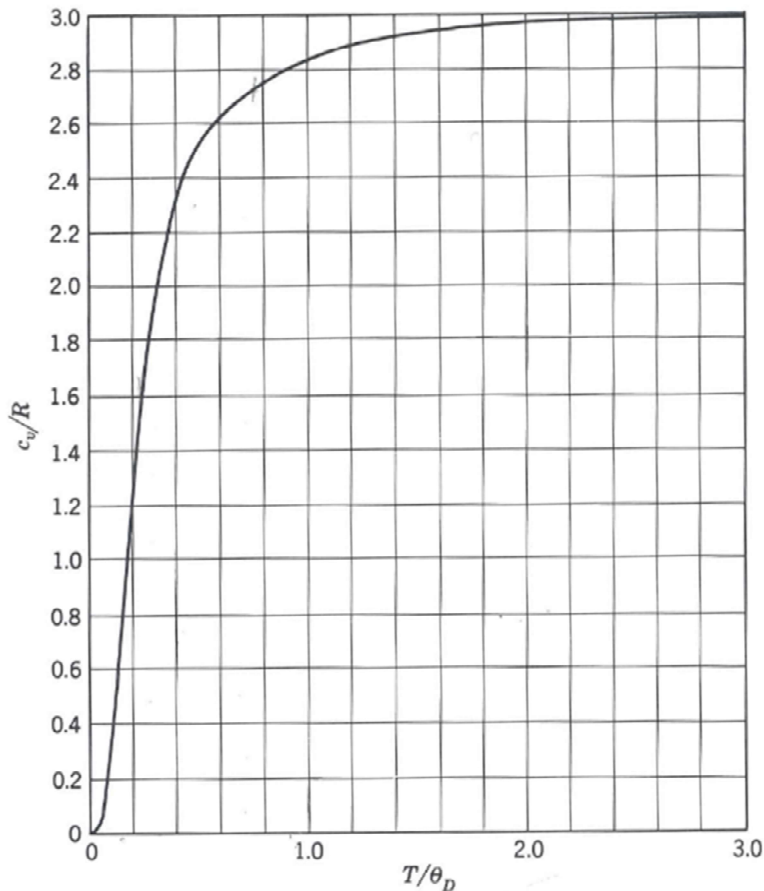


Fig. 2.8. The Debye specific heat function.

$$c_v = \frac{9RT^3}{\theta_D^3} \int_0^{\theta_D/T} \frac{x^4 e^x dx}{(e^x - 1)^2} = 3R \left(\frac{T}{\theta_D}\right)^3 D\left(\frac{T}{\theta_D}\right)$$

less than $\theta_D/12$

$$c_v = \frac{12\pi^4 RT^3}{5\theta_D^3} = \frac{233.78 RT^3}{\theta_D^3}$$

Table 2.1. Debye specific heat function

T/θ_D	c_v/R	T/θ_D	c_v/R	T/θ_D	c_v/R
0.08	0.1191	0.45	2.3725	1.60	2.9422
0.09	0.1682	0.50	2.4762	1.70	2.9487
0.10	0.2275	0.60	2.6214	1.80	2.9542
0.12	0.3733	0.70	2.7149	1.90	2.9589
0.14	0.5464	0.80	2.7781	2.00	2.9628
0.16	0.7334	0.90	2.8227	2.20	2.9692
0.18	0.9228	1.00	2.8552	2.40	2.9741
0.20	1.1059	1.10	2.8796	2.60	2.9779
0.25	1.5092	1.20	2.8984	2.80	2.9810
0.30	1.8231	1.30	2.9131	3.00	2.9834
0.35	2.0597	1.40	2.9248	4.00	2.9844
0.40	2.2376	1.50	2.9344	5.00	2.9900

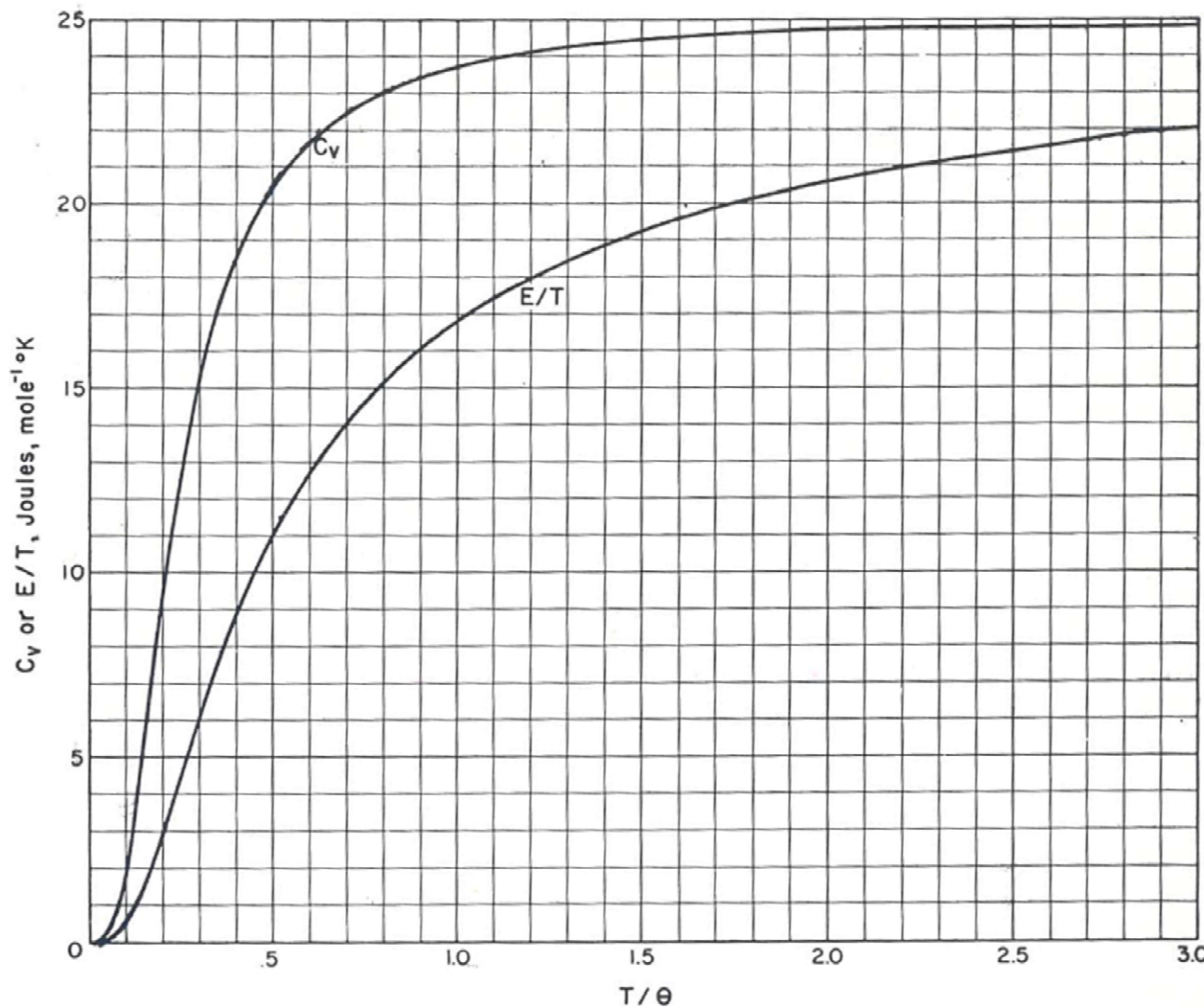


FIGURE 10.2. Debye specific heat (C_v) and internal energy (E) functions.

$$c_v = \frac{9RT^3}{\theta_D^3} \int_0^{\theta_D/T} \frac{x^4 e^x dx}{(e^x - 1)^2} = 3R \left(\frac{T}{\theta_D}\right)^3 D \left(\frac{T}{\theta_D}\right)$$

Table 2.2. Debye characteristic temperatures

Material	θ_D		Material	θ_D	
	K	°R		K	°R
Aluminum	390	702	Mercury	95	171
Argon	85	153	Molybdenum	375	675
Beryllium	980	1764	Neon	63	113
Calcium	230	414	Nickel	375	675
Chromium	440	792	Niobium	265	477
Copper	310	558	Platinum	225	405
Diamond	1850	3330	Silver	220	396
Gadolinium	160	288	Sodium	160	288
Germanium	290	522	Tantalum	245	441
Gold	180	324	White tin	165	297
Graphite	1500	2700	Gray tin	240	432
α -Iron	430	774	Titanium	350	630
γ -Iron	320	576	Tungsten	315	567
Lead	86	155	Vanadium	280	504
Lithium	430	774	Zirconium	280	504

By permission from Scott (1959).

Example: Enthalpy of a copper RF sc cavity (ALPI) (Nb sputtered on copper)

- Cylinder : diam 20 cm, height 50 cm, thickness 1 cm
- Cu density: 8.96 g/cm³, Cu molar weight: 63.54 g/mol, Cu Debye Temp $\theta_D = 310$ K
- Calculate: the enthalpy from 300 K to 80 K, and from 80 K to 4 K

Volume= 2983 cm³ Mass = 26728 g

From graph E/T vs T/ θ_D :

- at 300/310=0.97 read E/T= 16.7 J/mol-K => h(300)=16.7x300/63.54 = 78.8 J/g
- at 80/310=0.26 read E/T = 5 J/mol-K => h(80) K=5x80/63.54= 6.295 J/g
- at 4/310=0.01 read E/T= 0

Hence: Most of the energy is needed from 300 K to 80 K $(78.8-6.295)/78.8 = 0.92$ i.e. 92%

- From table Conte (see next slide): h(300)=79.6 J/g; h(80)= 6.02 J/g

THE GRAPH $\sigma(T)$ gives a very good estimation!

For a cavity: H(300)= 79.6J/g x 26728 g =2.13 MJ; H(80)=0.16 MJ;



Temp. °K)	Cuivre		Or		Argent	
	C _p (J/g °K)	H (J/g)	C _p (J/g °K)	H (J/g)	C _p (J/g °K)	H (J/g)
1	0,000 012	0,000 006	0,000 006	0,000 002	0,000 0072	0,000 0032
2	0,000 028	0,000 025	0,000 025	0,000 016	0,000 0239	0,000 0176
3	0,000 053	0,000 064	0,000 070	0,000 061	0,000 0595	0,000 0574
4	0,000 091	0,000 13	0,000 16	0,000 17	0,000 124	0,000 146
6	0,000 23	0,000 44	0,000 50	0,000 78	0,000 39	0,000 62
8	0,000 47	0,001 12	0,001 2	0,002 4	0,000 91	0,001 87
10	0,000 86	0,002 4	0,002 2	0,005 6	0,001 8	0,004 52
15	0,002 7	0,010 7	0,007 4	0,028	0,006 4	0,023 3
20	0,007 7	0,034	0,015 9	0,086	0,015 5	0,076
25	0,016	0,090	0,026 3	0,191	0,028 7	0,185
30	0,027	0,195	0,037 1	0,349	0,044 2	0,368
40	0,060	0,61	0,057 2	0,821	0,078	0,979
50	0,099	1,40	0,072 6	1,47	0,108	1,91
60	0,137	2,58	0,084 2	2,25	0,133	3,12
70	0,173	4,13	0,092 8	3,14	0,151	4,54
80	0,205	6,02	0,099 2	4,10	0,166	6,13
90	0,232	8,22	0,104 3	5,12	0,177	7,85
100	0,254	10,6	0,108 3	6,18	0,187	9,67
120	0,288	16,1	0,113 7	8,41	0,200	13,55
140	0,313	22,1	0,117 5	10,72	0,209	17,65
160	0,332	28,5	0,120 2	13,10	0,216	21,91
180	0,346	35,3	0,122 1	15,52	0,221	26,29
200	0,356	42,4	0,123 5	17,98	0,225	30,73
220	0,364	49,6	0,124 7	20,46	0,228	35,23
240	0,371	56,9	0,125 7	22,96	0,231	39,86
260	0,376	64,4	0,126 7	25,49	0,234	44,50
280	0,381	72,0	0,127 6	28,03	0,235	49,20
300	0,386	79,6	0,128 5	30,59	0,236	53,91

Temp. °K)	Aluminium		Béryllium		Titane	
	C _p (J/g °K)	H (J/g)	C _p (J/g °K)	H (J/g)	C _p (J/g °K)	H (J/g)
1	0,000 10*		1	0,000 051	0,000 025	0,000 013
2	0,000 28	0,000 025	2	0,000 108	0,000 105	0,000 051
3	0,000 53	0,000 064	3	0,000 176	0,000 246	0,000 116
4	0,000 91	0,000 13	4	0,000 261	0,000 463	0,000 209
6	0,000 23	0,000 44	6	0,000 50	0,001 21	0,000 496
8	0,000 47	0,001 12	8	0,000 88	0,002 6	0,000 944
10	0,000 86	0,002 4	10	0,001 4	0,004 9	0,001 60
15	0,002 7	0,010 7	15	0,004 0	0,018	0,000 842
20	0,007 7	0,034	20	0,008 9	0,048	0,001 61
25	0,016	0,090	25	0,017 5	0,112	0,002 79
30	0,027	0,195	30	0,031 5	0,232	0,004 50
40	0,060	0,61	35	0,051 5	0,436	0,039 2
50	0,099	1,40	40	0,077 5	0,755	0,057 1
60	0,137	2,58	50	0,142	1,85	0,099 2
70	0,173	4,13	60	0,214	3,64	0,146 7
80	0,205	6,02	70	0,287	6,15	0,189
90	0,232	8,22	80	0,357	9,37	0,230
100	0,254	10,6	90	0,422	13,25	0,267
120	0,288	16,1	100	0,481	17,76	0,300
140	0,313	22,1	120	0,580	28,4	0,352
160	0,332	28,5	140	0,654	40,7	0,391
180	0,346	35,3	160	0,713	54,4	0,422
200	0,356	42,4	180	0,760	69,2	0,446
220	0,364	49,6	200	0,797	84,8	0,465
240	0,371	56,9	220	0,826	101,0	0,480
260	0,376	64,4	240	0,849	117,8	0,493
280	0,381	72,0	260	0,869	135,0	0,504
300	0,386	79,6	280	0,886	152,5	0,514

*Supraconducteur.

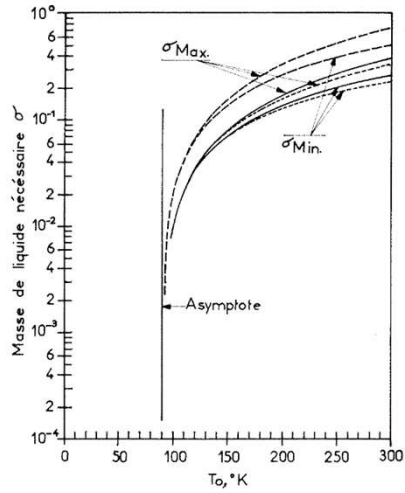


FIG. 5-9. — Variations des facteurs σ_{\min} et σ_{\max} avec la température. Cas de l'oxygène (26).

— Acier inoxydable
— - - Aluminium
- - - Cuivre.

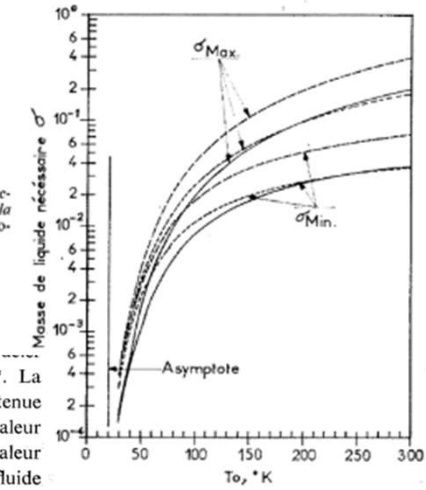


FIG. 5-11. — Variations des facteurs σ_{\min} et σ_{\max} avec la température. Cas de l'hydrogène (26).

— Acier inoxydable
— - - Aluminium
- - - Cuivre.

inoxydable, cuivre, aluminium. Il définit deux coefficients σ_{\min}^* et σ_{\max}^* . La valeur de σ_{\min} est déduite d'un calcul qui tient compte de toute la chaleur contenue dans le liquide, c'est-à-dire de la chaleur latente de vaporisation et de la chaleur sensible du gaz. La valeur de σ_{\max} par contre, ne tient compte que de la chaleur latente de vaporisation. σ_{\min} et σ_{\max} sont les rapports entre la masse de fluide et la masse à refroidir de la température T_a à la température T_c :

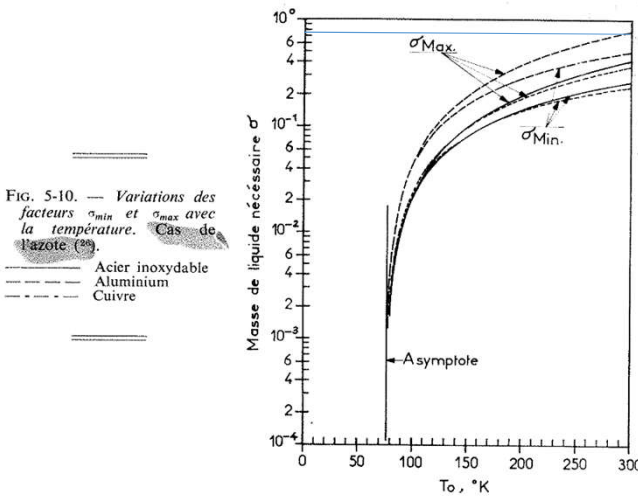


FIG. 5-10. — Variations des facteurs σ_{\min} et σ_{\max} avec la température. Cas de l'azote (26).

— Acier inoxydable
— - - Aluminium
- - - Cuivre.

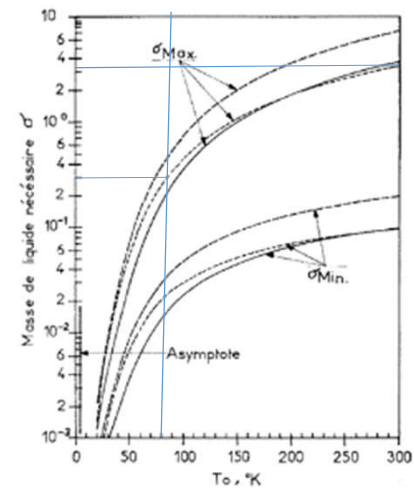


FIG. 5-12. — Variations des facteurs σ_{\min} et σ_{\max} avec la température. Cas de l'hélium (26).

— Acier inoxydable
— - - Aluminium
- - - Cuivre.

10.4 Cooling materials to 4.2 K using liquid helium

The volume of liquid helium required to cool a mass of metal from one temperature to another using the full enthalpy of the gas or using the latent heat alone was reported by J B Jacobs, Advances in Cryogenic Engineering, Volume 8, 1963, p. 529, as follows.

Cryogen		^4He	^3He	N_2
Initial temperature of metal		300 K	77 K	300 K
Final temperature of metal		4.2 K	4.2 K	77 K
Using the latent heat of vaporisation only *	Al	66.6	3.20	1.01
	St. Steel	33.3	1.43	0.53
	Cu	31.1	2.16	0.46
Using the enthalpy of the gas **	Al	1.61	0.22	0.64
	St. Steel	0.79	0.11	0.33
	Cu	0.79	0.15	0.29

Table 8 Amount of cryogenic fluid required to cool metals (litres/kg)



Amount of cryogens required to cool down 1 kg iron

Using	Latent heat only	Latent heat and enthalpy of gas
LHe from 290 to 4.2 K	29.5 litre	0.75 liter
LHe from 77 to 4.2 K	1.46 litre	0.12 litre
LN2 from 290 to 77 K	0.45 litre	0.29 litre

⇒ *recover enthalpy from cold gas (i.e. moderate flow of cryogen)*

⇒ *pre-cool with liquid nitrogen to save liquid helium*

Example: **Enthalpy of a copper RF sc cavity (ALPI) (Nb sputtered on copper)**

- Cylinder : diam 20 cm, height 50 cm, thickness 1 cm
- Cu density: 8.96 g/cm³, Cu molar weight: 63.54 g/mol, Cu Debye Temp= 310 K
- Calculate: the enthalpy from 300 K to 80 K, and from 80 K to 4 K

Volume= 2983 cm³ Mass = 26728 g

From graph E/T vs T/theta:

- at 300/310=0.97 read E/T= 16.7 J/mol-K => h(300)=16.7x300/63.54=78.8 Joule/g
- at 80/310=0.26 read E/T= 5 J/mol-K => h(80)=5x80/63.54=6.295 Joule/g
- at 4/310=0.01 read E/T= 0

Hence: Most of the energy is needed from 300 K to 80 K $(78.8-6.295)/78.8 = 0.92$ i.e. 92%

- From table Conte: h(300)=79.6 J/g; h(80)=6.02 J/g $(79.6-6.02)/79.6 = 0.924$

THE GRAPH σ (T) gives a very good estimation!

For a cavity: H(300)= 79.6J/g x 26728 g =2.13 MJ; H(80)=0.16 MJ;

How many kg (litres) of LHe are needed from 300 K to 80 K?

From calculation above: $(2.13-0.16) \times 10^6 \text{ J}/20.9 \text{ J/g}/125 \text{ g/l} = 754 \text{ litres}$ (only latent heat)

From graph of σ He: σ(300)=3.1; σ(80)=0.3; diff=2.8 kg(LHe)/kg(Cu)=> $2.8/0.125= 22.4 \text{ litreLHe/kg(Cu)}$

Hence $2.8 \text{ kg LHe} \times 26.7 \text{ kg (Cu)} = 74.76 \text{ kg LHe}$ or $74.76/0.125= 598 \text{ litre of LHe}$

The sigma graphs are also a good estimation of enthalpy.

How many kg (litres) of LN₂ are needed from 300 K to 80 K?

From graph of σ Nitrogen: $\sigma(300)=0.72$; $\sigma(80)=0$; $\text{diff}=0.72 \text{ kg(LHe)}/\text{kg(Cu)} \Rightarrow 0.72/0.800= 0.9 \text{ litreLN}_2/\text{kg(Cu)}$

Hence $0.9 \text{ kg LN}_2 \times 26.7 \text{ kg (Cu)}= 24.0 \text{ kg LN}_2$ or $24.0/0.800=30 \text{ litre of LN}_2$

From calculation above: $(2.13-0.16) \times 10^6 \text{ J}/199 \text{ J/g}/800 \text{ g/l} =12.4 \text{ litres (only latent heat)}$

The sigma graphs are also a good estimation of enthalpy.

How many kg (litres) of LHe are needed from 80 K to 4 K?

From graph of σ He: $\sigma(4)=0$; $\sigma(80)=0.3$; $\text{diff}=0.3 \text{ kg(LHe)}/\text{kg(Cu)} \Rightarrow 0.3/0.125= 2.4 \text{ litreLHe/kg(Cu)}$

Hence $0.3 \text{ kg LHe} \times 26.7 \text{ kg (Cu)}= 8.0 \text{ kg LHe}$ or $8.0/0.125=598 \text{ litre of LHe}$

From calculation above: $(2.13-0.16) \times 10^6 \text{ J}/20.9 \text{ J/g}/125 \text{ g/l} =64 \text{ litres (only latent heat)}$

The sigma graphs are also a good estimation of enthalpy.

How to select the appropriate material

The first selection of a material for low temperature use is the fracture toughness:

- Best are the **fcc** (face centered cubic) (AISI 300 series especially 304, 310, 316, CU, Al, brass,...)
- Less suitable the **bcc** (body centered cubic) (Cr, Fe, Mo, Ta, W, V, and nickel steel). They become brittle at low temperature
- The **hcp** (hexagonal close packed) are between the two above (Be, Ti, Zn,...)
- Resins material (epoxy) become also brittle at low temperature

Other important properties are:

- The tensile properties such as :
 - Young modulus, E (modulo di Young GPa)
 - Stress (carico, sollecitazione MPa)
 - Yield strength, σ_y (carico di snervamento 0.2 % Pa= N/m²)
 - Elastic strength, ϵ_y (deformazione elastica $\Delta L/L$)
 - Ultimate strength, σ_{ult} (massima resistenza alla trazione N/m²)
- Fracture toughness, K_{Ic} (**Resilienza**)
- Fatigue tolerance (**Tolleranza alle sollecitazioni ripetute**)
- creep (**cricca**)

How to select the appropriate material

6.6.1 TENSILE PROPERTIES

Before we look at tensile property data, we briefly review and define the Young's modulus, yield strength, elastic strain limit, and ultimate strength—all quantities used to describe the response of a material to a simple *tensile* force applied along the axis of a bar of the material. To generalize these properties for parts of different size, the axial force F is normalized by the part's cross-sectional area A and expressed as *stress* σ :

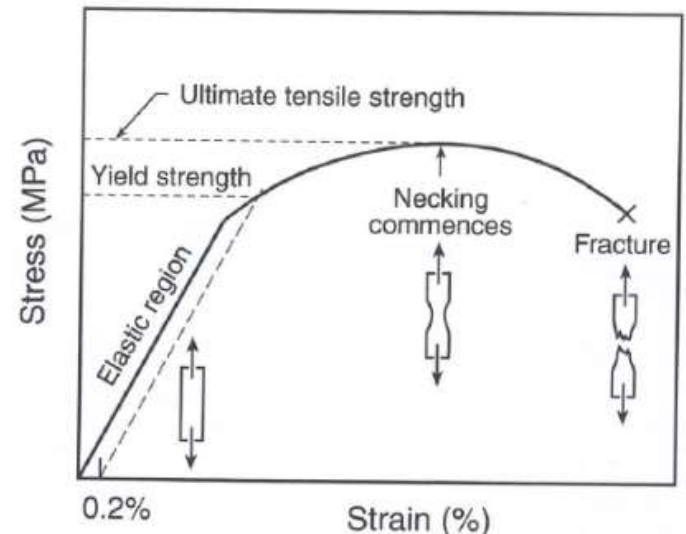
$$\sigma = F/A. \quad \text{Stress} \quad (6.19)$$

The units (SI) for stress are *pascals* ($\text{Pa} \equiv \text{N/m}^2$), and values are usually given in megapascals ($\text{MPa} = 10^6 \text{ Pa}$) because the numbers in common situations are so large.

The stress-induced change in length ΔL is usually normalized by the part's length L and expressed as *strain* ε :

$$\varepsilon = \Delta L/L, \quad \text{Strain} \quad (6.20)$$

(positive strain indicates elongation of the bar, and negative, strain compression). The units for strain are dimensionless, but for convenience and clarity, here we express the value as a percentage (%).



How to select the appropriate material

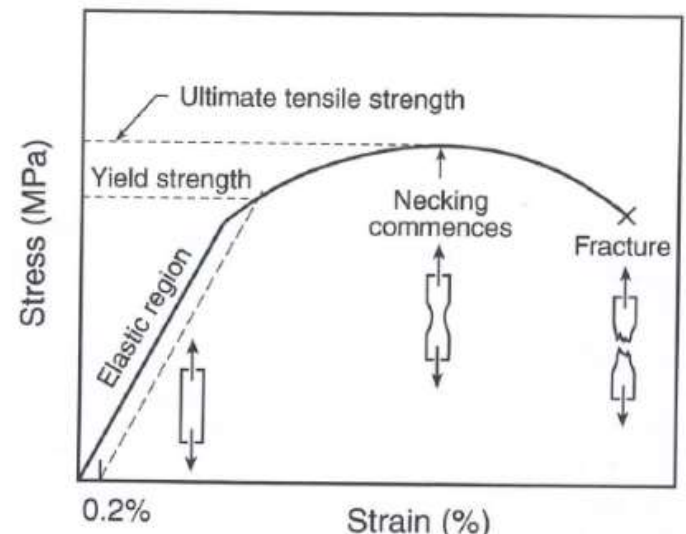
The relationship between axial stress σ and strain ϵ is illustrated for a typical metallic material in Fig. 6.15. When axial force is applied, the material at first deforms *elastically*; that is, it returns to its original size and shape when the force is removed. This results in the straight-line response of the material at the beginning of the diagram. The slope of this section of the curve determines the relative stiffness of the material and is designated as the *Young's modulus* E , usually expressed in gigapascals ($\text{GPa} = 10^9 \text{ Pa}$):

$$E = \sigma/\epsilon. \quad \text{Young's modulus} \quad (6.21)$$

Values of the Young's modulus are shown for a selection of metals in Fig. 6.16 and for common structural alloys in Appendix A6.10. Figure 6.16 shows that the Young's modulus usually changes little with temperature, increasing only slightly as temperature is lowered.

The end of the elastic (linear) region in Fig. 6.15 is an important point and indicates the onset of yielding, where the material starts to plastically deform. The stress corresponding to this onset point is designated as the *yield strength* σ_y . For most structural designs, this is the stress level to be avoided! Often parts are sized so that the maximum stress they experience is no more than half the material's yield strength, giving a safety factor of two. Values of yield strength are usually determined by use of the 0.2% offset method, as illustrated in Fig. 6.15 (i.e. 0.2% more strain than that at the end of the elastic region). The temperature dependence of the yield strength of common technical materials is shown in Figs 6.17 and 6.18, and tabulated for a few common metal alloys and polymers in the last table of Appendix A6.10.

After fracture toughness, yield strength is generally the main mechanical design factor. Figures 6.17 and 6.18 show that the yield strength of most materials (both ductile and brittle) increases moderately as temperature is lowered. Unlike the Young's modulus, the yield strength is strongly affected by extrinsic factors such as the amount of cold work introduced into the material as it is rolled, pressed, or drawn to smaller cross-sectional area. This is illustrated by comparing the



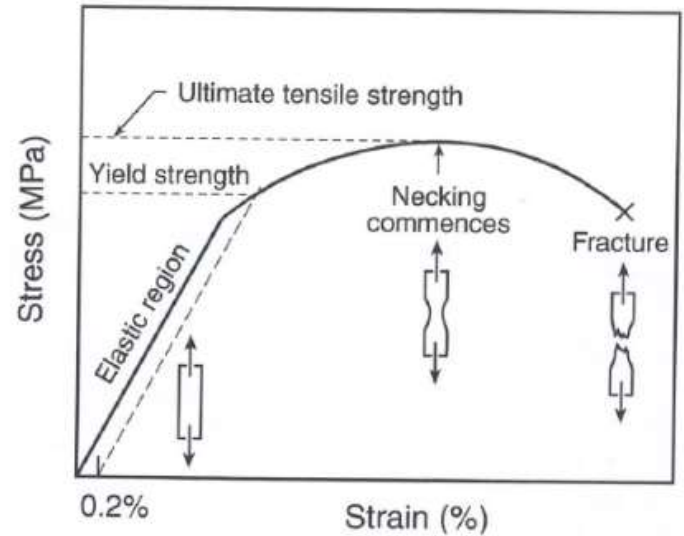
How to select the appropriate material

enormous differences between values of σ_y for annealed and cold-drawn materials, shown in Fig. 6.17 for copper and AISI 304 stainless steel.

The *elastic strain limit* (also called the *proportional limit* or *strain at yield*) is a significant design factor when choosing a material for a springy cryostat part that needs to bend elastically, such as spring clamps, extensometer arms, and bending beams. The elastic strain limit can be simply calculated as

$$\varepsilon_y = \sigma_y/E. \quad \text{Elastic strain limit} \quad (6.22)$$

Beryllium copper or precipitation-hardened aluminum alloys, for example, are materials having very high elastic strain limits, up to $\sim 1.0\%$. They are great materials for cryogenic parts that need to flex without fatiguing or breaking.



How to select the appropriate material

Resilienza: E' il lavoro per rompere una provetta di determinate dimensioni in un solo colpo con mazze a coltello

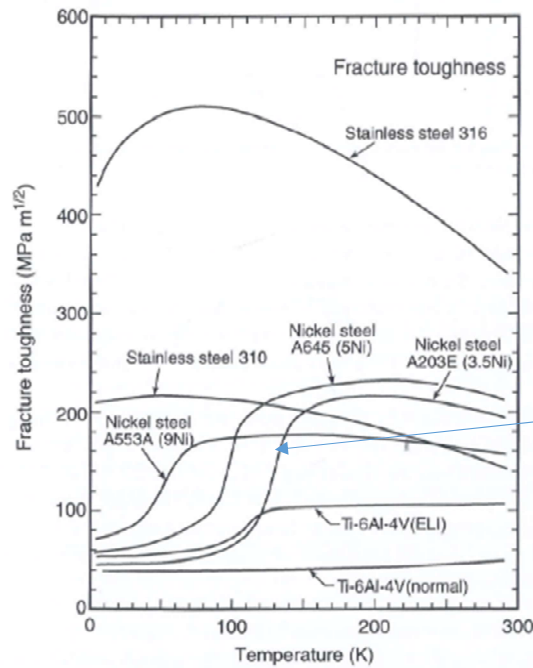
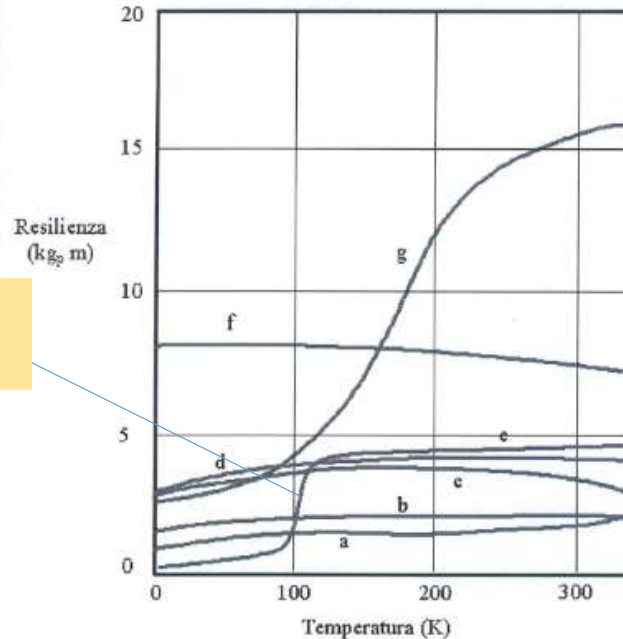


Fig. 6.20 Fracture toughness of various materials at low temperatures. Note that at low temperatures, the nickel steels (b.c.c. structure) decrease greatly in toughness and become brittle, whereas the austenitic stainless steels (f.c.c. structure) such as AISI 310 and 316 remain tough across the cryogenic temperature range. The Ti-6%Al-4%V alloys have an h.c.p. structure; their toughness drops more moderately. (Data compiled from Tobler and McHenry 1983, Mann 1978, and Fowlkes and Tobler 1976.) Tabulated data for some of these alloys are given in Appendix A.10.

To be avoided



a) alluminio; b) titanio; c) monel; d) rame legato; e) acciaio al carbonio; f) acciaio inox; g) acciaio al nichel

How to select the appropriate material

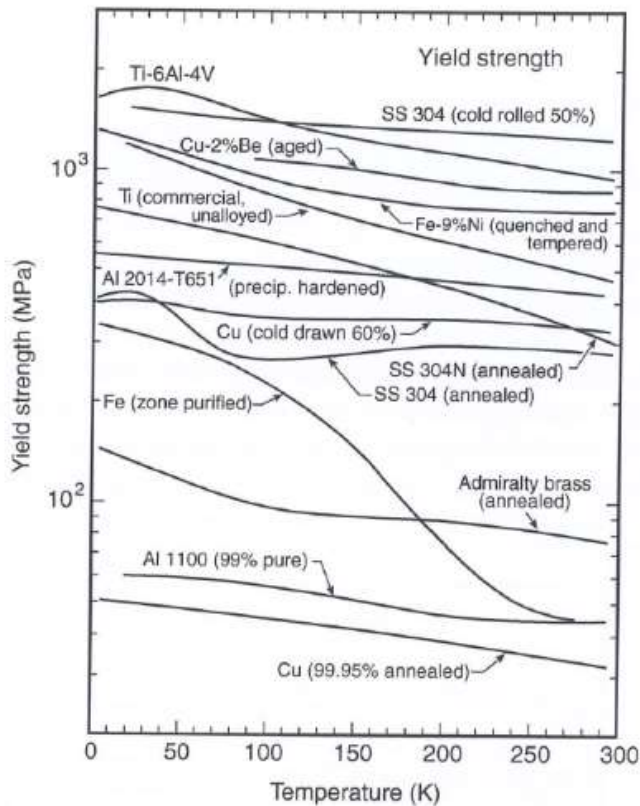


Fig. 6.17 Yield strength of common cryostat construction materials as a function of temperature. (Data compiled from Battelle 1977, Read and Reed 1979, Tobler 1976, Smith and Rutherford 1957, Warren and Reed 1963, Schramm et al. 1973, and Soffer and Molho 1967.) Appendix A6.10 gives tabulated values, along with mechanical data for additional materials.

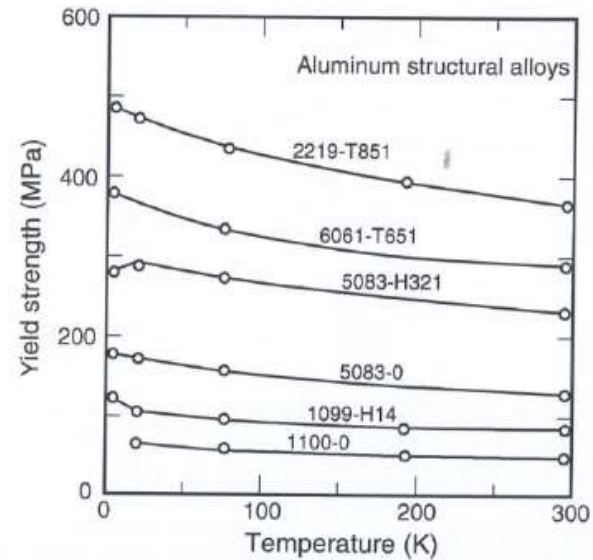


Fig. 6.18 Yield strength of structural aluminum alloys as a function of temperature (from Kaufman et al. 1968). Appendix A6.10 gives tabulated values, along with mechanical data for additional materials.

How to select the appropriate material

The last tensile property, the *ultimate tensile strength*, is usually not as important in practice, especially if the yield-strength limit is respected. Figure 6.15 shows that when ductile materials are strained beyond their yield strength, stress increases until the ultimate tensile strength is reached. (Brittle materials, on the other hand, fail at low strain in the elastic region of Fig. 6.15.) At the ultimate strength, necking commences, and if the material is strained further, the load it will support decreases. (If load is being controlled rather than strain, the material will fail at the onset of necking.) Eventually, at high enough strain, ductile materials pull apart and fail, as indicated by the \times in Fig. 6.15. Values of the ultimate strength for common cryostat materials

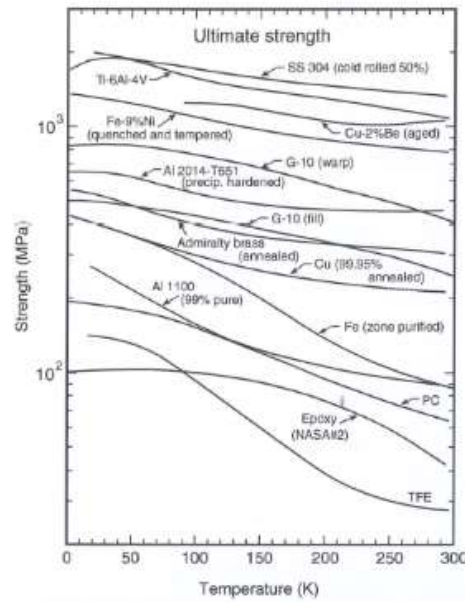


Fig. 6.19 Ultimate tensile strength of common cryostat construction materials as a function of temperature.
(Data compiled from Battelle 1977, Read and Reed 1979, Tobler 1976, Smith and Rutherford 1957, Warren and Reed 1963, Schramm et al. 1973, Soffer and Molho 1967, and Kasen et al. 1980.)

How to select the appropriate material

6.6.2 FRACTURE TOUGHNESS

As mentioned in the introduction, fracture toughness can be a show stopper in cryostat construction. The toughness parameter most commonly used for mechanical design is the plane-strain critical-stress intensity factor K_{Ic} [for further information, see, for example, the introductory material in Ruffin (1996)]. Values of K_{Ic} are shown for various construction materials in Fig. 6.20. This figure clearly shows the remarkable drop in fracture toughness around 100 K in b.c.c. materials, such as the very high-strength nickel steels (A203E, A553, and A645) and high-strength titanium alloys [Ti-6%Al-4%V, ELI Grade (ELI stands for a purer grade of titanium with extra-low interstitial element concentrations, which leads to higher

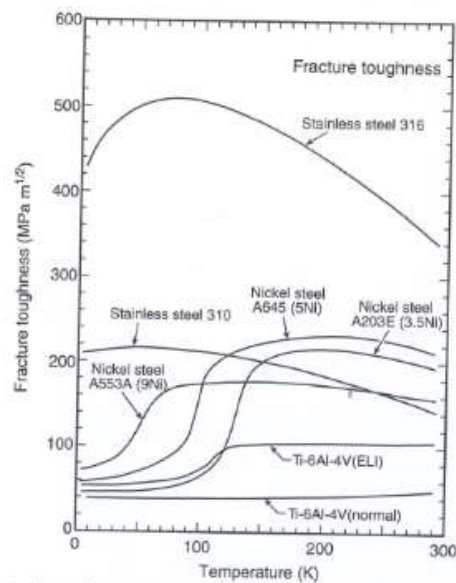


Fig. 6.20 Fracture toughness of various materials at low temperatures. Note that at low temperatures, the nickel steels (b.c.c. structure) decrease greatly in toughness and become brittle, whereas the austenitic stainless steels (f.c.c. structure) such as AISI 310 and 316 remain tough across the cryogenic temperature range. The Ti-6%Al-4%V alloys have an h.c.p. structure; their toughness drops more moderately. (Data compiled from Tobler and McHenry 1983, Mann 1978, and Fowlkes and Tobler 1976.) Tabulated data for some of these alloys are given in Appendix A.10.

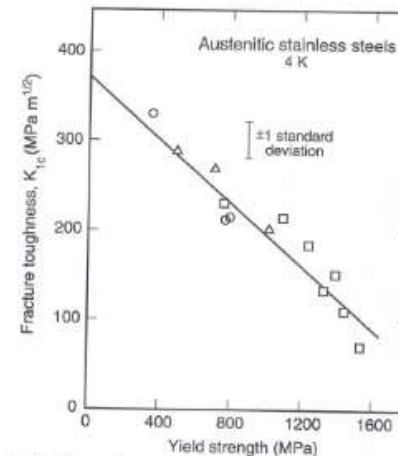


Fig. 6.21 Inverse relationship between fracture toughness and yield strength at 4 K for austenitic stainless steels (from Read and Reed 1981).

fracture toughness than for normal Ti-6%Al-4%V]. On the other hand, austenitic stainless steels are exceptionally tough. These are alloys of iron and chromium with enough nickel or manganese to stabilize the fracture-resistant f.c.c. (austenitic) crystal structure. Figure 6.20 and the tabulated data in Appendix A.10 show that the fracture toughness of austenitic AISI 310 and AISI 316 stainless steels do not exhibit a dip in toughness at low temperatures and have high strength as well. Thus, they make excellent structural materials for use at low temperatures.

Addition of nitrogen to the AISI 300 series steels increases their yield strength dramatically. For example, AISI 304 with additions of only 0.1–0.16 wt% nitrogen (designated AISI 304N), has approximately three times the yield strength of standard AISI 304 at 77 K. Furthermore, its strain-to-failure is higher at temperatures below 220 K. However, there is a trade-off: along with increased yield strength and strain-to-failure comes a significant loss in fracture toughness. Figure 6.21 shows that the toughness of austenitic stainless steels is generally *inversely proportional* to their yield strength.

How to select the appropriate material

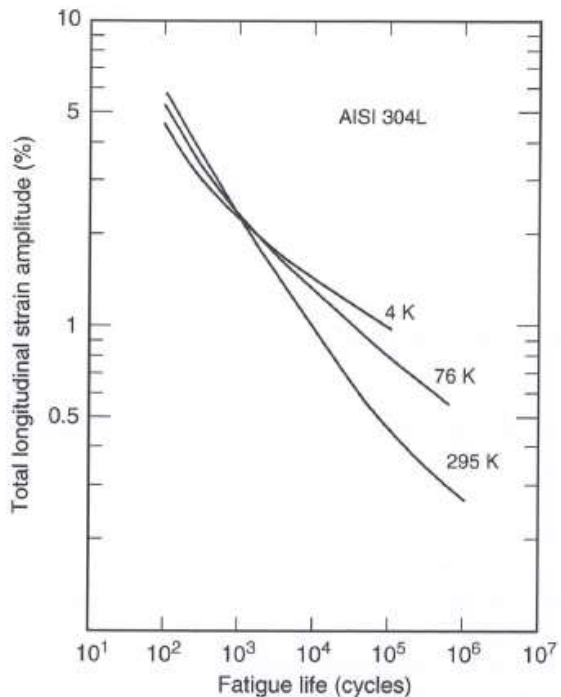


Fig. 6.22 Strain-cycling fatigue curves for AISI type 304L austenitic stainless steel at 295, 76, and 4 K (from Nachtigall 1975).

6.6.4 CREEP

Creep (plastic flow of a material) may occur when a material is subjected to a constant load over a long period. Generally, creep is not a significant factor at cryogenic temperature, except possibly at stresses exceeding the yield strength. Even soft materials that normally creep at room temperature (such as Pb–Sn solder or indium) have negligible creep at liquid-nitrogen temperature because there the thermal energy is insufficient to activate deformation and plastic flow.

How to select the appropriate material

6.6.5 MECHANICAL PROPERTIES OF TECHNICAL MATERIALS: SYNOPSIS

We described above each of the main mechanical properties that enter into selecting materials for cryostat construction and presented a wide range of material data for each property. Here, we sort the information differently and conclude this section by summarizing the salient mechanical properties for each group of materials:

Copper and aluminum: These f.c.c. metals remain ductile at low temperatures and, in pure annealed form, have very low strength. However, when alloyed, their strength increases remarkably, especially for compositions that precipitation-harden when given a heat treatment, as illustrated in Fig. 6.17 for the pure and alloyed forms of aluminum and copper.

Steels: Remember that although b.c.c. materials such as 9-nickel steel are the structural champions at room temperature, they become brittle at low temperatures and fracture at low strain. The f.c.c. austenitic stainless steels, on the other hand, generally remain ductile at low temperatures. However, be aware that the f.c.c. austenitic phase is *metastable* in most of these alloys, and so the common stainless-steel materials (such as AISI 304, 310, and 316) can partially transform to a b.c.c. or h.c.p. martensitic phase when cooled, deformed, or welded (Reed 1983). If this happens, the alloy becomes stronger, but less tough. Also the martensitic crystal phase that is formed is magnetic, raising the magnetic susceptibility of these materials considerably, which might be a concern in magnetic fields (Sec. 6.5). Among the austenitic stainless steels, AISI 310 and 316 stainless-steel alloys are less likely to transform at low temperatures (Appendix A6.8c) and so are preferable to AISI 304, but they are not as readily available commercially. AISI 310 and 316 are excellent cryogenic structural materials, especially for compositions with high nitrogen (N) and low carbon (L) (Appendix A6.9), which give superior strength and corrosion resistance. The modified compositions are usually designated by adding an L and/or an N after the AISI type number; that is AISI 316LN. Unfortunately, the L and N grades are even less available commercially than the 310 and 316 alloys.

Titanium: Titanium and titanium alloys are sometimes preferred structural materials for cryogenic service because of their high strength, low thermal conductivity, and low thermal contraction. Also, they have a magnetic susceptibility much lower than that of stainless steel. However, because of their h.c.p. crystal structure, the toughness of very high-strength titanium alloys (the ELI grades in Fig. 6.20) can decrease severely around 77 K. The more useful materials include Ti-6%Al-4%V and Ti-5%Al-2.5%Sn alloys, along with commercially pure titanium. The yield strengths of Ti-6%Al-4%V and commercial, unalloyed titanium

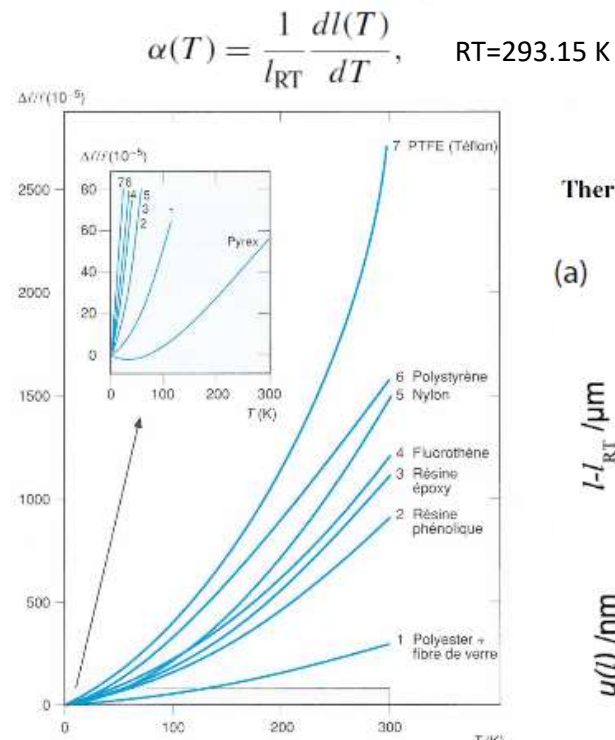
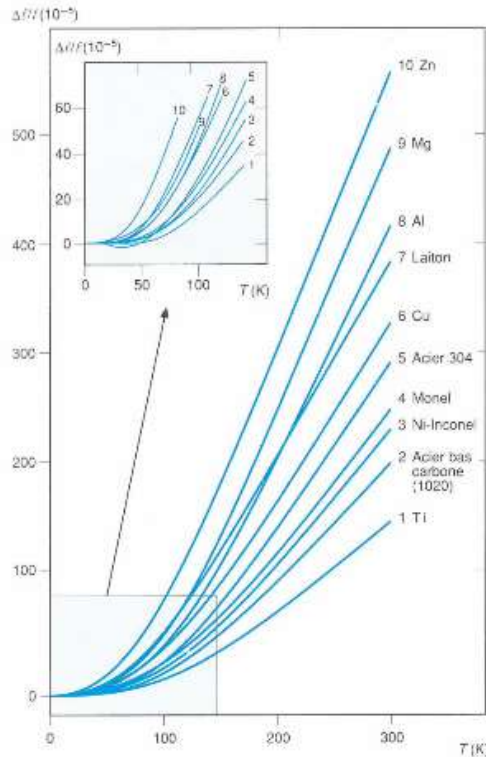
are shown in Fig. 6.17 (Ti-5Al-2.5Sn, which is not shown, has a temperature dependence similar to that of Ti-6%Al-4%V, but about 20% lower).

Polymers: Polymers have cryogenic strengths well below those of the common structural materials, as illustrated in Fig. 6.19. They are usually characterized by a glass transition temperature T_g below which they lose ductility. Commonly observed values of T_g range from 220–370 K. Polymers can exist in either amorphous or crystalline states. Crystalline polymers usually have more strength than amorphous polymers, but become extremely brittle below T_g .

Glasses: Glasses have an amorphous structure with local order, but no long-range crystalline order. At high temperatures (800 K and above) they behave as viscous liquids, flowing gradually under applied stress, but their lack of long-range crystalline order inhibits the formation and motion of dislocations at low temperatures, where they are extremely brittle. Although, theoretically, the strength of glasses can be extremely high, around 10 GPa(!), their lack of ductility makes them very susceptible to scratches and other stress concentrators at the surface. As a result, their failure stresses are extremely variable, with a minimum of only about 35 MPa. In compression, glass is quite strong, with failure believed to be initiated by the presence of tensile components of stress that cannot be eliminated. The strength of glasses usually increases down to liquid-nitrogen temperature. Be aware that glasses may fracture from thermal stresses on rapid cooling because of their low thermal conductivity, which results in nonuniform contraction and internal stresses. Fatigue damage usually does not accumulate in glasses because of their elastic, brittle nature.

(*Sticky stuff*—useful tapes, adhesives, glues, and materials for tying things down at cryogenic temperatures are listed in Appendix A3.10.)

The austenitics **stainless steels** such as 304 (1.4301) and 316 (1.4401) are however 'tough' at **cryogenic** temperatures and can be classed a '**cryogenic steels**'.



Thermal Expansion

Thermal expansion coefficient of single-crystal silicon from 7 K to 293 K

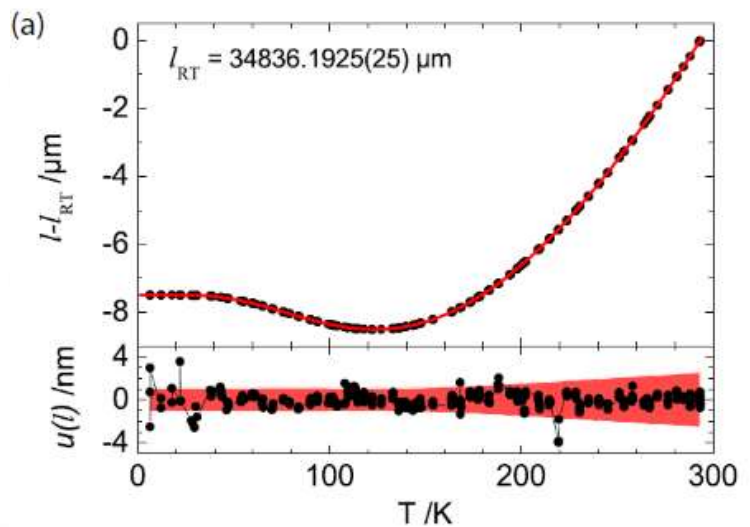
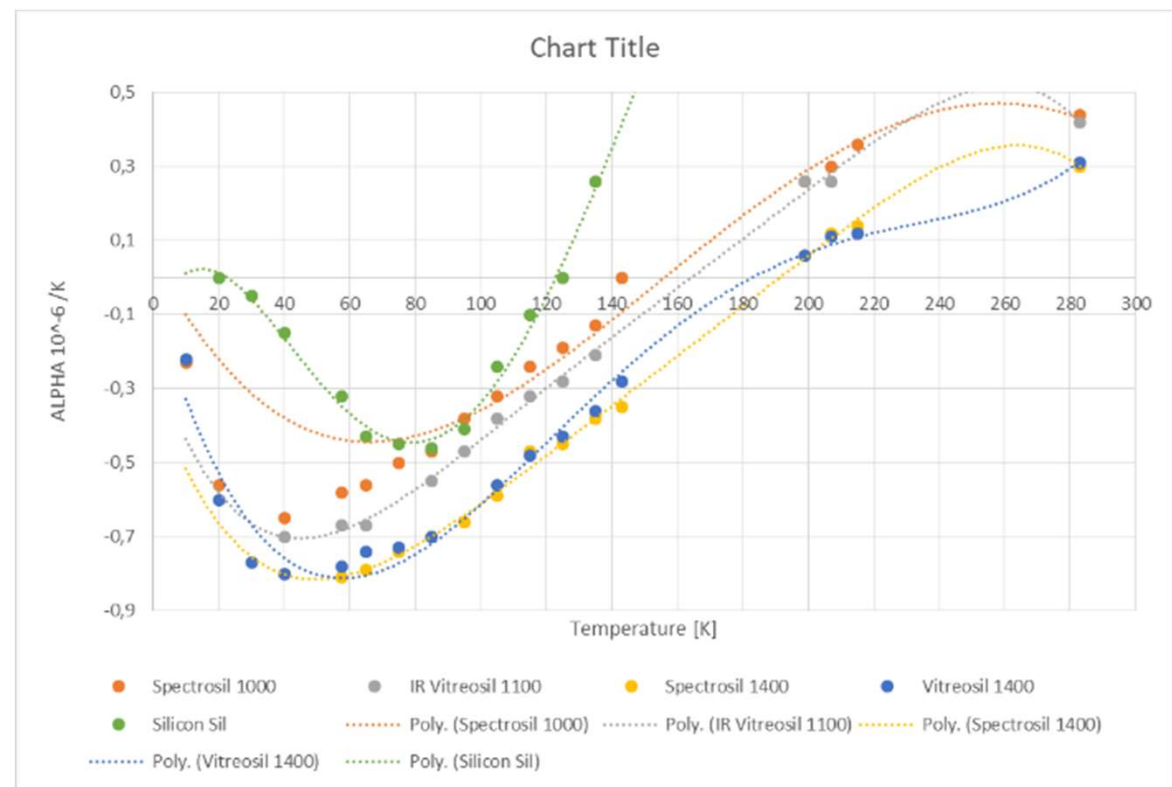


Fig. C. – Dilatation thermique linéaire moyenne de quelques métaux et plastiques [Conte].

THERMAL EXPANSION

10		-0,23			-0,22	
20		-0,56			-0,6	0
30		0,67			-0,77	-0,05
40		-0,65	-0,7	-0,8	-0,8	-0,15
57,5		-0,58	-0,67	-0,81	-0,78	-0,32
65		-0,56	-0,67	-0,79	-0,74	-0,43
75		-0,5		-0,74	-0,73	-0,45
85		-0,47	-0,55	-0,7	-0,7	-0,46
95		-0,38	-0,47	-0,66		-0,41
105		-0,32	-0,38	-0,59	-0,56	-0,24
115		-0,24	-0,32	-0,47	-0,48	-0,1
125		-0,19	-0,28	-0,45	-0,43	0
135		-0,13	-0,21	-0,38	-0,36	0,26
143		0		-0,35	-0,28	
199		0,26	0,26	0,06	0,06	1,38
207		0,3	0,26	0,12	0,11	1,56
215		0,36		0,14	0,12	
283		0,44	0,42	0,3	0,31	2,35



THERMAL EXPANSION

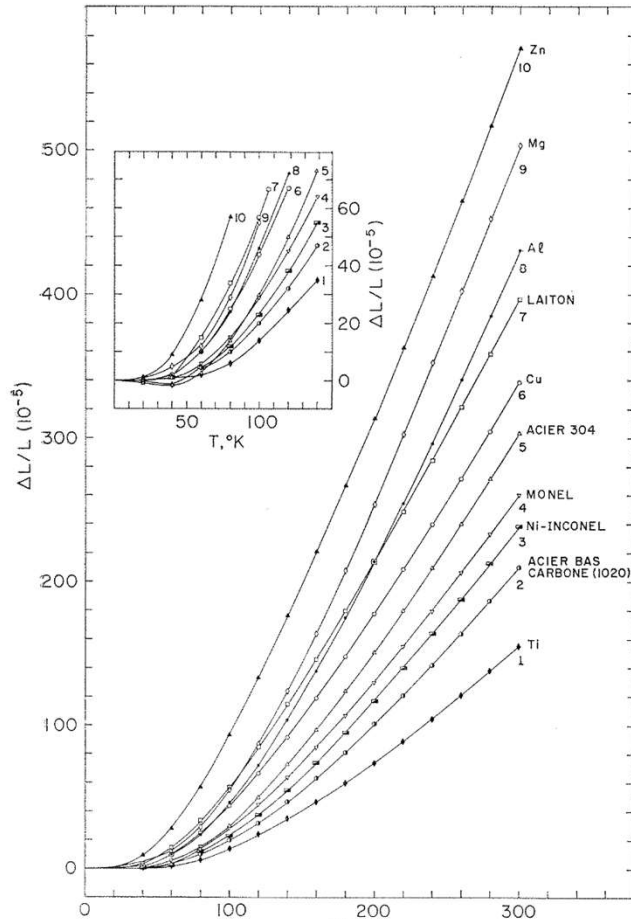


FIG. 2-41. — Dilatation thermique linéaire moyenne de quelques métaux (117).

$$\Delta L/L = \frac{L_T - L_0}{L_0}$$

Tableau II-35. — COEFFICIENT DE DILATATION THERMIQUE LINÉAIRE $\frac{1}{L} \cdot \frac{dL}{dT}$
(cm/cm °K) $\times 10^{-5}$ (116)

Matériaux	Température °K										
	10	20	40	60	80	100	120	140	200	240	300
Aluminium	-0,005	0,02	0,22	0,55	0,91	1,22	1,46	1,65	2,00	2,15	2,32
Béryllium		0,001	0,007	0,02	0,06	0,13	0,22	0,34	0,71	0,92	1,14
Laiton	0,001	0,05	0,37	0,76	1,06	1,29	1,44	1,54	1,74	1,81	1,91
Cuivre	0,004	0,03	0,23	0,55	0,84	1,05	1,20	1,32	1,52	1,59	1,68
Inconel	—	0,003	0,10	0,28	0,48	0,65	0,79	0,91	1,12	1,20	1,30
Indium	0,2	0,7	1,70	2,04	2,24	2,39	2,52	2,63	2,86	3,01	3,22
Monel	0,003	0,02	0,14	0,34	0,57	0,75	0,89	0,99	1,20	1,29	1,39
Acier 304	0,001	0,002	0,11	0,43	0,75	0,96	1,09	1,20	1,40	1,49	1,60
Acier 1020	—	0,001	0,08	0,23	0,40	0,55	0,68	0,78	0,99	1,08	1,19
Magnésium	0,005	0,04	0,33	0,81	1,22	1,54	1,76	1,94	2,32	2,44	2,55

THERMAL EXPANSION

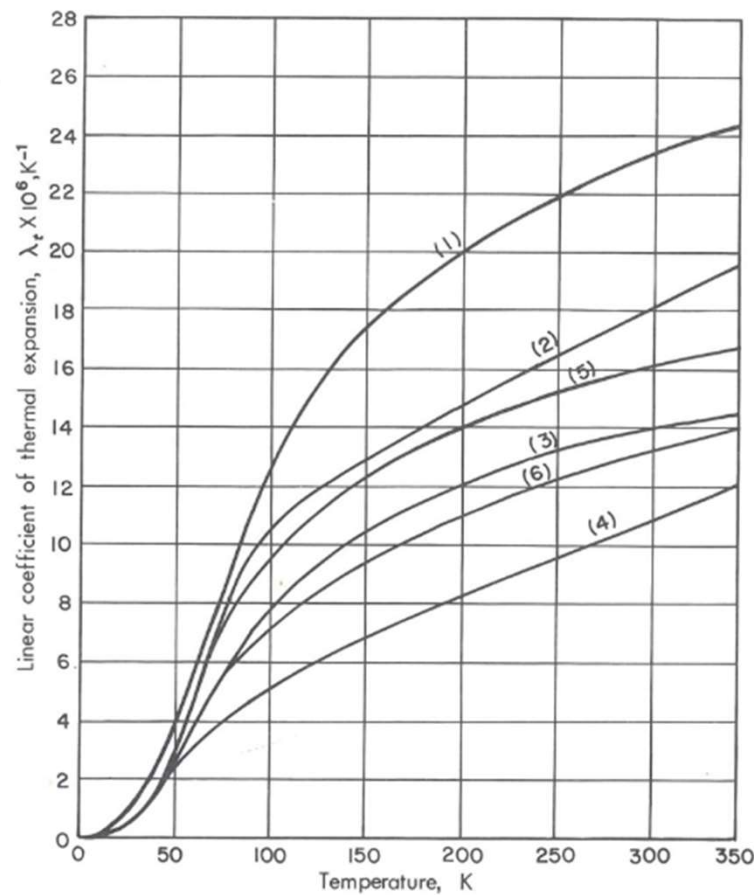


Fig. 2.10. Linear coefficient of thermal expansion for several materials at low temperature:
 (1) 2024-T4 aluminum; (2) beryllium copper; (3) K Monel; (4) titanium; (5) 304 stainless steel; (6) C1020 carbon steel (NBS Monograph 29, Thermal Expansion of Solids at Low Temperatures).

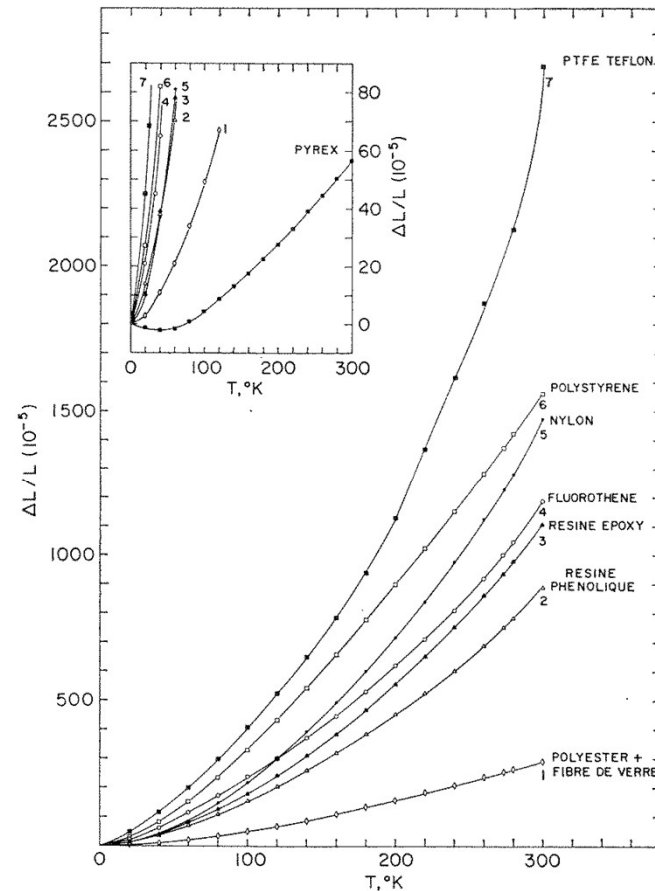


FIG. 2-42. — *Dilatation thermique linéaire moyenne de quelques plastiques.*

$$\Delta L/L = \frac{L_T - L_0}{L_0}$$

THERMAL EXPANSION

Table 7.18. Unit thermal expansion for several solids (Corruccini and Gniewek 1961).

$$e_t = \Delta L/L = \int_0^T \lambda_t dT; \text{ multiply the numbers in the table by } 10^{-5}$$

SS 304: $(307-17)/307=0.945$

Al: $(431-24)/431=0.944$

Temperature (K)	Beryllium Copper	Aluminum	1020 Steel	304 Stainless	Monel	Invar	Yellow Brass	Plexiglass	Teflon	Pyrex Glass	Nylon	Polystyrene
0	0	0	0	0	0	0	0	0	0	0	0	0
20	0	0	0	0	0	0	1	15	30	-1.0	10	28
40	1	2	1	0	1	0	4	60	80	-2.0	37	84
50	3	5	2	2	3	0	9	83	109	-1.9	58	118
60	7	10	4	5	6	0	16	110	140	-1.5	81	156
70	12	16	7	11	10	1	24	136	176	-0.6	110	196
80	20	24	10	17	15	2	34	170	210	+1.0	142	242
90	29	34	15	25	21	3	45	196	250	2.8	177	286
100	39	45	20	35	28	5	58	230	290	4.5	217	339
120	61	72	32	55	45	9	85	290	380	8.5	301	445
140	85	103	47	78	64	13	115	360	480	13.0	393	558
160	110	138	64	103	84	18	147	440	600	17.5	493	676
180	137	175	82	129	107	23	180	530	740	22.5	600	798
200	165	214	101	157	130	29	215	630	900	27.5	716	924
250	242	318	155	229	193	41	304	915	1390	41.7	1050	1250
300	329	431	210	307	261	54	397	1275	1600	57.0	1450	1601

THERMAL EXPANSION

Table 7.18. Unit thermal expansion for several solids (Corruccini and Gniewek 1961).

$$e_t = \Delta L/L = \int_0^T \lambda_t dT; \text{ multiply the numbers in the table by } 10^{-5}$$

Temperature (K)	Beryllium Copper	Aluminum	1020 Steel	304 Stainless	Monel	Invar	Yellow Brass	Plexiglass	Teflon	Pyrex Glass	Nylon	Polystyrene
0	0	0	0	0	0	0						
20	0	0	0	0	0	0						
40	1	2	1	0	1							
50	3	5	2	2	3							
60	7	10	4	5	6							
70	12	16	7	11	10							
80	20	24	10	17	15							
90	29	34	15	25	21							
100	39	45	20	35	28							
120	61	72	32	55	45							
140	85	103	47	78	64							
160	110	138	64	103	84							
180	137	175	82	129	107							
200	165	214	101	157	130							
250	242	318	155	229	193							
300	329	431	210	307	261							

Thermal expansion

Temperature [K]	SS 304 (Blue) $\Delta L/L \times 10^{-5}$	Al (Orange) $\Delta L/L \times 10^{-5}$
0	0	0
50	~10	~10
100	~50	~50
150	~100	~100
200	~150	~150
250	~200	~200
300	~250	~250

THERMAL EXPANSION

Table 7.18. Unit thermal expansion for several solids (Corruccini and Gniewek 1961).

$$e_t = \Delta L/L = \int_0^T \lambda_t dT; \text{ multiply the numbers in the table by } 10^{-5}$$

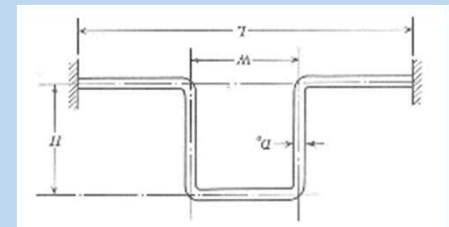
Temperature (K)	Beryllium Copper	Aluminum	1020 Steel	304 Stainless	Monel
0	0	0	0	0	0
20	0	0	0	0	0
40	1	2	1	0	1
50	3	5	2	2	3
60	7	10	4	5	6
70	12	16	7	11	10
80	20	24	10	17	15
90	29	34	15	25	21
100	39	45	20	35	28
120	61	72	32	55	45
140	85	103	47	78	64
160	110	138	64	103	84
180	137	175	82	129	107
200	165	214	101	157	130
250	242	318	155	229	193
300	329	431	210	307	261

Calculate the contraction of a cryogenic transfer line 10 m long, when cooled from 300 K to 4 K.

From table: $L(300)-L(4)/L(300) = (307-17) \times 10^{-5} \times 10 \text{ m} = 0.029 \text{ m} = 2.9 \text{ cm!!}$

If it were Aluminium $(431-24) \times 10^{-5} \times 10 \text{ m} = 0.041 \text{ m} = 4.1 \text{ cm}$

The anchorage point cannot usually stand the equivalent force: in order to compensate one can insert compensation boxes where the *lyra pipe* shape is adopted.



As an alternative bellows can be welded in the appropriate locations, even though bellows, being a weak part, should be, when possible, avoided in cryogenics.

PROPRIETA' DEI MATERIALI:

- Entalpia (Temperatura di Debye)
- Scelta del materiale
- Contrazione termica
- Conducibilita' termica

TRASMISSIONE DEL CALORE

- Nei solidi
- Nei gas
- Irraggiamento
- Isolamento termico
- Cenni di crio-pompaggio
- Current Leads (discendenti di corrente)

LINEE DI TRASFERIMENTO

- Caduta di pressione
- Termosifone
- Pompe di circolazione
- Valvole criogeniche
- Giunzioni a bassa temperatura
- Dimensionamento di valvole di sicurezza

HEAT CONDUCTION IN SOLIDS (FOURIER LAW)

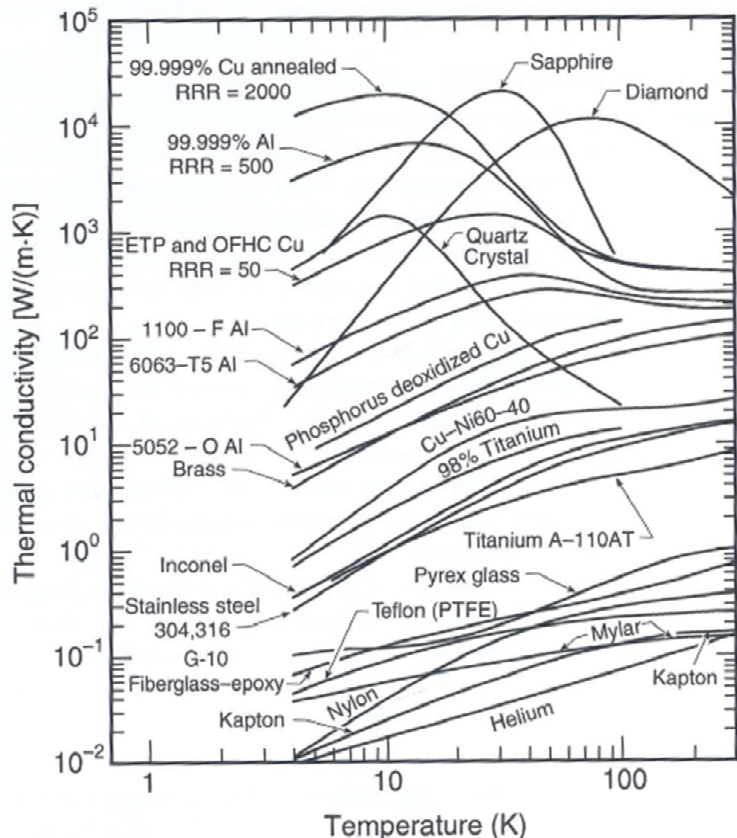


Fig. 2.1 Thermal conductivity of some common solids as a function of temperature (compiled from data in Radebaugh et al. 2001, Johnson 1960, White and Meeson 2002, and *Cryo. Mat. Prop. Prog.* 2001). Tabulated data for these and additional materials are given in Appendix A6.7.

$$\dot{q}_{\text{cond}} = A/L \int_{T_1}^{T_2} \lambda(T) dT = (A/L) \bar{\lambda} \Delta T,$$

$$\bar{\lambda} \equiv \Delta T^{-1} \int_{T_1}^{T_2} \lambda(T) dT, \quad \text{Mean thermal conductivity}$$

Strong dependence on temperature: but since

$$\nabla \cdot \nabla \int_{T_1}^{T_2} \lambda(T) dT = 0 \quad \nabla^2 \int_{T_1}^{T_2} \lambda(T) dT = 0$$

Then it exists a potential, and:

$$\dot{q}_{\text{cond}} = A/L \int_{T_1}^{T_2} \lambda(T) dT = A/L \left[\int_{4 \text{ K}}^{T_2} \lambda(T) dT - \int_{4 \text{ K}}^{T_1} \lambda(T) dT \right].$$

HEAT CONDUCTION IN SOLIDS

Thermal Conductivity Integrals

T[K]	ETP*	$\int_{\text{de}}^{\infty} \lambda dT$ [kW/m]						[W/m]				
		Copper	Copper alloys		Aluminum		Stainless steel	Constantan	Glass	Polymer		
6	0.80	0.0176	0.0047	0.00196	0.138	0.0275	0.0103	0.00063	0.0024	0.211	0.113	0.118
8	1.91	0.0437	0.0113	0.00524	0.342	0.0670	0.025	0.00159	0.0066	0.443	0.262	0.238
10	3.32	0.0785	0.0189	0.010	0.607	0.117	0.0443	0.00293	0.0128	0.681	0.44	0.359

15	8.02	0.208	0.0499	0.030	1.52	0.290	0.112	0.00816	0.0375	1.31	0.985	0.669
20	14.0	0.395	0.0954	0.0613	2.76	0.534	0.210	0.0163	0.0753	2.00	1.64	1.81
25	20.8	0.635	0.155	0.102	4.24	0.850	0.338	0.0277	0.124	2.79	2.39	1.44
30	27.8	0.925	0.229	0.153	5.92	1.23	0.490	0.0424	0.181	3.68	3.23	1.96
35	34.5	1.26	0.316	0.211	7.73	1.67	0.668	0.0607	0.244	4.71	4.13	2.59
40	40.6	1.64	0.415	0.275	9.62	2.17	0.770	0.0824	0.312	5.86	5.08	3.30
50	50.8	2.53	0.650	0.415	13.4	3.30	1.24	0.135	0.457	8.46	7.16	4.95
60	58.7	3.55	0.930	0.568	17.0	4.55	1.79	0.198	0.612	11.5	9.36	6.83
70	65.1	4.68	1.25	0.728	20.2	5.89	2.42	0.270	0.775	15.1	11.6	8.85
76	68.6	5.39	1.46	0.826	22.0	6.73	2.82	0.317	0.875	17.5	15.0	10.1
80	70.7	5.89	1.60	0.893	23.2	7.38	3.09	0.349	0.943	19.4	13.9	11.0
90	75.6	7.20	1.99	1.060	25.8	8.71	3.82	0.436	1.11	24.0	16.3	13.2
100	80.2	8.58	2.40	1.23	28.4	10.2	4.59	0.528	1.28	29.2	18.7	15.5
120	89.1	11.5	3.30	1.57	33.0	13.2	6.27	0.726	1.62	40.8	23.7	20.0
140	97.6	14.6	4.32	1.92	37.6	16.2	8.11	0.939	1.97	54.2	28.7	24.7
160	109	18.0	5.44	2.29	42.0	19.4	10.1	1.17	2.32	69.4	33.8	29.4
180	114	21.5	6.64	2.66	46.4	22.5	12.3	1.41	2.69	85.8	39.0	34.2
200	122	25.3	7.91	3.06	50.8	25.7	14.4	1.66	3.06	103.0	44.2	39.0
250	142	35.3	11.3	4.15	61.8	33.7	20.5	2.34	4.06	150.0	57.2	51.0
300	162	46.1	15.0	5.32	72.8	41.7	27.1	3.06	5.16	199.0	70.2	63.0

Sources
V. Johnson (1960), NBS Wright Air Development Div. (WADD) Technical Report 60-56, Part II, US Government Printing Office, Washington, D.C..

D. H. J. Goodall (1970), APT Division, Culham Science Center, Abingdon, Oxfordshire, UK.

*The high thermal conductivity of nearly pure metals is variable and strongly depends on their impurity content; see Sec. 6.4.2.

For pure metals Wiedemann-Franz law (ρ is the electrical resistivity):

$$\lambda \approx L_N T / \rho, \quad (2.4)$$

where L_N is the Lorenz number, $2.44 \times 10^{-8} \text{ V}^2/\text{K}^2$. (This is described in more detail in

HEAT CONDUCTION IN SOLIDS

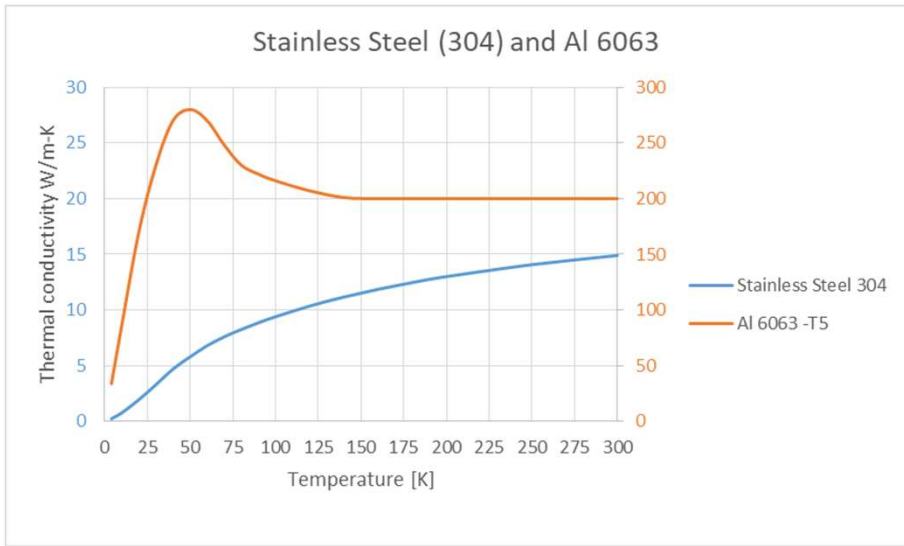
Tableau E. – Valeurs de l'intégrale $\int_{4,2}^T k(T) dT$ pour quelques matériaux.

Matériau	T (K)	6	8	10	15	20	60	80	300
Conducteurs (en W/cm)									
Cuivre extra-pur	166	382	636	1270	1790	2960	3090	4000	
Cuivre électroécroui	8,0	19,1	33,2	80,2	140	587	707	1620	
Argent	320	670	990	1610	1980	2570	2670	3570	
Aluminium extra-pur	73	168	280	600	907	1740	1840	2390	
Aluminium du commerce	1,38	3,42	6,07	15,2	27,6	170	232	728	
Or	41	93	149	274	364	612	682	1370	
Laiton	0,0531	0,129	0,229	0,594	1,12	10,4	17,7	172	
Plomb (normal)	27,0	37,3	42,4	49,0	52,5	73,8	81,3	160	
Titane	0,115	0,277	0,488	1,21	2,20	15,5	22,6	99,6	
Monel	0,0235	0,0605	0,112	0,315	0,618	5,23	8,24	52,5	
Acier inoxydable	0,0063	0,0159	0,0293	0,0816	0,163	1,98	3,49	30,6	
Isolants (en mW/cm)									
Verre	2,11	4,43	6,81	13,1	20,0	115	194	1990	
Téflon	1,13	2,62	4,4	9,85	16,4	93,6	139	702	
Plexiglas	1,18	2,38	3,59	6,69	10,1	68,3	110	630	
Nylon	0,321	0,807	1,48	4,10	8,23	85,9	142	895	

HEAT CONDUCTION IN SOLIDS

Table 7.9. Thermal conductivity (k_t , W/m-K) and thermal conductivity integral (K , W/m) for selected materials (Stewart and Johnson 1961) $K = \int_{4K}^T k_t dT$

Temperature (K)	Low-Carbon											
	Beryllium Copper		Aluminum (6063-T5)		Steel (C1020)		Stainless Steel (304)		Monel (drawn)		Teflon	
	k_t	K	k_t	K	k_t	K	k_t	K	k_t	K	k_t	K
4	1.9	0	34	0	3.0	0	0.24	0	0.43	0	0.046	0.0
10	4.8	19	86	360	11.5	43	0.77	2.9	1.74	6.3	0.096	0.44
20	10.6	95	170	1,650	24.0	222	1.95	16.3	4.30	36.4	0.141	1.64
30	16.2	229	230	3,650	32.0	502	3.30	42.4	6.90	92.9	0.174	3.23
40	21.0	415	270	6,200	38.6	867	4.70	82.4	9.00	173	0.193	5.08
50	26.1	650	280	8,950	47.6	1,310	5.80	135	10.95	273	0.208	7.16
60	30.0	930	270	11,700	53.6	1,810	6.80	198	12.09	368	0.219	9.36
70	33.7	1,250	248	14,300	57.5	2,360	7.60	270	13.06	513	0.228	11.6
80	37.0	1,600	230	16,700	60.0	2,950	8.26	349	13.90	647	0.235	13.9
90	40.1	1,990	222	19,000	61.8	3,550	8.86	436	14.63	791	0.241	16.3
100	43.0	2,400	216	21,100	62.9	4,170	9.40	528	15.27	940	0.245	18.7
120	48.4	3,300	207	25,300	64.1	5,450	10.36	726	16.26	1,260	0.251	23.7
140	53.3	4,320	201	29,300	64.6	6,750	11.17	939	17.34	1,590	0.255	28.7
160	57.6	5,440	200	33,300	64.8	8,050	11.86	1,170	18.25	1,950	0.257	33.8
180	61.5	6,640	200	37,300	64.9	9,350	12.47	1,410	19.02	2,320	0.258	39.0
200	65.0	7,910	200	41,300	65.0	10,700	13.00	1,660	19.69	2,710	0.259	44.2
250	72.4	11,300	200	51,300	65.0	13,900	14.07	2,340	21.02	3,730	0.260	57.2
300	78.5	15,000	200	61,300	65.0	17,200	14.90	3,060	22.00	4,800	0.260	70.2

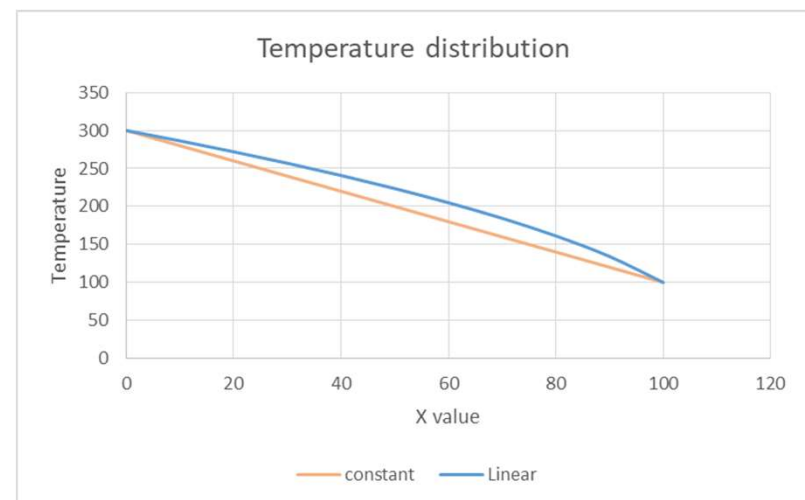


K	SS 304	Al 6063
4,00	0,24	34
10,00	0,77	86
20,00	1,95	170
30,00	3,3	230
40,00	4,7	270
50,00	5,8	280
60,00	6,8	270
70,00	7,6	248
80,00	8,26	230
90,00	8,86	222
100,00	9,4	216
120,00	10,36	207
140,00	11,17	201
160,00	11,86	200
180,00	12,47	200
200,00	13	200
250,00	14,07	200
300,00	14,9	200

HEAT CONDUCTION IN SOLIDS

Case (i): $k(T)$ const (e.g. Al from 300 K to 130 K)
 => Linear temperature distribution

Case (ii): $k(T)$ linear (e.g. SS from 300 K to 130 K)
 => Parabolic temperature distribution



$$\frac{\partial}{\partial x} \left(k \cdot \frac{\partial T}{\partial x} \right) = 0 \quad \text{if: } \lambda(T) = k = \text{constant}$$

$$k \cdot \frac{\partial T}{\partial x} = C_1 \quad k \cdot T = C_1 x + C_2$$

$$\text{If } x = 0 \quad T = T_0 \quad \text{if } x = L \quad T = T_L$$

$$\text{If } x = 0 \quad k \cdot T_0 = C_2$$

$$\text{If } x = L \Rightarrow k T_L = C_1 L + k T_0 \quad C_1 = k \cdot \frac{T_L - T_0}{L}$$

$$k \cdot T = k \cdot \frac{T_L - T_0}{L} x + k \cdot T_0 \Rightarrow \quad \color{red} T = \frac{T_L - T_0}{L} x + T_0$$

$$\frac{\partial}{\partial x} \left(\frac{T}{a} \cdot \frac{\partial T}{\partial x} \right) = 0 \quad \text{if: } \lambda(T) = \frac{T}{a}$$

Prima integrazione: $\frac{T}{a} \cdot \frac{\partial T}{\partial x} = C_1$

Separazione delle variabili $T \partial T = C_1 \cdot a \cdot \partial x$

Seconda integrazione $\frac{1}{2} T^2 = C_1 a x + C_2$

Condizioni al contorno: $x = 0: T = T_o; \quad x = L: T = T_L$

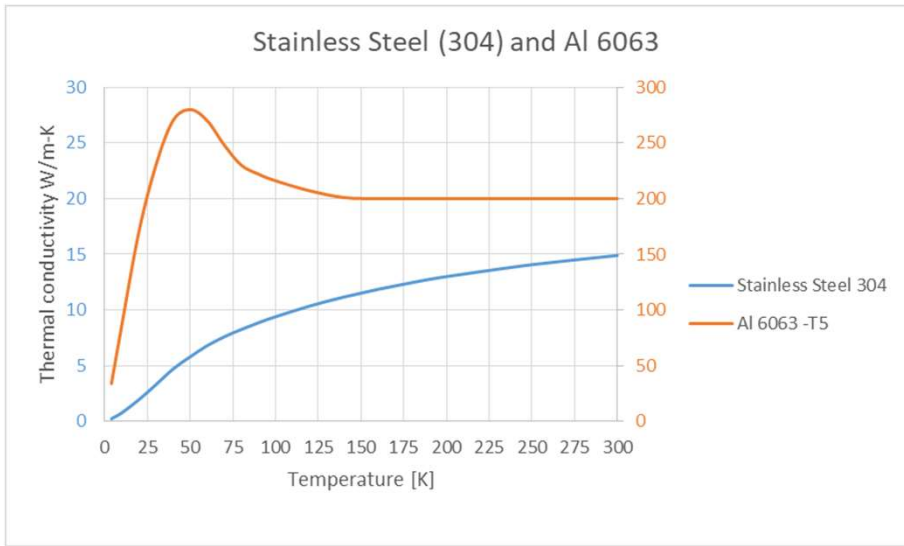
$x = 0: \frac{1}{2} T_o^2 = C_2; \quad x = L: \frac{1}{2} T_L^2 = C_1 a L + \frac{1}{2} T_o^2$

$$C_1 = \left(\frac{1}{2} T_L^2 - \frac{1}{2} T_o^2 \right) / a L = \frac{T_L^2 - T_o^2}{2 a L}$$

$$\frac{1}{2} T^2 = C_1 a x + C_2; \quad T^2 = 2 C_1 a x + 2 C_2$$

$$= 2 \frac{T_L^2 - T_o^2}{2 a L} a \cdot x + \frac{1}{2} T_o^2 \cdot 2$$

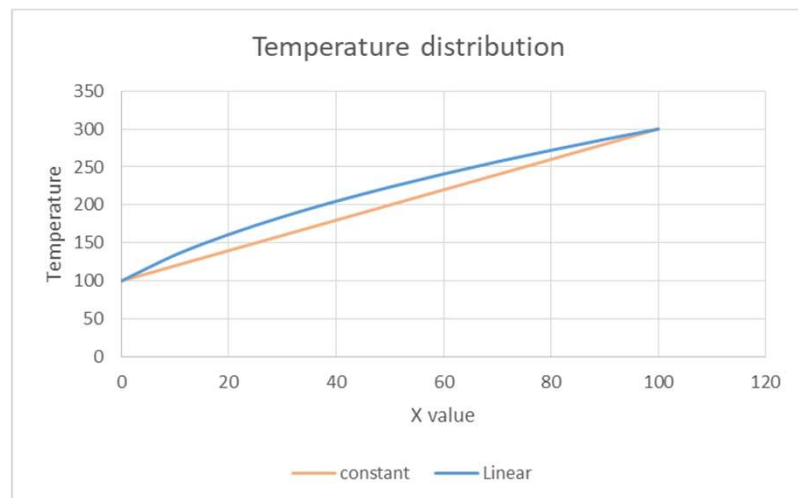
$$T^2 = \frac{T_L^2 - T_o^2}{L} x + T_o^2; \quad T = \sqrt{T_o^2 + \frac{T_L^2 - T_o^2}{L} x}$$



HEAT CONDUCTION IN SOLIDS

Case (i): $k(T)$ const (e.g. Al from 300 K to 130 K)
=> Linear temperature distribution

Case (ii): $k(T)$ linear (e.g. SS from 300 K to 130 K)
=> Parabolic temperature distribution



HEAT CONDUCTION IN SOLIDS

Let us now consider once again the case of a beam of area A and length L , as illustrated in Fig. 8, where heat is transferred along x , and where an internal energy is deposited inside its volume.

**Ref: Cryostat Design,
V. Parma, CERN-2014-005**

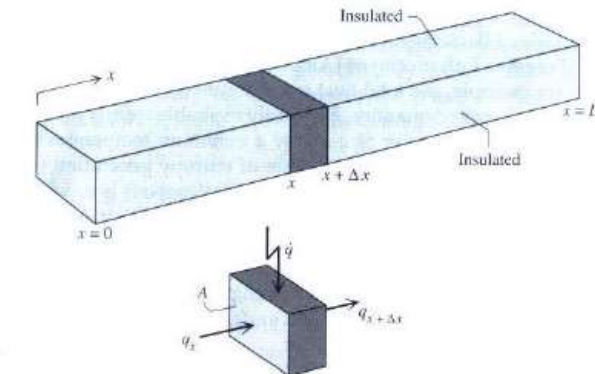


Fig. 7: One-dimension solid beam, with heat deposition \dot{q} and conduction heat flux along x

We can write the energy balance equation for an element $x + \Delta x$, introduce Fourier's law describing longitudinal heat transfer, and introduce the change of internal energy related to the heat capacity of the element as:

$$\frac{\partial}{\partial x} \left(k \cdot \frac{\partial T}{\partial x} \right) + \dot{q} = \rho c \frac{\partial T}{\partial t} \quad (6)$$

where the first term represents longitudinal conduction, \dot{q} is the internal heat deposited, and the term on the right-hand side represents the thermal inertia of the element related to its heat capacity (ρ is the density and c is the specific heat capacity).

If k is considered constant (valid for small changes of T), we can rewrite the equation as:

$$\frac{\partial^2 T}{\partial x^2} + \frac{\dot{q}}{k} = \frac{1}{\alpha} \frac{\partial T}{\partial t} \text{ with } \alpha = \frac{k}{\rho c}. \quad (7)$$

HEAT CONDUCTION IN SOLIDS

Thermal diffusivity α indicates how fast a thermal perturbation develops along the beam. A few cases of special interest are detailed below.

3.1.1 Steady-state beam with no heating

Of particular interest is the steady-state case ($\partial T / \partial t = 0$) in which there is no internal heat deposition ($\dot{q} = 0$). This is, for example, the case for any solid element having its extremities fixed in temperature (T_0 and T_L). Equation (6) is then simply re-written:

$$\frac{\partial}{\partial x} \left(k(T) \cdot \frac{\partial T}{\partial x} \right) = 0. \quad (8)$$

We can distinguish two cases of interest:

- (i) k is constant. By integrating and imposing the boundary conditions at the extremities, we find a linear temperature profile along the beam, given by:

$$T = T_0 + \frac{(T_L - T_0)}{L} \cdot x \quad (9)$$

and a constant heat flux along the beam, given by:

$$\dot{q} = k \cdot \frac{A}{L} (T_L - T_0); \quad (10)$$

- (ii) k is linear with T (in the example of impure metals, like steels and Al alloys). Let us assume $k = T/a$. By integrating and imposing the boundary conditions at the tips, we find a quadratic temperature profile along the beam, given by:

$$T = \sqrt{T_0^2 + \frac{T_L^2 - T_0^2}{L}} \cdot x \quad (11)$$

and a constant heat flux along the beam, given by:

$$\dot{q} = \frac{1}{2} \frac{A}{L} \cdot \frac{(T_L^2 - T_0^2)}{a}. \quad (12)$$

**Ref: Cryostat Design,
V. Parma, CERN-2014-005**

Support of a magnet/cavity with fixed temperature at both ends (e.g. 300 K and 4 K).

HEAT CONDUCTION IN SOLIDS

3.1.2 Steady-state beam with uniform heat deposition

Another relevant case is that of a structure that is thermally connected to a heat sink at a given temperature, and which is subject to uniformly distributed heating (Fig. 9). This is the case, for example, of a thermal shield that is actively cooled by a cryogenic line at a fixed temperature at one point, and on which radiation heat is uniformly distributed and transferred through solid conduction from the hottest point to the cooling point.

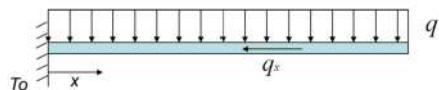


Fig. 9: Uniformly heated beam, cooled at one tip

Let L be the beam length, t its thickness, and w its width (perpendicular to the page). The beam is cooled at T_0 in $x = 0$. The uniform heat deposition along the beam is q (W m^{-2}).

Equation (6) can be re-written as:

$$\frac{d}{dx} \left(k(T) \cdot \frac{dT}{dx} \right) + \frac{q}{t} = 0. \quad (13)$$

Considering k to be constant (which is usually the case for thermal shields, as they should be designed to be quasi-isothermal), the equation can be integrated to yield the following temperature profile and heat flux along x :

$$T(x) = T_0 - \frac{q}{2 \cdot k(T)} \cdot x^2 + \frac{q \cdot L}{k(T)} \cdot x, \quad (14)$$

$t = \text{thickness}$

$$\dot{q}(x) = q \cdot w(x-L). \quad (15)$$

From Eq. (14), we can deduce the maximum ΔT along the beam, which may be the design objective achieved by providing a minimum thickness t . As previously mentioned, thermal shields are normally designed to be quasi-isothermal (typically within 5–10 K). So, by resolving t as a function of ΔT_{\max} we obtain the practical design formula to choose the minimum thickness:

$$t \geq \frac{q \cdot L^2}{2k \cdot \Delta T_{\max}}. \quad (16)$$

**Ref: Cryostat Design,
V. Parma, CERN-2014-005**

Thermal shield (actively cooled) at constant temperature

HEAT CONDUCTION IN SOLIDS

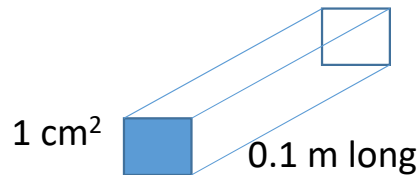
Calculate the heat transferred in Al 6063 with a cross section 1 cm^2 and a length of 0.1 m, when the end surfaces are maintained at 300 K and 80 K respectively. Compare the value found by K_{average} and KdT method:

In SI:

$$L = 0.1 \text{ m}$$

$$\Delta T = (300 - 80) \text{ K} = 220 \text{ K}$$

$$A = 1 \text{ cm}^2 = 10^{-4} \text{ m}^2$$



Temperature (K)	Beryllium Copper		Aluminum (6063-T5)	
	k_t	K	k_t	K
4	1.9	0	34	0
10	4.8	19	86	360
20	10.6	95	170	1,650
30	16.2	229	230	3,650
40	21.0	415	270	6,200
50	26.1	650	280	8,950
60	30.0	930	270	11,700
70	33.7	1,250	248	14,300
80	37.0	1,600	230	16,700
90	40.1	1,990	222	19,000
100	43.0	2,400	216	21,100
120	48.4	3,300	207	25,300
140	53.3	4,320	201	29,300
160	57.6	5,440	200	33,300
180	61.5	6,640	200	37,300
200	65.0	7,910	200	41,300
250	72.4	11,300	200	51,300
300	78.5	15,000	200	61,300

Table 7.9. Thermal conductivity (k_t , W/m-K) and thermal conductivity integral (K , W/m) for

selected materials (Stewart and Johnson 1961) $K = \int_{4K}^T k_t dT$

$$1. Q(W) = k_{\text{average}} A \Delta T / dx = [(230+200)/2] (300-80) / 0.1 \cdot 10^{-4}$$

$$= 47.3 \text{ W}$$

$$2. Q(W) = K(300) - K(80) A / L = (61300 - 16700) / 0.1 \cdot 10^{-4}$$

$$= 44.6 \text{ W}$$

HEAT CONDUCTION IN SOLIDS

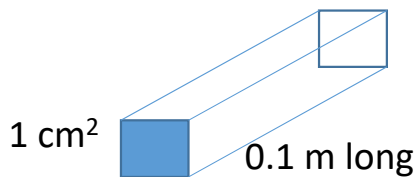
Calculate the heat transferred in Al 6063 with a cross section 1 cm^2 and a length of 0.1 m, when the end surfaces are maintained at 80 K and 4 K respectively. Compare the value found by K_{average} and $K_d T$ method:

In SI:

$$L = 0.1 \text{ m}$$

$$\Delta T = (80-4) \text{ K} = 220 \text{ K}$$

$$A = 1 \text{ cm}^2 = 10^{-4} \text{ m}^2$$



Temperature (K)	Beryllium Copper		Aluminum (6063-T5)	
	k_t	K	k_t	K
4	1.9	0	34	0
10	4.8	19	86	360
20	10.6	95	170	1,650
30	16.2	229	230	3,650
40	21.0	415	270	6,200
50	26.1	650	280	8,950
60	30.0	930	270	11,700
70	33.7	1,250	248	14,300
80	37.0	1,600	230	16,700
90	40.1	1,990	222	19,000
100	43.0	2,400	216	21,100
120	48.4	3,300	207	25,300
140	53.3	4,320	201	29,300
160	57.6	5,440	200	33,300
180	61.5	6,640	200	37,300
200	65.0	7,910	200	41,300
250	72.4	11,300	200	51,300
300	78.5	15,000	200	61,300

Table 7.9. Thermal conductivity (k_t , W/m-K) and thermal conductivity integral (K , W/m) for

selected materials (Stewart and Johnson 1961) $K = \int_{4K}^T k_t dT$

$$1. Q(W) = k_{\text{average}} A \Delta T / dx = [(230+34)/2] (80-4) / 0.1 \cdot 10^{-4}$$

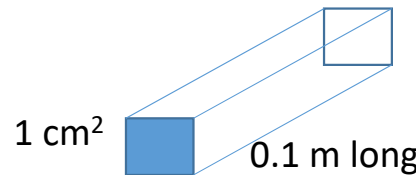
$$= 10.0 \text{ W}$$

$$2. Q(W) = K(80) - K(4) A / L = (16700 - 0) / 0.1 \cdot 10^{-4}$$

$$= 16.7 \text{ W}$$

HEAT CONDUCTION IN SOLIDS

Calculate the heat transferred in **SS 304** with a cross section 1 cm^2 and a length of 0.1 m, when the end surfaces are maintained at **300 K** and **80 K** respectively. Compare the value found by K_{average} and KdT method:



In SI:

$$L = 0.1 \text{ m}$$

$$DT = (300 - 80) \text{ K} = 220 \text{ K}$$

$$A = 1 \text{ cm}^2 = 10^{-4} \text{ m}^2$$

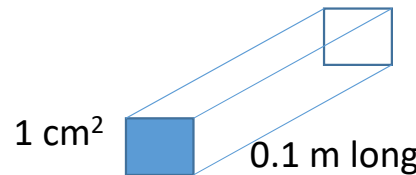
Table 7.9. Thermal conductivity (k_t , W/m-K) and thermal conductivity integral (K , W/m) for

selected materials (Stewart and Johnson 1961) $K = \int_{4K}^T k_t dT$

Temperature (K)	Beryllium Copper		Aluminum (6063-T5)		Low-Carbon Steel (C1020)		Stainless Steel (304)	
	k_t	K	k_t	K	k_t	K	k_t	K
4	1.9	0	34	0	3.0	0	0.24	0
10	4.8	19	86	360	11.5	43	0.77	2.9
20	10.6	95	170	1,650	24.0	222	1.95	16.3
30	16.2	229	230	3,650	32.0	502	3.30	42.4
40	21.0	415	270	6,200	38.6	867	4.70	82.4
50	26.1	650	280	8,950	47.6	1,310	5.80	135
60	30.0	930	270	11,700	53.6	1,810	6.80	198
70	33.7	1,250	248	14,300	57.5	2,360	7.60	270
80	37.0	1,600	230	16,700	60.0	2,950	8.26	349
90	40.1	1,990	222	19,000	61.8	3,550	8.86	436
100	43.0	2,400	216	21,100	62.9	4,170	9.40	528
120	48.4	3,300	207	25,300	64.1	5,450	10.36	726
140	53.3	4,320	201	29,300	64.6	6,750	11.17	939
160	57.6	5,440	200	33,300	64.8	8,050	11.86	1,170
180	61.5	6,640	200	37,300	64.9	9,350	12.47	1,410
200	65.0	7,910	200	41,300	65.0	10,700	13.00	1,660
250	72.4	11,300	200	51,300	65.0	13,900	14.07	2,340
300	78.5	15,000	200	61,300	65.0	17,200	14.90	3,060

HEAT CONDUCTION IN SOLIDS

Calculate the heat transferred in **SS 304** with a cross section 1 cm^2 and a length of 0.1 m, when the end surfaces are maintained at **80 K** and **4 K** respectively. Compare the value found by K_{average} and $K_d T$ method:



In SI:

$$L = 0.1 \text{ m}$$

$$\Delta T = (80-4) \text{ K} = 76 \text{ K}$$

$$A = 1 \text{ cm}^2 = 10^{-4} \text{ m}^2$$

Temperature (K)	Beryllium Copper		Aluminum (6063-T5)		Low-Carbon Steel (C1020)		Stainless Steel (304)	
	k_t	K	k_t	K	k_t	K	k_t	K
4	1.9	0	34	0	3.0	0	0.24	0
10	4.8	19	86	360	11.5	43	0.77	2.9
20	10.6	95	170	1,650	24.0	222	1.95	16.3
30	16.2	229	230	3,650	32.0	502	3.30	42.4
40	21.0	415	270	6,200	38.6	867	4.70	82.4
50	26.1	650	280	8,950	47.6	1,310	5.80	135
60	30.0	930	270	11,700	53.6	1,810	6.80	198
70	33.7	1,250	248	14,300	57.5	2,360	7.60	270
80	37.0	1,600	230	16,700	60.0	2,950	8.26	349
90	40.1	1,990	222	19,000	61.8	3,550	8.86	436
100	43.0	2,400	216	21,100	62.9	4,170	9.40	528
120	48.4	3,300	207	25,300	64.1	5,450	10.36	726
140	53.3	4,320	201	29,300	64.6	6,750	11.17	939
160	57.6	5,440	200	33,300	64.8	8,050	11.86	1,170
180	61.5	6,640	200	37,300	64.9	9,350	12.47	1,410
200	65.0	7,910	200	41,300	65.0	10,700	13.00	1,660
250	72.4	11,300	200	51,300	65.0	13,900	14.07	2,340
300	78.5	15,000	200	61,300	65.0	17,200	14.90	3,060

Table 7.9. Thermal conductivity (k_t , W/m-K) and thermal conductivity integral (K , W/m) for

selected materials (Stewart and Johnson 1961) $K = \int_{4K}^T k_t dT$

$$1. Q(W) = k_{\text{average}} A \Delta T / dx = [(8.26+0.24)/2] (80-4) / 0.1 \cdot 10^{-4}$$

$$= 0.32 \text{ W}$$

$$2. Q(W) = K(80) - K(4) A / L = (349-0) / 0.1 \cdot 10^{-4}$$

$$= 0.35 \text{ W}$$

HEAT CONDUCTION IN SOLIDS

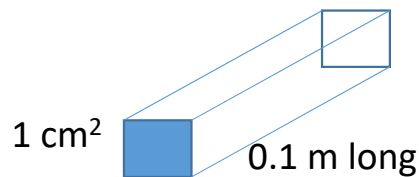
Calculate the heat transferred in copper berillium with a cross section 1 cm^2 and a length of 0.1 m, when the end surfaces are maintained at 300 K and 80 K respectively. Compare the value found by K_{average} and KdT method:

In SI:

$$L = 0.1 \text{ m}$$

$$\Delta T = (300 - 80) \text{ K} = 220 \text{ K}$$

$$A = 1 \text{ cm}^2 = 10^{-4} \text{ m}^2$$



Temperature (K)	Beryllium Copper	
	k_t	K
4	1.9	0
10	4.8	19
20	10.6	95
30	16.2	229
40	21.0	415
50	26.1	650
60	30.0	930
70	33.7	1,250
80	37.0	1,600
90	40.1	1,990
100	43.0	2,400
120	48.4	3,300
140	53.3	4,320
160	57.6	5,440
180	61.5	6,640
200	65.0	7,910
250	72.4	11,300
300	78.5	15,000

Table 7.9. Thermal conductivity (k_t , W/m-K) and thermal conductivity integral (K , W/m) for selected materials (Stewart and Johnson 1961) $K = \int_{4K}^T k_t dT$

$$1. Q(W) = k_{\text{average}} A \Delta T / dx = [(78.5 + 37.0)/2] (300-80)/0.1 \cdot 10^{-4}$$

$$= \mathbf{12.7 \text{ W}}$$

$$2. Q(W) = K(300) - K(80) A / L = (15000 - 1600) / 0.1 \cdot 10^{-4} = \mathbf{13.4 \text{ W}}$$

HEAT CONDUCTION IN SOLIDS

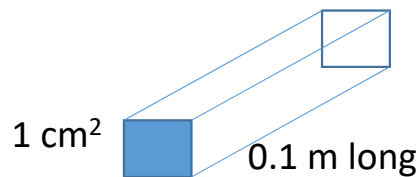
Calculate the heat transferred in **copper berillium** with a cross section 1 cm^2 and a length of 0.1 m, when the end surfaces are maintained at 80 K and 4 K respectively. Compare the value found by K_{average} and KdT method:

In SI:

$$L = 0.1 \text{ m}$$

$$\Delta T = (80-4) \text{ K} = 76 \text{ K}$$

$$A = 1 \text{ cm}^2 = 10^{-4} \text{ m}^2$$



Temperature (K)	Beryllium Copper	
	k_t	K
4	1.9	0
10	4.8	19
20	10.6	95
30	16.2	229
40	21.0	415
50	26.1	650
60	30.0	930
70	33.7	1,250
80	37.0	1,600
90	40.1	1,990
100	43.0	2,400
120	48.4	3,300
140	53.3	4,320
160	57.6	5,440
180	61.5	6,640
200	65.0	7,910
250	72.4	11,300
300	78.5	15,000

Table 7.9. Thermal conductivity (k_t , W/m-K) and thermal conductivity integral (K , W/m) for

$$\text{selected materials (Stewart and Johnson 1961)} \quad K = \int_{4K}^T k_t dT$$

$$1. Q(W) = k_{\text{average}} A \Delta T / L = [(37.0+1.9)/2] (80 - 4) / 0.1 \cdot 10^{-4}$$

$$= \mathbf{1.48 \text{ W}}$$

$$1. Q(W) = K(300) - K(80) A / L = (1600 - 0) / 0.1 \cdot 10^{-4}$$

$$= \mathbf{1.6 \text{ W}}$$

Liquid Helium Dewar with open neck

$$k(T) A \frac{dT}{dx} = Q(W) + \dot{m} C_p (T - T_{liquid})$$

If totally compensated $Q(W) = C_\lambda \dot{m}$; Latent heat = C_λ

$$Q = \frac{k(T) \frac{A}{L} dT}{1 + \frac{C_p}{C_\lambda} (T - T_{Liquid})} = \frac{A}{L} \bar{k} \cdot \int_{T_{Liquid}}^{T_0} \frac{dT}{1 + \frac{C_p}{C_\lambda} (T - T_{Liquid})};$$

$$z = 1 + \frac{C_p}{C_\lambda} \cdot (T - T_{Liquid}); dz = \frac{C_p}{C_\lambda} dT$$

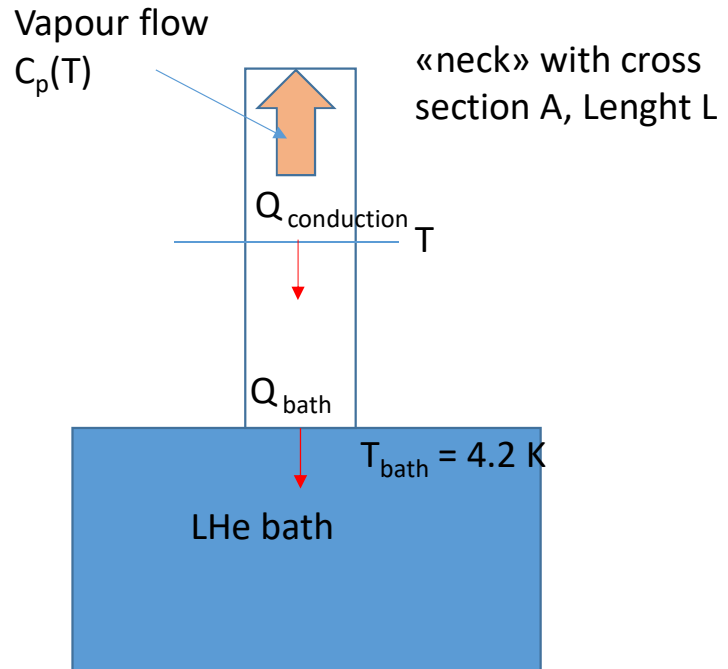
.....

.....

$$Q = \frac{A}{L} \bar{k} \cdot \frac{C_p}{C_\lambda} \cdot \ln(1 + \frac{C_p}{C_\lambda} \cdot (T - T_{Liquid})); \bar{k} = 0.07 \left(\frac{W}{cm \cdot K} \right)$$

$$Q \cdot \frac{L}{A} (W/cm) = 0.07 \left(\frac{W}{cm \cdot K} \right) 20.9 \left(\frac{J}{g} \right) / 5.2 \left(\frac{J}{g \cdot K} \right) \ln(1 + 5.2 \left(\frac{J}{g \cdot K} \right) / 20.9 \left(\frac{J}{g} \right)) \cdot (295 - 4.2) K = \textcolor{red}{1.21 W/cm}$$

If only conduction from table **30.6 W/cm**.



HEAT CONDUCTION IN THE RESIDUAL GAS

Cold temperature contributes to improve the vacuum by condensing molecules on the cold surface (cryopumping). Common gas, except He and H, are condensed at LHe temperature (see graph of vapour pressure vs temperature). In order to trap He and H additional material (e.g. Charcoal) are needed.

Case 1: $\lambda \ll L$ Viscous regime (hydrodynamic regime)

Case 2: $\lambda \gg L$ Molecular regime (free molecular regime)

λ : mean free path [m]

η : viscosity [Pa.s]

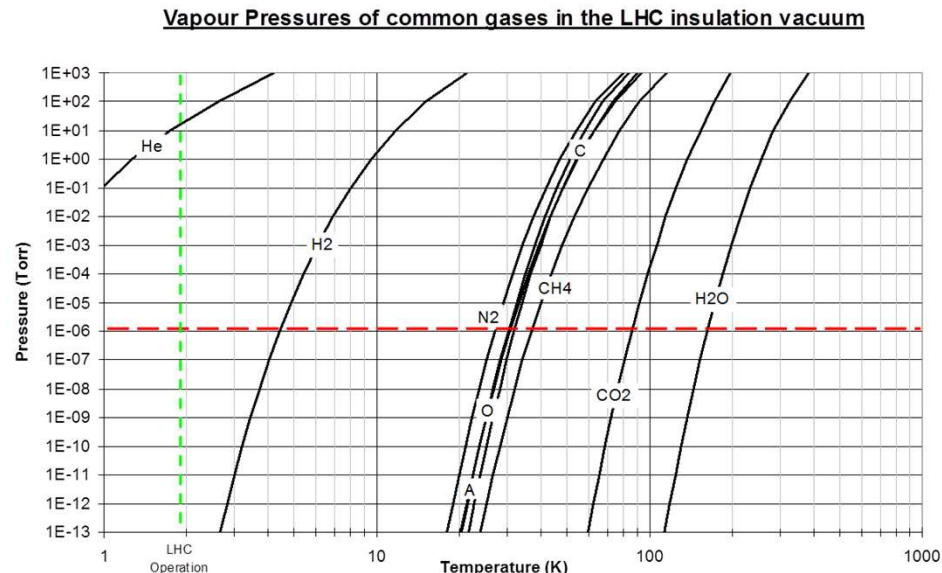
p : pressure [Pa]

T : temperature[K]

M: Molecular Mass

L: distance between walls

$$\lambda = 115 \frac{\eta}{p} \cdot \sqrt{\frac{T}{M}}$$



Note: calculations of heat transfer through gases are not as accurate as through solids! Some estimate is possible.

HEAT CONDUCTION IN THE RESIDUAL GAS

Le libre parcours moyen des molécules est donné par la relation :

$$L_p = 8,6 \cdot 10^3 \frac{\eta}{P} \sqrt{\frac{T}{M}}$$

L_p = libre parcours moyen en cm.

η = viscosité du gaz en poises, à la température T.

P = pression en micron de mercure, μHg .

T = température, $^{\circ}\text{K}$.

M = poids moléculaire; g.mole $^{-1}$.

Tableau XI. – Valeurs du libre parcours moyen ℓ_m (en cm) de molécules de gaz sous 0,13 Pa et du coefficient d'accommodation c_a (sans dimension) pour une surface métallique polie .

T(K)	Air		Hydrogène		Hélium	
	ℓ_m	c_a	ℓ_m	c_a	ℓ_m	c_a
300	5,1	0,8	9,5	0,3	15	0,3
77	0,87	1	1,8	0,5	3,2	0,4
20	–	–	0,30	1	0,67	0,6
4	–	–	–	–	0,11	1

$$\lambda = \frac{RT}{\sqrt{2\pi d^2 N_A p}} \begin{cases} R = \text{universal gas constant} = 8.31 \text{ J} \cdot \text{mol}^{-1} \cdot \text{K}^{-1}, \\ N_A = \text{Avogadro's number} = (6.02 \times 10^{23}) \cdot \text{mol}^{-1}, \\ d = \text{molecule diameter}. \end{cases}$$

HEAT CONDUCTION IN THE RESIDUAL GAS

For the residual gas if : $\lambda \gg L$ *Molecular regime (free molecular regime)*

$$Q = A\alpha \left(\frac{\gamma+1}{\gamma-1} \right) \sqrt{\frac{R}{8\pi M}} \frac{\Delta T}{\sqrt{T}} p \quad \text{with} \quad \gamma = \frac{C_p}{C_v},$$

A: surface receiving the heat flux

Tableau II-8. — VALEURS DE γ ET M POUR DIFFÉRENTS GAZ (29)

Nature du gaz	CO_2	O_2	N_2	N_e	H_2	${}^4\text{He}$
M : (g/mole) . . .	44,01	32	28,02	20,18	2,016	4
γ : (C_p/C_v) . . .	1,302	1,396	1,405	1,67	1,408	1,67

Tableau II-10. — COEFFICIENT D'ACCOMMODATION α_i ($i = 1$ ou 2) (21)

T (*K)	Hélium	Hydrogène	Air
300.	0,3	0,3	$\simeq 0,8$
80.	0,4	0,5	1
20.	0,6	1	—
4.	1	—	—

For the residual gas if : $\lambda \ll L$ *Viscous regime (hydrodynamic regime)*

The heat transfer is independent of the gas pressure.

The heat transfer follows the Fourier law ($\approx 1/L$)

Table 3: The thermal conductivity, k [$\text{mW}\cdot\text{m}^{-1}\cdot\text{K}^{-1}$] at 1 atm

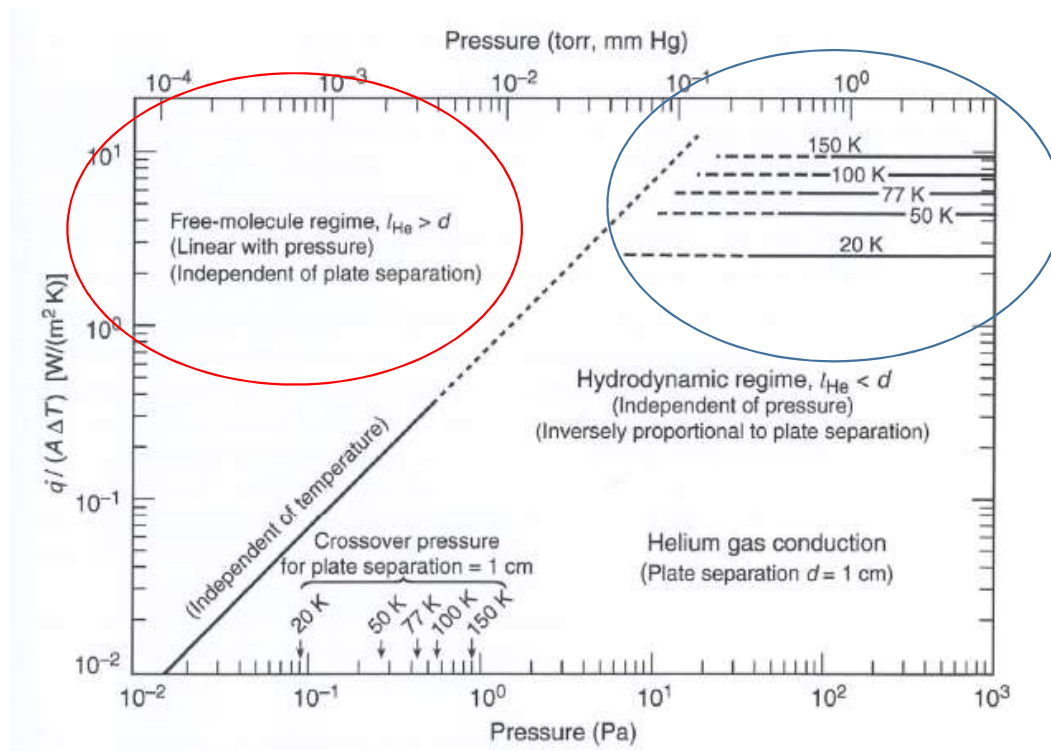
T (K)	${}^4\text{He}$	H_2	N_2
300	150,7	176,9	25,8
75*	62,4	51,6	7,23
20	25,9	15,7	
5	9,7		

HEAT CONDUCTION IN THE RESIDUAL GAS

$\lambda \gg L$: Molecular regime (free molecular regime)

$$Q/(A \Delta T) \propto p$$

Heat switches: molecules travel without collisions from one wall to the other. By varying the pressure one can couple/decouple the cooling between different parts



$\lambda \ll L$: Viscous regime (hydrodynamic regime)

$$\lambda \propto 1/p, N \propto p$$

Thermal cond $\propto \lambda N$

$Q/(A \Delta T)$ constant

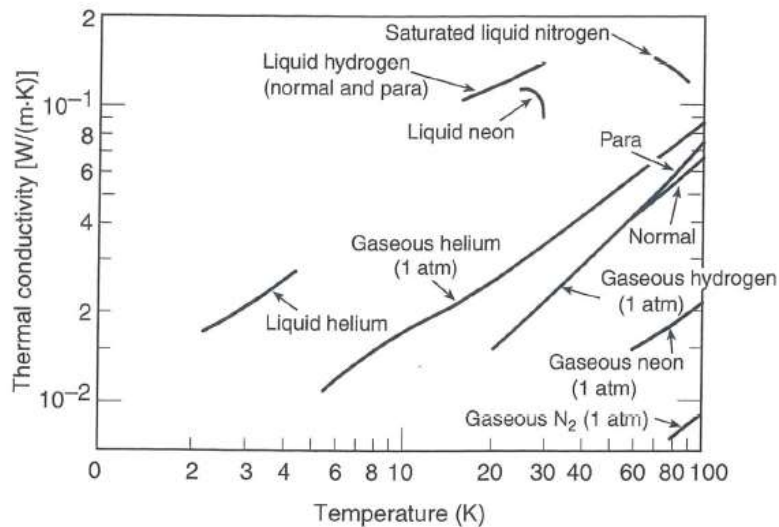
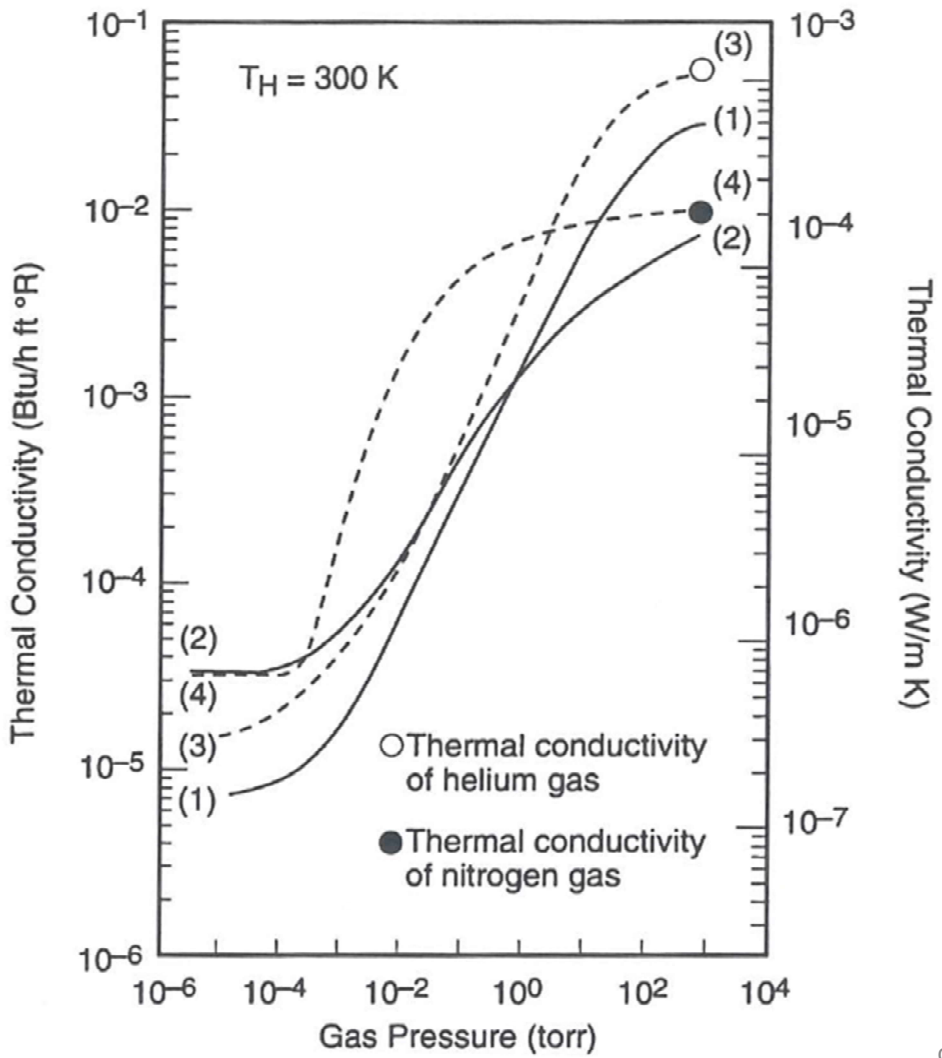
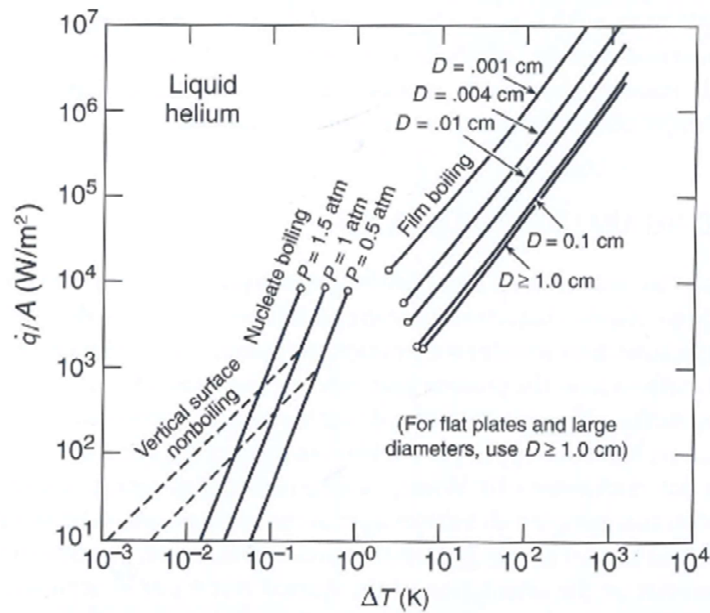


Fig. 2.3 Thermal conductivity of cryogenic gases and liquids as a function of temperature [gas data are measured at atmospheric pressure ($\sim 100 \text{ kPa}$) in the hydrodynamic regime, where λ is essentially independent of pressure]. Data are from Johnson (1960) and Goodall (1970); liquid neon data are from Loechtermann (1963).

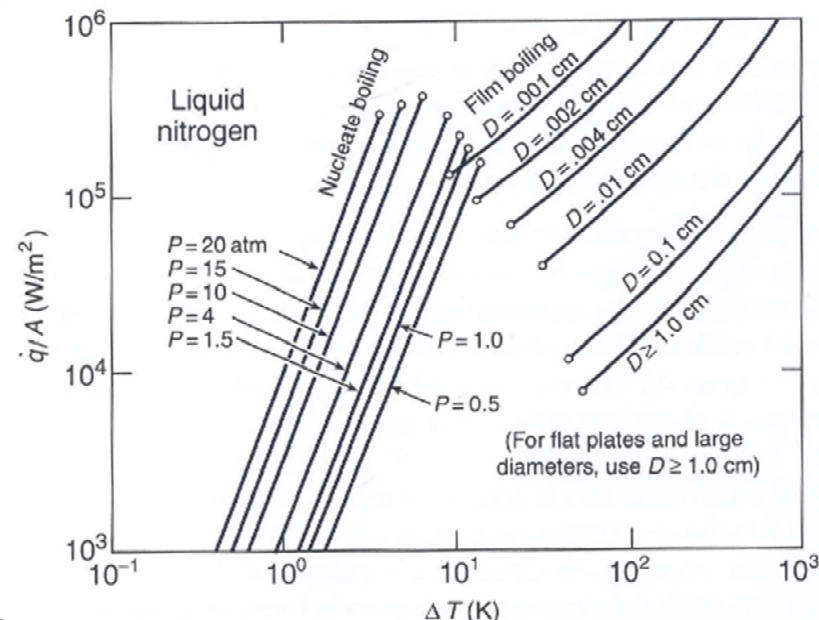
HEAT CONDUCTION THROUGH LIQUID/SOLID INTERFACE

- $< 10^4 \text{ W/m}^2$ or $\Delta T \leq 0.5 \text{ K}$
 - $Q/A = 6 \times 10^4 \Delta T^{2.5} [(\text{W/m}^2)(\text{K}^{-2.5})]$ *for LHe / solid interface*
 - Or $Q/A \geq 10^4 \Delta T^{2.5} [(\text{W/m}^2)(\text{K}^{-2.5})]$ *for LHe / solid interface, conservative approach*

- $< 2 \times 10^5 \text{ W/m}^2$ or $\Delta T \leq 10 \text{ K}$
 - $Q/A = 5 \times 10^2 \Delta T^{2.5} [(\text{W/m}^2)(\text{K}^{-2.5})]$ *for LN2 / solid interface*



R.Pengo, Introduzione



113

HEAT NATURAL CONDUCTION: HORIZONTAL PIPE IN AIR

Pipe diameter $d(m)$, $\Delta T (K)$ = temperature difference between the pipe and the air, $dS (m^2) = \pi \cdot d \cdot dx$

$$dQ (W) = h \cdot \Delta T \cdot dS$$

Downward: $h (W/m^2 \cdot K) = 1.3 (\Delta T / d)^{0.25}$

Upward : $h(W/m^2 \cdot K) = 2.5 (\Delta T / d)^{0.25}$

Example:

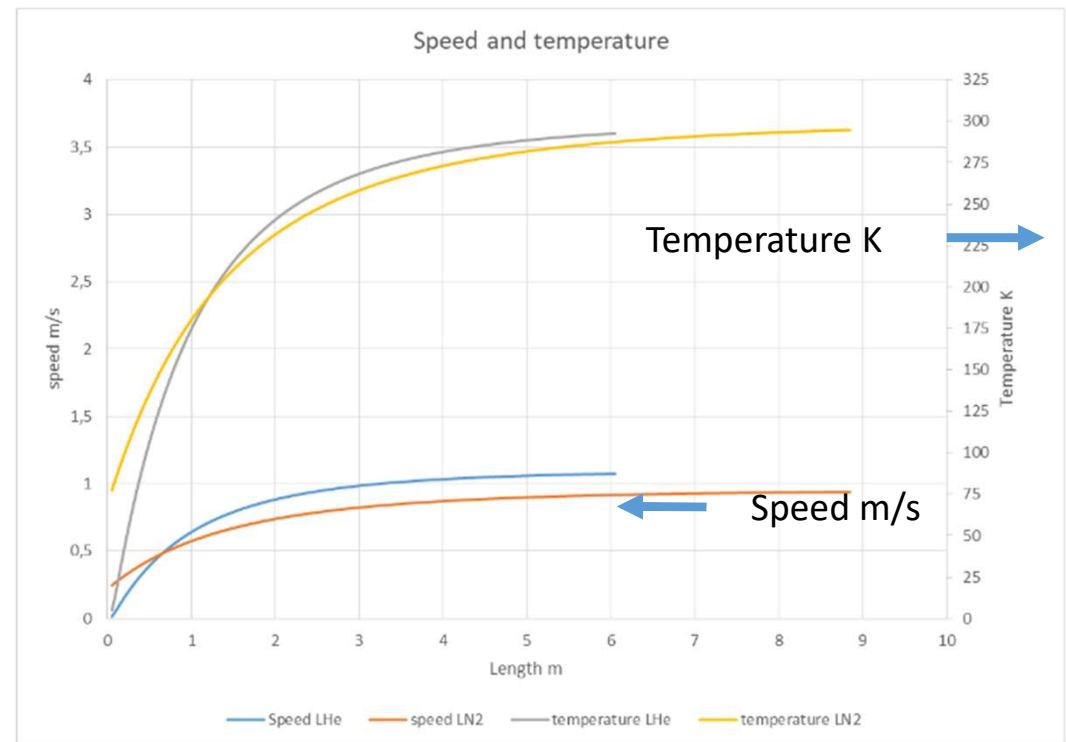
Diameter: 0.05 m,

Flow: 10 liter/hour (only vapour)

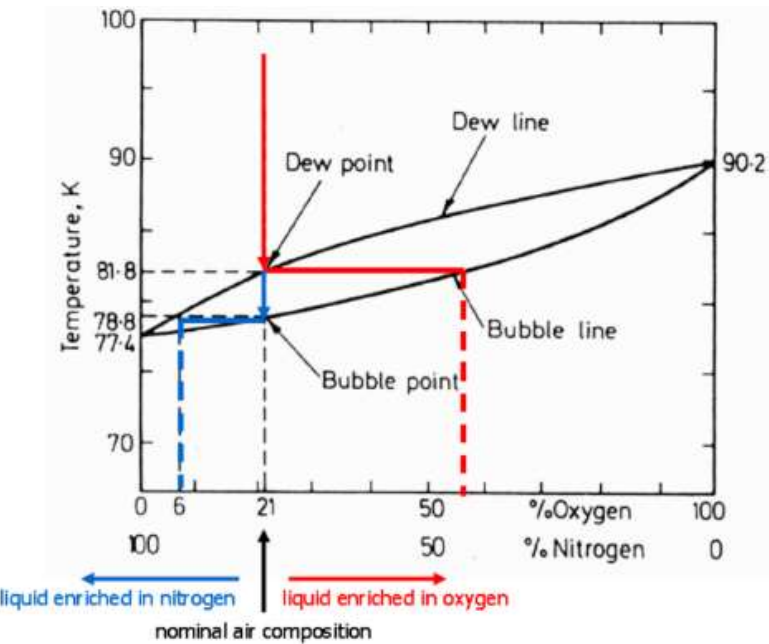
LHe: $10 \text{ litre} \cdot 0.125 \text{ kg/litre} / 3600 \text{ s} = 3.47 \cdot 10^{-4} \text{ kg/s}$

LN2: $10 \text{ litre} \cdot 0.800 \text{ kg/litre} / 3600 \text{ s} = 2.22 \cdot 10^{-3} \text{ kg/s}$

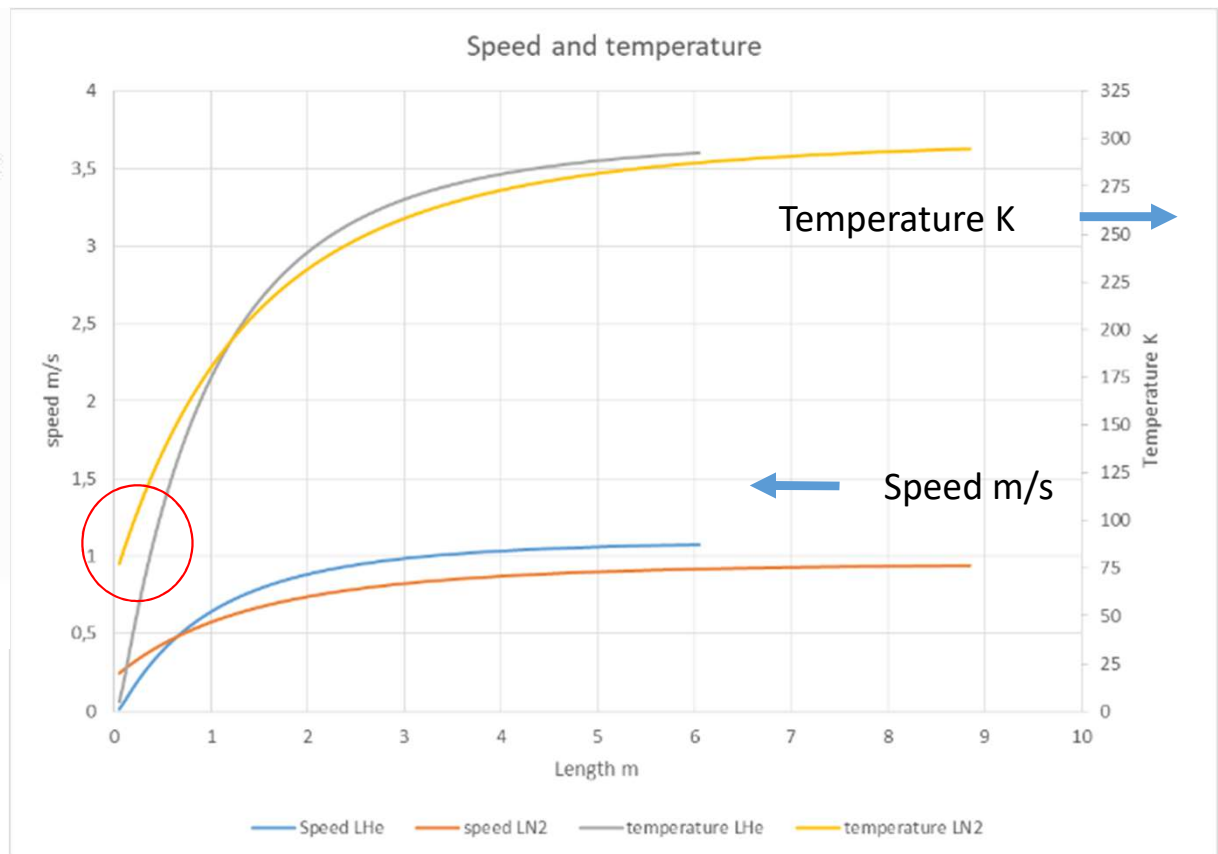
$c_p (Ghe) \approx 5200 \text{ J/kg}$ $c_p (GN2) \approx 1040 \text{ J/kg}$



HEAT NATURAL CONDUCTION: HORIZONTAL PIPE IN AIR



Danger: Oxygen enrichment in liquefied air



RADIATIVE HEAT TRANSFER

A body absorbs/emits energy by radiation according to, for a *black body*:

$$\lambda_{\max} T = 2898 \text{ } \mu\text{m} \cdot \text{K}^{-1}.$$

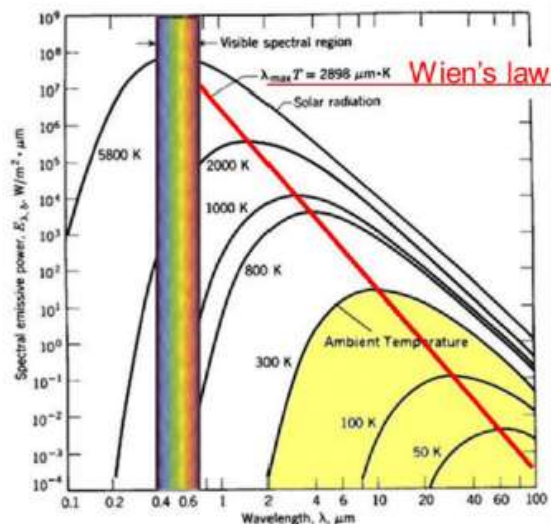


Fig. 11: The emissive power of a spectral blackbody

$$E^0 = \int_0^{\infty} \frac{C_1}{\lambda^5 (e^{C_2/\lambda T} - 1)} d\lambda = \sigma T^4 \quad \text{with} \quad \sigma = 5.67 \times 10^{-8} \text{ W} \cdot \text{m}^{-2} \cdot \text{K}^{-4}$$

For a real opaque surface material the emissive power is only a fraction $\epsilon(T)$ of the black body: $E^0 = \epsilon \sigma T^4$; $\epsilon = 1 - R$ (reflectivity)

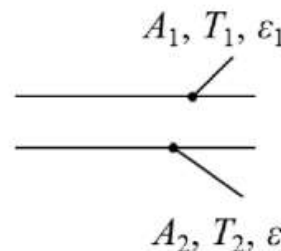
Table 4: The total emissivity of various metals at three different temperatures

	300 K	78 K	4.2 K
3M black paint (80 μm) on a copper surface	0.94	0.91	0.89
Polished aluminium (33 μm roughness)	0.05	0.023	0.018
Polished copper (41 μm roughness)	0.10	0.07	0.05
304 Polished stainless steel (27 μm roughness)	0.17	0.13	0.08

RADIATIVE HEAT TRANSFER

The thermal exchange q_{12} between two surfaces A_1 at T_1 with ε_1 and A_2 at T_2 with ε_2 depends also on the geometrical factor (view factor) F_{12}

$$q_{12} = \sigma(T_1^4 - T_2^4) / \left(\frac{1-\varepsilon_1}{\varepsilon_1 A_1} + \frac{1}{A_1 F_{12}} + \frac{1-\varepsilon_2}{\varepsilon_2 A_2} \right), \quad A_i F_{ij} = A_j F_{ji} \quad \sum_{j=1}^N F_{ij} = 1.$$

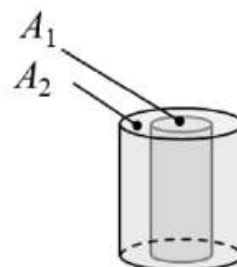


$$A_1, T_1, \varepsilon_1$$

$$A_2, T_2, \varepsilon_2$$

$$A = A_1 = A_2, \quad F_{12} = 1, \quad q_{12} = \frac{\sigma A_1 (T_1^4 - T_2^4)}{\frac{1}{\varepsilon_1} + \frac{1}{\varepsilon_2} - 1};$$

Examples: Large parallel plates (above) and long concentric cylinders (below)



$$\frac{A_1}{A_2} = \frac{r_1}{r_2}, \quad F_{12} = 1, \quad q_{12} = \frac{\sigma A_1 (T_1^4 - T_2^4)}{\frac{1}{\varepsilon_1} + \frac{1-\varepsilon_2}{\varepsilon_2} \left(\frac{r_1}{r_2} \right)}.$$

RADIATIVE HEAT TRANSFER

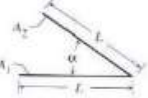
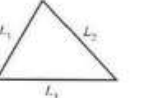
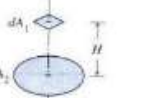
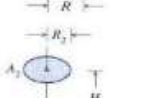
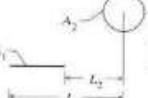
Configuration	Geometric View Factor
	Two infinitely long plates of width L , joined along one of the long edges: $F_{12} = F_{21} = 1 - \sin \frac{\alpha}{2}$
	Two infinitely long plates of different widths (H, L), joined along one of the long edges and with a 90° angle between them: $F_{12} = \frac{1}{2}[1 + x - (1 + x^2)^{1/2}]$ where $x = H/L$
	Triangular cross section enclosure formed by three infinitely long plates of different widths (L_1, L_2, L_3): $F_{12} = \frac{L_1 + L_2 - L_3}{2L_1}$
	Disc and parallel infinitesimal area positioned on the disc centerline: $F_{12} = \frac{R^2}{H^2 + R^2}$
	Parallel discs positioned on the same centerline: $F_{12} = \frac{1}{2} \left\{ x - \left[x^2 - 4 \left(\frac{x_2}{x_1} \right)^2 \right]^{1/2} \right\}$ where $x_1 = \frac{R_1}{H}$, $x_2 = \frac{R_2}{H}$, and $X = 1 + \frac{1 + x_2^2}{x_1^2}$
	Infinite cylinder parallel to an infinite plate of finite width ($L_1 - L_2$): $F_{12} = \frac{R}{L_1 - L_2} \left(\tan^{-1} \frac{L_1}{H} - \tan^{-1} \frac{L_2}{H} \right)$
	Two parallel and infinite cylinders: $F_{12} = F_{21} = \frac{1}{\pi} \left[\left(X^2 - 1 \right)^{1/2} + \sin^{-1} \left(\frac{1}{X} \right) - X \right]$ where $X = 1 + \frac{L}{2R}$

Fig. 14: View factors for given geometries

Tableau II-1. — VALEURS DE E EN FONCTION DES POUVOIRS ÉMISSIFS e_1 ET e_2 DES SURFACES A_1 ET A_2 AUX TEMPÉRATURES T_1 ET T_2 ($T_1 < T_2$) (3)

	Réflexion spéculaire	Réflexion diffuse
Plaques parallèles	$\frac{e_1 e_2}{e_2 + (1-e_2)e_1}$	$\frac{e_1 e_2}{e_2 + (1-e_2)e_1}$
Longs cylindres coaxiaux $L \gg R$	$\frac{e_1 e_2}{e_2 + (1-e_2)e_1}$	$\frac{e_1 e_2}{e_2 + \frac{A_1}{A_2}(1-e_2)e_1}$
Sphères concentriques	$\frac{e_1 e_2}{e_2 + (1-e_2)e_1}$	$\frac{e_1 e_2}{e_2 + \frac{A_1}{A_2}(1-e_2)e_1}$

More configurations in: H:Y: Wong, Heat Transfer for engineers, Longman 1977

Tableau G. — Émissivité totale normale de quelques métaux.

Métal	T (K)	ε_n
Or	300 80	0,02 0,01
Argent	300 80 4	0,02 0,01 0,005
Aluminium commercial brut	300 80 4	0,25 0,12 0,07
Aluminium poli mécanique	300 80 4	0,20 0,10 0,06
Aluminium poli électrolytique	300 80 4	0,15 0,08 0,04
Chrome	300	0,08
Cuivre poli mécanique	300 80 4	0,10 0,06 0,02
Étain	300 80 4	0,050 0,012 0,013
Nickel	300 80	0,05 0,02
Laiton poli	300 80 4	0,03 0,03 0,02
Acier inoxydable 18-8	300 80 4	0,20 0,12 0,10

RADIATIVE HEAT TRANSFER

Tableau II-2. — POUVOIR ÉMISSIF « e » DES MATERIAUX (4-8)

Materiaux	Température de la surface (°K)		
	300	78	4.2
Aluminium recuit électropoli	0,03	0,018	0,011
Aluminium commercial	0,08	0,03	
Aluminium sur mylar (2 côtés)		0,04	
Cuivre (poli mécaniquement)	0,013	0,069	0,008
Cuivre (commercial poli électro)	0,030	0,019	0,015
Argent	0,020	0,008	
Laiton 65/35 poli	0,060	0,029	0,018
Laiton 65/35 oxydé	0,60	0,029	
Acier inox 302	0,08	0,048	
Acier inox 304	0,15	0,061	
Étain (25 μ)	0,05	0,013	0,012
Monel	0,17	0,11	
Or (37 μ sur verre ou plexi)	0,02	0,01	
Or (12 μ sur verre ou plexi)		0,016	
Or (0,25 μ sur verre ou plexi)		0,063	
Acier inox doré 12 μ		0,025	
Acier inox doré 2,5 μ		0,027	
Cuivre doré 12 μ	0,04	0,025	

RADIATIVE HEAT TRANSFER

Most of the radiation happens between 300 K and 4 K
happens between 300 K and 77 K:

$$300 \text{ K to } 77 \text{ K: } q_{300-77}/A = 5.67 \times 10^{-8} \times (300^4 - 77^4) = 457 \text{ W/m}^2$$

$$300 \text{ K to } 4 \text{ K: } q_{300-4}/A = (5.67 \times 10^{-8} \times (300^4 - 4^4)) = 459 \text{ W/m}^2$$

Only 2 W/m² between 77 K and 4 K

$$\sigma = 5.67 \times 10^{-8} \text{ W} \cdot \text{m}^{-2} \cdot \text{K}^{-4}; \varepsilon=1; F_{12}=1$$

Most of the radiation happens between 300 K and 4 K
happens between 300 K and 77 K:

$$293 \text{ K to } 77 \text{ K: } q_{293-77}/A = 5.67 \times 10^{-8} \times (293^4 - 77^4) = 416 \text{ W/m}^2$$

$$293 \text{ K to } 4 \text{ K: } q_{293-4}/A = (5.67 \times 10^{-8} \times (293^4 - 4^4)) = 418 \text{ W/m}^2$$

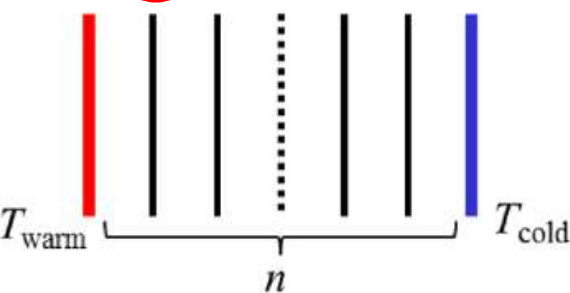
Only 2 W/m² between 77 K and 4 K

$$\sigma = 5.67 \times 10^{-8} \text{ W} \cdot \text{m}^{-2} \cdot \text{K}^{-4}; \varepsilon=1; F_{12}=1$$

RADIATIVE HEAT TRANSFER

It is important to note that by inserting 1 or n floating shields between the hot and the cold surface one can reduce the radiation up to $1/(n+1)$ times (MLI multilayer insulation):

Table 5: Passive shielding heat transfer as a function of the intermediate surface number

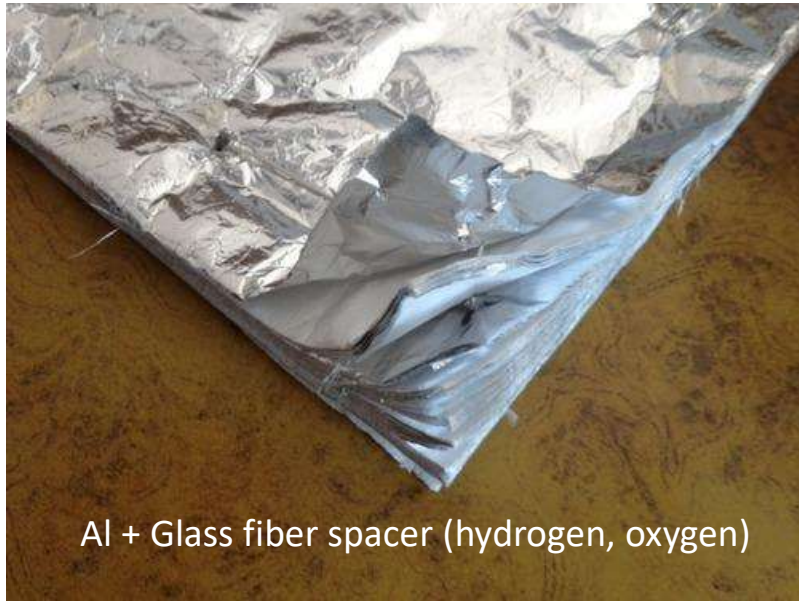
$q = \frac{\varepsilon\sigma}{2-\varepsilon} (T_{\text{warm}}^4 - T_{\text{cold}}^4)$	$q = \frac{1}{2} \frac{\varepsilon\sigma}{2-\varepsilon} (T_{\text{warm}}^4 - T_{\text{cold}}^4)$	$q = \frac{1}{n+1} \frac{\varepsilon\sigma}{2-\varepsilon} (T_{\text{warm}}^4 - T_{\text{cold}}^4)$
 T_{warm}	 T_{cold}	 T_{warm} T_{cold}

$$T^4 = \frac{T_{\text{warm}}^4 + T_{\text{cold}}^4}{2}$$

$$T_i^4 = T_{\text{cold}}^4 + \frac{T_{\text{warm}}^4 + T_{\text{cold}}^4}{i+1}$$

RADIATIVE HEAT TRANSFER

MLI is used to reduce the radiation power, when cleanliness is not required as e.g. Not suitable for Superconducting RF cavities environnement. It consists of a number of reflecting (Al , 400 ångström, 1 ångström = 10^{-10} m) thin layers, in vacuum, of polyethylene films interspaced by thin insulating materials as polyether nets or glass fiber.



Al + Glass fiber spacer (hydrogen, oxygen)



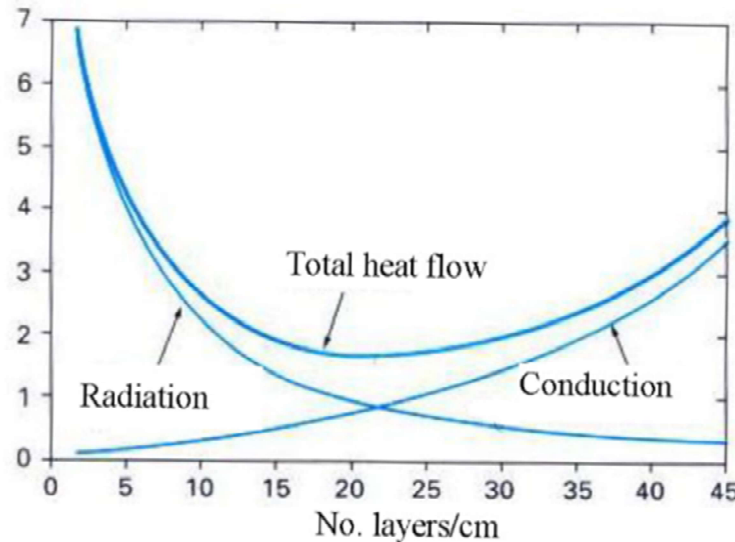
Polyester spacer (helium, nitrogen)
between polyethylene with 400
ångström Al deposit.

RADIATIVE HEAT TRANSFER

It can be shown that there is an optimum value for the number of layers per unit thickness equal to 20-25 layers/cm. The actual value of equivalent heat conduction depends strongly on the vacuum level but also on the ability to install the MLI, avoiding to tight/compress them, overlapping the junctions, etc.

LHC measured values:

- 30 layers between 300 K and 50 K $\sim 1 \text{ W/m}^2$
- 10 Layers between 50 K and 1.9 K $\sim 50 \text{ mW/m}^2$



Total heat flow as a function of MLI packing density

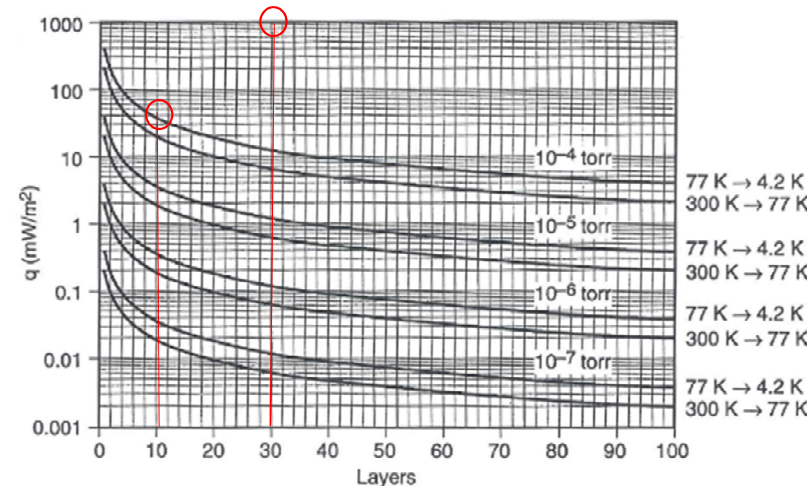


Figure 3-41 Gas conduction versus number of layers (nitrogen as interstitial gas).

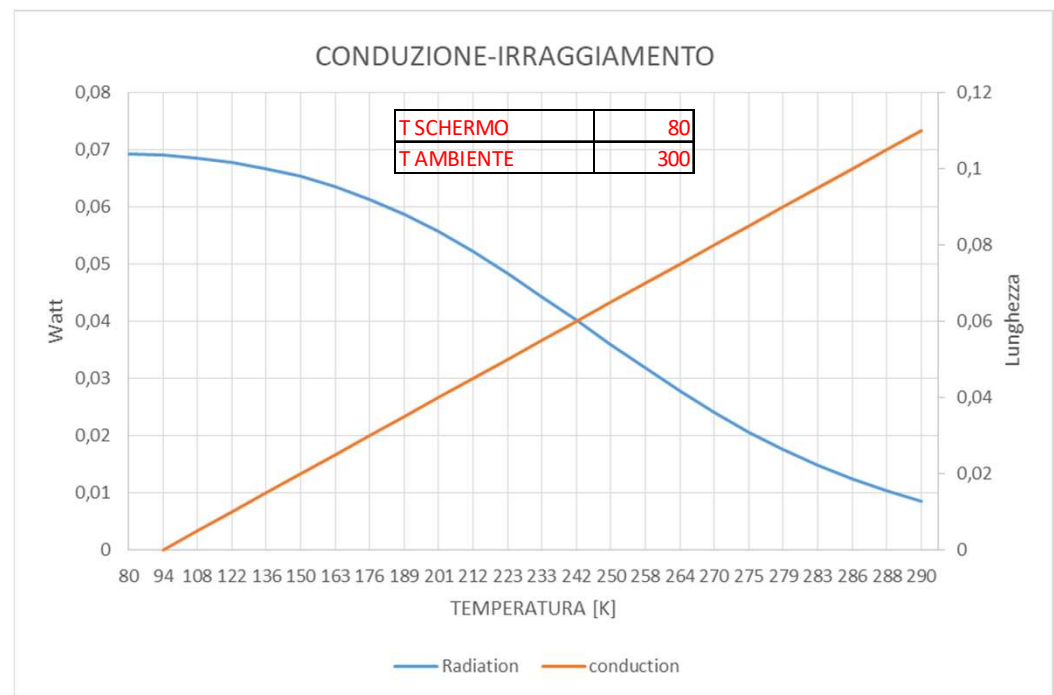
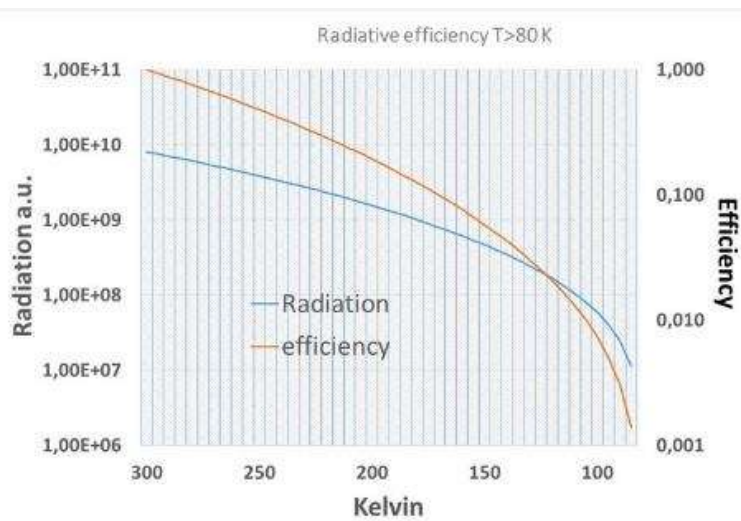
RADIATIVE HEAT TRANSFER

Typical heat fluxes at vanishingly low temperature
between flat plates [W/m²]

Black-body radiation from 290 K	401
Black-body radiation from 80 K	2.3
Gas conduction (100 mPa He) from 290 K	19
Gas conduction (1 mPa He) from 290 K	0.19
Gas conduction (100 mPa He) from 80 K	6.8
Gas conduction (1 mPa He) from 80 K	0.07
MLI (30 layers) from 290 K, pressure below 1 mPa	1-1.5
MLI (10 layers) from 80 K, pressure below 1 mPa	0.05
MLI (10 layers) from 80 K, pressure 100 mPa	1-2

RADIATIVE HEAT TRANSFER

Radiative cooling of a mirror, supported by a PEEK tube, from a shield at 80 K.



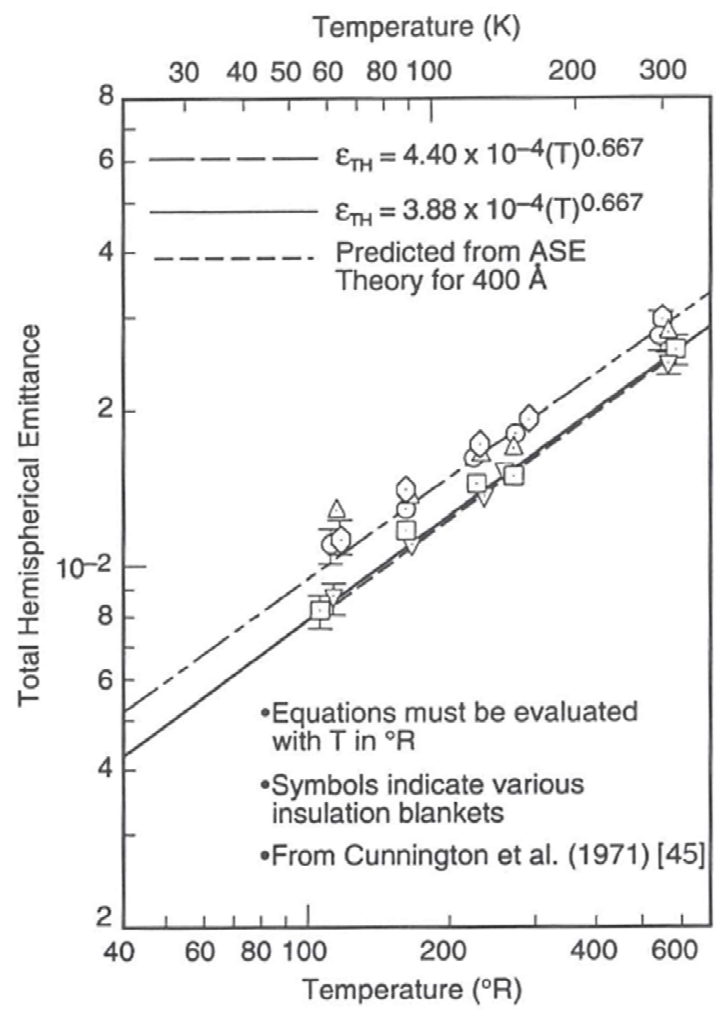


Figure 3-23 Total hemispherical emittance of double-aluminized 1/4-mil Mylar as a function of temperature.

Cryopumping (highlights only)

It allows to obtain very low vacuum level ($< 10^{-2}$ Pa or 10^{-4} mbar) by means of Cryocondensation and Cryosorption:

- Crycondensation

- the molecules adhere to the cold surface and form a layer.
 - re-sublimation (gaseous->solid)
 - condensation (gaseous-> liquid)

Tableau VII. — Propriétés des cryodépôts et énergies de sublimation et de condensation de divers gaz entre la température de 300 K ou 100 K et la température de la surface froide (77, 20 ou 4 K).

Grandeurs	H ₂ O*	CO ₂	O ₂	Ar	N ₂	H ₂
T _s (K)	77	77	20	20	20	4
ρ (kg/m ³)	100 à 800	1 600	1 360	1 600	900	80
k [W/(m . K)]	0,1 à 7	1	—	1,2	0,1 à 0,4	0,2 à 100
E _T (kJ/kg)	2 816	602	287	201	263	420
H ₁₀₀ – H _T (kJ/kg)	—	—	360	243	350	1 424
H ₃₀₀ – H _T (kJ/kg)	3 130	—	542	350	563	4 077

* neige.

9.Cryopumping (highlights only)

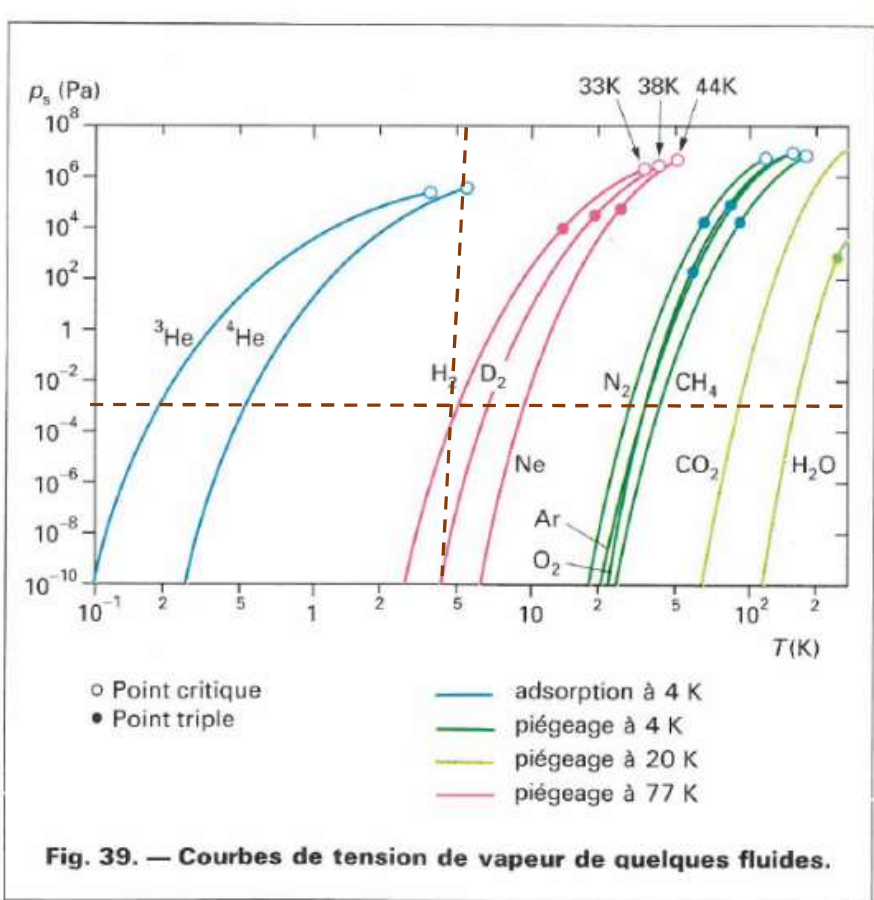


Fig. 39. — Courbes de tension de vapeur de quelques fluides.

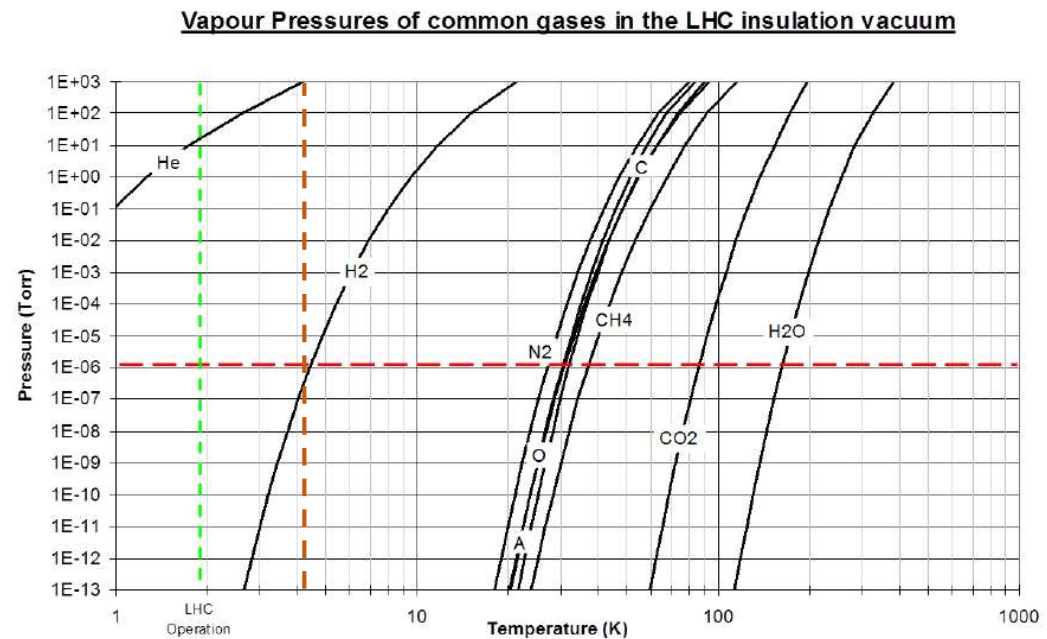


Fig. 10: Vapour pressures of common gases in the LHC insulation vacuum
 100 K: water, and all hydrocarbons (e.g. Oil vapours)
 20 K: to condense air (N_2 and O_2)
 4 K : Hydrogen isotopes and neon

9.Cryopumping (highlights only)

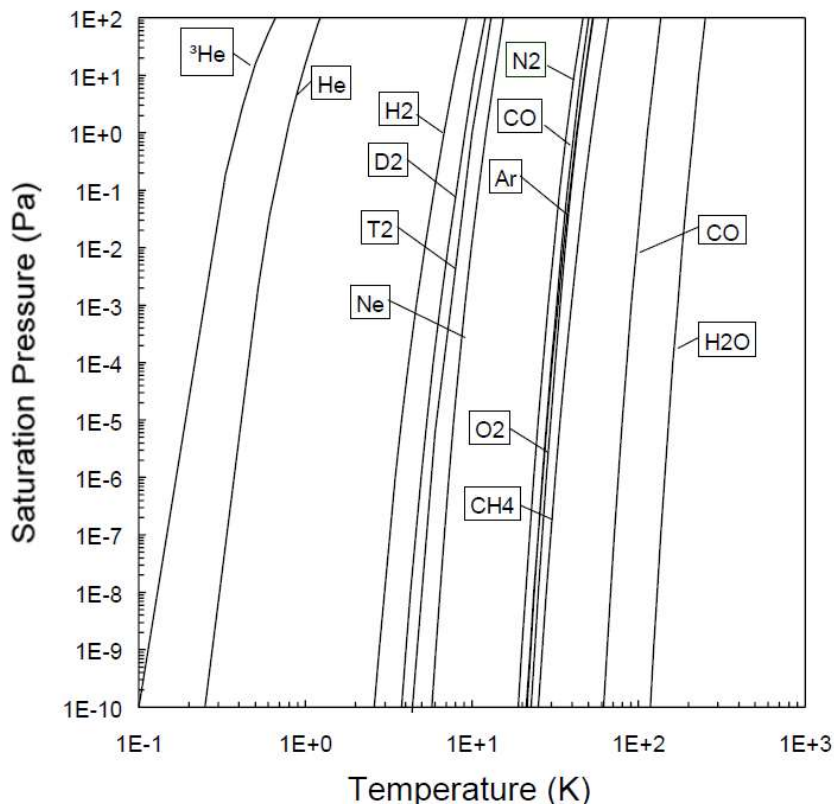


Fig. 1: Saturation curves of common gases

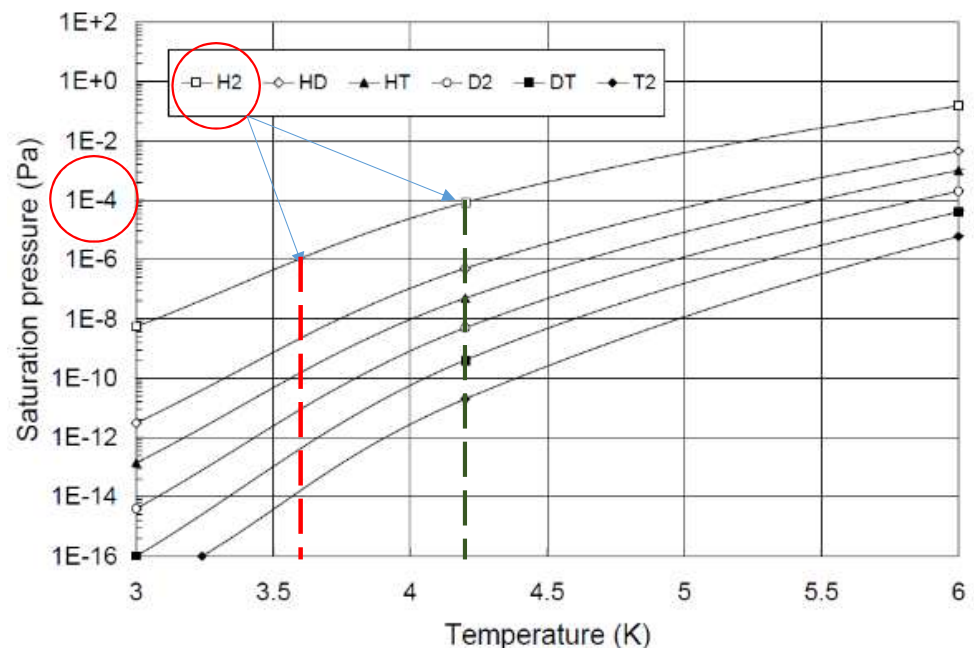


Fig. 2: Sublimation pressures of the six hydrogen isotopomers [8]

For practical applications it is recommended to provide for oversaturation of the gas by **TWO ORDER OF MAGNITUDE** in pressure. In order to establish a pressure of 10^{-4} Pa during pumping of H₂ (at 4.2 K), the cold surface must be at 3.6 K.

9.Cryopumping (highlights only)

It allows to obtain very low vacuum level (< 10⁻² Pa or 10⁻⁴ mbar) by means of Cryocondensation and Cryosorption:

- Cryocondensation
 - the molecules adhere to the cold surface and form a layer.
- Cryosorption
 - the molecules adhere on a solid «porous» surface, which is the adsorbant element
 - physical (ad)sorption or physisorption
 - The equilibrium pressure of the adsorbed gas is much lower than the saturation pressure for cryocondensation. The gas can be retained at considerably higher temperature than would be required for condensation. (Essential for cryopumping He, H and Neon)

9.Cryopumping (highlights only)

- Porous materials with high sorption capacity, such as molecular sieves or activated charcoal are most used as sorbent materials
- However layers of condensed gas frost (Argon, CO₂, SF₆) may also be applied
- It is possible to bind Helium and Hydrogen in the 5 K temperature range and to achieve pressure of 10⁻⁷ Pa (10⁻⁹ mbar).

Zeolite molecular sieves: are (size 3 Å, 4 Å, 5 Å) hydrated aluminosilicates (synthetically produced or from volcanic ash). Usually adopted till 77 K. Their temperature regeneration is quite high 300 C (hydrophilic character)

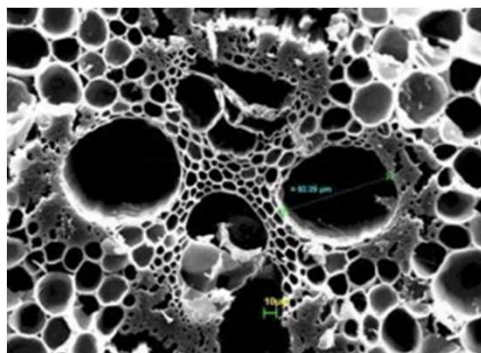
Cryocondensates: Typical combinations are He/Ar, He/SF₆, H₂/CO₂ usually some µm thick. (E.g. for Argon the ratio is 20 atoms of Ar for 1 atom of He at 4.5 K.)

Activated charcoal: is the most recommended material. It is obtained from coconut shell (mostly) or wood, peat, lignite,.. To activate the charcoal two procedures are used:

- chemically: phosphoric acid is added to the parent prior carbonization
- physically: gasification of carbon by introduction of oxygen

The activation temperature is about 400 K.

9.Cryopumping (highlights only)



- Some general characteristics of the most common adsorbents used in cryogenics.
- A critical component is the «glue»



Charcoal

Zeolites



Tableau VIII. — Caractéristiques physiques des adsorbants utilisés en cryogénie.

Matériau	Surface massique m ² /g	Volume poreux cm ³ /g	Masse volumique apparente g/cm ³	Capacité thermique massique J/(g·K)	Dimension moyenne d'un pore 10 ⁻¹⁰ m	Température de régénération (durée 24-72 h) °C	Forme (1) (dimensions commerciales) mm
Charbon actif noix de coco	1000 à 1200	0,7	0,5	1,0	5 à 20	20 à 200	G(0,5 × 1,40 à 2,4 × 4,8 mm) P, C, T
Tamis moléculaire 5A	800	0,75	0,69	1,0	5	250 à 420	C (1,6 à 3,2) P, S
Tamis moléculaire 13X	510	1,3	0,64	1,0	10	380	C(1,6 à 3,2) P, S
Alumine activée	320 à 360	0,40	0,74 à 0,80	1,0	22 et 44	350	S(0,2 à 1,0)
Silicagel (type R)	750 à 800	0,45	0,72	0,92	22	175	G

(1) G = granulés sans forme définie, P = poudre, C = bâtonnets cylindriques, T = tissus (utilisés dans les hottes de cuisine, par exemple), S = granulés sphériques.

Charcoal:
1000 m²/g
0.5 g/cm³



$$1 \text{ cm}^3 = 0.5 \text{ g} = 500 \text{ m}^2$$

$$1 \text{ g} = 2 \text{ cm}^3 = 2000 \text{ m}^2$$

Electrical connection into the cryostat

- A cryostat typically contains superconducting RF cavities and/or superconducting magnets
 - An electrical connection between the outside (at 300K) and the sc device is needed
 - The connection should be capable of carrying the necessary power with the minimum use of cryogenic power.
- Superconducting cavities: usually a (commercial or home made) coaxial cable (50 Ohm) from 300 K to 4 K
- The RF power P_{cold} dissipated into the RF cavity is of the order of few Watts (max ca. 50 W). ALPI-HIE Isolde-ESS 5-12 W (old LEP cavities ca. 50 W)
 - To minimize the heat load optimize A/L and when possible anchor to intermediate temperature (e.g. LN2 temperature)
 - Stored energy is low $Q = 2 \cdot \pi \cdot v = \omega \cdot U_{\text{stored}} / P_{\text{cold}}$

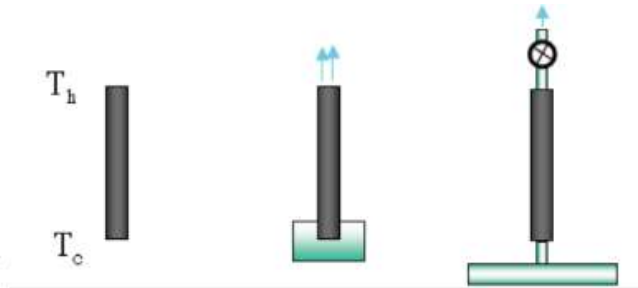
Superconducting magnets: the connection from the outside to the coil is obtained by means of “current leads” (CL).

Three types mainly of CL are used:

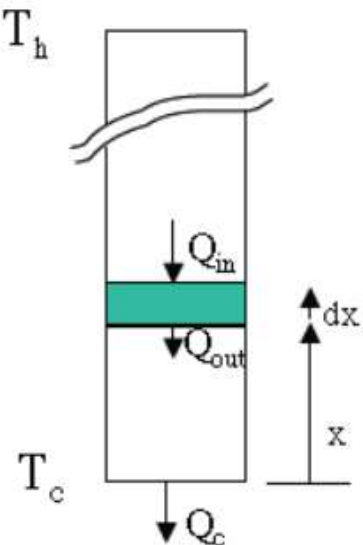
- Conduction cooled CL (for low current)
- Gas/vapor cooled CL (or forced flow cooled CL)
- Hybrid HTS CL

Conventional

- Conduction cooled
- Vapor cooled
- Forced-flow cooled



Electrical connection into the cryostat: conduction cooled CL



- Energy balance on control volume:

$$Q_{in} - Q_{out} + Q_{gen} = 0$$

$$\left(kA \frac{dT}{dx} \Big|_{x+dx} - kA \frac{dT}{dx} \Big|_x \right) + \frac{I^2 \rho}{A} dx = 0 \quad \text{note that if } dT/dx > 0, Q_{in} > 0$$

$$\frac{d}{dx} \left(k \frac{dT}{dx} \right) + \rho J^2 = 0$$

- Change variables: let $s = k \frac{dT}{dx}$

$$\frac{ds}{dx} + \rho J^2 = 0; \Rightarrow \frac{ds}{dT} \frac{dT}{dx} + \rho J^2 = 0$$

$$\frac{s}{k} \frac{ds}{dT} + \rho J^2 = 0; \Rightarrow s ds = -k \rho J^2 dT$$

$$s = \frac{Q}{A}; \Rightarrow ds = \frac{dQ}{A}; \quad \int_c^k Q dQ = \frac{1}{2} Q^2 \Big|_c^k = -I^2 \int_{T_c}^{T_k} k \rho dT$$

Ref. US Particle
accelerator
school 2004

Electrical connection into the cryostat: conduction cooled CL

CRYOGENIC EQUIPMENT 405

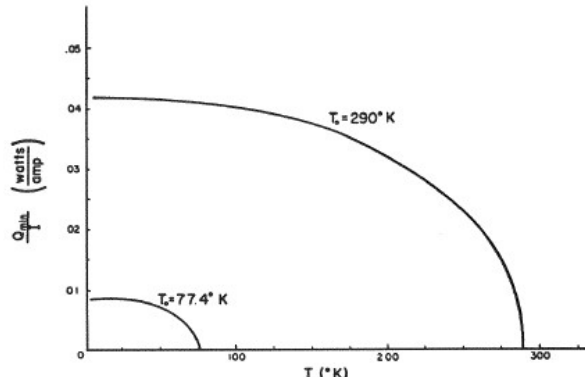


Figure 9-41 Heat conducted to low-temperature region by optimum, conduction-cooled copper lead connecting temperature T_0 to lower temperature T (from Ref. [50]).

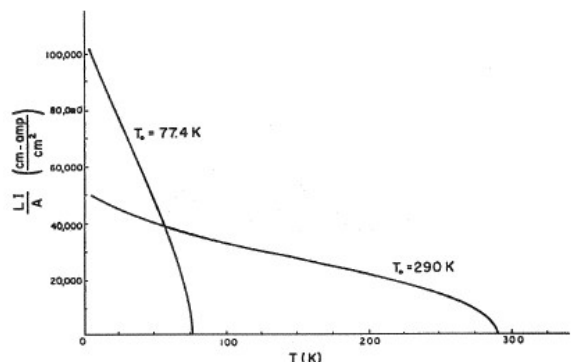
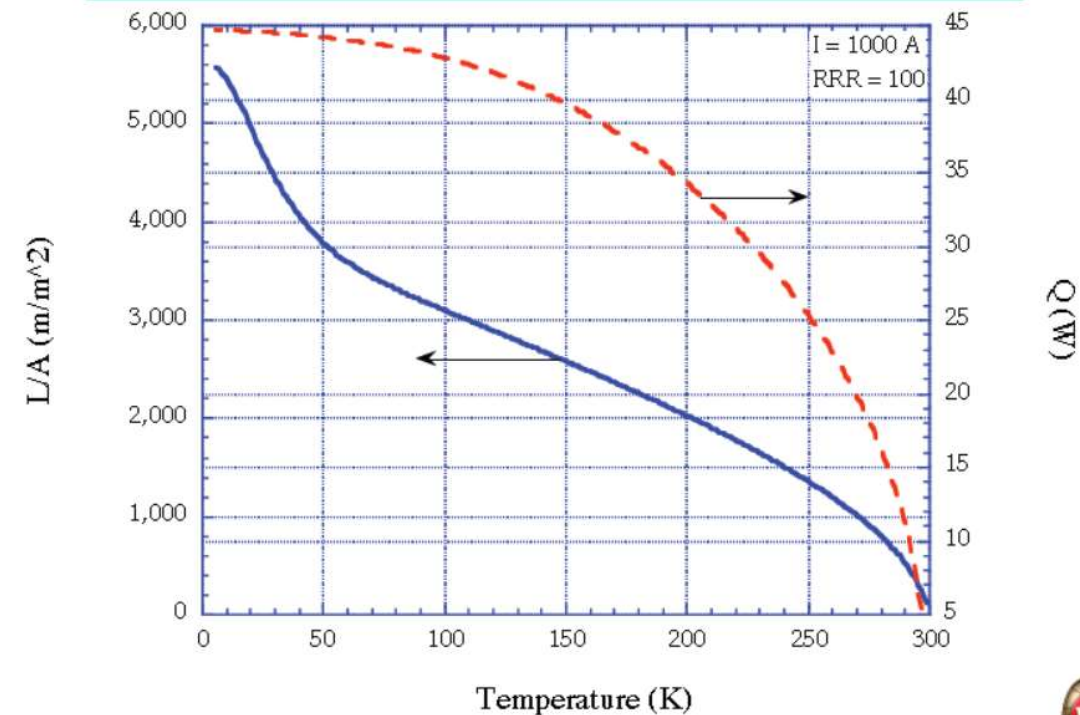


Figure 9-42 Ratio of length to cross section of optimum conduction-cooled lead connecting temperature T_0 to lower temperature T (from Ref. [50]).

Conduction Cooled Lead: Sample Results



For 1000 Amps one CL dissipates at 4 K ca. 45 W, a pair ca. 90 W!!
i.e. $90 \text{ J/s} / 20.9 \text{ J/g} / 125 \text{ g/liter} \times 3600 \text{ s/hour} = 124 \text{ liter/hour}!!$

Electrical connection into the cryostat: conduction cooled CL

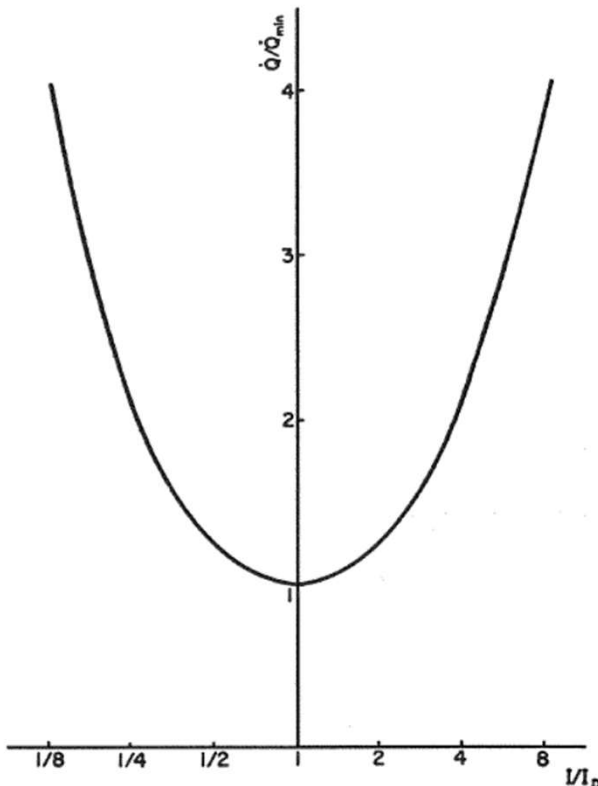


Figure 9-43 Comparison of heat flow from lead a current I , higher or lower than design value I_D , with heat flow that would occur if the lead were optimized for a new current I (from Ref. [50]).

$$\frac{Q_L}{(Q_L)_{\min}} = \frac{1}{2} \left(\frac{I}{I_{\text{opt}}} + \frac{I_{\text{opt}}}{I} \right)$$

For $I = 2 \cdot I_{\text{opt}}$; $Q_L/(Q_L)_{\min} = 1.25$

For twice the current only 25 % higher dissipation

THE REVIEW OF SCIENTIFIC INSTRUMENTS

VOLUME 30, NUMBER 2

Optimum Input Leads for Cryogenic Apparatus

RICHARD MC FEE

Department of Electrical Engineering, Syracuse University, Syracuse 10, New York

(Received September 2, 1958; and in final form, December 9, 1958)

Electrical connection into the cryostat: vapour cooled CL

Energy balance at steady state is given by:

$$\frac{I^2 \rho}{A} + \frac{d}{dx} \left(Ak \frac{dT}{dx} \right) - \dot{m} C_p \frac{dT}{dx} = 0$$

Goal is to minimize \dot{m} with $\dot{m} = \frac{1}{C_L} kA \frac{dT}{dx} \Big|_{x=0}$

Transfer coefficient f
between the vapour and
the copper should be
inserted

For cryogenic engineers is more useful to convert in terms of g/s:

Conduction cooled is 47 mW/A : for 1000 A $2 \cdot 47 \text{ J/s} / 20.9 \text{ J/g} = 4.5 \text{ g/s}$; 130 litre/hour!!

Since 1 g/s = 120 W @ 4.5 K 540 Watt @ 4.5 K!!! (not realistic)

Vapour cooled is 1.04 mW/A: for 1000 A, 0.1 g/s ; 2.9 litre/hour

Since 1 g/s = 120 W @ 4.5 K , 12 W @ 4.5 K

ATLAS (CMS) 21 kA: for a pair of leads

$2 \cdot 1.04 \cdot 21 / 20.9 = 2.1 \text{ g/s}$, i.e. 250 W @ 4.5 K!!

In refrigeration mode (in reality 50% more, 3 g/s).

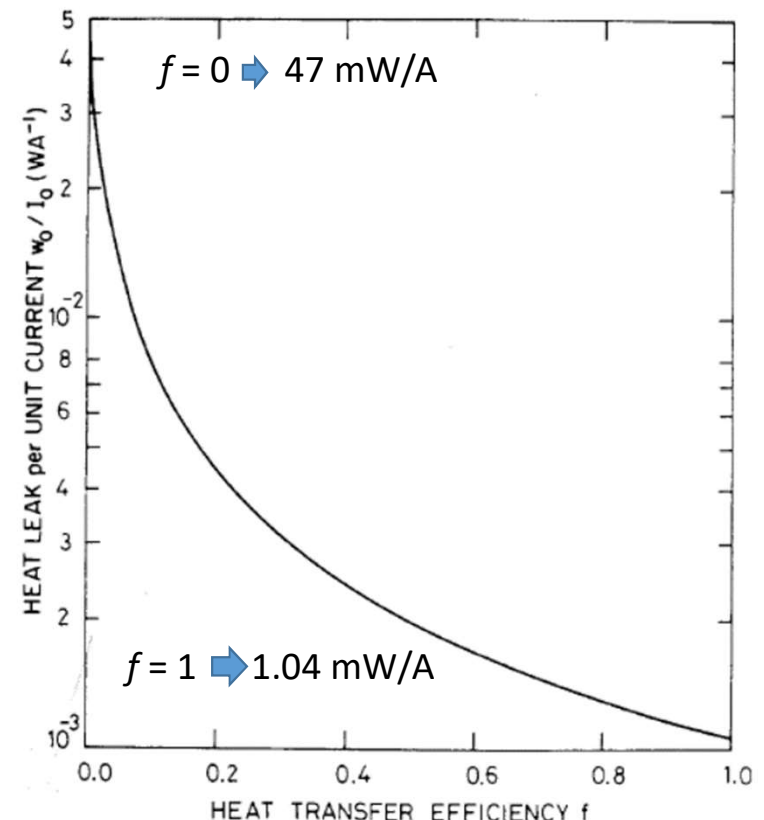


Fig. 11.2. Heat leak caused by an optimized current lead as a function of the efficiency of heat transfer to the boil-off gas stream.

Electrical connection into the cryostat: vapour cooled CL

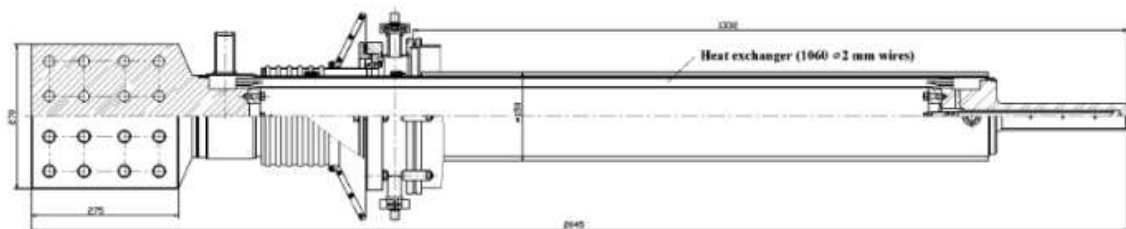


Fig. 1. The current lead design.

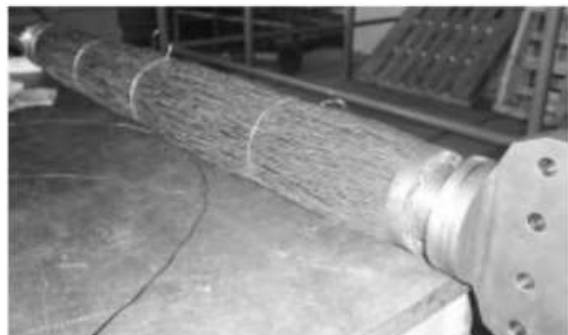


Fig. 2. The heat exchanger.

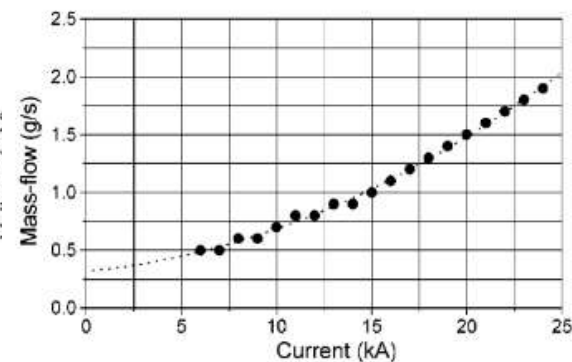


Fig. 8. Mass-flow rate (per one lead) versus current.

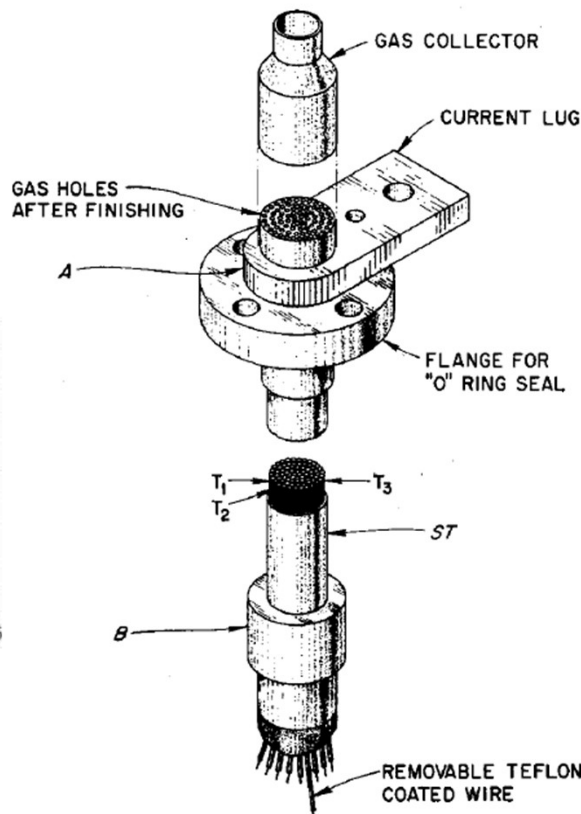


FIG. 1. Construction details for vapor cooled current lead. Woven wire tubes T_1 , T_2 , . . . , are soldered into current contacts A and B by dipping. Removable Teflon wires (contact B) insure a gas entrance hole into each of the woven tubes after solder dipping.

Electrical connection into the cryostat: hybrid CL

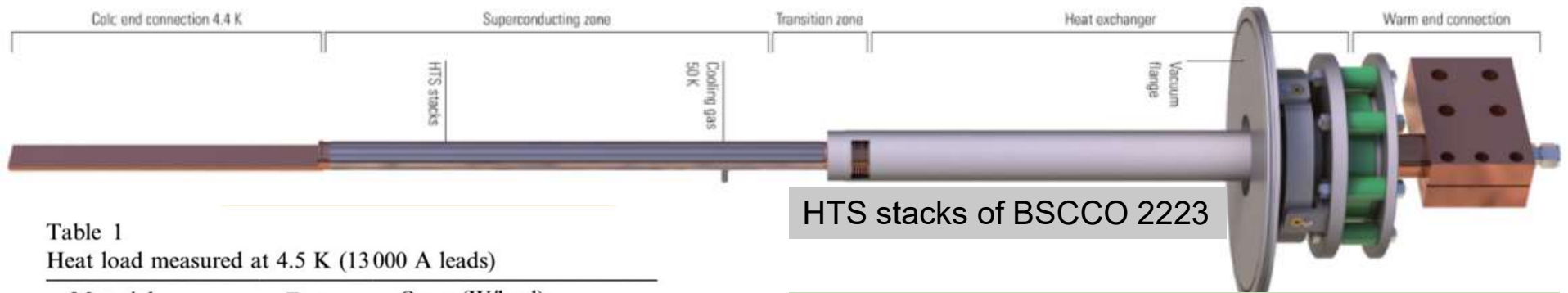


Table 1
Heat load measured at 4.5 K (13 000 A leads)

Material	T_{HTS} (K)	$Q_{4.5 \text{ K}}$ (W/lead)	
		0 A	13 000 A
Bi-2223 tapes	50	0.88	0.95
Bi-2223 tapes	50	1.16	1.74
Bi-2212 MCP	50	1.15	1.3
Bi-2223 AFM	40	1.62	1.68
Bi-2223 tapes	40	0.64	0.715
Bi-2223 tapes ^a	40	1.11	—
Y-123 MT	30	0.75	0.95
Bi-2212 DIP	30	0.82	1.3
Bi-2223 tapes	30	0.81	1.1

^a 13 000 A not achieved.

HTS stacks of BSCCO 2223

For a vapour cooled CL at 13000 A:
 $1.04 \cdot 10^{-3} \cdot 13000 \text{ W} = 13.5 \text{ W}$

For hybrid CL (LHC) the average value is 1.2 W!

Other insulation techniques than vacuum insulation

- **Porous insulation**
 - low gas density embedded (nitrogen), apparent thermal insulation is that of the gas
 - it limits the heat transfer by convection and radiation
 - No linearity as expected but constant
- **Powders & Fibers**
 - perlite (from volcanic rocks, 100-1600 micron)
 - colloidal silica (150-200 angstrom ca. 15-20 nm)
 - silica gel (water is replaced by alcohol, hygroscopic)
 - Note: the vacuum required with powder insulation is much less than with High Vacuum or MLI (\Rightarrow vacuum pump protection!)
 - 300 K \rightarrow 80 K : evacuated powders are superior to HV (powder limits the radiation load) see example
 - 80 K \rightarrow 10 K solid conduction is greater so it is not used in this temperature range
- **Microspheres insulation**
 - hollow spheres, conductivity $\approx 10^{-4}$ W/m-K
- **Specific powder insulation**
 - Adding copper or Aluminium flakes reduce the radiant heat.
 - Gas filled powders on fibrous materials (used T $>$ 77 K or 81.5 K for air condensation).

Other insulation techniques than vacuum insulation

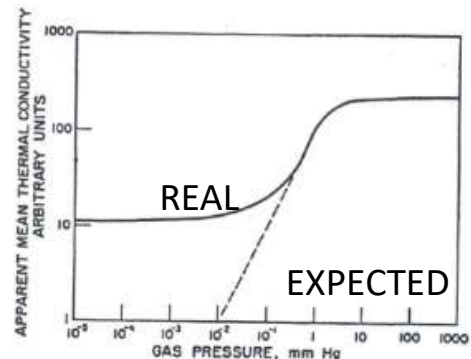


FIGURE 7.8 Variation of the apparent thermal conductivity of an insulating powder as the pressure of the interstitial gas is changed.

TABLE 7.13 Apparent Mean Thermal Conductivity of Some Selected Foams

Foam	Density (g/cm ³)	Boundary temp. (K)	Test space pressure	Conductivity [μW/(cm · K)]
Polystyrene	0.039	300, 77	1 atm	330
	0.046	300, 77	1 atm	260
	0.046	77, 20	10 ⁻⁵ mm Hg	81
Epoxy resin	0.080	300, 77	1 atm	330
	0.080	300, 77	10 ⁻² mm Hg	168
	0.080	300, 77	4 × 10 ⁻³ mm Hg	130
Polyurethane	0.08–0.14	300, 77	1 atm	330
			10 ⁻³ mm Hg	120
Rubber	0.08	300, 77	1 atm	360
Silica	0.16	300, 77	1 atm	550
Glass	0.14	300, 77	1 atm	350

Source: Kropschot 1959 and 1963.

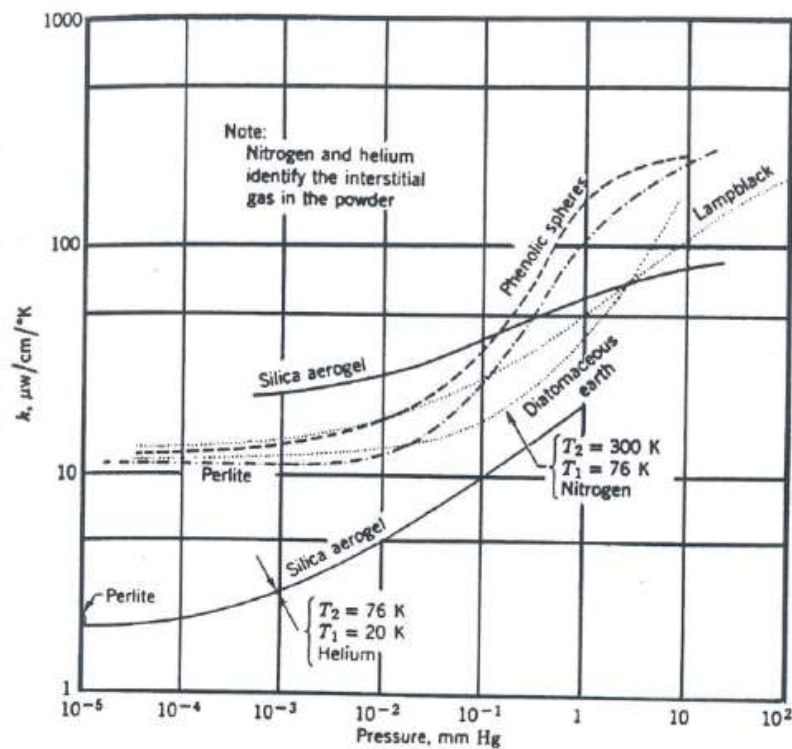


FIGURE 7.9 Apparent mean thermal conductivities of several powders as a function of interstitial gas pressure.

Other insulation techniques than vacuum insulation

Solid foam:

- Polystyrene, Polyurethanes, rubber, silicons (CO_2 used for manufacturing)
 - Gas (air) can penetrate the porous material
 - high expansivity (2-5 times Aluminium, 4-10 times SS)
 - during cooling they will shrink more and then crack, where air and/or moisture can enter
- e.g. Thermal conductivity of Polyurethane : @ 1 atm 0.330 mW/cm-K , @ 10^{-3} torr 0.120 mW/cm-K

-Example: cryostat containing Liquid Argon, is a big box 20 m long and quared faces of 6 m x 6 m.

-The total area is $(4 \times 20 \times 6 + 2 \times 6 \times 6) \text{ m}^2 = 552 \text{ m}^2$

- thermal insulation is 0.80 m of polyurethane (see above).

-@ 1 atm $Q(W) = (552 \times 10^4 \text{ cm}^2 / 80 \text{ cm}) \times 330 \times 10^{-6} \text{ W/cm-K} \times (300 - 80) = 5009 \text{ W}$ (113 l/h LN2)

- @ 10^{-3} Torr $Q(W) = (552 \times 10^4 \text{ cm}^2 / 80 \text{ cm}) \times 120 \times 10^{-6} \text{ W/cm-K} \times (300 - 80) = 1822 \text{ W}$ (41 l/h LN2)

Radiation only:

Assume $\epsilon = 0.1$; $Q = 24912 \text{ Watt}$ (560 l/h LN2)

PROPRIETA' DEI MATERIALI:

- Entalpia (Temperatura di Debye)
- Scelta del materiale
- Contrazione termica
- Conducibilita' termica

TRASMISSIONE DEL CALORE

- Nei solidi
- Nei gas
- Irraggiamento
- Isolamento termico
- Cenni di crio-pompaggio
- Current Leads (discendenti di corrente)

LINEE DI TRASFERIMENTO

- Caduta di pressione
- Termosifone
- Pompe di circolazione
- Valvole criogeniche
- Giunzioni a bassa temperatura
- Dimensionamento di valvole di sicurezza

Esempio di calcolo di pressure drop di una linea di trasferimento

$$\Delta p = \frac{1}{2} \psi \frac{LG^2}{D\rho} \quad \text{where} \quad G = \frac{4m}{\pi D^2},$$

and ψ is a dimensionless factor which is given by

$$\psi = 64 \left(\frac{\eta}{GD} \right)$$

for laminar flow (Poiseuille flow) or

$$\psi = 0.316 \left(\frac{GD}{\eta} \right)^{-0.25}$$

for turbulent flow (see Fig. 3.2).

In most applications the flow is turbulent, $Re > 2300$. From
*G.K.White. Experimental techniques in low-temperature
 physics, Oxford press.*

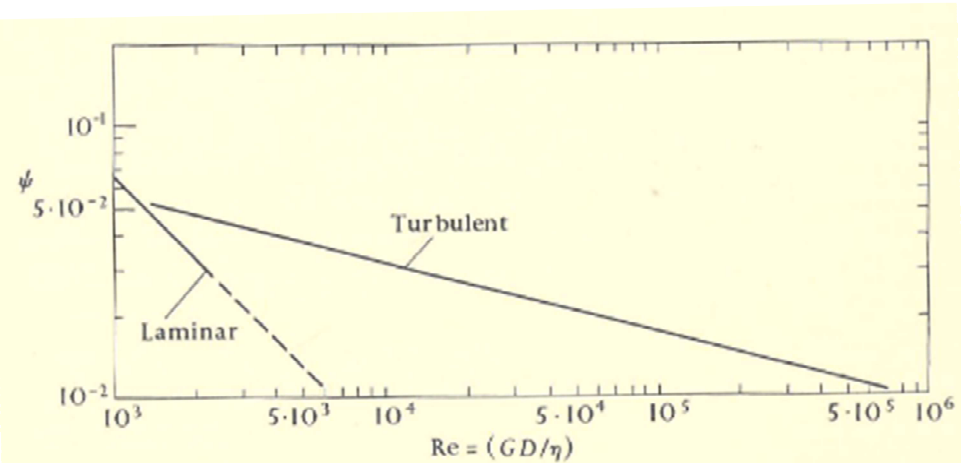


FIG. 3.2. The dimensionless factor ψ as a function of the Reynolds number.

L: pipe length [m]
 ρ: density [kg/m³]
 η: viscosity [Pa·sec]
 D: pipe diameter [m]
 ψ: dimensionless factor

Esempio di calcolo di pressure drop di una linea di trasferimento

mined by Darcy's equation:

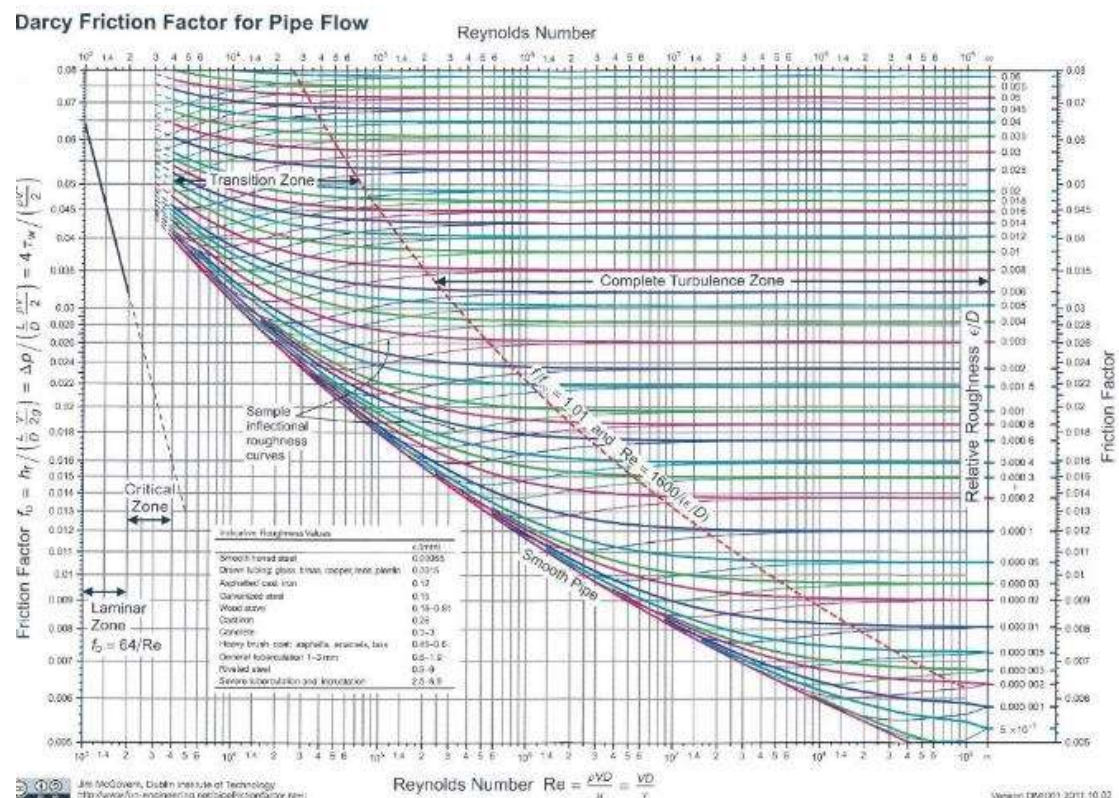
$$h_f = f \frac{L v^2}{D 2g}$$

where h_f = head loss due to friction
 f = friction factor
 L = length of conduit
 D = diameter of conduit
 v = velocity of flow
 g = acceleration of gravity

Table 6-1 Typical wall roughness values for commercial conduits (from [1]†)

Material (new)	Roughness (ϵ)	
	f	m
Riveted steel	0.003–0.03	0.0009–0.009
Concrete	0.001–0.01	0.0003–0.003
Wood stave	0.0006–0.003	0.0002–0.0009
Cast iron	0.00085	0.00026
Galvanized iron	0.0005	0.00015
Asphalted cast iron	0.0004	0.0001
Commercial steel or wrought iron	0.00015	0.000046
Drawn brass or copper tubing	0.000005	0.0000015
Glass and plastic	"smooth"	"smooth"

Moody diagram



Esempio di calcolo di pressure drop di una linea di trasferimento

mined by Darcy's equation:

$$h_f = f \frac{L}{D} \frac{v^2}{2g}$$

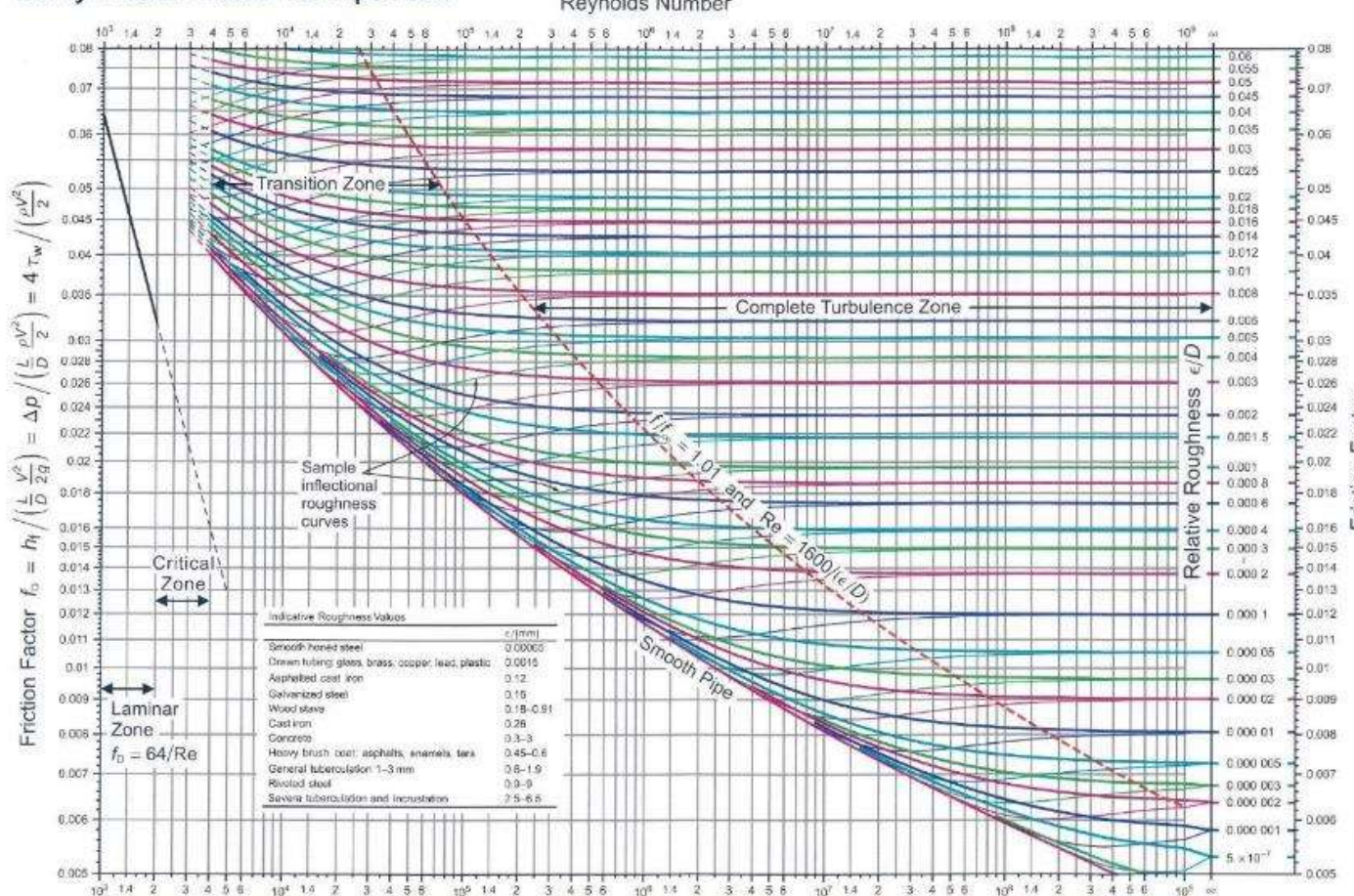
where h_f = head loss due to friction
 f = friction factor
 L = length of conduit
 D = diameter of conduit
 v = velocity of flow
 g = acceleration of gravity

Table 6-1 Typical wall roughness values for commercial conduits (from [1]†)

Material (new)	Roughness (r)	
	ft	m
Riveted steel	0.003-0.03	0.0009-0.009
Concrete	0.001-0.01	0.0003-0.003
Wood stave	0.0006-0.003	0.0002-0.0009
Cast iron	0.00085	0.00026
Galvanized iron	0.0005	0.00015
Asphalted cast iron	0.0004	0.0001
Commercial steel or wrought iron	0.00015	0.000046
Drawn brass or copper tubing	0.000035	0.0000015
Glass and plastic	"smooth"	"smooth"

Esempio di calcolo di pressure drop di una linea di trasferimento

Darcy Friction Factor for Pipe Flow



Moody diagram

Esempio di calcolo di pressure drop di una linea di trasferimento [Metodo 1]

Example: transfer LHe from a dewar (connected to a liquefier/refrigerator) to N cryostats where in total 500 W are dissipated. The LHe in the dewar is at 1.3 bar absolute, i.e. 4.5 K. **Case of pure liquid helium.**

$Q(W) = c_\lambda \text{ [J/g]} \cdot m \text{ [g/s]} = c_\lambda \text{ [J/kg]} \cdot m \text{ [kg/s]}$, c_λ latent heat,

$L = 30 \text{ m}$, D (guess) $25 \text{ mm} = 0.025 \text{ m}$

m : mass flow = $500 \text{ W}/20.9 \text{ J/g} = 23.9 \text{ g/s} = 0.0239 \text{ kg/s}$

η (from HePak) = $3.0 \times 10^{-6} \text{ Pa} \cdot \text{s}$; $G = 4 \text{ m}/(\pi D^2) = 4 \times 0.0239/\pi (0.025)^2 = 48.6887$

$Re = GD/\eta = 403887 \Rightarrow$ turbulent flow

$\Psi = 0.316 (Re)^{-0.25} = 0.01253$;

$DP = 0.5 \cdot 0.01253 \cdot 30 \cdot (48.6887)^2 / (0.025 \cdot 119.0)$

= **150 Pa** = 1.5 mbar

Example: transfer LHe from a dewar (connected to a liquefier/refrigerator) to N cryostats where in total 500 W are dissipated. The LHe in the dewar is at 1.3 bar absolute, i.e. 4.5 K. **Case of pure helium vapor.**

$Q(W) = c_\lambda \text{ [J/g]} \cdot m \text{ [g/s]} = c_\lambda \text{ [J/kg]} \cdot m \text{ [kg/s]}$, c_λ latent heat,

$L = 30 \text{ m}$, D (guess) $25 \text{ mm} = 0.025 \text{ m}$

m : mass flow = $500 \text{ W}/20.9 \text{ J/g} = 23.9 \text{ g/s} = 0.0239 \text{ kg/s}$

η (from HePak) = $1.4 \times 10^{-6} \text{ Pa} \cdot \text{s}$; $G = 4 \text{ m}/(\pi D^2) = 4 \times 0.0239/\pi (0.025)^2 = 48.6887$

$Re = GD/\eta = 884852 \Rightarrow$ turbulent flow

$\Psi = 0.316 (Re)^{-0.25} = 0.0103$;

$DP = 0.5 \cdot 0.0103 \cdot 30 \cdot (48.6887)^2 / (0.025 \cdot 22.07)$

= **664 Pa** = 6.64 mbar

Esempio di calcolo di pressure drop di una linea di trasferimento [Metodo 2]

Example: transfer LHe from a dewar (connected to a liquefier/refrigerator) to N cryostats where in total 500 W are dissipated. The LHe in the dewar is at 1.3 bar absolute, i.e. 4.5 K. **Case of pure liquid helium.**

$Q(W) = c_\lambda \text{ [J/g]} \cdot m \text{ [g/s]} = c_\lambda \text{ [J/kg]} \cdot m \text{ [kg/s]}$, c_λ latent heat,
 $L = 30 \text{ m}$, D (guess) $25 \text{ mm} = 0.025 \text{ m}$
 m mass flow = $500 \text{ W}/20.9 \text{ J/g} = 23.9 \text{ g/s} = 0.0239 \text{ kg/s}$; density = 119 kg/m^3
 η (from HePak) = $3.0 \times 10^{-6} \text{ Pa} \cdot \text{s}$; $Re = GD/\eta = 403887 \Rightarrow$ turbulent flow;
From Moody diagram for a smooth pipe,
Head [m] = $0.014 \cdot 30 \cdot (0.41)^2 / (0.025 \cdot 2 \cdot 9.81) = 0.1405 \text{ [m]}$; $DP = 0.1405 \cdot g \cdot 119 = \textcolor{red}{164 \text{ Pa}}$

Example: transfer LHe from a dewar (connected to a liquefier/refrigerator) to N cryostats where in total 500 W are dissipated. The LHe in the dewar is at 1.3 bar absolute, i.e. 4.5 K. **Case of pure helium vapor.**

$Q(W) = c_\lambda \text{ [J/g]} \cdot m \text{ [g/s]} = c_\lambda \text{ [J/kg]} \cdot m \text{ [kg/s]}$, c_λ latent heat,
 $L = 30 \text{ m}$, D (guess) $25 \text{ mm} = 0.025 \text{ m}$
 m mass flow = $500 \text{ W}/20.9 \text{ J/g} = 23.9 \text{ g/s} = 0.0239 \text{ kg/s}$; density = 22.07 kg/m^3
 η (from HePak) = $1.4 \times 10^{-6} \text{ Pa} \cdot \text{s}$; $Re = GD/\eta = 884852 = \rho D v / \eta >$ turbulent flow
From Moody diagram for a smooth pipe
Head [m] = $0.012 \times 30 \times (2.21)^2 / (0.025 \times 2 \times 9.81) = 22 \text{ m}$; $DP = 22 \times g \times 22.07 = \textcolor{red}{771 \text{ Pa}}$

Esempio di calcolo di pressure drop di una linea di trasferimento [Metodo 3]

Case of pure liquid helium.

$Q(W) = c_\lambda \text{ [J/g]} \cdot m \text{ [g/s]} = c_\lambda \text{ [J/kg]} \cdot m \text{ [kg/s]}$, c_λ latent heat,
 $L = 30 \text{ m}$, D (guess) $25 \text{ mm} = 0.025 \text{ m}$
 m mass flow = $500 \text{ W}/20.9 \text{ J/g} = 23.9 \text{ g/s} = 0.0239 \text{ kg/s}$; density = 119 kg/m^3
 η (from HePak) = $3.0 \times 10^{-6} \text{ Pa} \cdot \text{s}$; $Re = GD/\eta = 403887 \Rightarrow$ turbulent flow; [e.g. Barron, Cryogenic Engineering]
 $f = 64/Re$ if $Re < 2300$;
 $f = 0.316 Re^{-0.25}$ if $3000 < Re < 50000$;
 $f = 0.184^{-0.20}$ if $Re > 50000$;
 $Re = \rho v D/\mu = 403887$
 $f = 0.184 \times 403887^{-0.20} = 0.0139$
 $DP = L f G^2/2 \rho D = 0.0139 \times 11961.24 = 166.5 \text{ Pa}$

Case of pure helium vapor.

$Q(W) = c_\lambda \text{ [J/g]} \cdot m \text{ [g/s]} = c_\lambda \text{ [J/kg]} \cdot m \text{ [kg/s]}$, c_λ latent heat,
 $L = 30 \text{ m}$, D (guess) $25 \text{ mm} = 0.025 \text{ m}$
 m mass flow = $500 \text{ W}/20.9 \text{ J/g} = 23.9 \text{ g/s} = 0.0239 \text{ kg/s}$; density = 22.07 kg/m^3
 η (from HePak) = $1.4 \times 10^{-6} \text{ Pa} \cdot \text{s}$; $Re = GD/\eta = 884852 = \rho D v / \eta >$ turbulent flow
 $f = 64/Re$ if $Re < 2300$;
 $f = 0.316 Re^{-0.25}$ if $3000 < Re < 50000$;
 $f = 0.184^{-0.20}$ if $Re > 50000$;
 $Re = \rho v D/\mu = 884852$
 $f = 0.184 \times 884852^{-0.20} = 0.0119$
 $DP = L f G^2/2 \rho D = 0.0119 \times 64294 = 765 \text{ Pa}$

Esempio di calcolo di termosifone

Supponiamo di voler raffreddare un magnete usando solo la forza di gravità: termosifone (ALEPH, CMS;..)

The pressure drop ΔP_f due to the friction in the turbulent flow is given by [3] [6] (in SI units):

$$\Delta P_f = \rho * f * (L * v^2) / (2 * D)$$

is the fluid density [kg/m^3]

f is the friction factor

L is the length of the pipe [m]

v is the velocity of the fluid [m/s]

D is the diameter of the pipe [m]

$$\Delta P_f = 8 * f * (L * m^2) / (\pi^2 * \rho * D^5)$$

For a simplified thermosyphon calculation let x be fraction of vapor produced:

$$x = q / (c_L * m) = q / (c_L * \rho * S * v)$$

q is the heat load [W]

c_L is the latent heat [J/kg]

S is the pipe cross-section [m^2]

m is the mass flow [kg/s].

Esempio di calcolo di termosifone

Supponiamo di voler raffreddare un magnete usando solo la forza di gravità: termosifone (ALEPH, CMS;..)

The complete thermosiphon loop is composed of a U-shape circuit vertically oriented and a helium phase separator vessel located in elevated position. The downstream branch is

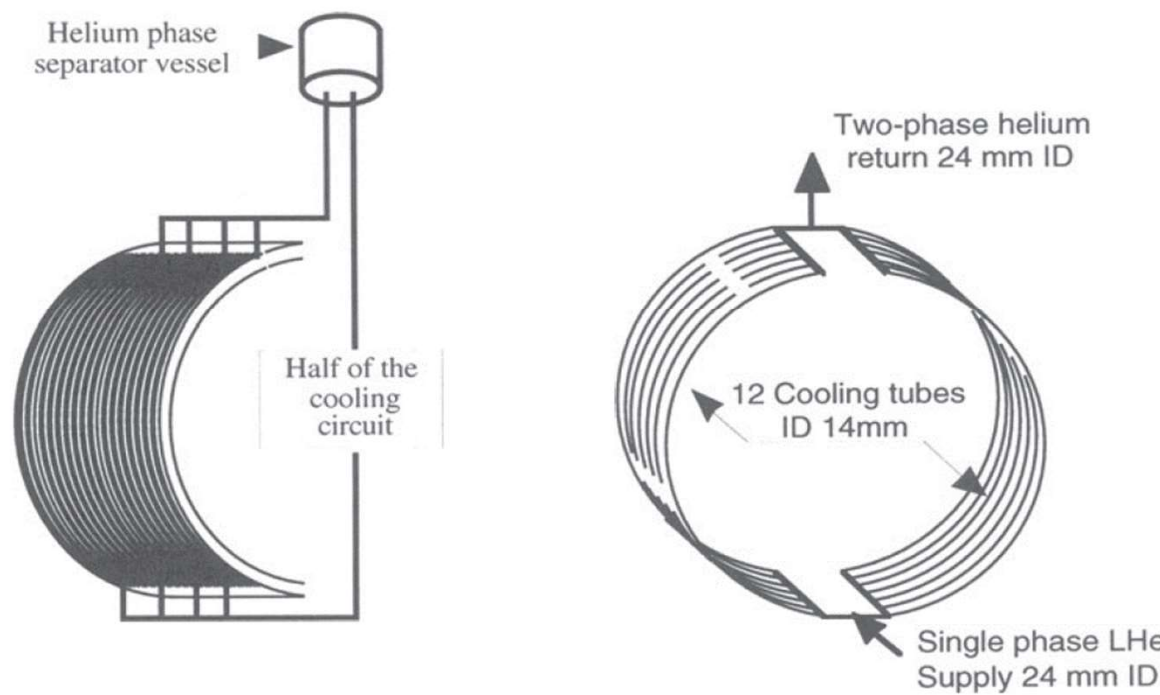


Figure 1. Cooling circuit of the CMS solenoid in a thermiphon mode. The 8 sub-circuits are connected by pair to the phase separator vessel. Inlet and outlet are situated at opposite side.

Esempio di calcolo di termosifone

The subscripts L and G stand for liquid and gas respectively.

If the difference in volume, due to the input heat load, were empty, then the pressure difference ΔP_L would be given by:

$$\Delta P_L = x * \rho_L * g * h$$

From the above value one has to subtract the amount ΔP_V

$$\Delta P_V = x * \rho_L * g * h * (\rho_G / \rho_L),$$

which is due to the vapor, in order to obtain the total ΔP_{Th} for the thermosyphon:

$$\Delta P_{Th} = \Delta P_L - \Delta P_V = q * (\rho_L - \rho_G) * g * h / (c_L * \rho_L * S * v).$$

Since the fraction of vapor is of the order of a few percent, i.e. $\rho \approx \rho_L$, one can assume that:

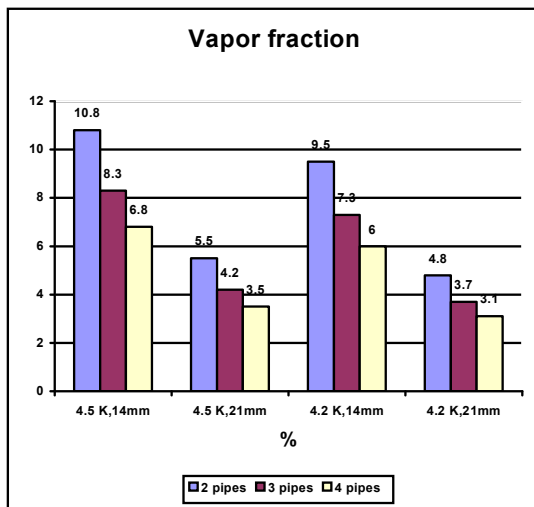
$$\Delta P_f \approx \rho_L * f * (L * v^2) / (2 * D).$$

By substitution of the values for helium at 4.5 K (or at 4.2 K), for $q = 185$ W, as calculated in this report, and solving the resulting equations in v , one obtains the total mass flow given in the following tables. In the calculation the correction (of the order of few percent) due to the bends was not taken into account. The presence of bends in the circuit gives, as a consequence, a reduced value of the velocity and a decrease in mass flow as well as an increase in the value of vapor fraction.

Esempio di calcolo di termosifone

Table A1 Summary of the mass flow for the racetrack cooling system @ 4.5 K. Each of the pipes is 21 m long.

Number of pipes	Pipe diameter (mm)	Velocity (m/s)	Vapor fraction %	Mass flow (l/h)
4 x 2 = 8	14	0.62	10.8	2749
4 x 2 = 8	21	0.54	5.5	5402
4 x 3 = 12	14	0.54	8.3	3601
4 x 3 = 12	21	0.47	4.2	7078
4 x 4 = 16	14	0.49	6.8	4363
4 x 4 = 16	21	0.43	3.5	8575



The simplified calculation, given above, shows that the thermosyphon cooling is feasible, with a pipe diameter of 21 mm and a three- or four-pipe geometry. The above calculations have been also successfully compared to the values published for the ALEPH case, and an agreement better than 10 % was found (see the text below).

Esempio di calcolo di termosifone

Note. In the following an example of the calculation, for comparison only, is outlined for the ALEPH thermosyphon. The total input load given is 200 W, divided in 52 pipes in parallel each 8.7 m long and 14 mm in diameter. The flow is taken as turbulent [3] [6] with an $\varepsilon / D = 1.5 \cdot 10^{-6} [\text{m}] / 1.4 \cdot 10^{-2} [\text{m}] = 1.1 \cdot 10^{-4}$. The pressure drop due to the friction is then

$$\Delta P_f = f \cdot v^2 \cdot 38964 .$$

With the notation used above, and for the ALEPH case, the thermosyphon pressure drop is given by

$$\Delta P_{Th} = 50.95/v.$$

Solving the equation for v and with $f = 0.02$, extracted from the usual Moody diagram [3][6], one obtains $v = 0.40 [\text{m/s}]$. The total flow, for the 52 pipes in parallel is given by the following expression:

$$Q[\text{l/h}] = S \cdot v = 1.54 \cdot 10^{-4} [\text{m}^2] \cdot 0.40 [\text{m/s}] \cdot 3600 [\text{s/h}] \cdot 1000 [\text{l/m}^3] \cdot 52 = \mathbf{11614 [\text{l/h}]},$$

where S is the cross section of the pipes and v the calculated velocity, to be compared to the value of 11000 [l/h] quoted in ref. [9].

The reduction due to the bends of the pipes in the circuit should be of the order of a few percents and it has not been taken into account in the calculation because its exact number was unknown. The correction would bring the calculated value closer to the one quoted in [9].

Esempio di calcolo di head di una pompa e dell'efficienza

Quite often is necessary to have a higher mass flow and/or a higher pressure head than that available from a JT circuit of a given refrigerator.

Suppose we need 1.6 kW to cool a big magnet (ATLAS): the refrigerator has a max JT flow of 295 g/s (5000 W) and a the available D_p is less than 300 mbar. We need to dissipate ca. 1600 W, i.e. more than 36% vapor will be produced. In case of all vapor the heat load would produce the temperature increase according to:

$$Q(W) = C_p m \Delta T.$$

The task is achieved by adding a Liquid helium pump and leaving the refrigerator to work in a closed cycle.

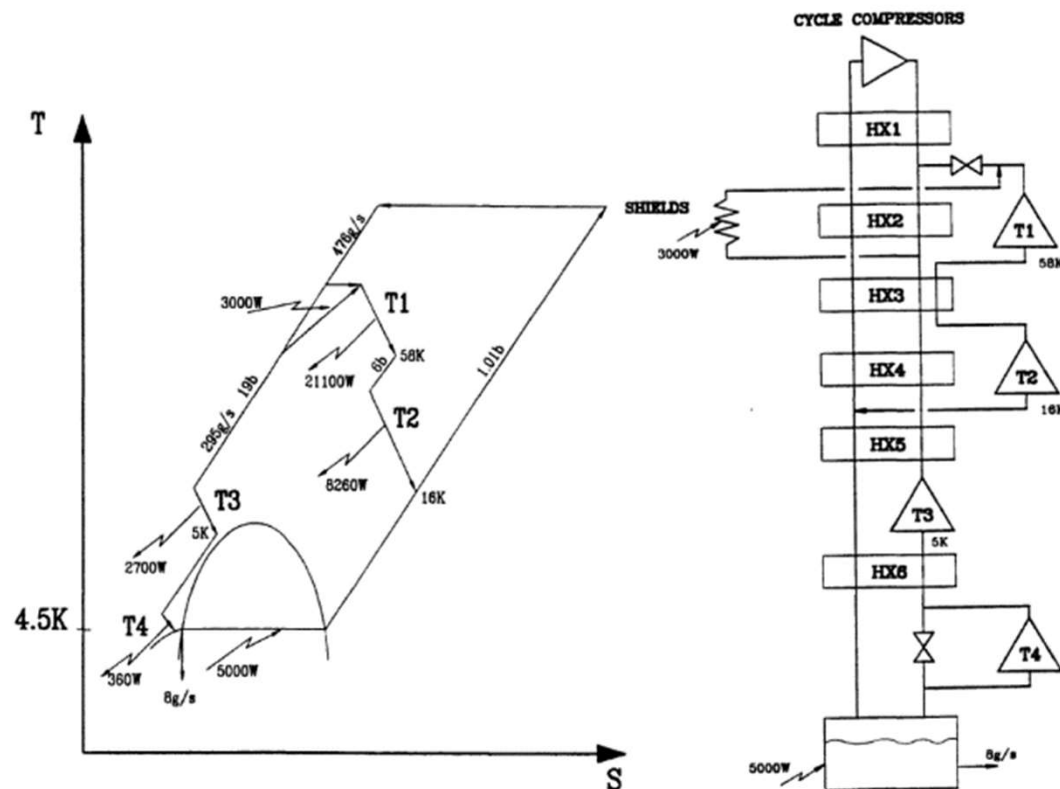
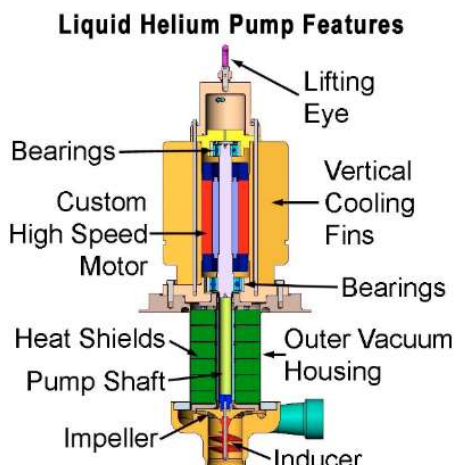
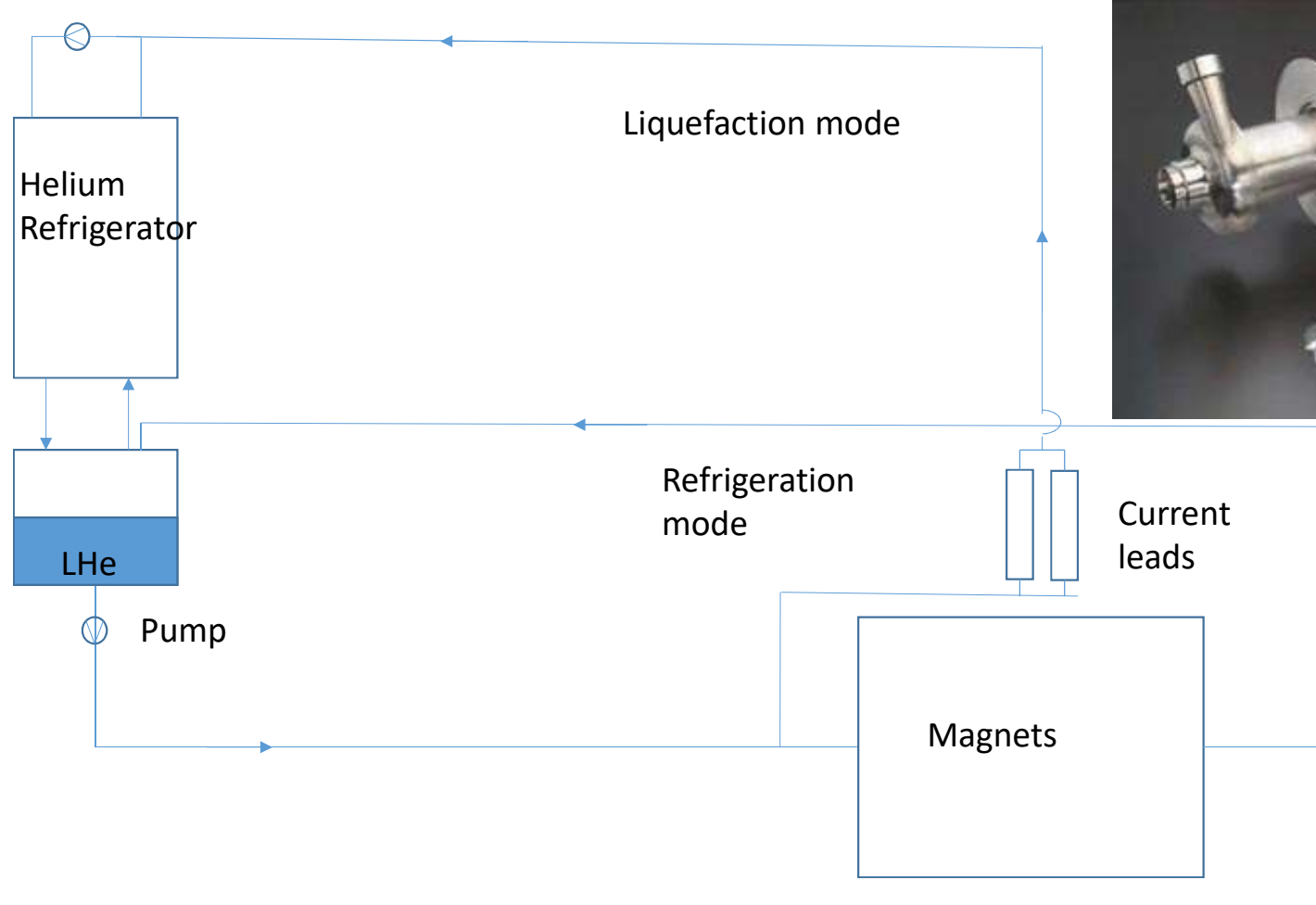


Figure 1. The 6 kW cycle.

Esempio di calcolo di head di una pompa e dell'efficienza



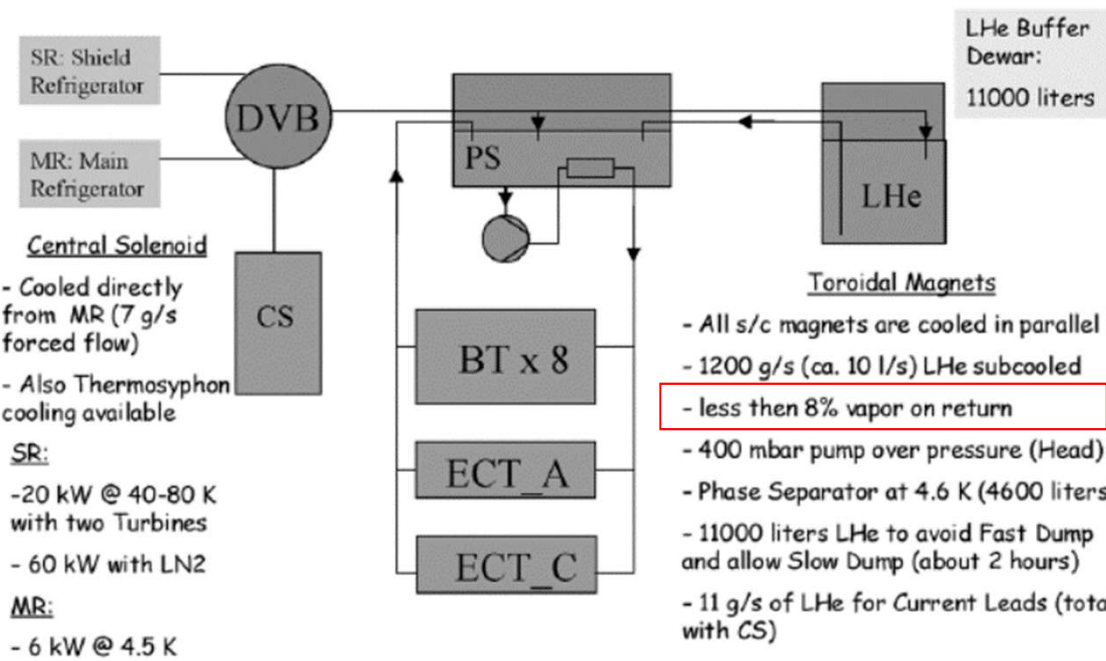


Fig. 1. A schematic view of the cryogenic ATLAS cooling system is shown.

The advantage in mass flow and pressure head is paid by the efficiency of the pump, ca. 60%.

$$(1.2 \text{ kg/s} \times 40000 \text{ Pa}) / 120 \text{ kg/s} = \\ = 400 \text{ W}$$

Since efficiency is 0.6 the refrigerator has to produce:
400 W/0.6= 670 W.

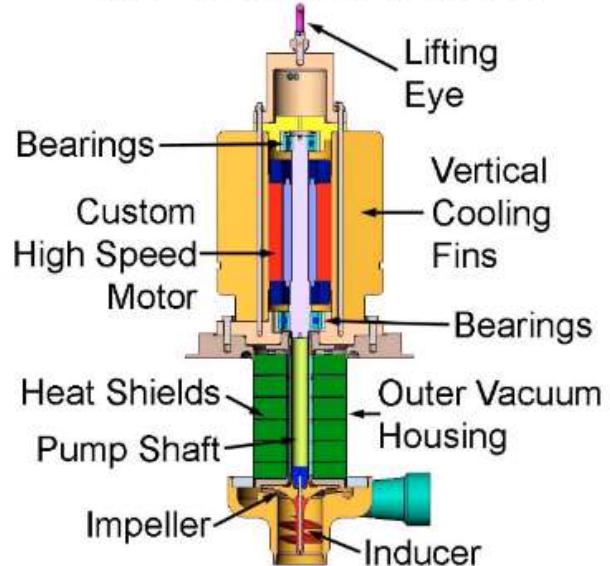
The use of a LHe pump has to be avoided when possible.

ciency η is calculated as follows:

$$\eta = \frac{\dot{m} \int_{P_1}^{P_2} \frac{dp}{\rho}}{W} = \frac{\dot{m}}{W} \frac{\Delta P}{\rho}, \quad \text{R.Pengo, et al., Cryogenics 50 (2010) 8–12} \quad (2)$$

where \dot{m} is the LHe mass flow (kg/s), $\Delta P = P_2 - P_1$ is the pressure head across the pump (Pa), ρ is the density of LHe (kg/m³), W (W) is the net heat load at the test station. The efficiency calculated

Liquid Helium Pump Features



Esempio di calcolo del flow coefficient K_v ($C_v=1.17 K_v$) di una valvola

K_v -value

The K_v -value is a parameter defining the flow rate of valves. It describes the amount of water from 5° to 30°C which flows through the valve at a pressure loss of 1 bar. The K_{vs} -value describes the K_v -value when the valve is 100% open.

For water 5-30°C applies:

$$K_v = \frac{Q}{\sqrt{\Delta p}}$$

General Liquid Flow Formula:

$$K_v = Q \sqrt{\frac{P}{1000 \Delta p}}$$

Conversion of K_v in C_v
 $C_v = 1,17 \times K_v$

Conversion of C_v in K_v
 $K_v = 0,86 \times C_v$

Explanations:

K_v	m^3/h	flow rate parameter
Q	m^3/h	volume flow rate
	kg/m^3	specific gravity
P_1	bar	pressure before the valve
P_2	bar	pressure after the valve
Δp	bar	pressure drop through the valve
		$\Delta p = P_1 - P_2$

The linear flow characteristic curve allows the flow rate to be directly proportional to the valve travel ($\Delta q/\Delta x$ equals a constant) or in terms of the inherent valve characteristic, $f(x) = x$.

An equal percentage valve starts initially with a slow increase in flow rate with valve position which dramatically increases as the valve opens more.

The term equal percentage for a slow opening characteristic curve may at first be confused with the description of a linear characteristic curve.

However, for an equal percentage valve, $\Delta q/\Delta x$ at any stage, is proportional to the flow rate q at that moment. This is in contrast with a linear characteristic for which $\Delta q/\Delta x$ is constant.

That $\Delta q/\Delta x$ is proportional to q , may be rephrased as $\Delta q/q$ is proportional to Δx . This means the percentage change Δq with respect to the current flow rate q (that is $(\Delta q/q) \times 100$), is equal at every valve travel position x for the same change in valve travel Δx , hence the term 'equal percentage'.

The inherent valve characteristic for an equal percentage valve is exponential in nature

Esempio di calcolo del flow coefficient K_v ($C_v = 1.17 K_v$) di una valvola

K_v -value

The K_v -value is a parameter defining the flow rate of valves. It describes the amount of water from 5° to 30°C which flows through the valve at a pressure loss of 1 bar. The K_{vs} -value describes the K_v -value when the valve is 100% open.

Conversion of K_v in C_v

$$C_v = 1.17 \times K_v$$

Conversion of C_v in K_v

$$K_v = 0.86 \times C_v$$

For water 5-30°C applies:

$$K_v = \frac{Q}{\sqrt{\Delta p}}$$

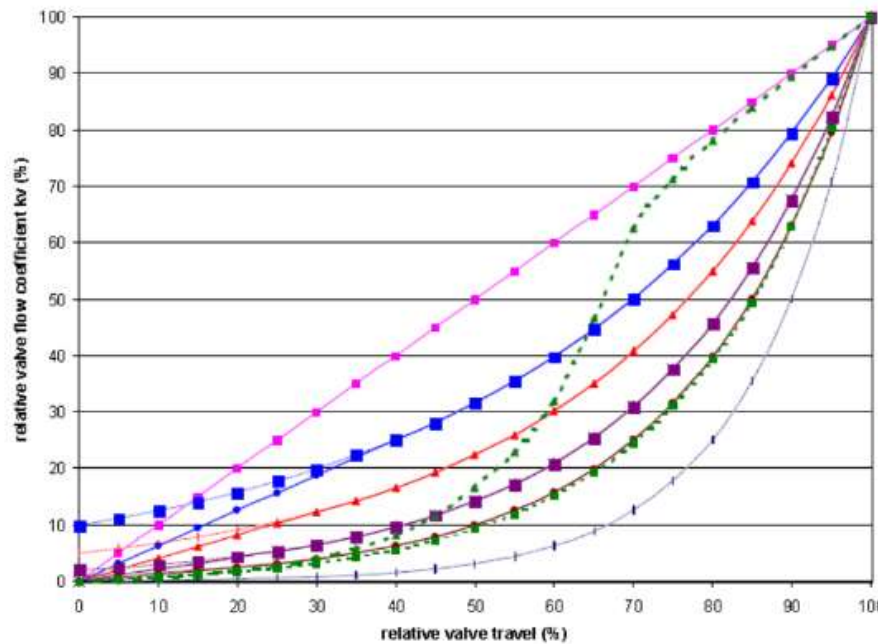
General Liquid Flow Formula:

$$K_v = Q \sqrt{\frac{\rho}{1000 \Delta p}}$$

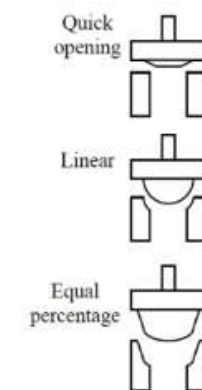
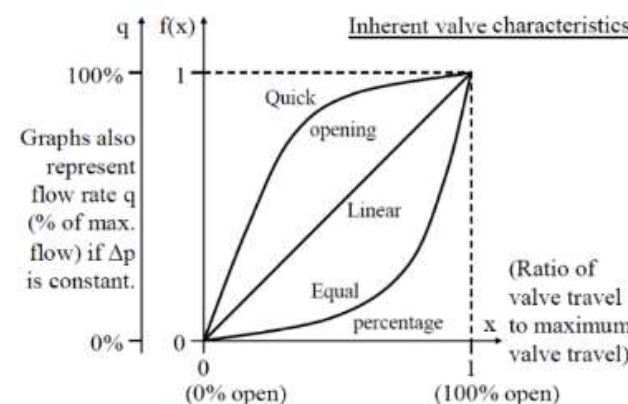
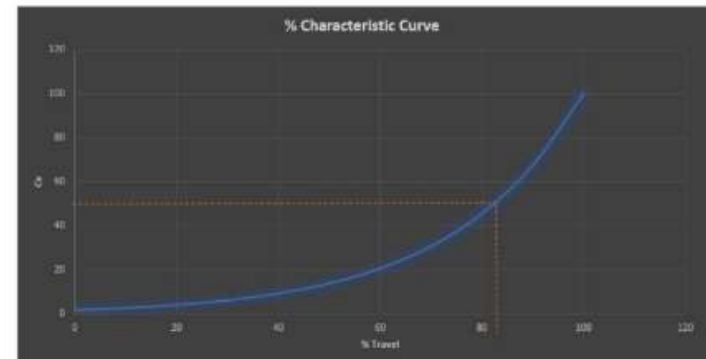
Explanations:

K_v	m^3/h	flow rate parameter
Q	m^3/h	volume flow rate
	kg/m^3	specific gravity
p_1	bar	pressure before the valve
p_2	bar	pressure after the valve
Δp	bar	pressure drop through the valve
		$\Delta p = p_1 - p_2$

Esempio di calcolo del flow coefficient K_v ($C_v=1.17 K_v$) di una valvola



Graphs also represent flow rate q (% of max. flow) if Δp is constant.



Esempio di calcolo del flow coefficient K_v ($C_v=1.17 K_v$) di una valvola

Definitions of valve flow characteristics:

Equal percentage flow characteristics (eq-%, =%):

An ideal equal percentage flow characteristics would yield the same percentage of kv-flow increase for each percentage increment of travel. In the example that follows, this increase is 47% over the previous kv-value for each 10% increase in travel (i.e. rangeability factor 1:50).

Expressed mathematically: $\Phi = \Phi_0 * e^{nh}$

Where: Φ = fraction of kv

Φ_0 = lowest fraction of rated kv (usually at $h \approx 0$) that conform to the specific flow characteristic

e = 2.7183, the base of the natural logarithm

n = $\log_e(1/\Phi_0)$

h = fraction of rated travel

For $\Phi_0 = 0.02$ (= 1:50) the values of Φ shown in table follows are calculated:

An ideal Equal Percentage Flow Characteristic:

$h =$	0.00	0.05	0.10	0.20	0.30	0.40	0.50	0.60	0.70	0.80	0.90	1.00
$\Phi =$	0.020	0.024	0.030	0.044	0.065	0.096	0.141	0.209	0.309	0.457	0.676	1.000

Linear flow characteristics (lin):

In an ideal linear flow characteristics the kv values increases by the same increment for each fraction of travel:

Expressed mathematically: $\Phi = \Phi_0 + m * h$

Where: Φ = fraction of kv

m = the slope of versus travel, $(\Phi - \Phi_0)/h$

Assuming $\Phi_0 = 0$ (= ideal) or $\Phi_0 = 0.02$, Φ has the values shown in table follows:

An ideal Linear Flow Characteristic:

$h =$	0.00	0.05	0.10	0.20	0.30	0.40	0.50	0.60	0.70	0.80	0.90	1.00
$\Phi = (\Phi_0 = 0)$	0.000	0.050	0.100	0.200	0.300	0.400	0.500	0.600	0.700	0.800	0.900	1.000
$\Phi = (\Phi_0 = 0.02)$	0.020	0.069	0.118	0.216	0.314	0.412	0.510	0.608	0.706	0.804	0.902	1.000

Esempio di calcolo del flow coefficient K_v ($C_v=1.17 K_v$) di una valvola

Specification:

Valve Sizing Formulas (k_v -Value)

The calculation for the k_v -value is standardized in DIN EN 1534. For a provisional, simplified sizing for control valves the following basic formulas are usable.

p_1 upstream pressure, in bar
 p_2 downstream pressure, in bar
 Δp pressure drop, in bar
 Q flow of liquids, in m^3/h
 W flow in kg/h

ρ specific gravity, in general and for liquids, in kg/m^3
 ρ_g specific gravity of gases at 273K and 1013mbar, in kg/m^3
 Q_g volumetric flow for gases at 273K and 1013mbar in m^3/h
 T_1 temperature in K, upstream
 v_1 specific volume of vapor at p_1 and T_1 , in m^3/kg
 v_2 specific volume of steam/vapour at p_2 and T_2 , in m^3/kg
 v^* specific volume of steam/vapour at $p_1/2$ and T_1 , in m^3/kg

Liquid Service:

m^3/h	kg/h
$k_v = Q \sqrt{\frac{p}{1000 * \Delta p}}$	$k_v = \frac{W}{\sqrt{1000 * \rho * \Delta p}}$

Gas Service:

subcritical flow i.e. $p_2 > p_1/2$ and $\Delta p < p_1/2$	
m^3/h	kg/h
$k_v = \frac{Q_g}{519} \sqrt{\frac{\rho_g * T_1}{\Delta p * p_2}}$	$k_v = \frac{W}{519} \sqrt{\frac{T_1}{\rho_g * \Delta p * p_2}}$

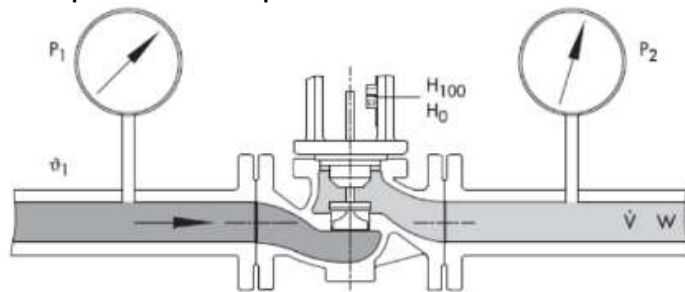
critical flow i.e. $p_2 < p_1/2$ and $\Delta p > p_1/2$	
m^3/h	kg/h
$k_v = \frac{Q_g}{259.5 * p_1} \sqrt{\rho_g * T_1}$	$k_v = \frac{W}{259.5 * p_1} \sqrt{\frac{T_1}{\rho_g}}$

Vapour / Steam Service:

subcritical flow i.e. $p_2 > p_1/2$ and $\Delta p < p_1/2$	
kg/h	kg/h
$k_v = \frac{W}{\sqrt{1000} \sqrt{\frac{v_2}{\Delta p}}}$	$k_v = \frac{W}{\sqrt{1000}} \sqrt{\frac{2 * v^*}{p_1}}$

Esempio di calcolo del flow coefficient K_v ($C_v=1.17 K_v$) di una valvola

The procedure specified in the IEC 60534 standard



p_1 Upstream pressure
 p_2 Downstream pressure
 H Travel
 V Volume flow rate in m^3/h (gases)
 W Mass flow rate in kg/h (liquids, steam)
 ρ Density in kg/m^3
 $(\text{general}, \text{also in liquids})$
 ρ_1 Density upstream of the valve in kg/m^3
 $(\text{in gases and vapors})$
 ϑ_1 Temperature in $^\circ\text{C}$ upstream of the valve

Medium Pressure drop	Liquids		Gases		Steam
	m^3/h	kg/h	m^3/h	kg/h	kg/h
$p_2 > \frac{p_1}{2}$			$K_V = \frac{\dot{V}_G}{519} \sqrt{\frac{p_0 T_1}{\Delta p \rho}}$	$K_V = \frac{W}{519} \sqrt{\frac{T_1}{p_0 \Delta p p_2}}$	$K_V = \frac{W}{31.62} \sqrt{\frac{v_2}{\Delta p}}$
$\Delta p < \frac{p_1}{2}$	$K_V = \dot{V} \sqrt{\frac{P}{1000 \Delta p}}$	$K_V = \frac{W}{\sqrt{1000 \rho \Delta p}}$			
$p_2 < \frac{p_1}{2}$			$K_V = \frac{\dot{V}_G}{259.5 p_1} \sqrt{p_0 T_1}$	$K_V = \frac{W}{259.5 p_1} \sqrt{\frac{T_1}{\rho}}$	$K_V = \frac{W}{31.62} \sqrt{\frac{2v^*}{p_1}}$
$\Delta p > \frac{p_1}{2}$					

where:

p_1 [bar] Absolute pressure p_{abs}

ρ [kg/m^3] Density of liquids

p_2 [bar] Absolute pressure p_{abs}

ρ_G [kg/m^3] Density of gases at 0°C and 1013 mbar

Δp [bar] Absolute pressure p_{abs} (differential pressure $p_1 - p_2$)

v_1 [m^3/kg] Specific volume (v found in the steam table) for p_1 and ϑ_1

T_1 [K] $273 + \vartheta_1$

v_2 [m^3/kg] Specific volume (v found in the steam table) for p_2 and ϑ_1

\dot{V}_G [m^3/h] Flow rate of gases,
related to 0°C and 1013 mbar

v^* [m^3/kg] Specific volume (v found in the steam table) for $\frac{p_1}{2}$ and ϑ_1

Esempio di calcolo del flow coefficient K_v ($C_v=1.17 K_v$) di una valvola

Suppose we have to feed a cryostat with four cavities each dissipating 7 W RF at 4.5 K. The cavities are housed in a cryostat whose static heat load is 12 W at 4.5 K: total heat load is 50 W i.e. $50W/20.9 \text{ J/g} = 2.39 \text{ g/s}$.

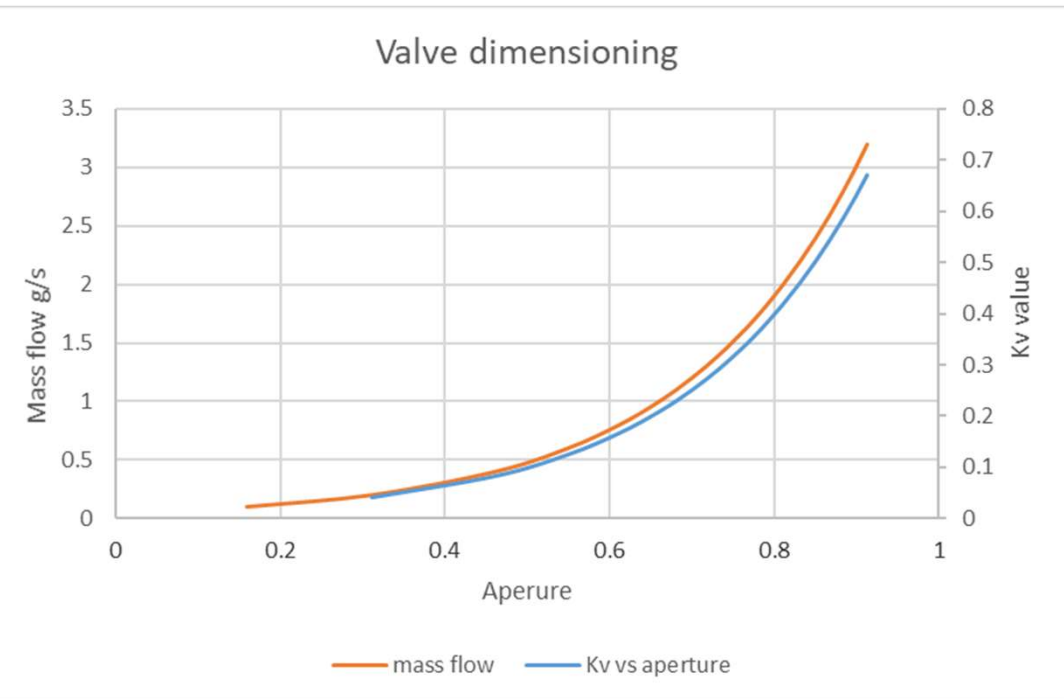
Calculate the appropriate K_v of the cryogenic valve

Case 1: Feeding fluid is pure liquid helium at $P_1 = 1.3 \text{ bar abs}$, $P_2 = 1.1 \text{ Bar abs}$ in the cryostat, i.e. $\Delta P = 0.2 \text{ bar}$

Density ρ of LHe at 4.5 K is 118 g/liter (or Kg/m^3). From the previous formulas:

$$K_v = 2.39 \cdot 3.6 / \sqrt{1000 \cdot \rho \cdot \Delta P} = 0.056 \Rightarrow K_v \text{ chosen is } 2 \cdot 0.056 = 0.112;$$

K_v installed	Aperture					K_v/K_v installed	Aperture
g/s	K_v	def 1:50	def 1:100			Proportiona l	
0.1	0.002334	0.011502	0.160286	0.020921		1.792392	
0.2	0.004669	0.0188686	0.310801	0.041841		3.584784	
0.4	0.009337	0.036587	0.461316	0.083682		5.377176	
0.6	0.014006	0.0469516	0.549362	0.125523		7.169567	
0.8	0.018675	0.0543054	0.611831	0.167364			
1	0.023344	0.0600094	0.660286	0.209205		8.961959	
1.2	0.028012	0.06467	0.699877	0.251046		10.75435	
1.4	0.032681	0.0686104	0.73335	0.292887		12.54674	
1.6	0.03735	0.0720238	0.762346	0.334728		14.33913	
1.7	0.039684	0.0735735	0.775511	0.355649		15.23533	
1.8	0.042019	0.0750346	0.787922	0.376569		16.13153	
2	0.046687	0.0777278	0.810801	0.41841		17.92392	
2.2	0.051356	0.0801641	0.831497	0.460251		19.71631	
2.4	0.056025	0.0823883	0.850392	0.502092		21.5087	
2.6	0.060694	0.0844344	0.867773	0.543933		23.30109	
2.8	0.065362	0.0863288	0.883865	0.585774		25.09349	
3	0.070031	0.0880924	0.898847	0.627615		26.88588	
3.2	0.0747	0.0897421	0.912861	0.669456		28.67827	



Esempio di calcolo del flow coefficient K_v ($C_v=1.17 K_v$) di una valvola

Suppose we have to feed a cryostat with four cavities each dissipating 7 W RF at 4.5 K. The cavities are housed in a cryostat whose static heat load is 12 W at 4.5 K: total heat load is 50 W i.e $50W/20.9 J/g = 2.39 \text{ g/s}$.

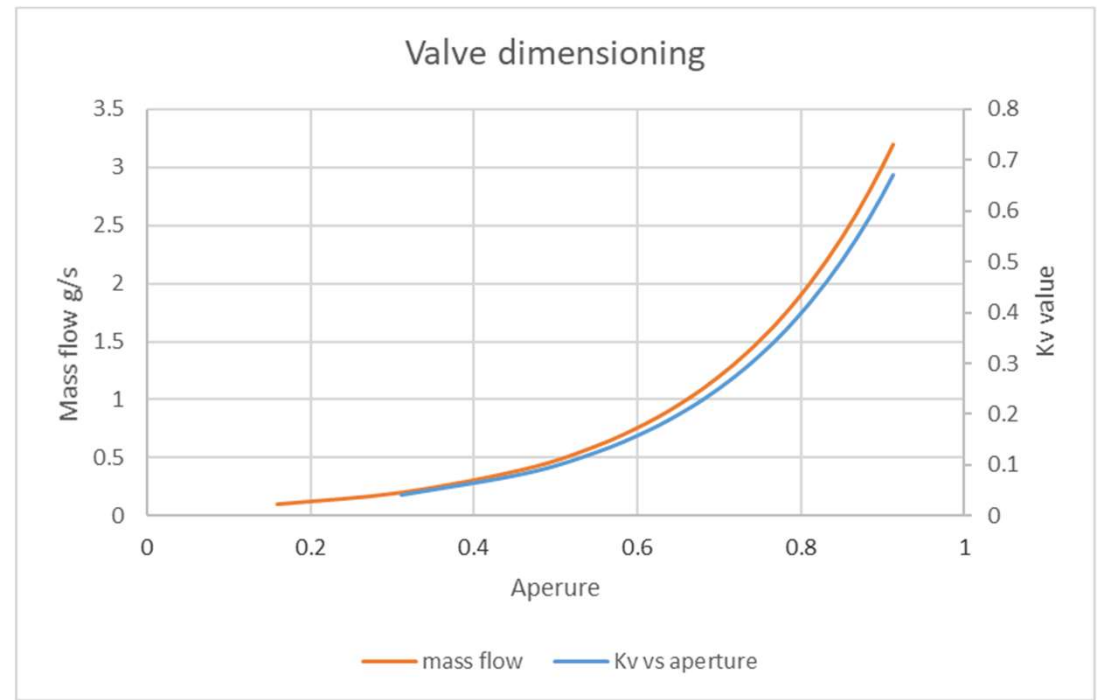
Calculate the appropriate K_v of the cryogenic valve

Case 2: Feeding fluid is pure vapor helium at $P_1 = 1.3 \text{ bar abs}$, $P_2 = 1.1 \text{ Bar abs}$ in the cryostat, i.e. $\Delta P = 0.2 \text{ bar}$

Density ρ of LHe at 4.5 K is 22.1 g/liter (or Kg/m^3). From the previous formulas:

$$K_v = 2.39 \cdot 3.6/\sqrt{1000 \cdot \rho \cdot \Delta P} = 0.129 \Rightarrow K_v \text{ chosen is } 2 \cdot 0.129 = 0.259;$$

Kv installed		Aperture				Aperture	
g/s	Kv	def 1:50	def 1:100	Kv/Kv installed	Proportiona l		
0.1	0.005412	0.011502	0.160286	0.020921			
0.2	0.010824	0.018686	0.310801	0.041841	0.773098		
0.4	0.021648	0.036587	0.461316	0.083682	1.546196		
0.6	0.032473	0.0469516	0.549362	0.125523	2.319294		
0.8	0.043297	0.0543054	0.611831	0.167364	3.092391		
1	0.054121	0.060094	0.660286	0.209205	3.865489		
1.2	0.064945	0.06467	0.699877	0.251046	4.638587		
1.4	0.07577	0.0686104	0.73335	0.292887	5.411685		
1.6	0.086594	0.0720238	0.762346	0.334728	6.184783		
1.7	0.092006	0.0735735	0.775511	0.355649	6.571332		
1.8	0.097418	0.0750346	0.787922	0.376569	6.957881		
2	0.108242	0.0777278	0.810801	0.41841	7.730979		
2.2	0.119067	0.0801641	0.831497	0.460251	8.504077		
2.4	0.129891	0.0823883	0.850392	0.502092	9.277174		
2.6	0.140715	0.0844344	0.867773	0.543933	10.05027		
2.8	0.151539	0.0863288	0.883865	0.585774	10.82337		
3	0.162364	0.0880924	0.898847	0.627615	11.59647		
3.2	0.173188	0.0897421	0.912861	0.669456	12.36957		



Esempio di calcolo del flow coefficient K_v ($C_v=1.16 K_v$) di una valvola

Technical Valve Data's

	Standard	Optional on request	
Valve size DN (Nominal Valve Size) Valve bore / Valve travel	Size DN Dia. of valve bore (mm)	Valve travel (mm)	Greater DN on request Longer travel on request, special diameter on valve bore on request e.g.
DN2	2mm	/ 10mm	
DN4	4mm	/ 10mm	
DN6	6mm	/ 10mm	
DN8	8mm	/ 10mm	
DN10	10mm	/ 10mm	
DN15	15mm	/ 10mm	DN150 140 / 70
DN20	20mm	/ 16mm	DN200 190 / 95
DN25	25mm	/ 16mm	DN250 240 / 120
DN32	32mm	/ 16mm	DN250spez. 270 / 135
DN40-36	36mm	/ 20mm	DN300 285 / 145
DN40	40mm	/ 32mm	
DN50	50mm	/ 32mm	
DN65	65mm	/ 32mm	
DN80	80mm	/ 40mm	
DN100	100mm	/ 50mm	
DN125	120mm	/ 65mm	
k_vs value range as control resp. digital valve ($c_v=1.16 \cdot k_v$) i.e. different flow plugs for k_v , value range, see catalogue no. 921104	Size DN as control valve DN2 0.007...0.070-lin DN4 0.050...0.186-lin DN6 0.09...0.80=% DN8 0.20...2.20=% DN10 0.33...2.80=% DN15 1.00...5.80=% DN20 5.3...11.0=% DN25 6.8...14.7=% DN32 12.6...21.8=% DN40-36 16.0...33.0=% DN40 20.6...43.3=% DN50 31.5...71.0=% DN65 52...98=% DN80 63...160=% DN100 ?...240=% DN125 ?...370=%	as digital valve <0.007; greater values for k_v or C_v respectively, linear flow character- istics or any other special flow char- acteristics	
PN (Nominal Pressure, bar)	PN25 respective PN10 as indicated i.e. same valve could be used as PN6, PN10, PN16 and PN 20 respectively Body and bellows are designed for 25bar and 10bar respectively, for details see specification no. 930922 (pressure load calculation)	PN40, PN50/PN63, PN100 and more	
Heat load to the system	See page 7		

Da verificare con un esempio reale
ATLAS il caso di pre-raffreddamento
misto

DN 8

Size DN	as control valve	as digital valve
DN2	0.007...0.070-lin	-
DN4	0.050...0.186-lin	-
DN6	0.09...0.80=%	0.9-dig
DN8	0.20...2.20=%	2.5-dig
DN10	0.33...2.80=%	3-dig
DN15	1.00...5.80=%	6-dig
DN20	5.3...11.0=%	12-dig
DN25	6.8...14.7=%	15-dig
DN32	12.6...21.8=%	25-dig
DN40-36	16.0...33.0=%	35-dig
DN40	20.6...43.3=%	45-dig
DN50	31.5...71.0=%	75-dig
DN65	52...98=%	100-dig
DN80	63...160=%	170-dig
DN100	?...240=%	260-dig
DN125	?...370=%	390-dig

Metodi di giunzione piu' usati in criogenia

- But Welding (Saldatura di testa): TIG, Laser, Electron-beam (SS-SS, Al-Al, SS-Cu,...)
- For SS-Al joints special transitions Al-SS parts obtained by friction.
- Vacuum Brazing (Brasatura sotto vuoto) (SS-Cu, Cu-Cu, metals-ceramics,..)
- Seals/couplings (guarnizioni/Flangiature) (SPG, CF, Johnston/bayonet, Indio, Elicoflex, Al, ...)
- Possible use of other materials (e.g. for Cryo-valves) Kel-F, Vespel SP1,Teflon,..)
- No Viton O-ring at low temperature! (=>**Space Shuttle Challenger incident, 1986**)

Dimensioning of a Pressure Relief Valve

b) Détermination des caractéristiques d'une soupape

La détermination de la section de passage du gaz dans une soupape est réglementée par la C.G.A. (36) en fonction de la nature des conteneurs et de leur contenu. On trouvera tous les détails nécessaires à ces calculs dans les parties S-1-2 et S-1-3.

Le code A.S.M.E. (114)* donne, pour la détermination de la surface de passage du gaz en fonction du débit gazeux, la relation :

$$A = \frac{\dot{m} (T/M)^{\frac{1}{2}}}{C Kd P_{max}} \quad (5-13)$$

A = surface de passage du gaz.

\dot{m} = débit masse du fluide.

T = température du gaz entrant dans la soupape.

M = masse moléculaire du gaz.

C = coefficient d'expansion donné par :

$$C = 520 \left[\gamma \left(\frac{2}{\gamma + 1} \right)^{\frac{\gamma+1}{\gamma-1}} \right]^{\frac{1}{2}} \quad (5-14)$$

Les valeurs de C en fonction de γ sont portées dans le tableau V-5. (Les valeurs de $\gamma = C_p/C_v$ ont été données dans le tableau II-8.)

Kd = coefficient de décharge donné par le constructeur :

$$Kd = \frac{\text{débit réel}}{\text{débit théorique}}$$

$P_{max} = 1,1 P + \text{pression atmosphérique}$.

(P_{max} et P pression absolue).

Dimensioning of a Pressure Relief Valve

b) Détermination des caractéristiques d'une soupape

La détermination de la section de passage du gaz dans une soupape est réglementée par la C.G.A. (36) en fonction de la nature des conteneurs et de leur contenu. On trouvera tous les détails nécessaires à ces calculs dans les parties S-1-2 et S-1-3.

Le code A.S.M.E. (114)* donne, pour la détermination de la surface de passage du gaz en fonction du débit gazeux, la relation :

$$A = \frac{\dot{m} (T/M)^{\frac{1}{2}}}{C Kd P_{\max}} \quad (5-13)$$

A = surface de passage du gaz.

\dot{m} = débit masse du fluide.

T = température du gaz entrant dans la soupape.

M = masse moléculaire du gaz.

C = coefficient d'expansion donné par :

$$C = 520 \left[\gamma \left(\frac{2}{\gamma + 1} \right)^{\frac{\gamma+1}{\gamma-1}} \right]^{\frac{1}{2}} \quad (5-14)$$

Les valeurs de C en fonction de γ sont portées dans le tableau V-5. (Les valeurs de $\gamma = C_p/C_v$ ont été données dans le tableau II-8.)

Tableau V-5. — VALEURS DE C EN FONCTION DE γ (114)*

γ	C	γ	C	γ	C
1,00	315	1,26	343	1,52	366
1,02	318	1,28	345	1,54	368
1,04	320	1,30	347	1,56	369
1,06	322	1,32	349	1,58	371
1,08	324	1,34	351	1,60	372
1,10	327	1,36	352	1,62	374
1,12	329	1,38	354	1,64	376
1,14	331	1,40	356	1,68	379
1,16	333	1,42	358	1,70	380
1,18	335	1,44	359	2,00	400
1,20	337	1,46	361	2,20	412
1,22	339	1,48	363		
1,24	341	1,50	364		

Kd = coefficient de décharge donné par le constructeur :

$$Kd = \frac{\text{débit réel}}{\text{débit théorique}}$$

$P_{\max} = 1,1 P + \text{pression atmosphérique.}$
(P_{\max} et P pression absolue).

Tableau II-8. — VALEURS DE γ ET M POUR DIFFÉRENTS GAZ (35)

Nature du gaz	CO ₂	O ₂	N ₂	N _e	H ₂	⁴ He
M : (g/mole) . . .	44,01	32	28,02	20,18	2,016	4
γ : (C _p /C _v) . . .	1,302	1,396	1,405	1,67	1,408	1,67

The correlations are based on the assumption that the gas, at the exit in the atmosphere, cannot have a speed higher than the speed of sound.

Dimensioning of a Pressure Relief Valve

Tableau 1 – Densités de flux recommandées pour le calcul de la puissance thermique

Fluide cryogénique	ϕ sans superisolant (W/cm ²)	ϕ avec 10 couches de superisolant (W/cm ²)	ϕ avec 20 couches de superisolant (W/m ²)	ϕ avec 30 couches de superisolant (W/cm ²)
LHe	3,8 [1] [2]	0,62 [1] [2]	0,33 [1] [2]	0,21 [1] [2]
LH ₂	10 [3]	0,62 [1] [2]	0,33 [1] [2]	0,21 [1] [2]
LNe	6,5 [4]	0,62 [1] [2]	0,33 [1] [2]	0,21 [1] [2]
LN ₂	0,25 [5]	0,05 [6]	0,04 [6]	0,028 [6]
LO ₂	0,25 [5]	0,05 [6]	0,04 [6]	0,028 [6]
LAr	0,25 [5]	0,05 [6]	0,04 [6]	0,028 [6]

Normes et standards

NF EN 13458	Réceptacles fixes isolés sous vide	NF EN ISO 4126-6 08-04	Dispositifs de sécurité pour protection contre les pressions excessives. Partie 6 : applications, sélection et installation des dispositifs de sûreté à disque de rupture
NF EN 1251	Réceptacles transportables isolés sous vide		
NF EN 13648-3 12-02	Réceptacles cryogéniques, dispositifs de protection contre les surpressions. Partie 3 : détermination du débit à évacuer, capacité et dimensionnement	NF EN ISO 4126-7 09-13	Dispositifs de sécurité pour protection contre les pressions excessives. Partie 7 : données communes
NF EN ISO 4126-1 07-04	Dispositifs de sécurité pour protection contre les pressions excessives. Partie 1 : soupapes de sûreté		

Dimensioning of a Pressure Relief Valve

A cryostat housing a liquid helium reservoir, a horizontal cylinder as in picture. The total surface is= $2 \cdot 0.5^2 \cdot \pi/4 + 0.5 \cdot \pi \cdot 1 = 1.96 \text{ m}^2$. Let us assume that only 50% of the reservoir has LHe the rest has vapor, i.e. the wetted surface is $1.96/2 = 0.98 \text{ m}^2$

In case of vacuum rupture the reservoir undergoes a heat load (experimentally measured) as follows:

Case 1: **6 kW/m²**, if the reservoir is wrapped with 10 layers of MLI

Case2: **40 kW/m²** with no MLI.

Case 3 (fire): 70 kW/m²

The latent heat of LHe is $(307741-9944) \text{ J/kg} = 20798 \text{ J/kg}$ or 20.8 J/g .

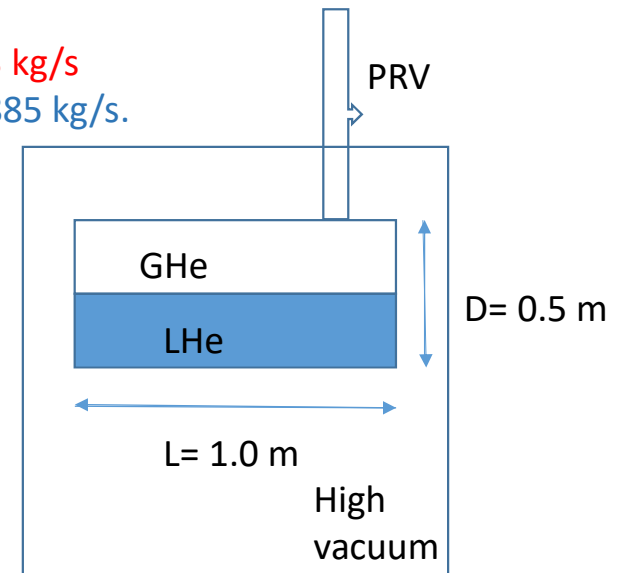
Case 1 : the mass flow generated is $6000 \text{ W} \cdot 0.98 \text{ m}^2 / 20.8 \text{ J/g} = 283 \text{ g/s}$ or **0.283 kg/s**

Case 2: the mass flow generated is $40000 \text{ W} \cdot 0.98 \text{ m}^2 / 20.8 \text{ J/g} = 1885 \text{ g/s}$ or **1.885 kg/s**.

Our cryostat design imposes not to exceed 6 bar absolute,

so the Pressure Relief Valve must open at this pressure.

According to the formula which gives the minimum area of the PRV orifice



The temperature T has to be calculated according to a isochoric transformation. Usually it is chosen between 10 and 20 K.

Dimensioning of a Pressure Relief Valve

In our example we choose T= 15 K.

Case 1: with MLI

)											
gamma	1.67		mdot	0.283227		T	15	P	6	Kd	0.78
	1.854651										
	base	0.74906367		exp	3.985075		Coefficient	377.864			
	Area	0.000244854	Diam	0.018	m	17.7	mm				

PRV minimum diameter is 18 mm

Case 2: no MLI

)											
gamma	1.67		mdot	1.888179		T	15	P	6	Kd	0.78
	1.854651										
	base	0.74906367		exp	3.985075		Coefficient	377.864			
	Area	0.001632357	Diam	0.046	m	45.6	mm				

PRV minimum diameter is 46 mm.

In case of a magnet quench the stored energy $\frac{1}{2} \cdot L \cdot i^2$ has to be taken into account.

Dimensioning of a Pressure Relief Valve

In case of a magnet quench the stored energy $\frac{1}{2} \cdot L \cdot i^2$ has to be taken into account.

The electromagnetic energy stored in the magnet is usually dumped into external resistors and/or diodes. The latter to limit the voltage during the discharge.

With the detailed knowledge of the design of the magnet it is possible to estimate the heat load as a function of time i.e. the power (Watt/m²) associated and the related mass flow generated at the opening of the PRV, and its dimensioning.

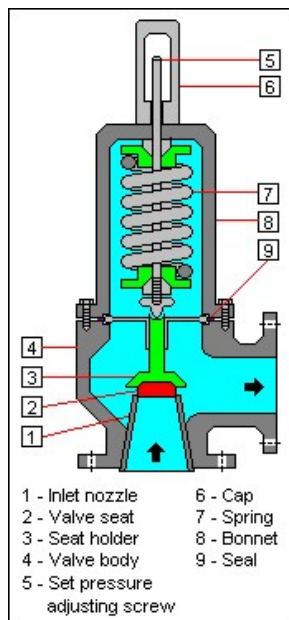
Sometimes it is also necessary (advisable) to measure the heat load by inducing some quenches (Fast dump), and to measure the mass flow associated through a PRV.

$$\int_0^\infty J^2 dt = \int_{T_0}^{T_m} \frac{C}{\rho} dT = U(T_m) \quad (8-62)$$

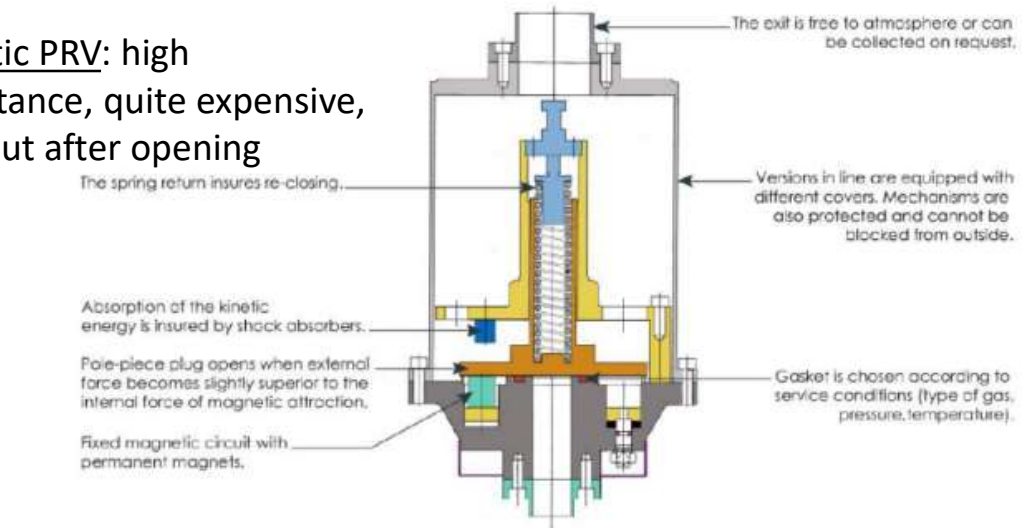
The function U contains only the properties of the materials used in the winding and therefore has a universal validity allowing the determination of the final temperature T_m

Dimensioning of a Pressure Relief Valve

Spring-loaded PRV: Most used type, sometimes does not shut properly (dust or alignment) and so it leaks. Needs maintenance so usually double with three-way valve.



Magnetic PRV: high conductance, quite expensive, does shut after opening



Rupture disk as PRV: high conductance, does not shut and the apparatus can be irreversibly damaged, usually set in parallel at a higher opening pressure

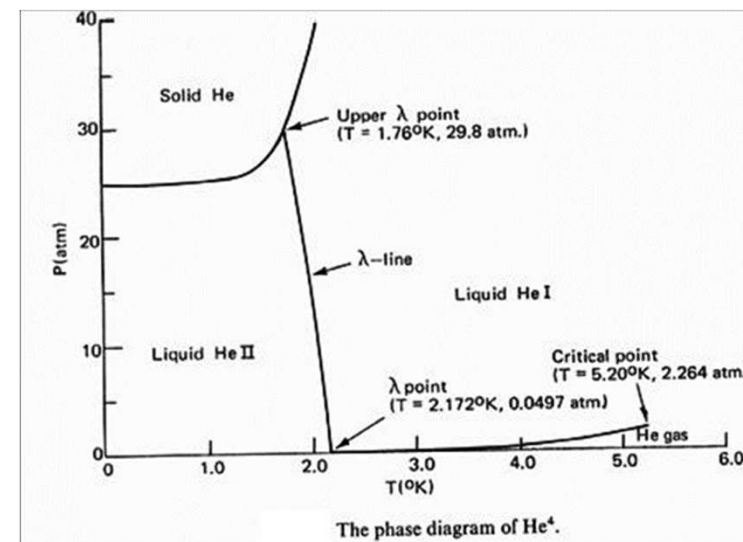
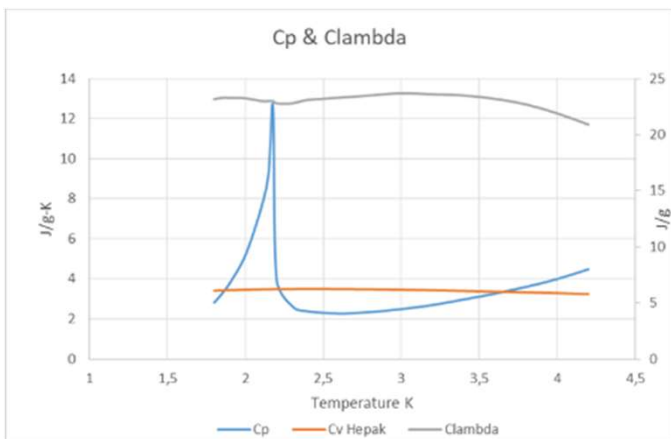
CENNI DI CRIOGENIA CON T< 4 K

- Superfluidita'
- Resistenza di Kapitza
- Cenni di criogenia con T< 1 K
- Superconduttività (Magneti, Cavità RF)

Superfluidita'e superconduttività' cenni

T(K)	P _{svp} (Pa)
1.0	15.57
1.2	81.48
1.4	282.00
1.6	746.36
1.8	1,638.41
2.0	3,129.26
2.1768	5,041.80
2.2	5,335.15
2.4	8,354.10
2.6	12,372.07
2.8	17,551.76
3.0	24,047.07
3.2	32,009.97
3.4	41,594.70
3.6	52,956.31
3.8	66,247.39
4.0	81,619.69
4.2	99,233.46
4.4	119,269.30
4.6	141,930.40
4.8	167,429.50
5.0	196,003.90
5.1953	227,462.30

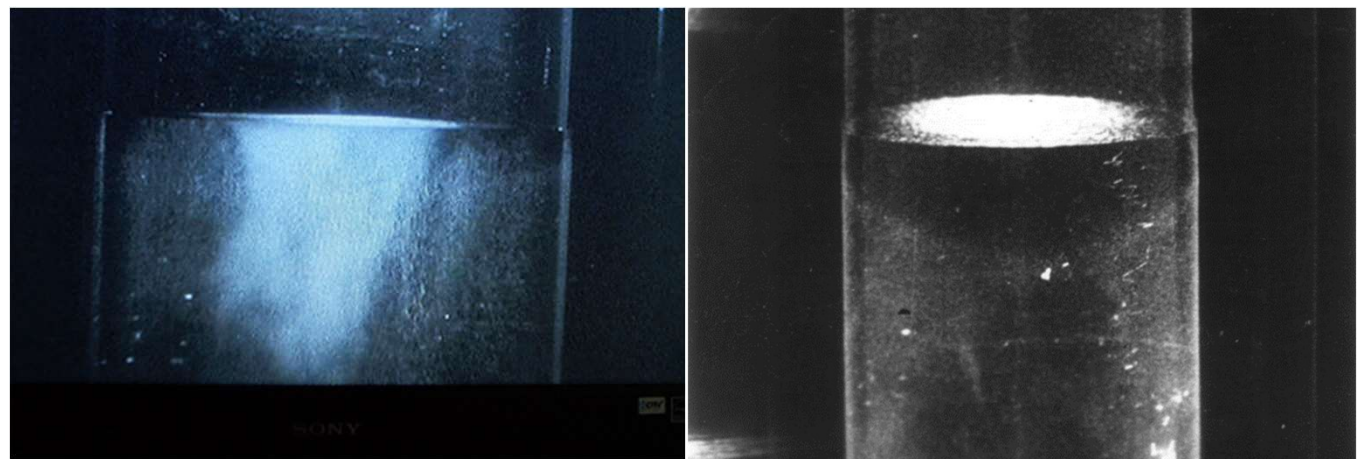
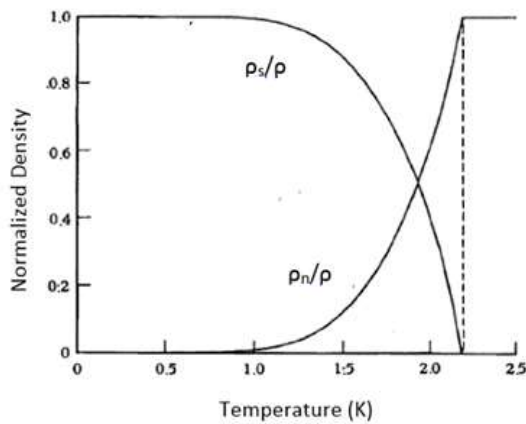
- By pumping on a He⁴ bath, it is possible to lower the bath temperature (see table). A physical limit is at about 1 K
- Below 1 K a mixture He³- He⁴ is used
- At 2.17 K one observes that the Cp diverge and recovers just below, i.e. it can be integrated (see picture. The shape of λ gives the name «lambda point»
- The liquid become superfluid, a quantum fluid with no viscosity and very high thermal conductivity



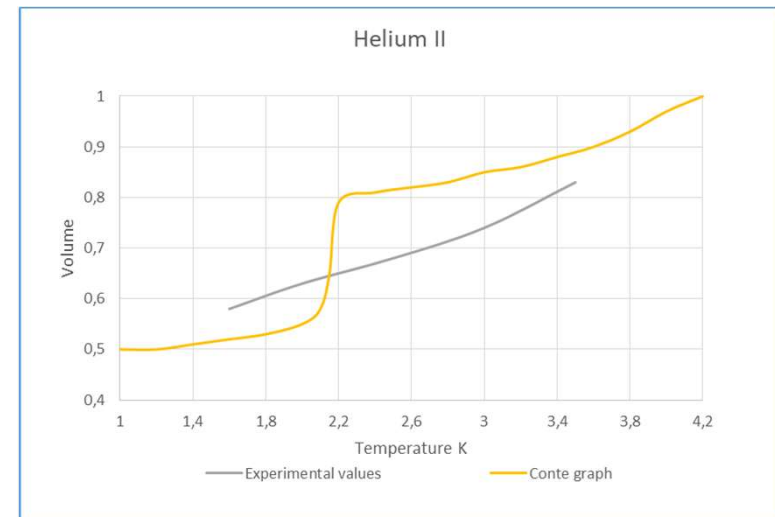
- The very high thermal conductivity λ is such that the bubbles disappear (see photo)
- At 2 K: $\lambda = 2 \text{ kW}/(\text{m}\cdot\text{K}) !!$
[for Cu: $\lambda = 0.2 \text{ kW}/(\text{m}\cdot\text{K})$]

[Temperature < 4K] cenni

- By pumping on the bath, the temperature is lowered
- The transition at 2.17 K is paid by the vaporization of a good part of LHe (50 to 60) % (see graph)
- If C_λ and C_p are the latent heat and the specific heat at the same temperature T, one can write:
- $C_\lambda \cdot dm = m \cdot C_p \cdot dT ; \ln \frac{m}{m_0} = \int_{4.2}^T \frac{C_p}{C_\lambda} dT ;$
with the initial mass equal to m_0
- The helium superfluid, named He II, is a mixture of normal He and superfluid He. The ratio, as a function of T, is given in the graph below.



R.Pengo, Introduzione alla criogenia, Bologna ottobre 2019



Velocità di pompaggio necessaria per mantenere la temperatura $T < T_\lambda$ ($T < 2.17$ K) in elio superfluido di-fasico? [La pompa è a 295K]

- Supponiamo heat load 1 W @ T

- Supponiamo il calore latente $C_\lambda \simeq 20.9 \text{ J/g} = 4 \cdot 20.9 \text{ J/mol}$

$$Q(\text{W}) = \dot{m} \cdot C_\lambda \quad 1 \text{ W} = \dot{m} (\text{g/s}) \cdot 20,9 (\text{J/g})$$

$$\dot{m} = \frac{1}{20,9} (\text{g/s}) = \frac{1}{4 \cdot 20,9} \left[\frac{\text{mol}}{\text{sec}} \right]$$

$$PV = nRT \rightarrow P \cdot \dot{V} = \dot{n} R T ; \quad \dot{V} = (\dot{n} R T)/P ; \quad \dot{V} \left[\frac{\text{m}^3}{\text{s}} \right] = \frac{\frac{1}{4 \cdot 20,9} \left[\frac{\text{mol}}{\text{s}} \right] \cdot 8,31 \left[\frac{\text{J}}{\text{mol} \cdot \text{K}} \right] \cdot 295 \text{K}}{287 [\text{Pa}]}$$

$$= 0.1022 \frac{\text{m}^3}{\text{s}} = 368 \frac{\text{m}^3}{\text{h}} \quad @ 1.4 \text{ K; } 33,3 \frac{\text{m}^3}{\text{h}} \quad 1 \text{ W @ 2.0 K}$$

$$333 \frac{\text{m}^3}{\text{h}} \quad 10 \text{ W} \quad @ 2.0 \text{ K}$$

T [K]	P [Pa]
1.4	287
1.6	287
1.8	1662
2.0	3169

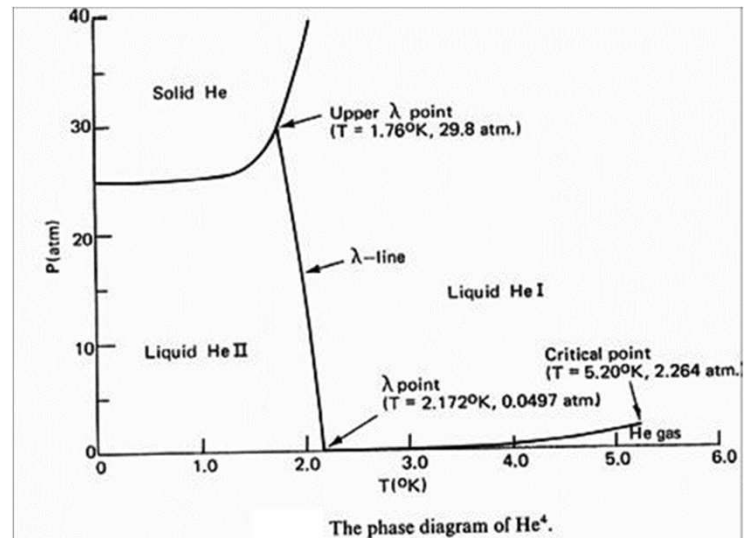
[Superfluidita'e superconduttività cenni]

Tableau B. – Tension de vapeur de ^3He et ^4He en fonction de la température.

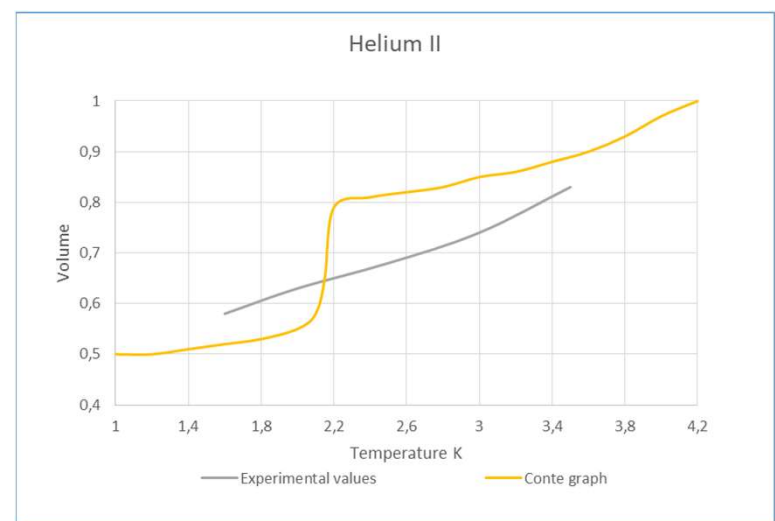
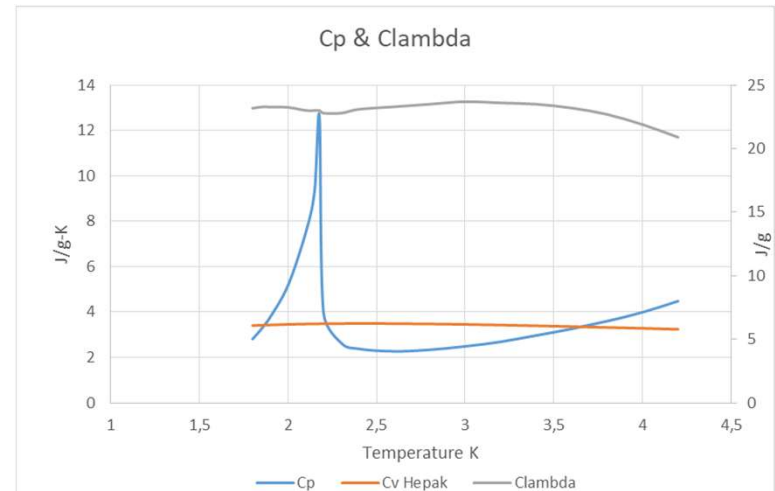
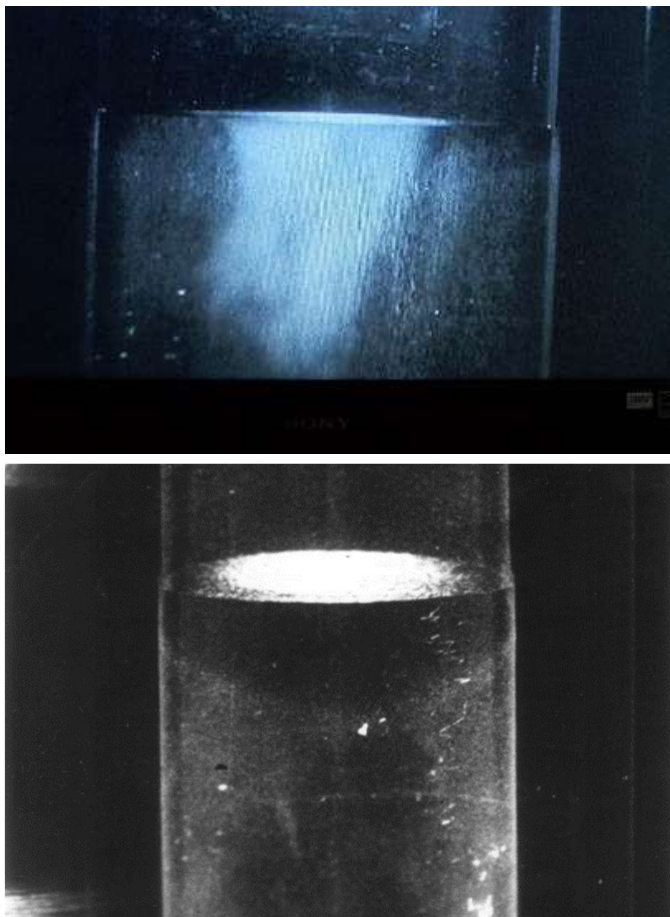
Tension de vapeur	Température (K)	
Pa (mm Hg à 20 °C (1))	^3He	^4He
26,6 (0,2)	0,524 0	1,055 0
66,6 (0,5)	0,599 4	1,168 6
$1,33 \times 10^2$ (1)	0,670 2	1,269 3
$2,66 \times 10^2$ (2)	0,754 8	1,385 7
$6,66 \times 10^2$ (5)	0,896 1	1,569 9
$1,33 \times 10^3$ (10)	1,032 3	1,738 7
$2,66 \times 10^3$ (20)	1,203 6	1,941 5
$6,66 \times 10^3$ (50)	1,496 4	2,289 4
$1,33 \times 10^4$ (100)	1,789 2	2,633 4
$2,66 \times 10^4$ (200)	2,161 4	3,061 2
4×10^4 (300)	2,424 2	3,359 3
$5,33 \times 10^4$ (400)	2,634 2	3,595 8
$6,66 \times 10^4$ (500)	2,812 0	3,795 3
8×10^4 (600)	2,967 8	3,969 5
$9,33 \times 10^4$ (700)	3,107 4	4,125 0
$10,1 \times 10^4$ (760)	3,185 1	4,211 1
$10,6 \times 10^4$ (800)	3,234 7	4,266 1
$11,6 \times 10^4$ (875)	3,33	⋮
$22,3 \times 10^4$ (1685)		5,20

(1) avec $g = 9,80665 \text{ m/s}^2$.

T(K)	p _{svp} (Pa)
1.0	15.57
1.2	81.48
1.4	282.00
1.6	746.36
1.8	1,638.41
2.0	3,129.26
2.1768	5,041.80
2.2	5,335.15
2.4	8,354.10
2.6	12,372.07
2.8	17,551.76
3.0	24,047.07
3.2	32,009.97
3.4	41,594.70
3.6	52,956.31
3.8	66,247.39
4.0	81,619.69
4.2	99,233.46
4.4	119,269.30
4.6	141,930.40
4.8	167,429.50
5.0	196,003.90
5.1953	227,462.30



Temperature < 4K cenni



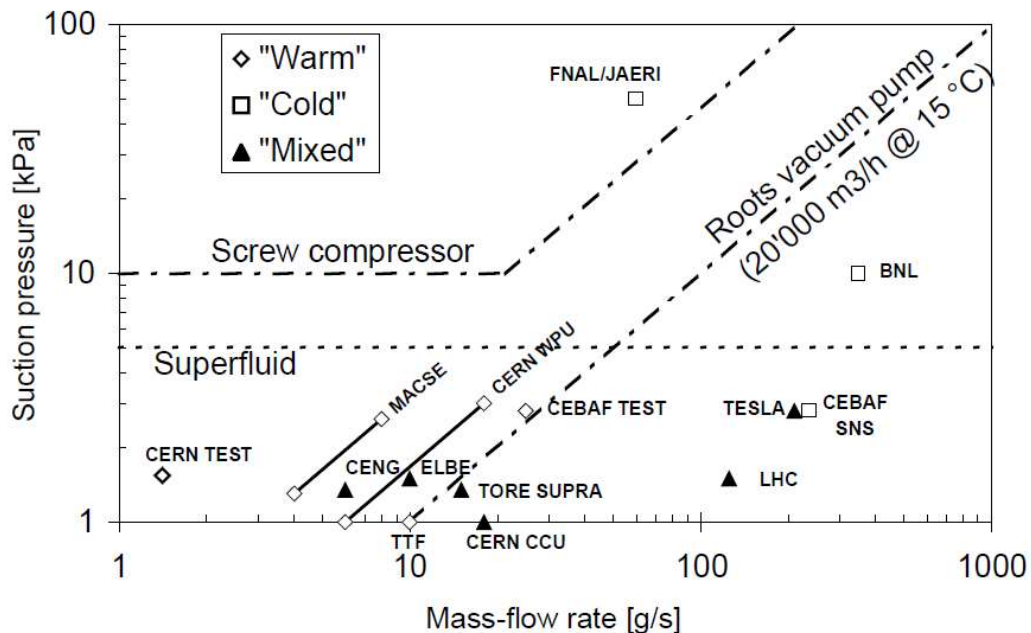


Fig. 20: The range of application of low-pressure helium compression techniques



- The cold compressor CC pumps the 1.8 K (16 mbar) cold vapour to higher pressure.
- A stack of CC is necessary to reach atmospheric pressure.
- The roots pumping speed ($20\ 000\ m^3/h$) is calculated for 300 W at 1.8 K (see previous calculations)

Velocità di pompaggio necessaria per mantenere la temperatura $T < T_\lambda$ ($T < 2.17$ k) in elio superfluido di-fasico? [La pompa è a 295k]

- Supponiamo heat load 1 W @ T
- Supponiamo il calore latente $C_\lambda \simeq 20.9 \frac{J}{g} = 4 \cdot 20.9 \frac{J}{mol}$

$$Q (W) = \dot{m} \cdot C_\lambda \quad 1 \text{ W} = \dot{m} (\frac{g}{s}) \cdot 20,9 (\frac{J}{g})$$

$$\dot{m} = \frac{1}{20,9} (\frac{g}{s}) = \frac{1}{4 \cdot 20,9} \left[\frac{mol}{sec} \right]$$

$$PV = nRT \rightarrow P \cdot \dot{V} = \dot{n} R T ; \quad \dot{V} = (\dot{n} R T)/P ; \quad \dot{V} \left[\frac{m^3}{s} \right] = \frac{\frac{1}{4 \cdot 20,9} \left[\frac{mol}{s} \right] \cdot 8,31 \left[\frac{J}{mol \cdot K} \right] \cdot 295K}{287 [Pa]}$$

$$= 0.1022 \frac{m^3}{s} = 368 \frac{m^3}{h} \quad @ 1.4 \text{ k; } 33,3 \frac{m^3}{h} \quad 1 \text{ W} @ 2.0 \text{ K}$$

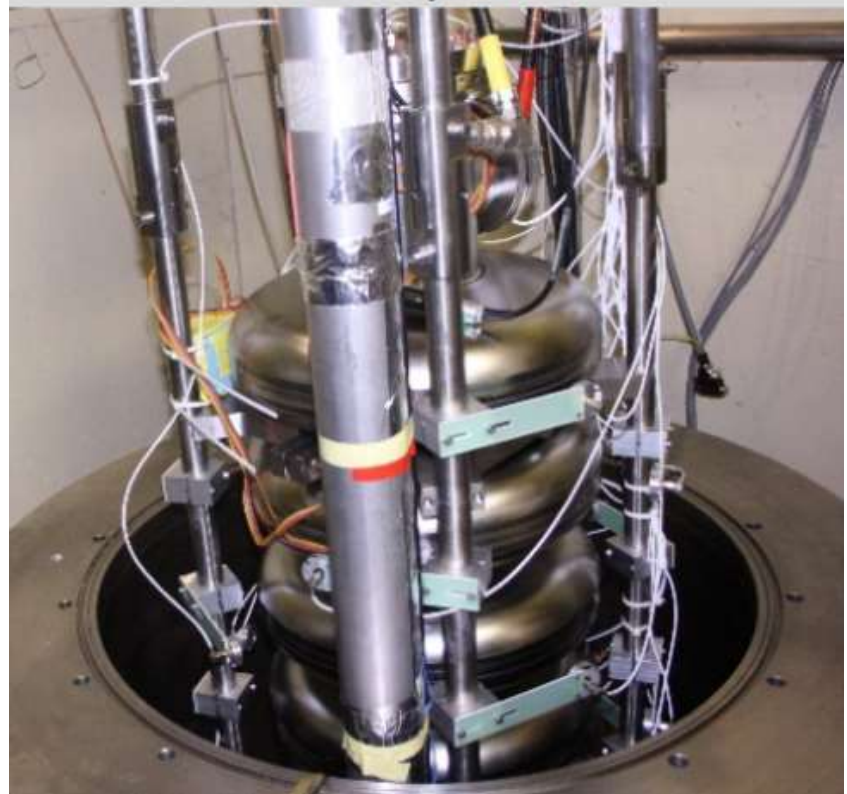
$$333 \frac{m^3}{h} \quad 10 \text{ W} \quad @ 2.0 \text{ K}$$

T [k]	P [Pa]
1.4	287
1.6	746
1.8	1662
2.0	3169

TWO PHASE He II: CONTINOUS PUMPING



*Insertion of MB cavity into LASA
test cryostat*



PRESSURIZED He II

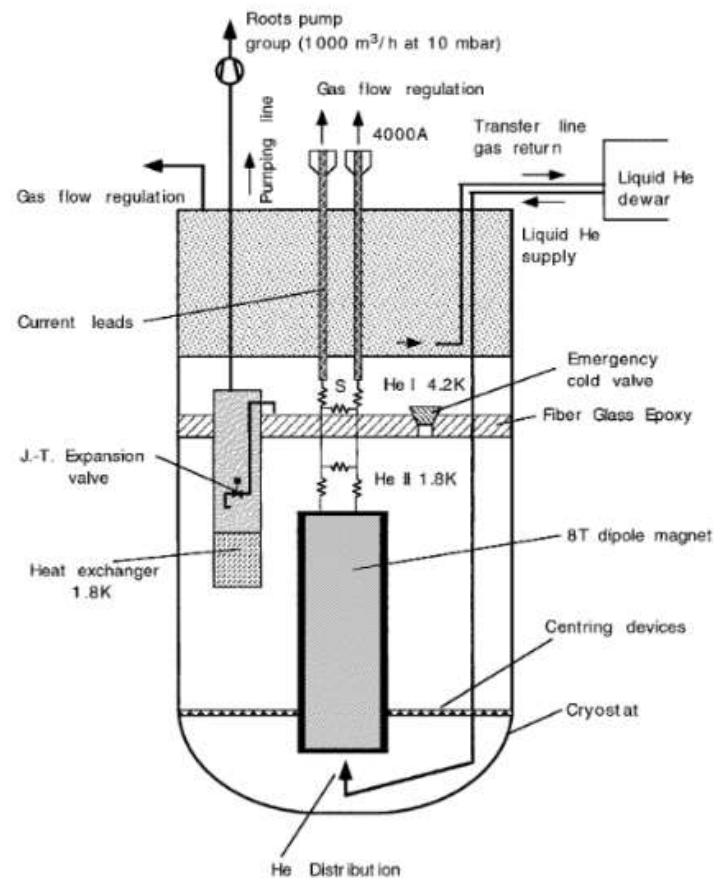


Figure 3. Schematic drawing of the cryostat.



The Kapitza resistance (conductance)

- At low ΔT no boiling occurs and the heat transfer between He II and a solid surface is controlled by the Kapitza conductance such that $h_k = q/\Delta T$ (q in kW/m^2)
- (At high ΔT the heat transfer is determined primarily by the character of the vapour film)
- If a block of copper is immersed in He II, sizeable DT between the Cu and the bath can be measured
- (Nowdays the Kapitza conductance has been extended also to the interface between a metal and water at room temperature). In general it is neglected (also for He I) being strongly dependent of T.
- For small ΔT the experimental values are:
 - clean surface $h_k = 0.9 T^3 \text{ kW/m}^2$
 - dirty surface $h_k = 0.4 T^3 \text{ kW/m}^2$
- For large ΔT :
 - $q_s = \alpha \cdot (T_s^n - T_b^n)$
 - α and n adjustable parameters (see next table)

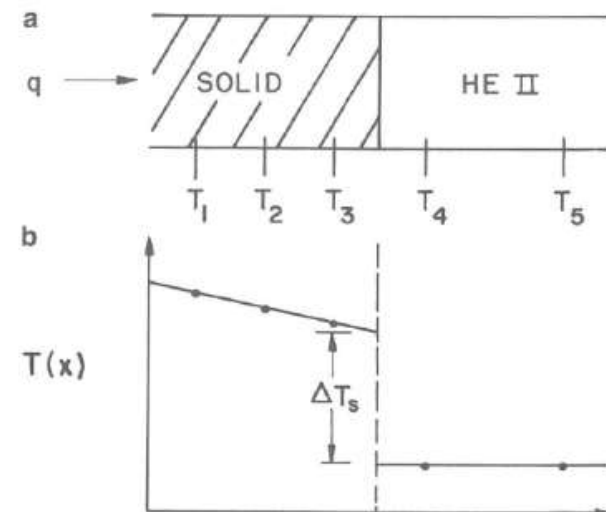


Fig. 7.32 Schematic of Kapitza conductance experiment: (a) temperature sensors located in the vicinity of a solid-He II interface and (b) temperature profile

Note: The dependence from T^3 comes from solid state physics: the heat flux is $q = \sigma T^4$, and for small ΔT , $h_k = q/\Delta T$ implies that $q = 4 \sigma T^3$. Theoretically for Cu it would be $h_k = 4.4 T^3 \text{ kW/m}^2 \text{ K}$. (The σ is only an analogy to the photon radiation correlation).

The Kapitza conductance

$$h_{K_0} = \lim_{\Delta T \rightarrow 0} \frac{\dot{q}}{\Delta T}$$

Where ΔT is the temperature difference between the two media, and \dot{q} the heat flux through the interface. The Kapitza conductance can be ideally defined in the limit where q and ΔT are vanishing (the 0 subscript of K_0 refers to ΔT vanishing, i.e. $\Delta T \rightarrow 0$) as:

$$h_K = \frac{\dot{q}}{\Delta T}$$

Using the latter definition, and the difference between the heat incident on the high temperature side and that on the low temperature side, namely:

$$\Delta \dot{q} = \dot{q}(T + \Delta T) - \dot{q}(T)$$

then

$$h_K = \frac{\Delta \dot{q}}{\Delta T} = \frac{\dot{q}(T + \Delta T) - \dot{q}(T)}{\Delta T} \quad (11)$$

On the other hand, equation (10) could also be simplified (in a form analogous to the Stefan-Boltzman law of photon heat transport) such as:

$$\dot{q} = \sigma T^4$$

where

$$\sigma = \frac{4\pi^5 k_B^4 \rho_L c_L}{15 h^3 \rho_S c_S^3}$$

Consequently

$$\begin{aligned} \Delta \dot{q} &= \sigma(T + \Delta T)^4 - \sigma T^4 \\ &= \sigma T^3 \Delta T [1 + \frac{3}{2} \frac{\Delta T}{T} + (\frac{\Delta T}{T})^2 + \frac{1}{4} (\frac{\Delta T}{T})^3] \end{aligned}$$

$$h_K = 4\sigma T^3$$

which gives us the final expression for the Kapitza conductance:

$$h_K = \frac{16\pi^5 k_B^4 \rho_L c_L}{15 h^3 \rho_S c_S^3} T^3 \quad (12)$$

The Kapitza resistance (conductance)

Table 7.4 High heat flux Kapitza conductance fitting parameters for metals at 1.8 K

Metal	Surface condition	T_s at 10 kW/m ²	α (kW/m ² ·K ⁿ)	n	References
Cu	As received	3.1	0.486	2.8	
	Brushed and baked	2.85	to		
	Annealed	2.95	0.2	3.8	[65]
	Polished	2.67	0.455	3.45	[67]
	Oxidized in air for 1 month	2.68	0.46	3.46	[67]
	Oxidized in air at 200°C for 40 min	2.46	0.52	3.7	[67]
	50-50 PbSn solder coated	2.43	0.76	3.4	[67]
	Varnish coated	4.0	0.735	2.05	[67]
Pt	Machined	3.9	0.19	3.0	[62]
Ag	Polished	2.8	0.6	3.0	[62]
Al	Polished	2.66	0.49	3.4	[63]

Copper at 2.1 K, heat flux 5 kW/m²

Small DT, surface as received:

$$h_k = 0.4 T^3 \text{ kW}/(\text{m}^2 \cdot \text{K}) = 0.4 \cdot 2.1^3 = 3.7 \text{ kW}/(\text{m}^2 \cdot \text{K})$$

$$T_s = T_b + q/h_k = 2.1 + 5/3.7 = 2.1 + 1.35 = \mathbf{3.45 \text{ K}}$$

Large DT, surface as received:

$$q_s = \alpha \cdot (T_s^n - T_b^n); \alpha = 0.486 \text{ kW}/(\text{m}^2 \cdot \text{K})$$

$$, n = 2.8$$

$$T_s = (q/\alpha - T_b^n)^{1/n}$$

$$T_s = (5/0.486 - 2.1^{2.8})^{1/2.8} = \mathbf{2.82 \text{ K}}$$

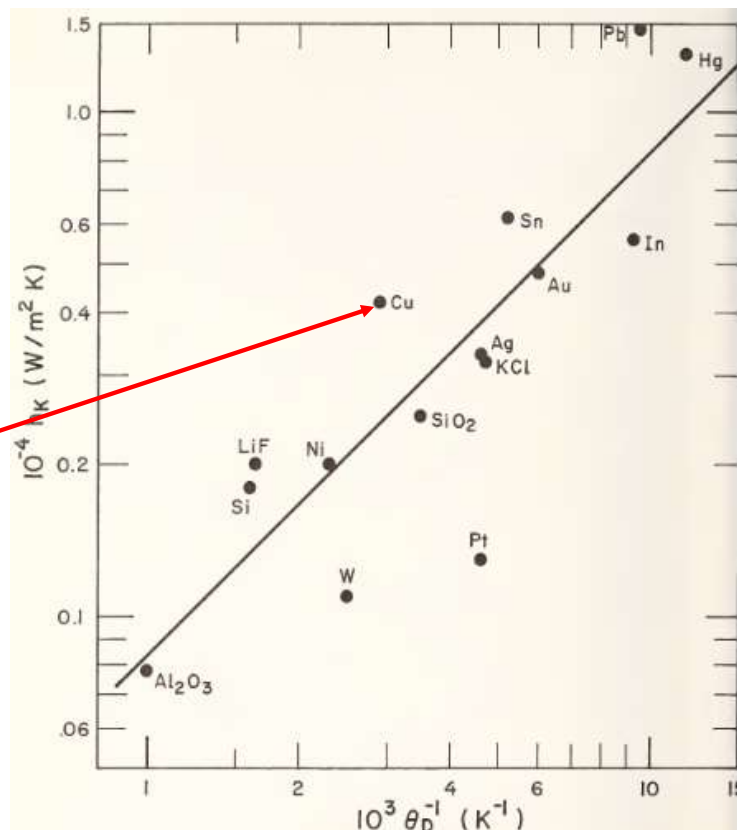


Figure 1. Kapitza conductance at 1.5 K – largest values observed for each solid are plotted. From Challis (1968). Ag data from Frederking (1968).

The Kapitza resistance (conductance)

heat flow in turbulent He II, the nonlinear heat conductivity equation can be used to describe the heat conducted by internal convection,

$$q_{ic} = - \left(f(T, p)^{-1} \frac{dT}{dx} \right)^{1/3} \quad (7.56)$$

where $f'(T, p)$ is the same temperature-dependent heat conductivity function. The

If $q = 1 \text{ kW/m}^2$ in He II at 1.8 K turbulent flow one needs ca. 1000 m to have $0.1 \text{ K} = \Delta T$.

$$\Delta x (\text{m}) = 9749 \times 0.1 / 1^3 = 975 \text{ m}$$

$$[\Delta x (\text{m}) = 9281 \times 0.1 / 1^3 = 928 \text{ m (at 1 bar)}].$$

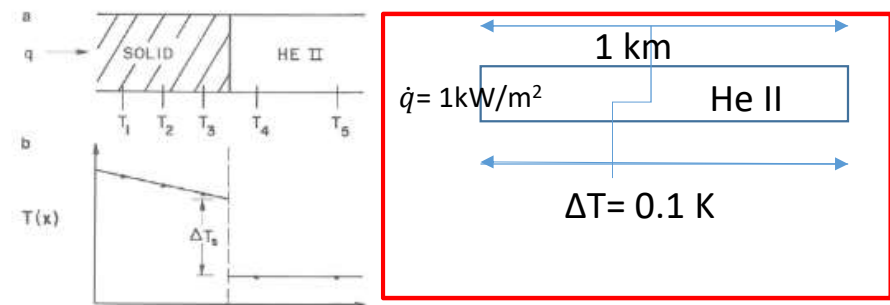


Fig. 7.32 Schematic of Kapitza conductance experiment: (a) temperature sensors located in the vicinity of a solid-He II interface and (b) temperature profile

Appendix A3 Turbulent He II heat conductivity function, $f^{-1}(T, p)$, $\text{kW}^3/\text{m}^5 \text{ K}$

TEMP (K)	SVP	0.1 MPa	0.25 MPa	0.5 MPa	1 MPa	1.5 MPa	2 MPa	2.5 MPa
1.4	396.88	389.91	374.74	356.23	343.23	322.94	291.98	279.18
1.42	492.09	483.16	464.00	440.23	421.71	394.09	352.60	331.46
1.44	607.04	595.63	571.54	541.13	515.08	477.78	422.59	389.82
1.46	745.02	730.50	700.32	661.55	625.36	575.38	502.50	453.88
1.48	909.64	891.23	853.58	804.33	754.62	688.14	592.62	522.84
1.5	1,104.84	1,081.57	1,034.78	972.45	904.87	817.11	692.86	595.36
1.52	1,334.81	1,305.52	1,247.60	1,169.02	1,078.03	963.05	802.68	669.54
1.54	1,603.96	1,567.21	1,495.81	1,397.13	1,275.74	1,126.23	920.88	742.74
1.56	1,916.77	1,870.84	1,783.17	1,659.73	1,499.25	1,306.30	1,045.52	811.63
1.58	2,277.66	2,220.49	2,113.27	1,959.50	1,749.17	1,502.09	1,173.75	872.13
1.6	2,690.81	2,619.91	2,489.35	2,298.61	2,025.27	1,711.38	1,301.68	919.55
1.62	3,159.86	3,072.31	2,914.01	2,678.47	2,326.23	1,930.69	1,424.35	948.79
1.64	3,687.69	3,580.03	3,388.95	3,099.42	2,649.33	2,155.11	1,535.63	954.68
1.66	4,275.95	4,144.16	3,914.56	3,560.40	2,990.12	2,378.07	1,628.42	932.58
1.68	4,924.68	4,764.10	4,489.55	4,058.54	3,342.20	2,591.24	1,694.78	879.06
1.7	5,631.79	5,437.10	5,110.43	4,588.75	3,696.87	2,784.58	1,726.45	792.94
1.72	6,392.53	6,157.71	5,771.08	5,143.29	4,042.96	2,946.41	1,715.47	676.33
1.74	7,198.86	6,917.20	6,462.18	5,711.32	4,366.75	3,063.84	1,655.15	535.73
1.76	8,038.89	7,703.03	7,170.71	6,278.62	4,652.08	3,123.42	1,541.29	382.86
1.78	8,896.31	8,498.36	7,879.58	6,827.27	4,880.66	3,112.10	1,373.74	234.57
1.8	9,749.90	9,281.59	8,567.29	7,335.65	5,032.79	3,018.70	1,157.98	111.09
1.82	10,573.23	10,026.21	9,207.86	7,778.62	5,088.44	2,835.73	906.67	31.12
1.84	11,334.63	10,700.85	9,771.03	8,128.11	5,028.94	2,561.60	640.58	1.49
1.86	11,997.49	11,269.75	10,222.94	8,354.22	4,839.10	2,203.13	388.07	
1.88	12,521.14	11,693.80	10,527.32	8,426.88	4,510.05	1,777.95	181.76	
1.9	12,862.33	11,932.24	10,647.41	8,318.24	4,042.50	1,316.21	50.37	
1.92	12,977.62	11,945.21	10,548.69	8,005.91	3,450.25	860.57	2.39	
1.94	12,826.67	11,697.28	10,202.53	7,476.91	2,763.44	462.82		
1.96	12,376.63	11,161.98	9,590.84	6,732.33	2,030.59	174.52		

Temperature < 1K cenni

Table 12.2 Temperatures, in kelvin, at which the vapor pressures of ${}^4\text{He}$ and ${}^3\text{He}$ reach specified values

p (torr)	10^{-4}	10^{-3}	10^{-2}	10^{-1}	1	10	100
${}^4\text{He}$	0.56	0.66	0.79	0.98	1.27	1.74	2.64
${}^3\text{He}$	0.23	0.28	0.36	0.47	0.66	1.03	1.79

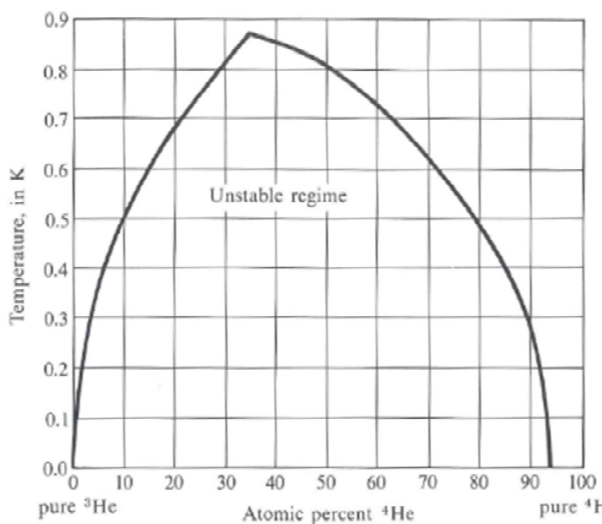


Figure 11.7 Liquid mixtures of ${}^3\text{He}$ and ${}^4\text{He}$.

Below 0.87 K, ${}^3\text{He}$ and ${}^4\text{He}$ are immiscible like oil and water. The concentrated ${}^3\text{He}$ phase floats on top of the dilute ${}^3\text{He}$ phase. If the amount of ${}^4\text{He}$ is increased the excess of ${}^3\text{He}$ will evaporate resulting by cooling the bath. To obtain a cyclic process ${}^3\text{He}$ - ${}^4\text{He}$ mixture has to be separated e.g. by distillation. Temperatures as low as 8 mK can be obtained.

The lowest temperature accessible by evaporation cooling is [a problem of vacuum technology](#). As T drops the equilibrium vapor pressure drops, and so the rate at which helium gas and its heats of vaporization can be extracted from LHe bath.

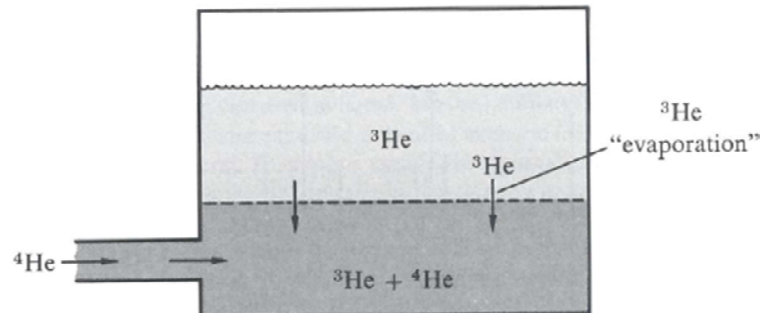


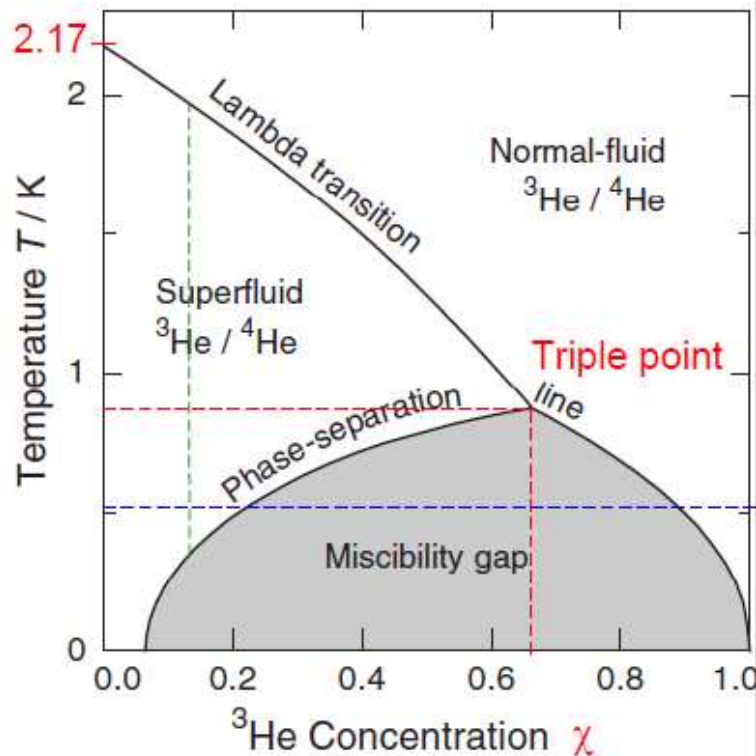
Figure 12.5 Cooling principle of the helium dilution refrigerator. Liquid ${}^3\text{He}$ is in equilibrium with a ${}^3\text{He}$ - ${}^4\text{He}$ mixture. When ${}^4\text{He}$ is added to the mixture, ${}^3\text{He}$ evaporates from the pure ${}^3\text{He}$ fluid and absorbs heat in the process.

Two phase region (miscibility gap)

- He³-rich component (on right part of phase-separation line) has He³ content between 67% (triple point) and 100% at T=0
- He⁴-rich component (on left part of phase-separation line) has He³ content between 67% (triple point) and 6% at T=0
- Finite He³ solubility at T=0: Both isotopes have the same Van der Waals potentials, but He³ atoms are lighter hence have larger zero-point motion
 - He³ atom is closer to He⁴ atoms than other He³ atoms
 - He³-He⁴ bonding is stronger than He³-He³

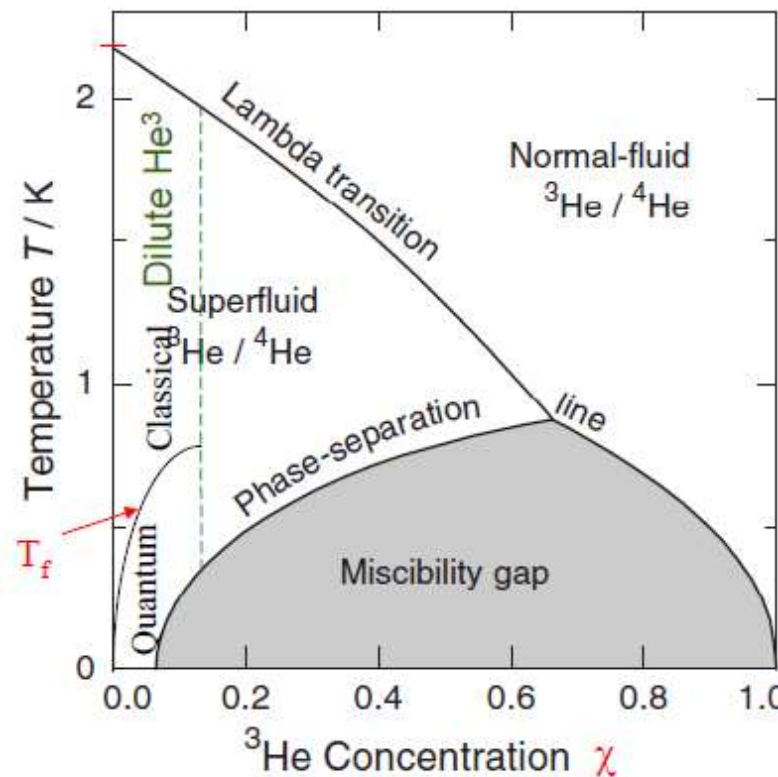
Liquid He³-He⁴ phase diagram

- Above 0.87K: transition between normal and superfluid
- Increasing χ lowers transition temperature
- **Miscibility gap** below 0.87K: no homogeneous mixture; two liquids (grey region in graph)
- He³-rich liquid floats above He⁴-rich liquid (denser)



Dilute He³-He⁴ II liquid mixtures

- In region $\chi < 0.15$ as T decreases He³ atoms are separated by increasing proportion of superfluid He⁴ (Landau two-fluid theory)
- Creates system of weakly interacting fermions in a sea of He⁴ bosons
- At small concentrations He³ atoms can be described as a free gas in a massive vacuum
- He³ atoms must displace He⁴ atoms as they move
- Described as effective mass $m_3^* = 2.4m_3$



[Temperature < 1K] cenni

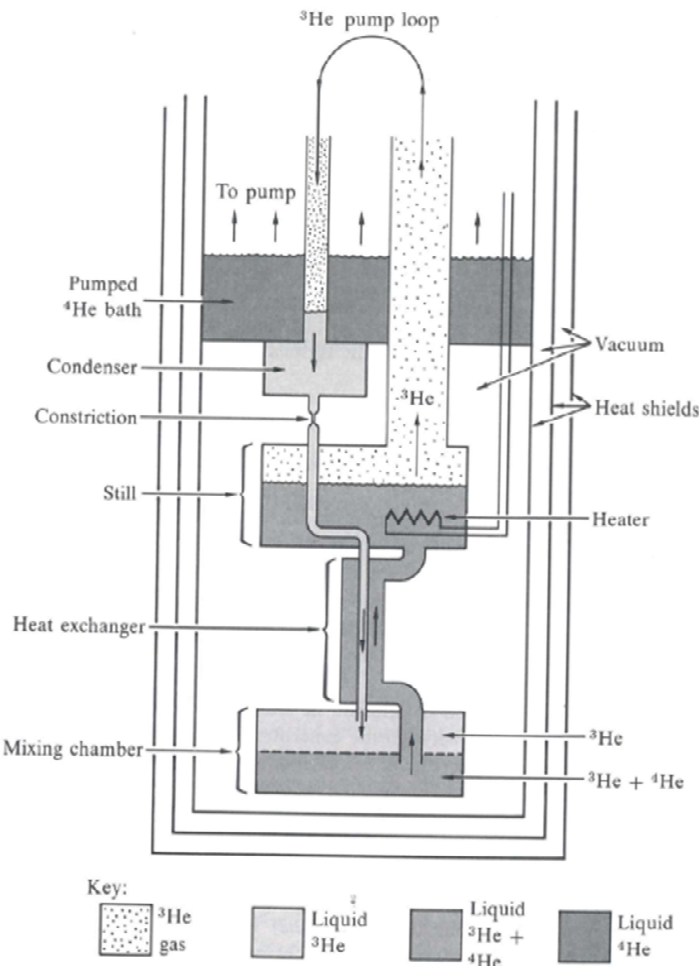
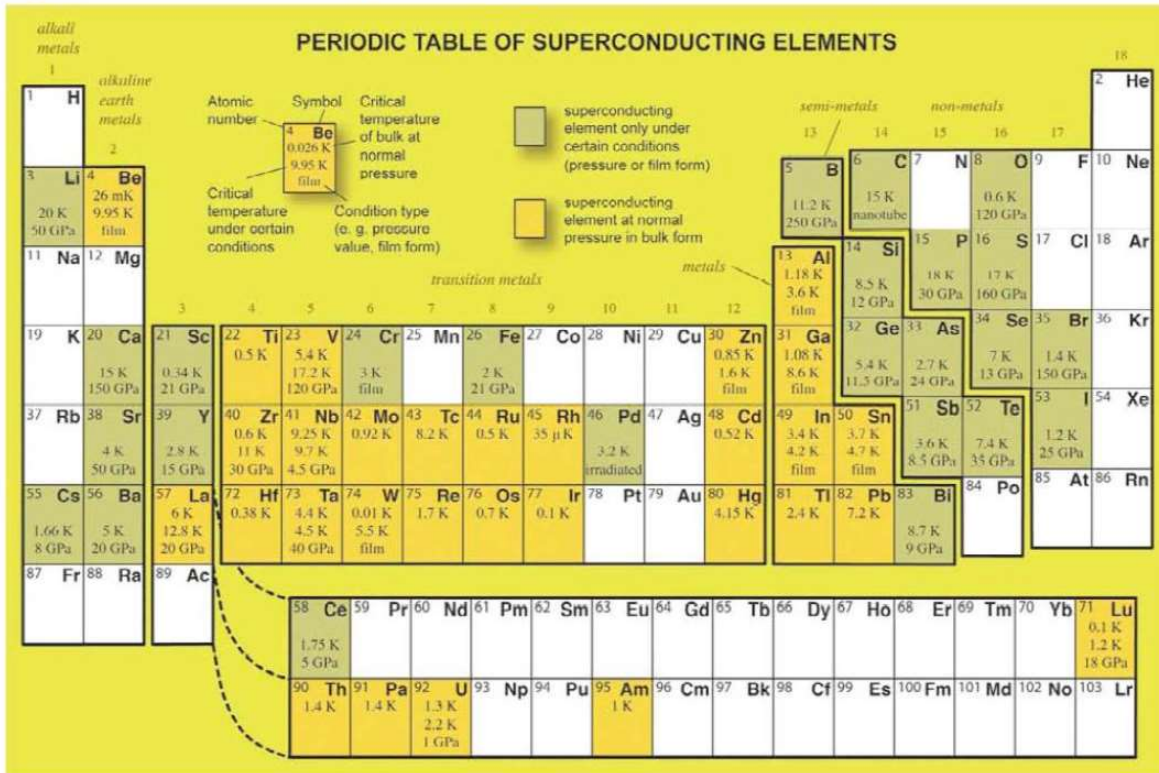


Figure 12.6 Helium dilution refrigerator. Precooled liquid ^3He enters a mixing chamber at the lower end of the assembly, where cooling takes place by the quasi-evaporation of the ^3He atoms into the denser ^3He - ^4He mixed phase underneath. The quasi-gas of ^3He atoms dissolved in liquid ^4He then diffuses through a counterflow heat exchanger into a still. There the ^3He is distilled from the ^3He - ^4He mixture selectively, and is pumped off. To obtain a useful ^3He evaporation and circulation rate, heat must be added to the still, to raise its temperature to about 0.7 K, at which temperature the ^4He vapor pressure is still much smaller. Thus, the ^4He does not circulate to any appreciable extent; the ^3He moves through a nearly stationary background of ^4He . The pumped-off ^3He is returned to the system and is condensed in a condenser that is cooled to about 1 K by contact with a pumped ^4He bath. The constriction below the condenser takes up the excess pressure generated by the circulation pump over the pressure in the still. The liquified ^3He is cooled further, first in the still, then in the counterflow heat exchanger, before re-entering the mixing chamber.

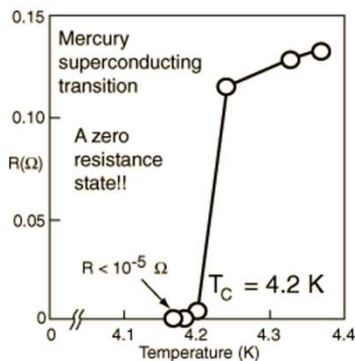
Table 12.2 Temperatures, in kelvin, at which the vapor pressures of ^4He and ^3He reach specified values

p (torr)	10^{-4}	10^{-3}	10^{-2}	10^{-1}	1	10	100
^4He	0.56	0.66	0.79	0.98	1.27	1.74	2.64
^3He	0.23	0.28	0.36	0.47	0.66	1.03	1.79

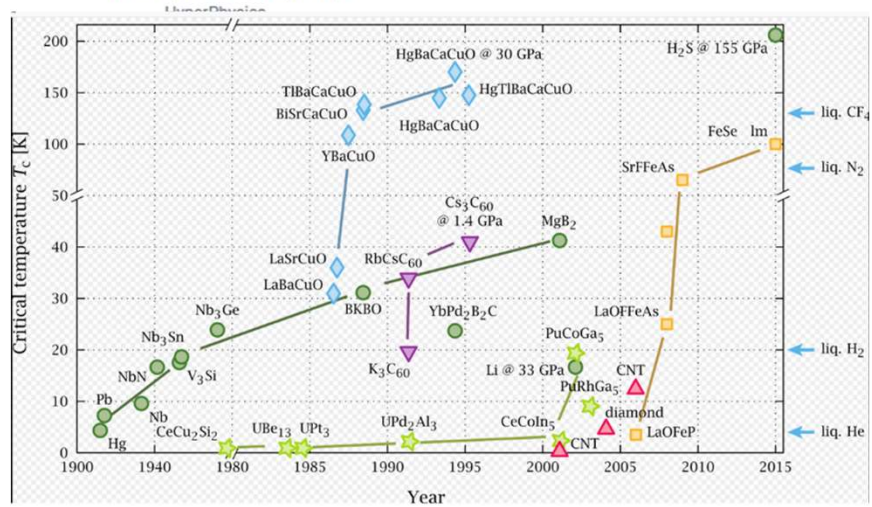
Superconducting elements



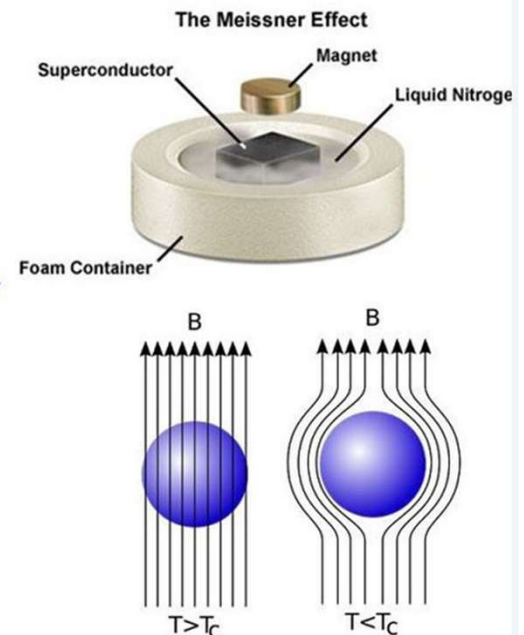
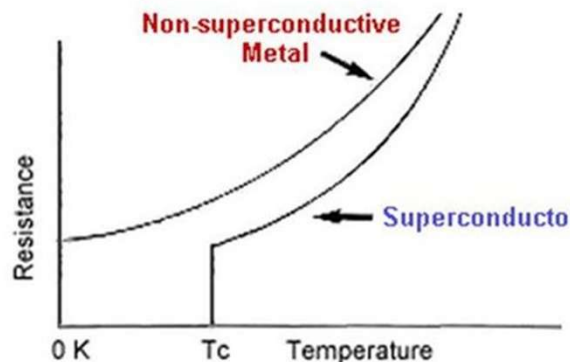
[Superconductivity] cenni



The discovery of superconductivity took place in 1911 using mercury. | Credit: H. K. Onnes, Commun. Phys. Lab. 12, 120, (1911) /

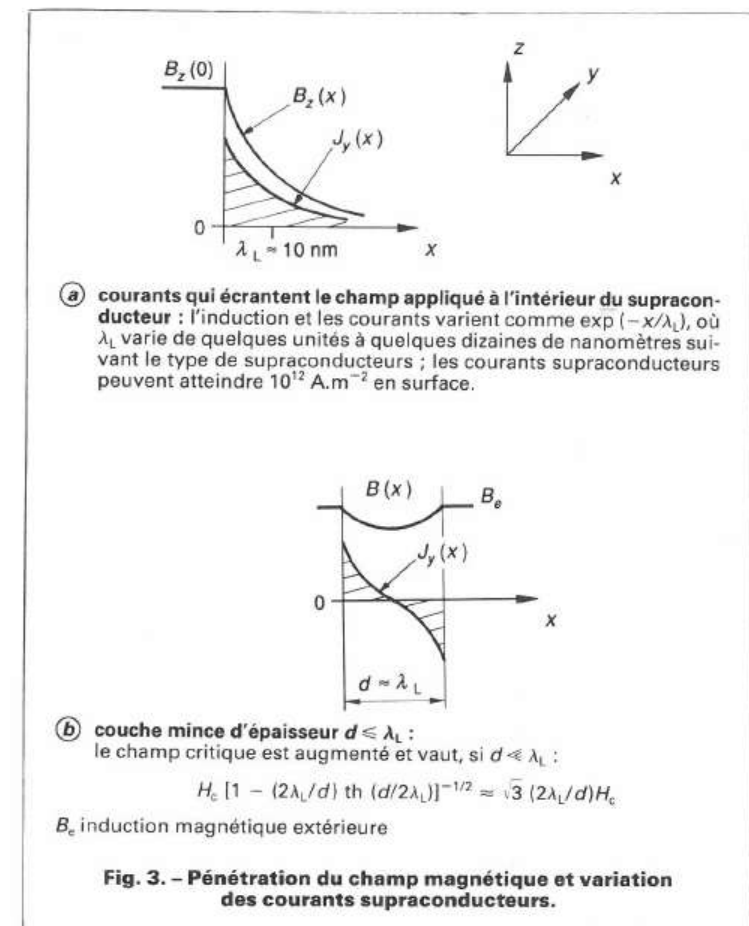
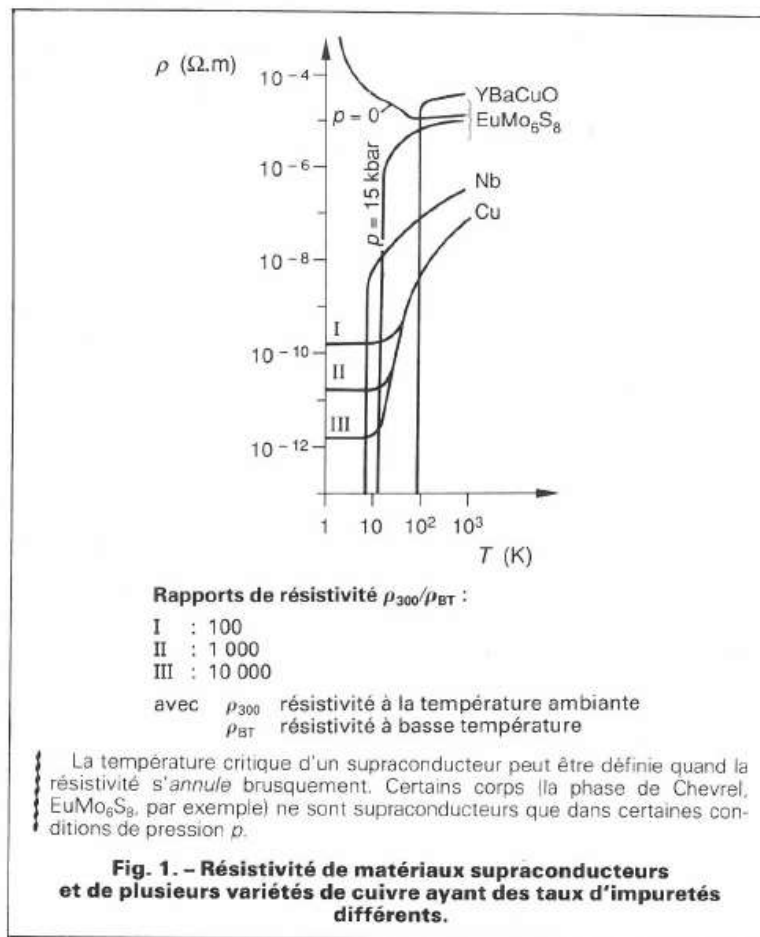


- ◆ Zero resistivity
- ◆ Perfect diamagnetism



[Superconductivity] cenni

- Temperatura critica: T alla quale la resistenza e' nulla (non solo piccola). La transizione a R = 0 avviene in modo repentino, in dipendenza della purezza del materiale. (almeno inferiore a 10^{-25} Ohm)
- In DC e' propriamente R=0 Ohm.
- In AC solo a frequenze «ottiche» si comporta come un materiale resistivo normale. A 50 Hz la densita' di corrente $J_n/J_s = 10^{-10}$
- Dopo la scoperta nel 1911 per il Hg, molti altri materiali sono stati scoperti. In particolare dal 1986 alcuni ad «alta temperatura» (praticamente a temperatura ambiente).



[Superconductivity] cenni

- Effetto Meissner: Poiche' il flusso di B deve conservarsi, affiche' all'interno del superconduttore sia B=0, si devono instaurare delle correnti di «schermatura» di segno opposto. Il campo diminuisce esponenzialmente verso l'interno
- Se il sc e' sottile $d \ll \lambda_L$

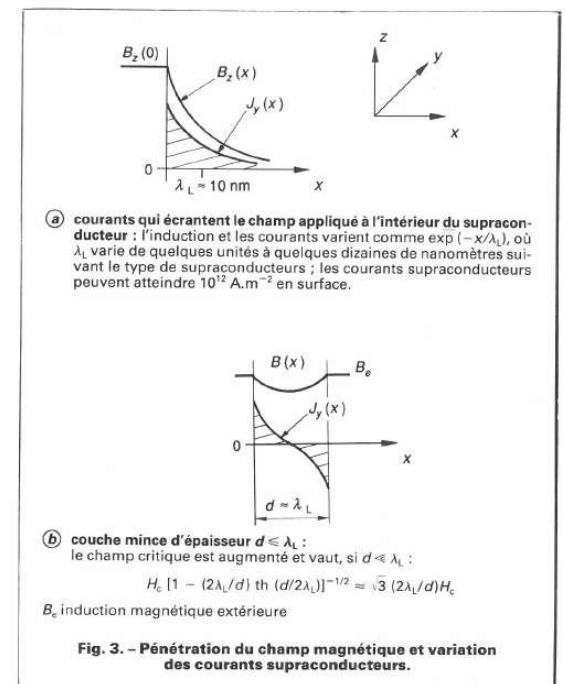
λ_L , longueur de pénétration de London, vaut typiquement 50 nm pour les supraconducteurs à $T_c < 25$ K ; elle varie avec la température suivant une loi :

$$\lambda_L(T) = \lambda_L(0) (1 - \theta^4)^{-\frac{1}{2}}$$

avec $\theta = T/T_c$ température réduite.

L'hypothèse de London conduit à l'effet Meissner et montre que le champ s'amortit exponentiellement de la surface extérieure vers l'intérieur (fig. 3a). Il en est de même des courants qui écrivent le champ appliqué ; les densités de courant peuvent atteindre 10^{12} A/m².

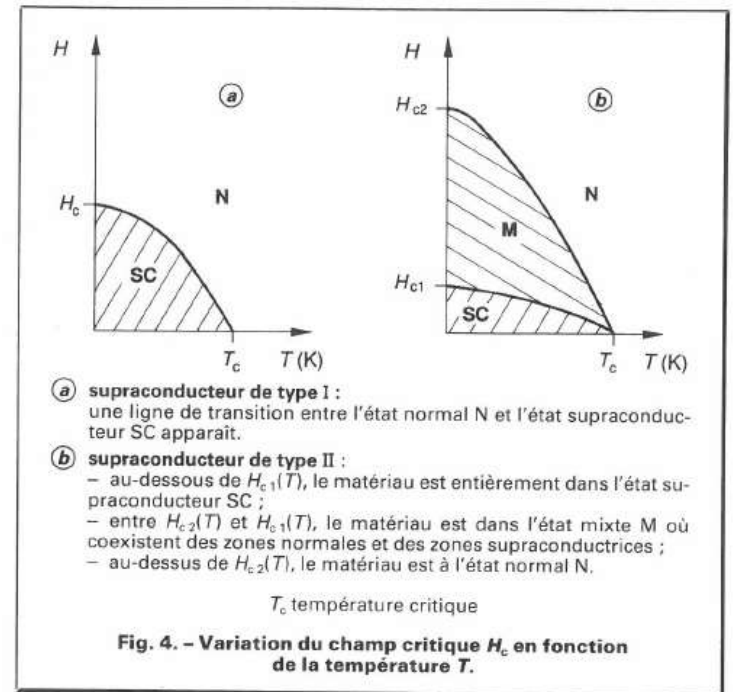
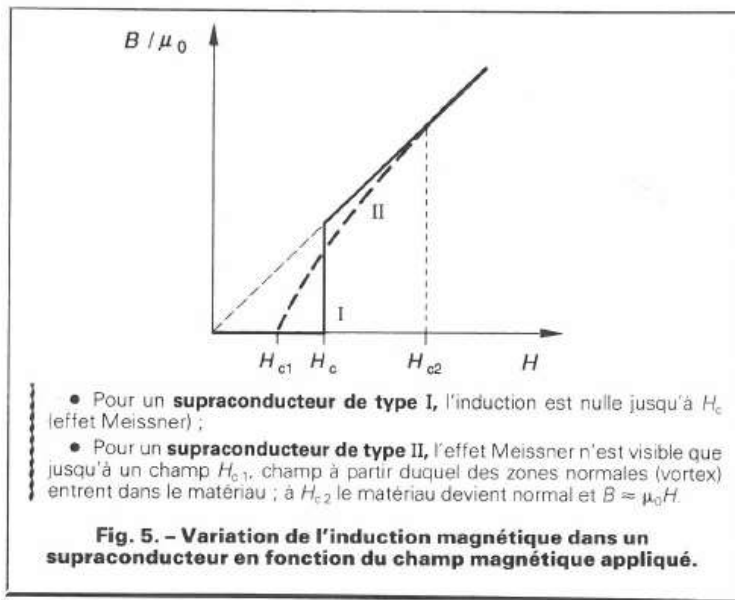
Dans le cas de films minces (d'épaisseur $d \leq \lambda_L$), le champ magnétique pénètre dans le film et l'effet Meissner est incomplet (fig. 3b).



[Superconductivity] cenni

- Campo critico: Il valore del campo magnetico H_c al di sopra del quale il materiale superconduttore diviene normale.
- E' funzione della temperatura :

$$H_c(T) = H_c(0) [1 - \theta^2]; \quad \theta = T/T_c$$



[Superconductivity] cenni

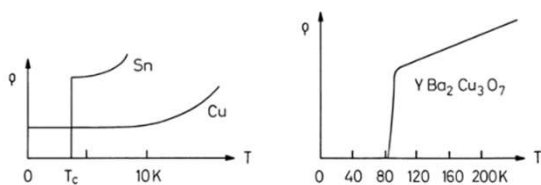


Figure 1: The low-temperature resistivity of copper, tin and $\text{YBa}_2\text{Cu}_3\text{O}_7$.

Al	Hg	Sn	Pb	Nb	Ti	NbTi	Nb_3Sn
1.14	4.15	3.72	7.9	9.2	0.4	9.4	18

Table 1: Critical temperature T_c in K of selected superconducting materials for vanishing magnetic field.

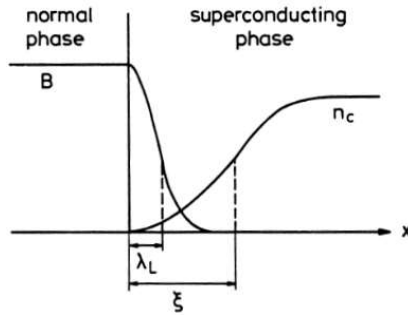


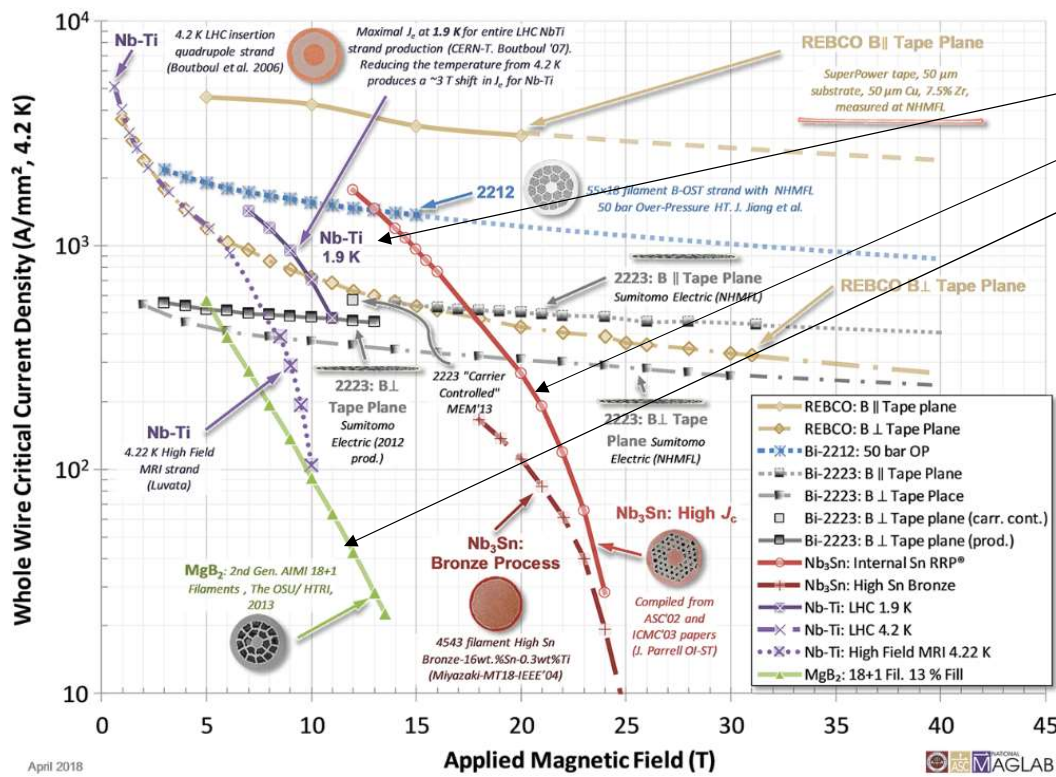
Figure 2: The exponential drop of the magnetic field and the rise of the Cooper-pair density at a boundary between a normal and a superconductor.

La teoria basilare della superconduttività è stata definita dalla BCS (Bardeen, Cooper e Schiffer, 1957):

- Gli elettroni avendo la stessa carica ($-e$) si respingono
- Nei cristalli si può avere un'interazione elettrone-fonone cioè con le vibrazioni del cristallo
- È stato dimostrato che due elettroni con spin opposto possono formare una *coppia di Cooper* di spin nullo (statistica di Bose-Einstein)
- La coppia si comporta come un'unica particella, bosone
- I due elettroni si trovano ad una distanza ξ (lunghezza di coerenza) ma si muovono insieme senza dissipare energia
- Per rompere una coppia occorre un'energia $2 \Delta(0) = 3.5 k T_c$
- Es. $T_c = 10 \text{ K}$, $k = 1.38 \cdot 10^{-23} \text{ J/K}$; $eV = 1.6 \cdot 10^{-19} \text{ Joule}$
- $2 \Delta(0) k T_c \approx 5 \cdot 10^{-22} \text{ J}$; $\Delta(0) k T_c \approx 2 \cdot 10^{-22} \text{ J}$

material	In	Pb	Sn	Nb
λ_L [nm]	24	32	≈ 30	32
ξ [nm]	360	510	≈ 170	39

[Superconductivity] cenni: Magneti



Of major interest :
 NbTi (1.9 K LHC),
 Nb₃Sn (HL-LHC),
 MgB₂(MRI cryogen-free),

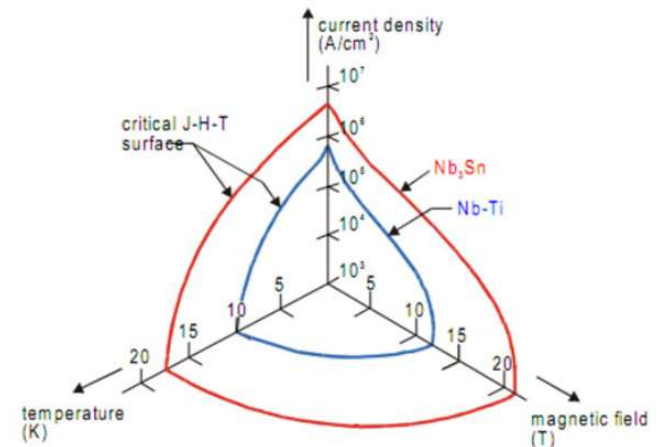


Figure 1.2: The critical surface of Niobium-Titanium and Niobium-3-Tin.

[Superconductivity] cenni: Magneti

Per la criogenia sono importanti:

- L'energia immagazzinata $\frac{1}{2} L \cdot I^2$ (per la sicurezza)
- La massa del magnete
- Lo scambio termico con l'elio di raffreddamento, a bagno (LHC) o indirectly cooled (ATLAS,CMS)
- Es. $E_{\text{dipole}} = 0.5 L \cdot I^2$ dipole Energy stored in one dipole is 7.6 MJoule
- For all 1232 dipoles in the LHC: 9.4 GJ
- In case of quench (spontaneous or induced) the energy can be dumped on an external circuit (with resistors and/or diodes) or in the magnet itself (or shared between the two).
- In some small magnets the dumping circuit is in the bath.

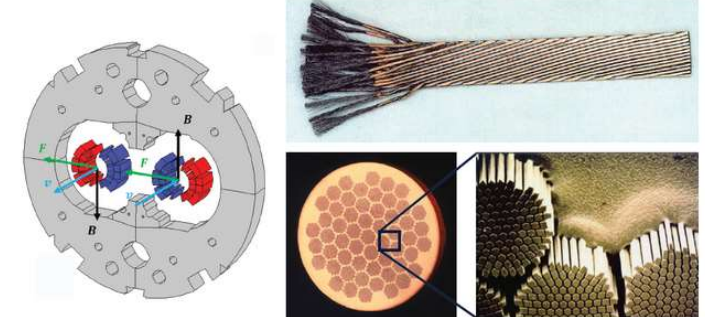
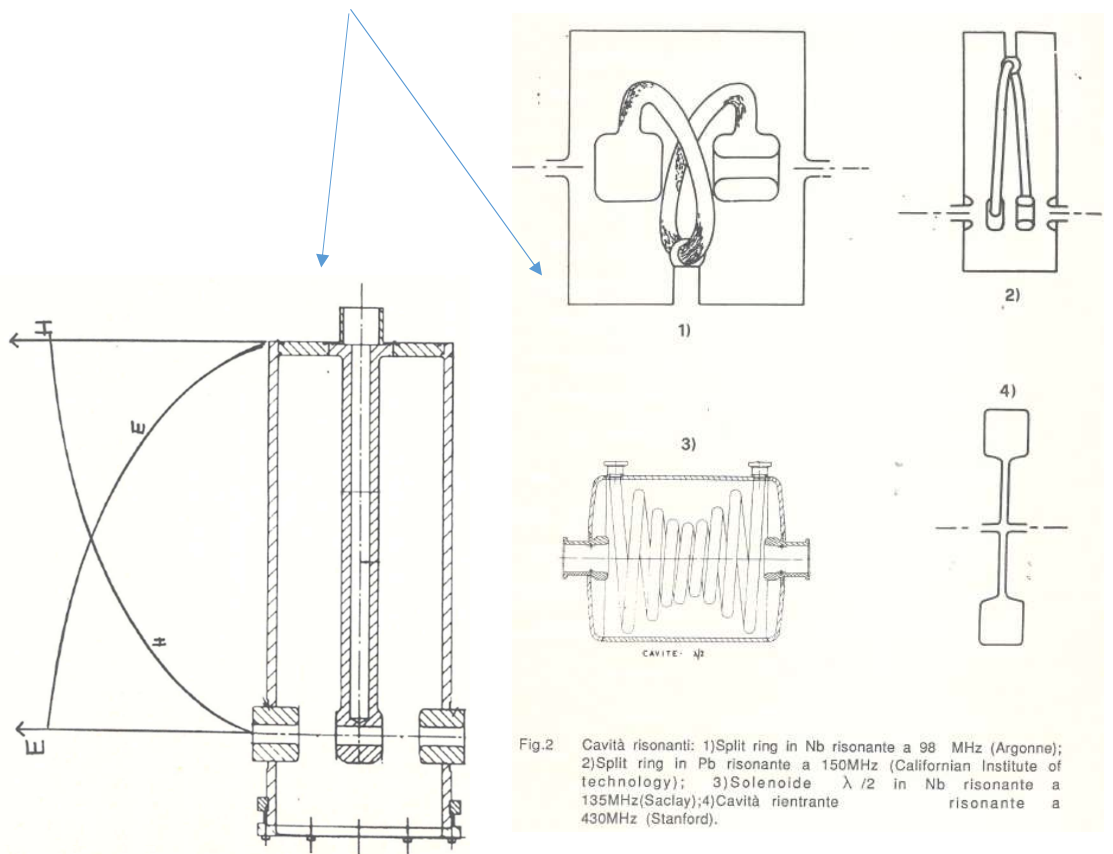
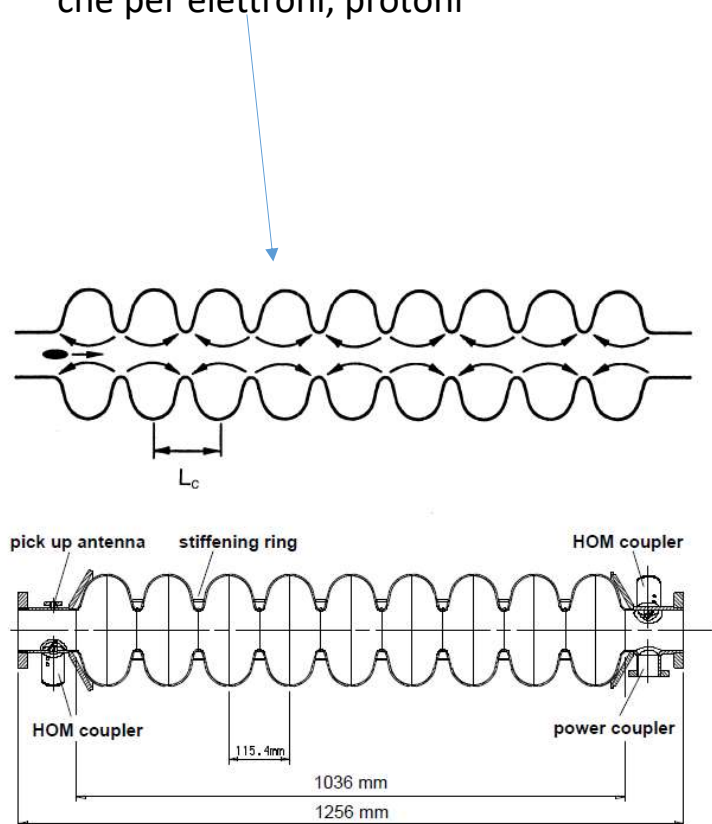


Figure 3. Left: A cross section of the LHC main dipole. Red and blue domains represent the superconducting coils keeping the particles in a circular trajectory. The gray domain represents the iron yoke. Right: High-current superconducting magnets in the Large Hadron Collider are based on cables made of superconducting microfilaments embedded in a copper matrix.



[Superconductivity] cenni: cavita' risonanti

- L'applicazione maggiore dell RF cavities e' per acceleratori, sia per ioni pesanti che per elettroni, protoni



[Superconductivity] RF cavities

Il valore del fattore di merito Q è forse la quantità più importante tra quelle misurate in pratica, per conoscere la bontà di un risonatore.

In analogia ai circuiti a costanti concentrate esso si definisce come:

$$Q_L = \frac{2\pi U}{(-dU/dt) T} \quad (5)$$

$$= \omega \frac{\text{en. immagazzinata}}{\text{pot. dissipata}} \quad (6)$$

dove $U = U_0 e^{-\omega t / Q_L}$ è l'energia immagazzinata ($T = 1/\nu$; ν = frequenza di risonanza).

Q_L è cioè 2π volte il numero di cicli necessario affinché l'energia dell'oscillazione diminuisca di un fattore $1/e$.

Il valore del fattore di merito rende immediatamente evidente la differenza tra cavità superconduttrici e normal-conduttrici: per le prime si ottengono, tipicamente, valori di Q dell'ordine di 10^7 - 10^9 e più, per le seconde, invece, di 10^4 . Questo è in stretta relazione con la differenza dei medesimi ordini di grandezza, tra la resistenza superficiale (che è definita in appendice) dei superconduttori utilizzati in cavità risonanti (10^{-8} - $10^{-9} \Omega$) e

- **Per la criogenia sono importanti:**
- L'energia immagazzinata (per la sicurezza)
- La potenza dissipata in He I a 4 K o in He II a 2 K.
 - XFEL (1.3 GHz), la potenza dinamica (RF) è attorno a 60W, energia accumulata ≈ 80 J. ($Q=1 \times 10^{10}$)
 - ESS (700 MHz), $Q=5 \times 10^9$ dissipano circa 100 W con un'energia accumulata di 120J.
 - ALPI, 160 MHz $P=7$ W
 - $U \approx 0.2$ J (≈ 3 - 4 J per PIAVE)

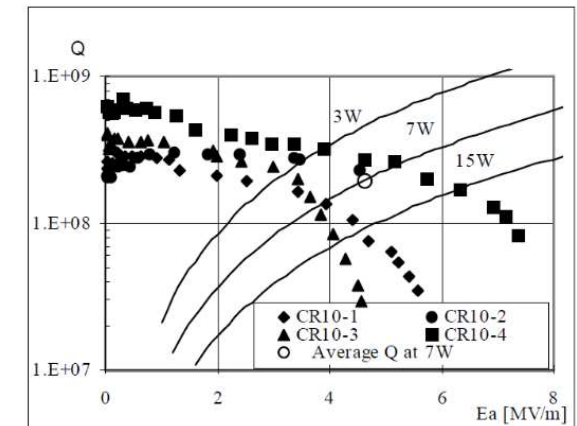
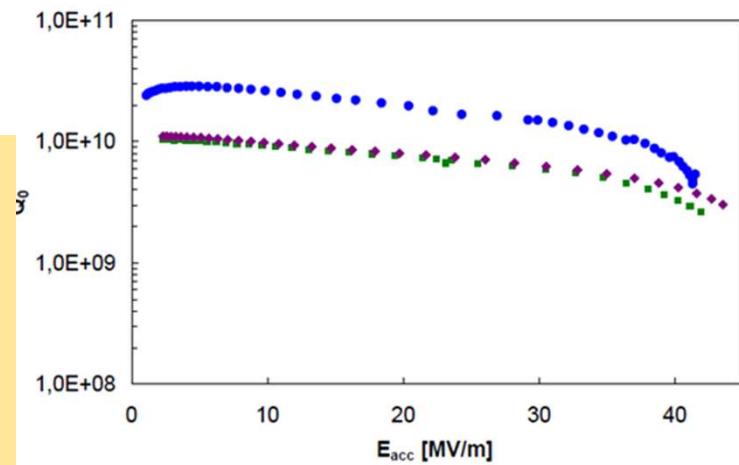


Figure 5: On line performance of Nb sputtered QWRs

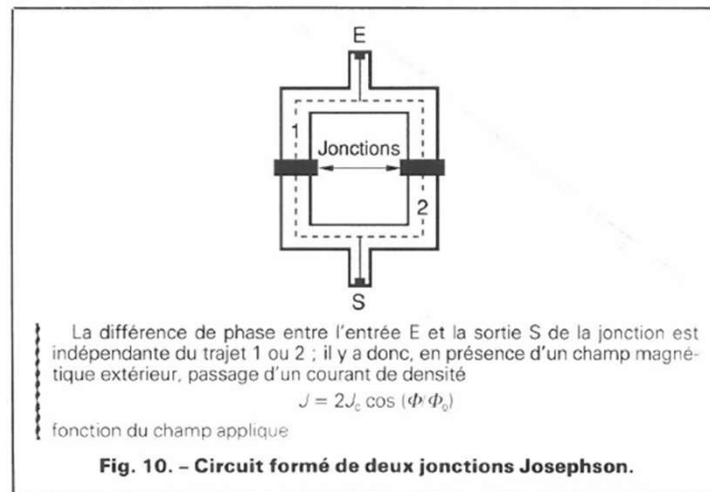
[Superconductivity] Josephson junction

- Due superconduttori sono a contatto attraverso un sottile strato di materiale isolante
- Una densità di corrente J_c può attraversare la barriera senza che vi sia applicata una tensione (effetto Josephson continuo)
- Se si applica una tensione U , appare una corrente di frequenza $v = \omega/2 \cdot \pi = 2 \cdot e \cdot U/h$ (effetto Josephson alternato)
- Esempio : $U = 10^{-6}$ Volt ; $h = 6.626 \cdot 10^{-34}$
 $v = 2 \cdot 1.6 \cdot 10^{-19} \cdot 10^{-6} / 6.626 \cdot 10^{-34} = 483.6$ Mhz
- Se si applica una tensione alternata

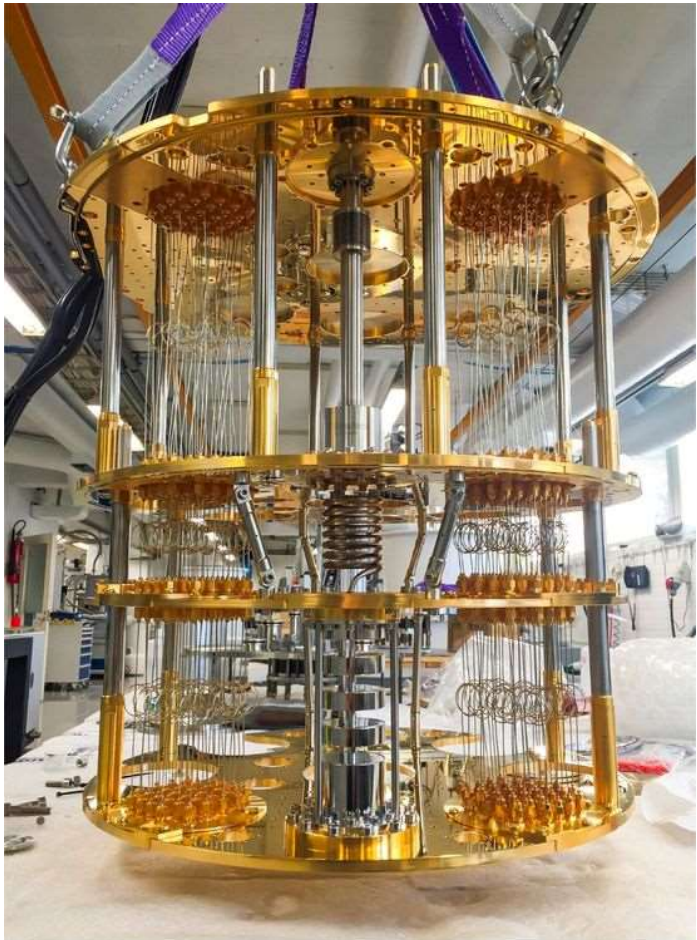
$$U = U_0 + \bar{U} \sin \omega t$$

La densità di corrente J ha un valore medio non nullo se è un multiplo di $\omega = 4 \pi \cdot e \cdot U_0/h$
- L'analogo avviene in presenza di un campo magnetico che produce un flusso ϕ , appare una corrente

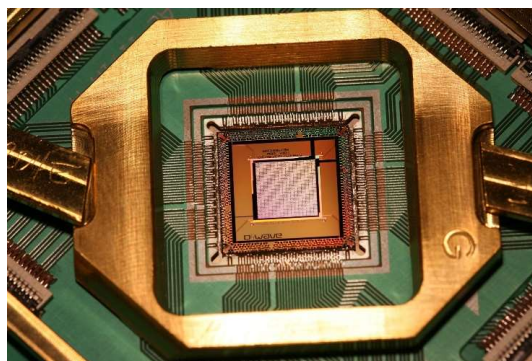
$$J = 2 \cdot J_c \cdot \cos(\phi/\phi_0)$$
- per un circuito con due giunzioni
- Questo effetto è utilizzato negli SQUID (Superconducting Quantum Interference Device) come magnetometri, voltmetri, frequency mixer,...)
- L'effetto Josephson è alla base della costruzione dei *qubits*



[Superconductivity] Josephson junction



Cryogenics for
Quantum computers



1000 qubits